International Agricultural Engineering Journal

CONTENTS

International Agricultural Engineering Journal

An International Journal on Research and Development in Agricultural Engineering
Published by the Asian Association for Agricultural Engineering (AAAE)

INTERNATIONAL

AGRICULTURAL ENGINEERING

JOURNAL

DESIGN OF A G-SHAPED LOAD CELL FOR TWO-RANGE WEIGHING APPLICATION

Fan-She Lin[*] and Tshen-Chan Lin[†]

ABSTRACT

This paper presents the design of a novel G-shaped load cell for measurement of two ranges of weight loading. In the first range of light weight loading (0 to 22 kgf for 20 mm-width or 0 to 42 kgf for 30 mm-width load cell), there was no contact between the two special components of the load cell. In the second range of heavy weight loading (22 to 50 kgf for 20 mm-width or 42 to 50 kgf for 30 mm-width load cell), contact between the two components occurs. The software of Finite Element analysis Method - Integrated Design Engineering and Analysis Software (FEM - I-DEAS) - was used in the structural analysis of the load cell. The results of FEM were used to simulate the displacement response of the load cell. Prototypes of the G-shaped load cells with a width of 20 or 30 mm were manufactured and tested. The strains of the G-shaped load cell under certain loads were measured, and the relationship of load weight and displacement was established. Our results showed that for the 20 mm-width load cell, the maximal relative error for using the regression equations to estimate the weight is 1.67%. For the 30 mm-width load cell, the maximal relative error for using the regression equations is 2.29%. The G-shaped load cell is a one-step, two-range weighing system with good accuracy, which could prove beneficial to the agricultural products sorting process.

Keywords: *Load cell; Weighing machine; Finite element analysis.* © 2007 AAAE

1. INTRODUCTION

The weighing system plays a key role in the sorting and processing of agricultural products. The load cell is the major sensing element of the system. Characteristics including simple geometry, small size, and high sensitivity are the important properties for an ideal load cell. Most load cells have limited weighing range in order to maintain the linear property for accurate measurement. Shen (1989) developed a micro-computerized weighing device that employed a load cell to measure the weight of fruits individually. His results showed that the output voltage greatly correlated with the weight of fruits.

The load cell consists of a structural body and two strain gages. The strain gages are glued onto specific locations of the surface of the load cell's structural body for maximal stress. When the structure is subject to loading, the strain gages change their resistance which results in an output of voltage signal. The weight can then be measured. The smaller the area of moment inertia of the structure, the larger the

strain and the more significant the signal becomes. Therefore, hollowing the structure of the load cell is an effective way to obtain higher sensitivity. Furthermore, the range of measurement of the load cell is limited in order to maintain the linearity. When the load is over the limit, another load cell with higher range needs to be used.

Typically, the load cell is either C-shaped or S-shaped. Wang (1994) applied the finite element analysis and optimal design methods to design an S-shaped load cell. The interior of the load cell was hollowed out to reduce the stiffness of the structure. By doing so, they were able to obtain a stronger voltage output signal when subject to loading and therefore achieve higher weighing sensitivity. Lia (1998) investigated the importance of the location of the strain gages and the size of load cell and deduced that the sensitivity of the load cell was highly dependent on the deformed capability of the load cell. The author used COmbined System MOdeling and Simulation (COSMOS) FEM code to analyze the load cell to establish the location for maximal stress. The

---

[*] Graduate Student, National Chung Hsing University, Department of Bio-Industrial Mechatronics Engineering, Taichung, Taiwan, R.O.C.

[†] Professor and Corresponding Author, National Chung Hsing University, Department of Bio-Industrial Mechatronics Engineering, Taichung, Taiwan, R.O.C.

strain gages were glued onto these locations to achieve high sensitivity of the load cell. Hert's contact was known as the simplest contact problem (Ma, 1997). A linear, elastic, and isotropic material was considered in this contact problem. The contact area is smaller compared to the size of the structures. There exists no friction between the structural components.

In our study, a G-shaped load cell was designed. The theory of our design for the load cell is to use the phenomenon of contact between two components of the body of the load cell when subject to loading of heavy weight that does not happen upon loading of light weight. Two ranges of measurement can be obtained. Due to the very small contact surface area of the two components, friction was neglected. I-DEAS is used to analyze the strain and stress of the load cell when subject to loading. According to the simulation results, prototypes of the load cell with a width of 20 or 30 mm were manufactured. The specialized G-shaped load cell was then subject to loading test. The relation of load weight and displacement of load cell is thus established.

2. MATERIALS AND METHODS

2.1 Design of G-shaped Load Cell

In order to overcome the aforementioned shortages, a G-shaped load cell was developed. The theory to design a G-shaped load cell is to utilize the concept of the contact of structural components upon heavy loading as compared to no contact between structural components upon light loading. Two ranges of weight measurement can therefore be theoretically achieved. In the first range (light weight loading), there is no contact between structural components, therefore only two sets of strain gages output signals. In the second range (heavy weight loading), contact happens between two components of the structural body. All four sets of strain gages output signals. The geometric scheme of the prototype of a G-shaped load cell is shown in Fig. 1. The photo of the prototype of a G-shaped load cell is shown in Fig. 2. In Fig. 1, the upper frame is denoted as A; the lower frame is denoted as B; the screw is denoted as C; the left stem is denoted as D; the right stem is denoted as E; and the base is denoted as F. The screw C is treated as the contactor and the frame B is treated as the target upon
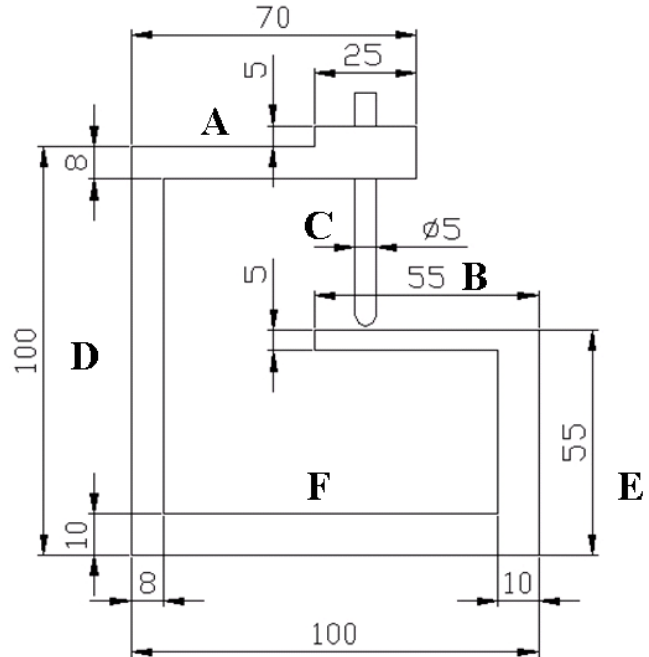
Fig. 1: Geometry of G-shaped load cell (unit: mm)

Fig. 2: A photographical view of the G-shaped load cell prototype

contact during heavy loading. The screw, nut, and washer were assembled to maintain a gap of 1 mm between the tip of the screw and the target.

2.2 Material of Load Cell

1) Body of structure: Dimensions of each part of the load cell is shown in Fig. 1. Two load cells, with a width of 20 mm or 30 mm, were manufactured and tested. The structural body is made from aluminum alloy metal, 6061 Al-Mg-Si. With a mechanical property of E = 70,000 MPa, G = 27,000 MPa, $\nu = 0.3$, and Yield stress = 250 MPa.
2) Screw: Carbon steel, M6×1, with one taped end; E = 200,000 MPa; G = 80,000 MPa; $\nu = 0.25$.

2.3 Finite Element Model

1) Element type: Solid Elements were used.
2) Mesh:
   i. Auto Meshing: Near contact area, *Local Mesh Option* in I-DEAS is used and fine meshes with a length of 0.5 mm are generated. For the rest area, *Free Mesh Option* is used and meshes with a length of 3 mm are automatically established.
   ii. Mesh for the tip of screw: The tip of screw, shown in Fig. 3, is used for contact. Theoretically, it is a point. It cannot be used as contact element when using I-DEAS. Some modification is needed. The tip is converted to a small circular region shown in Fig. 4. This small circular region may make contact with frame B, the target, during heavy loading.
   iii. Contact: The *search distance* is set to be 3 mm when solving contact problem.

2.4 Hardware and Software for Experiment and Analysis

1) Hardware
   i. Strain Gage: KFG-5-120-C1-23, manufactured by KYOWA Co. (Tokyo, Japan). Its gage factor is 2.1.
   ii. Signal amplifier: WGI-300A, manufactured by KYOWA Co. (Tokyo, Japan). The readout is shown on the display panel or acquired by a DAQ device.
   iii. Wheatstone bridge: DBB-120A, manufactured by KYOWA Co. (Tokyo, Japan).
2) Software: I-DEAS (SDRC, 2001) is used to analyze the structure model of the G-shaped load cell.
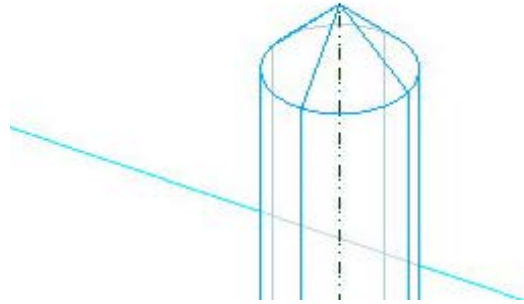
Fig. 3: The tip of screw model
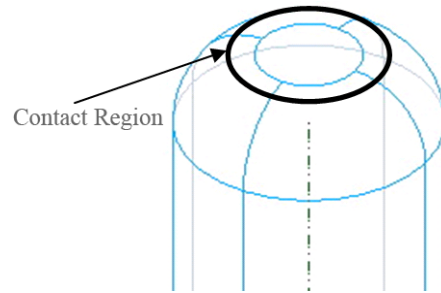
Fig. 4: The modified tip of the screw model

2.5 Experimental Procedure

The experimental setup is shown in Fig. 5. The strain gages were glued onto the regions of maximal displacement in order to obtain a more significant signal. In this study, the strain gages for frame A were 25 mm to the centerline of loading, as shown in Figs. 6 and 7. The strain gages for frame B were 15 mm to the right stem E. Four strain gages with half-bridge circuits were used. The signal amplifier was re-set each time before measuring.

Two ranges of load weight were tested in our experiment. During the first range, i.e. the light weight loading, the tip of the screw did not touch frame B. During the second range, i.e. the heavy weight loading, contact between the screw and frame B was made.

In order to compare the results of the simulation to measurement, a command of I-DEAS, Anchor Node Create, was used to place an "anchor" at the location where the strain gage was glued onto the prototyped model. Then, I-DEAS added one node at that location of the model. The displacement was evaluated. This procedure is very important in comparing the FEM results with measured data.
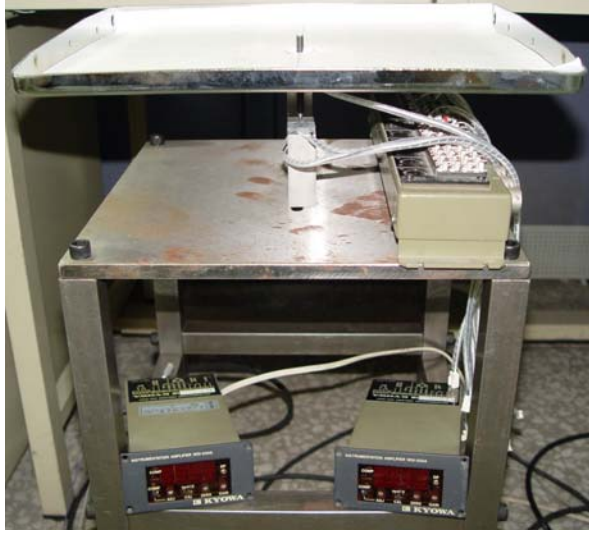
Fig. 5: Experimental setup

Fig. 6: The location of strain gage in the upper portion
of frame A
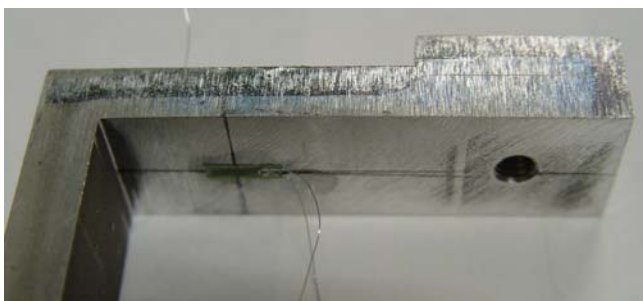
Fig. 7: The location of strain gage in the lower portion
of frame A

The load is placed as near the center of the plate as possible. The loads from 10 kgf to 50 kgf were measured. Each load was measured three times and the averaged readout recorded.

3. RESULTS AND DISCUSSION

Our results showed that with our G-shaped load cell for a two range weighing system, the displacements of the measured data were smaller than that of the analyzed data. Conceptually, in our load cell contact between the tip of screw C with frame B happens when the displacement of the tip of the screw is over 1 mm. The analyzed results showed that at that instant the location of the strain gages on frame B did not displace. But, we obtained signal output produced from the strain gages on frame B. Plots of displacements vs. loads of load cells are shown in Figs. 8 and 9. The results are summarized as follows:

1) For the load cell with a width of 20 mm: The contact did not happen until the load was 21 kgf. Table 1 shows the slopes of the curves for measured and analyzed data for the load cell.

   i. Measured Results: No signal output was recorded from the strain gages on frame B until the loads reached 22 kgf. The loads fall into three intervals – [0, 22), [22, 27], (27, 50] – as discussed below. During [0, 22), the no contact stage, there was a linear relation between loads and displacement of frame A and the slope is 0.01389. During [22, 27] when there was contact between the screw and frame B, the slope of the displacements vs. loads of frame A is 0.00811 and the slope of the displacements vs. loads of frame B is -0.00160. During (27, 50] when displacements from frame A and from frame B were recorded, the slope of the displacements vs. loads of frame A is 0.00370 and the slope of the displacements vs. loads of frame B is 0.00222.

   ii. Analyzed Results: The displacement of the location of strain gages on frame B occurred when the loads were over 26 kgf according to the analyzed results. The relation of the displacement vs. the load of frame A differs from that of the measured data. The structure appears to be stiffer. However, this is one of the phenomena of an FEM model. The loads fall into three intervals – [0, 27), [27, 33], (33, 50] – as discussed below. During [0, 27), the no contact stage, there is a linear relation between displacements and loads and slope is 0.01428. During [27, 33],

Table 1: The slope of the curves for measured and analyzed data for load cell with a width of 20 mm

Loading Stage	Measured Data		Analyzed Data	
	Slope (frame A)	Slope (frame B)	Slope (frame A)	Slope (frame B)
No Contact	0.01389	-	0.01428	-
First Stage	0.00811	-0.00160	0.00430	0.00300
Second Stage	0.00370	0.00222	0.00162	0.00263

the first stage of contact, the slope of the displacements vs. loads of frame A is 0.00430 and the slope of the displacements vs. loads of frame B is 0.00300. During (33, 50], the second stage of contact, the slope of the displacements vs. loads of frame A is 0.00162 and the slope of the displacements vs. loads of frame B is 0.00263.

iii. Regression Equations: According to the response curves of the load cell with different loads, three intervals – no contact, contact in the first stage and contact in the second stage - are corresponding to light, medium, and heavy loads. Three linear regression equations were obtained. Using these equations, we estimated the weight of loads. The equations were summarized as follows. The voltage signal was used in the following equations.

a) No contact: No contact happens. The equation is

$$F = mv + b \qquad (1)$$

where F (in kgf) is load and v (in mV) is the measured voltage of frame A. m is 33.49 and b is -1.42. The maximal relative error was 1.67%.

b) Contact in the first stage: Contact happened and frame B displaced to produce signals. Voltage signals are produced from the strain gages of frame A as well as frame B. The equation is

$$F = m_1 v_1 + m_2 v_2 + b \qquad (2)$$

where v_1 and v_2 are measured voltages from frame A and frame B respectively. The coefficients m_1 is 57.28 and m_2 is -0.73. The coefficient b is -16.90. The maximal relative error was 1.12%.

c) Contact in the second stage: The equation is the same as Eq. (2) but with different coefficients where m_1 is 116.87 and m_2 is 14.81. The coefficient b is -63.10. The maximal relative error was 0.95%.

2) For the load cell with a width of 30 mm: The contact did not happen until the load was 31 kgf. The displacement of frame B occurred only when the loads were over 42 kgf according to the analyzed results. As a result, no signal output was produced from the strain gages on frame B until the load reached 42 kgf. The curves of displacements vs. loads are composed of two segments for both measured and analyzed data. The loads fall into two intervals – [0, 42], [42, 50] – as discussed below. Table 2 shows the slopes of the curves for measured and analyzed data for load cell.

Table 2: The slope of the curves for measured and analyzed data for a load cell with a width of 30 mm

Loading Stage	Measured Data		Analyzed Data	
	Slope (frame A)	Slope (frame B)	Slope (frame A)	Slope (frame B)
First Stage	0.00923	-	0.00946	-
Second Stage	0.00599	0.00214	0.00375	0.00200

i. Measured Results: When the loads were within the range of [0, 42), the slope of the curve of displacements vs. loads of frame A is 0.00923. The slope of the curve of displacements vs. loads of frame A is 0.00599 and the slope of the curve of displacements vs. loads of frame B is 0.00214 when the loads were within the range of [42, 50].

ii. Analyzed Results: When the loads were within the range of [0, 42), the slope of the curve of displacements vs. loads of frame A is 0.00946. The slope of the curve of displacements vs. loads of frame A is 0.00375 and the slope of the curve of displacements vs. loads of frame B is 0.00200 when the loads were within the range of [42, 50].

iii. Regression Equations: According to the response curves of load cell with different loads, two intervals – no contact and contact - are corresponding to light and heavy loads. Two linear regression equations were obtained. Using these equations, we estimated the weight of loads. The equations were summarized as follows.
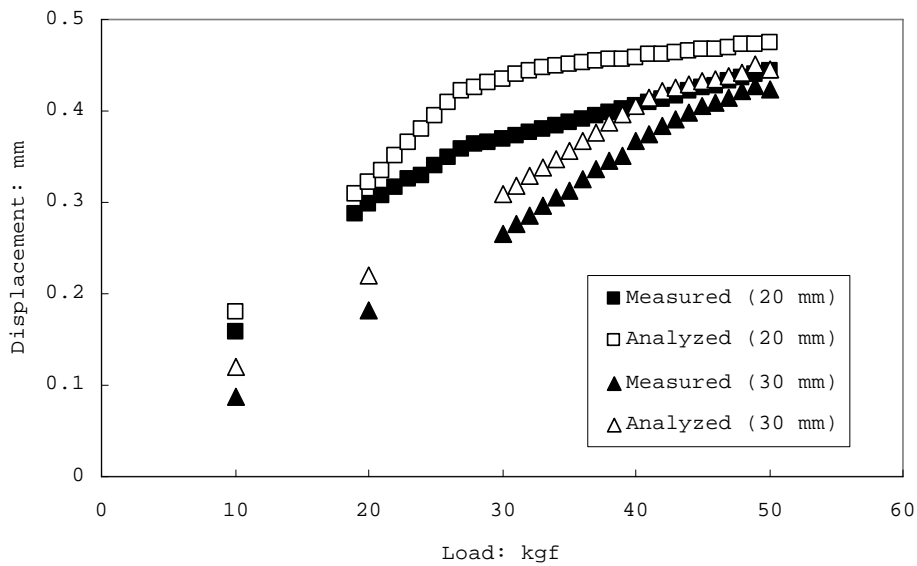
Fig. 8: Plot of displacements vs. loads of frame A of a load cell
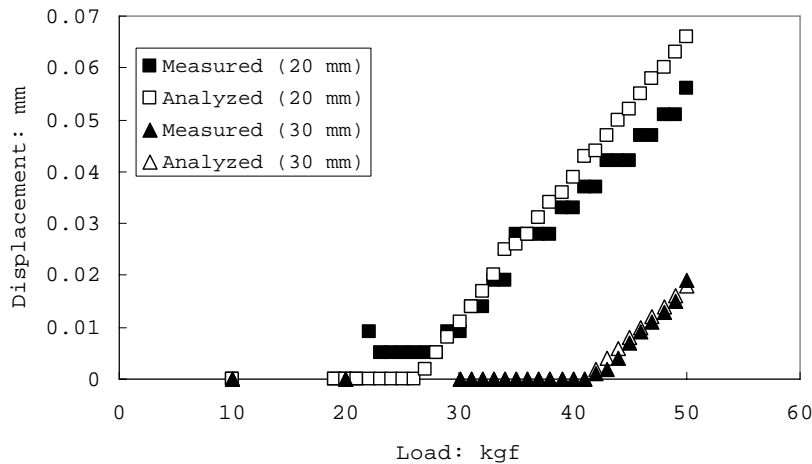
Fig. 9: Plot of displacements vs. loads of frame B of a load cell

a) No contact: No contact happens. The equation is

$$F = mv + b \qquad (3)$$

where F (in kgf) is load and v (in mV) is the measured voltage of frame A. m is 50.40 and b is 0.74. The maximal relative error was 2.29%.

b) Contact: Contact happened and both frame A and frame B displaced to produce signals. Voltage signals are produced from the strain gages of frame A as well as frame B. The equation is

$$F = m_1 v_1 + m_2 v_2 + b \qquad (4)$$

where v_1 and v_2 are measured voltages from frame A and frame B respectively. The coefficients m_1 is 31.94 and m_2 is 132.82. The coefficient b is 15.38. The maximal relative error was 0.58%.

4. CONCLUSIONS

A G-shaped load cell for two ranges of loading measurement was established in this study. The FEM model had been evaluated and compared with the experimental results. The displacements of the frame of load cell by measurement were smaller than by analysis when subject to the same loading. However, the trends of displacement of the structure were very consistent. The results show that the maximal relative errors of the regression equations is 1.67% for a load cell with a width of 20 mm, and 2.29% for a load cell with a width of 30 mm. In order to obtain more significant voltage signals, the strain gages were cemented on the location of the maximal stress. However, the actual location of the strain gage needs to be determined with the consideration of easy fabrication in mind.

REFERENCES

1. Wang, C. C. (1994). Shape Optimum Design on Force Transducers, Master Thesis, Dep. of Mechanical Eng., Feng Chia University (in Chinese).
2. Shen, D. G. (1989). A Study on Weighing and Grading Device for Agricultural Products and Microcomputer Control System, Master Thesis. Dep. of Agricultural Eng., National Taiwan University (in Chinese).
3. Ma, L. C., Pong, Z. S., Xi, D. B., Shen, G. L. and Z. F. Tao (1993). Strain Measurements and Transmission Technology. Beijing: Chinese Instrumentation Publisher (in Chinese).
4. Lia, F. Y. (1998). Design Optimization of Strain Gauge Pressure Transducer, Master Thesis, Dep. of Mechanical Eng., DA-YEH University (in Chinese).
5. Hack, R. S. and A. A. Becker (1998). Frictional contact analysis under tangential loading using a local axes boundary element formulation. International Journal of Mechanical Sciences, Vol. 41, pp. 419-436.
6. Structural Dynamics Research Corporation (SDRC). 2001. I–DEAS 9 Analysis Pre- and Post-Processing. pp. 197-217.

RESPONSE OF DRIP IRRIGATED POTATO UNDER VARIABLE IRRIGATION LEVELS

D.M. Denis[*] and J. Lordwin Girish Kumar[†]

ABSTRACT

With declining ground water tables and lack of adequate surface water supplies for irrigation, Indian farmers must adopt efficient irrigation systems to grow more food with less water. The drip irrigation system offers a huge potential to farmers to grow more cash crops with limited water supplies. The main objective of this study was to conduct research experiments to determine the viability of a drip irrigation system to grow potatoes under varying degrees of management practices. To accomplish the objective field studies were conducted for two years (2003 and 2004) on clay loam soil in the northern region of Allahabad to study the effect of eight water management levels (equivalent to pan evaporation replenishment of 25, 50, 75, 100, 125, 150, 175 and 200%) on potato yield, irrigation production efficiency, and economics of a potato production system using the drip irrigation method. The highest average potato yield of 48.98 tonnes/ha was observed at water use equivalent to 150% of pan evaporation replenishment. The maximum irrigation production efficiency of 106.26 kg/m^3 was observed. Also, drip irrigation at 150% of pan evaporation replenishment resulted in the highest benefit cost ratio. The seasonal water applied and marketable yield of potato showed quadratic relationship (R^2=0.9830), which can be used for allocating irrigation water within and between the crops. The results of this study clearly indicate that the drip irrigation system is profitable for potato production inspite of high initial investment.

Keywords: *Drip; Pan evaporation; Replenishment; Water; Irrigation levels.* © 2007 AAAE

1. INTRODUCTION

Potato (*Solanum tuberosum* L.) is one of the most important and popular crops throughout the world. The crop has attained great importance and popularity during the past two decades. Potato is one of the unique crops grown in the country having high productivity and supplementing food needs. Potato is rich in carbohydrates, proteins, phosphorus, calcium, vitamin C, and vitamin A. India ranks fourth in the area and third in the world for potato production. In India potato is produced in an area of 1.4 Million ha with a production of 25 Million tonnes and productivity of 17.86 tonnes per ha as per FAO figures for the year 2004. However, during 2004-2005, estimated production was around 26.5 Million MT. In India, Uttar Pradesh is the largest producer with a production of about 9.8 Million tonnes during 2004-2005 from an area of 0.44 Million ha. This low yield is caused, in part, by improper and unscientific methods of irrigation. Potato crop thrives well in all the soil textures that have good internal drainage. It is relatively sensitive to soil water deficits.

Water resource is the most dominant limiting factor for crop diversification and production in India, particularly in the northern region. Water for irrigation is becoming both scarce and expensive due to significant depletion of surface and subsurface water resources caused by erratic rainfall and over-exploitation. Improper water management practices not only waste expensive and scarce water resources but also decreases marketable yield, water use efficiency and economic return and leads to water logging and salinity, which can be partly corrected by expensive drainage systems (Singh, 1987; Singh and Mohan, 1994; Imtiyaz *et al*., 2000 a, b, c, d). Irrigation scheduling is a critical management input to ensure adequate soil moisture for optimum plant growth yield, quality, water use efficiency and economic return. Irrigation scheduling which determines the timing and amount of irrigation water is governed by many complex factors but microclimate plays the

---

[*] Assistant Professor, Department of Soil Water Land Engineering and Management Agricultural Institute - Deemed University, Allahabad – 211007 (U.P), India

[†] Assistant professor and Corresponding Author, P.O.Box: 1501, Department of Water Resources Engineering, Faculty of Engineering, Bahir Dar University, Bahir Dar, Ethiopia.E-mail: lordwingirish@rediffmail.com

most important role. Therefore, it is important to develop irrigation scheduling techniques under prevailing climatic conditions in order to utilize scarce and expensive water resources efficiently and effectively for crop production. Numerous studies were carried out in the past on the development and evaluation of irrigation scheduling techniques under a wide range of irrigation system and management, soil, climate and crop conditions (Hagan and Laborde, 1964; Jensen *et al.*, 1970; Mishra and Pant, 1981; Wanjura *et al.*, 1990).

Drip irrigation is the most efficient method to deliver water and nutrients to the plants. It is one of the latest methods of irrigation, which is becoming increasingly popular in areas with water scarcity. It is a method of watering plants frequently with a volume of water approaching the consumptive use of the plants, thereby minimizing losses such as conveyance, deep percolation, run-off and soil evaporation. In this method, irrigation is accomplished by the devices called 'emitters' or 'drippers' at selected spacing to deliver water at the soil surface near the base of the plants. The system applies water slowly to keep the soil moisture within the desired range of plant growth. The micro irrigation system, which includes drip and micro-sprinklers, with its ability to apply small but frequent water applications has been found superior in terms of water saving, yield and irrigation production efficiency (Theodore, 1980: Fekadu and Teshome, 1988; Shrivastava *et al.*, 1994).

With this background consideration, a comprehensive field study was undertaken on sandy loam soil at the Irrigation Research Farm of Allahabad Agricultural Institute - Deemed University, Allahabad, to determine the response of drip irrigated potato under variable irrigation management schemes on marketable yield, irrigation production efficiency and economic return of potato under limited water availability conditions.

2. MATERIALS AND METHODS

Field experiments were conducted on potato crop over a period of two years 2003–2004 through 2004–2005. *Kufri Badshah* was selected which is 100–110 days vegetable crop of the locality and is suited to the prevailing climate in the winter season (November–March) of the year. The crop was grown from 17th November, 2003 to 5th March, 2004 during the first experiment and 24th November, 2004 to 8th March,

2005 during the second experiment. Twenty four experimental plots having 8.4 m^2 each and with row to row and plant to plant spacing of 60 cm x 20 cm were used for the field experiments. Application of fertilizers was done as per the recommendation for the cv. *Kufri Badshah*. Prior to sowing, farm yard manure was incorporated into the soil at the rate of 35 tonnes per hectare. Single super phosphate and muriate of potash were also incorporated along with farm yard manure @ 500 kg ha^{-1} and 300 kg ha^{-1}, respectively. Urea application was done in split dosage, one before sowing and the next at 30 days after sowing, at the rate of 266.60 kg ha^{-1} per application. The experiment consisted of eight irrigation treatments. The details of the treatments are as follows:

Experimental treatments for different Irrigation management schemes

Scheme	% of pan evaporation replenishment used in the irrigation
I_1	25
I_2	50
I_3	75
I_4	100
I_5	125
I_6	150
I_7	175
I_8	200

The daily evaporation data from USWB class A pan for a period of five years were collected from Meteorological Station, Bamrauli, Allahabad, Uttar Pradesh. Crop was irrigated when the sum of daily mean (5 years) of pan evaporation reached approximately a pre-determined value of 16.3 mm (rooting depth in m x plant available soil moisture in fraction). The crop was irrigated by the surface drip irrigation method. The drip irrigation system was designed and installed to meet the objectives of the proposed research work. The irrigation water was pumped directly from borehole to the concrete tank. The irrigation water was lifted from the concrete tank with the help of motor to the drip irrigation system. A

screen filter was installed on the mainline to minimize dripper blockage. PVC pipes of 50 mm and low density polyethylene pipes (LDPE) of 12 mm diameter were used for sub-main and lateral lines. The lateral line was laid to each crop row. Plants of potato were watered by 4 ℓ h^{-1} non-pressure compensated on line drippers. The space between drippers was 0.5m x 0.5 m. The sub-main line was connected to a water meter and a control valve in order to deliver the desired amount of water to the respective treatments. Standard cultural practices were adopted during the crop growing seasons. The crops were harvested from $3^{rd} – 5^{th}$ March during the first experiment and $6^{th} – 8^{th}$ March during the second experiment.

In order to assess the economic viability of the drip irrigation system under variable irrigation, both fixed and operating costs were included. Total cost of production, gross return and net return under different irrigation levels were estimated on the following assumptions:

Salvage value of the components	0
Useful life of tube well, pump motor and pump house	25 years
Useful life of drip irrigation systems	8 years
Useful life of weeding and spraying equipment	7 years
Interest rate	14%
Repair and maintenance	7.5%
Number of crops per year	2

The fixed cost including water development (tube well, pump, motor, pump house and other accessories) and irrigation systems, Poly Vinyl Chloride (PVC) and Low Density Polyethylene pipes (LDPE) for main, sub-main and laterals, filters, fertilizer unit, pressure gauges, control valves, water meter, drippers and other accessories, was calculated for different irrigation levels by the following approach (James and Lee, 1971).

$$CRF = \frac{i(1+i)^n}{(1+i)^n - 1} \qquad (1)$$

where

CRF = Capital recovery factor
i = Interest rate (fraction)
n = Useful life of the component (years)

Annual fixed cost/h = CRF x fixed cost/ha   (2)

Annual fixed cost/ha/season =
$$\frac{Annual\ fixed\ \cos t\,/\,ha}{2} \qquad (3)$$

The operating cost including labour (system installation, irrigation, planting, weeding, cultivation, fertilizer, chemical application, harvesting, etc.), land preparation, fertilizers, chemicals, water pumping, repair, maintenance (tube well, pump, electric motor, pump house, irrigation systems, etc.) was estimated.

The gross return was calculated taking into consideration the marketable yield and current wholesale price of potato. Subsequently, the net return for potato was calculated considering total cost of production (fixed and operating costs) and gross return.

Net return (Rs./ha) = Gross return (Rs./ha) – Total cost of production (Rs./ha)   (4)

The benefit cost ratio (B/C) was calculated as follows:

$$\frac{B}{C} = \frac{Gross\ return\ (Rs./ha)}{Total\ cost\ production\ (Rs./ha)} \qquad (5)$$

Statistical tool used in the data analysis

One way classified data has been used for the data analysis. When a set of observations is distributed over the different level of factor, they form one-way classified data. For Ex: Let us take a factor, say, at K levels. Let there be n_i observations denoted by $Y_{ij} \begin{pmatrix} j = 1,2,...,n_1 \\ i = 1,2,...,k \end{pmatrix}$ against the ith level. Then the observations y_{ij} classified in K groups according to the K levels of the factor are said to form one way classified data.

3.   RESULTS AND DISCUSSION

3.1 Yield and Irrigation Production Efficiency

In both 2003-2004 and 2004-2005 growing seasons, irrigation levels significantly influenced the marketable yield of potato (Table 2). In both years, the highest marketable yield (48.42 – 49.54 t/ha) was observed when irrigation during the crop-growing season was performed at 150% of pan evaporation replenishment. A further increase in the amount of irrigation resulted from 175% pan evaporation replenishment and did not increase the marketable yield of potato. The irrigation production efficiency (99.86 – 112.67 kg/m^3) was recorded at 25% of pan evaporation replenishment. Irrigation production efficiency decreased significantly with an increase in irrigation levels because the increase in marketable yield was less than the seasonal water applied. Irrigation at 200% of pan evaporation replenishment gave significantly minimum irrigation production efficiency (46.13–46.62 kg/m^3) because it increased the seasonal water application considerably but decreased the marketable yield (Table 1). Singh and Mohan (1994) reported a reduction in sugarcane yield when irrigation was applied beyond IW/CPE ratio of 1.0. Singh *et al.* (1997) observed that the reduction in plant growth and yield of Palma Rosa at higher irrigation levels resulted from IW/CPE ratios of 1.1 to 1.5.

3.2 Water Applied – Yield Relationship

The relationship between seasonal water applied and marketable yield of potato is shown in Fig. 1. The seasonal water applied for potato ranged from 32 to 255 mm, whereas marketable yield ranged from (32.96–49.50 t/ha). The seasonal water applied and marketable yield of potato (R^2=0.9830) exhibited strong quadratic relationship. The marketable yield of potato increased with an increase in seasonal water applied approximately up to 193 mm and thereafter yield tended to decline.

The results revealed that higher seasonal water application did not increase evapotranspiration as well as marketable yield but it increased deep percolation. The quadratic yield–water applied relationship probably resulted from nutrients leaching through deep percolation and poor aeration. Strong quadratic relationship between yield and seasonal irrigation regimes, soil and climatic conditions were reported by many researchers (Singh, 1987; Farah *et al.*, 1997; Howell *et al.*, 1997; Tiwari and Reddy, 1998).

3.3 Economic Return

The total cost of production for potato at different irrigation levels is presented in Table 3. The total cost of production (fixed and operating costs) in pan evaporation replenishment (irrigation levels), because the pumping cost (which includes diesel and oil) was insignificant as compared to other expenses. The labour cost to perform major farm activities represented 26.84% of the total expenditure. The fixed costs and costs for repair and maintenance contributed 38.02% and 2.85% to the total costs. The net return of potato increased sharply from 25% to 150% pan evaporation replenishment due to the sharp increase in marketable yield. The net return from 150 to 200% pan evaporation replenishment did not increase considerably because of the insignificant improvement in marketable yield. This was due to the fact that irrigation at 150% of pan evaporation replenishment resulted in optimum plant growth and development coupled with a significant improvement in irrigation production efficiency. The maximum net return of potato was found Rs. 70,197/ha. The benefit cost ratio (B/C) which indicates gross revenue per unit investment was influenced by irrigation levels. The irrigation at 150% of pan evaporation replenishment gave the maximum benefit cost ratio (1.80), because increase in gross return was higher as compared to total cost of production. Similar results were reported by some researchers under a wide variety of irrigation systems and regimes, soil crop and climatic conditions (Shrivastava *et al.*1994; Singh *et al.* 1997; Tiwari and Reddy 1998; Imtiyaz *et al.* 2000a).

3.4 Relationship Between Water Applied, Gross Return, Net Return and Benefit Cost Ratio

The relationship between seasonal water applied and gross return of potato is shown in Fig. 2. The seasonal water applied ranged from 32 to 255 mm whereas gross return ranged from Rs. 110080–156736/ha. The seasonal water applied and gross return of potato exhibited strong quadratic relationship (R^2 = 0.9867). The gross return increased with an increase in seasonal water applied approximately up to 212 mm and thereafter gross return tended to decline.

Table 1: Analysis of variance table for one way classification

Sources of variation	Degree of Freedom	Sum of squares	Mean square = $\dfrac{sum\,of\,square}{deg\,ree\,of\,freedom}$	F
Between level of the factors	k-1	$\sum \dfrac{T_i^2}{n_i} - \dfrac{G^2}{n}$	s_t^2	$\dfrac{st^2}{s^2}$
Within levels of the factors(Error)	n-k	**By subtraction**	s^2	
Total	n-1	$\sum y_{ij}^2 - \dfrac{G^2}{n}$		

n_i = numbers of observations, $n = \sum n_i$

k = levels

$\sum \dfrac{T_i^2}{n_i}$ = uncorrected treatment sum of squares

$\dfrac{G^2}{n}$ = Correction term, where G is the Grand total

$\sum y_{ij}^2$ = Corrected total sum of squares

s_t^2 = treatment mean square

s^2 = error mean square

Table 2: Effect of pan evaporation replenishment on marketable yield and irrigation production efficiency of potato

Treatment (pan evaporation replenishment,%)	Seasonal water applied, mm	Mean marketable yield (t/ha)		Mean irrigation production efficiency (kg/m^3)	
		2003	2004	2004	2005
25	32	35.84	32.96	112.67	99.86
50	64	39.67	38.19	63.36	59.67
75	95	42.68	39.54	44.73	41.62
100	127	44.01	46.67	34.59	36.74
125	159	46.71	47.41	29.37	29.81
150	191	48.42	49.54	25.37	25.93
175	223	47.32	48.62	21.25	21.80
200	255	46.13	46.62	18.13	18.51
C. D. (0.05)	-	1.03	2.714	0.86	2.57

The relationship between seasonal water applied and net return of potato is shown in Fig. 3. The seasonal water applied remains the same whereas the net return ranged from Rs. 25115 to 70197/ha. The seasonal water applied and net return of potato exhibited strong quadratic relationship (R^2 = 0.9910). The net return increased with an increase in seasonal water applied approximately up to 210 mm and thereafter net return tended to decline. The relationship between water applied and benefit cost ratio is shown in Fig. 4. The seasonal water applied remains the same whereas the benefit cost ratio ranged from 1.29 to 1.80. The seasonal water applied and benefit cost ratio of potato exhibited a strong quadratic relationship (R^2 = 0.986). The benefit cost ratio increased with an increase in seasonal water applied up to 167 mm and thereafter it tended to decline.

4. CONCLUSIONS

The experimental results from both years (2003 and 2004) showed that 150% of pan evaporation replenishment resulted in the highest marketable yield of potato. The irrigation at 25% evaporation replenishment produced higher irrigation production efficiency. Irrigation with 200% pan evaporation replenishment reduced the irrigation production efficiency because it increased the seasonal water application considerably without a significant improvement in marketable yield. The net return of potato increased sharply from 25% to 150% evaporation replenishment. In both years, seasonal water applied and marketable yield of potato exhibited strong quadratic relationship. Irrigation water production functions developed in the present investigations can be used for allocating water within and between the above-mentioned crop, comparing irrigation production efficiency and economic analysis.

Finally, the overall results clearly suggest that in order to obtain an optimum yield, irrigation production efficiency and net return of potato in the semi-arid climate of northern regions of Allahabad, crop during the winter season should be irrigated at 150% of pan evaporation replenishment. Furthermore, an irrigation management approach using pan evaporation data is simple and can be adopted easily by farmers. In spite of the high initial investment, drip irrigation for potato production in Allahabad is highly profitable. Clogging of the drippers is the main concern, but it can be minimized by using appropriate filters and flushing out the main, sub-main and lateral lines regularly.

ACKNOWLEDGEMENTS

REFERENCES

1. Farah, S. M., Salih, A. A., Taha, A. M., Ali, Z. I. and I. A. Ali (1997). Grains Sorghum response to supplementary irrigation under post-rainy season conditions. Agric Water Manage, 33: 31 – 41.

2. Fekadu, Y. and T. Teshome (1998). Effect of drip and furrow irrigation and plant spacing on yield of tomato at Dire Dawa, Ethiopia. Agric Water Manage 35: 201 – 207.

3. Hagan, R. M. and J. F. Laborde (1964). Plants as indicator of need for irrigation. Proceedings of the 8th Congress on Soil Science, Bucharest, Romania, Vol. 11: pp. 399-422.

4. Howell, T. A., Schneider, A. D. and S. R. Evett (1977). Subsurface and surface micro-irrigation of corn – Southern High Plains. Transactions of the ASAE, 40 (3): 635 – 641.

5. Imtiyaz, M., Mgadla, N. P., Chepete, B. and S. K. Manase (2000a). Marketable yield, water use efficiency and economic return of cabbage, carrot and onion as influenced by irrigation schedules. In: Proceedings of International Agricultural Engineering Conference, Asian Institute of Technology, Bangkok pp. 321 – 328.

6. Imtiyaz, M., Mgadla, N. P. and S. K. Manase (2000b). Response of six vegetable crops to irrigation schedules. Agric Water Management 45: 331– 342.

7. Imtiyaz, M., Mgadla, N. P. and S. K. Manase (2000c). Response of green mealies to water levels under sprinkler and drip irrigation. In : Proceedings of International Agricultural Engineering Conference, Asian Institute of Technology, Bangkok pp. 343 – 350.

8. Imtiyaz, M., Mgadla, N. P., Manase, S. K., Chendo, K., Mothobi, E. O. (2000d). Yield and economic return of vegetable crops under variable irrigation. Irrig. Sci. 19: pp. 87 – 93.
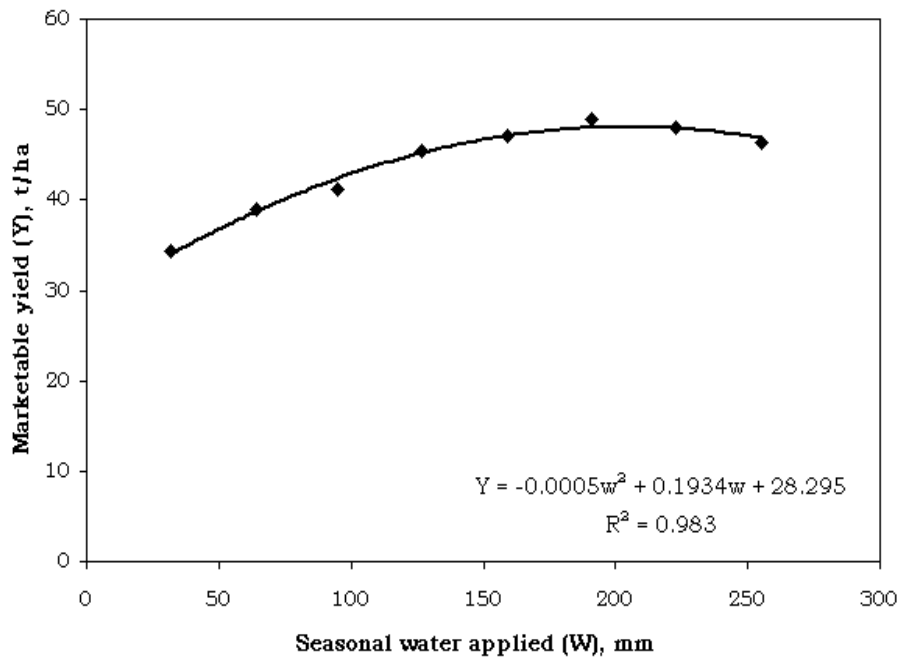
Fig. 1: Seasonal water applied vs. Marketable yield

Within the figure:
$$Y = -0.0005w^2 + 0.1934w + 28.295$$
$$R^2 = 0.983$$
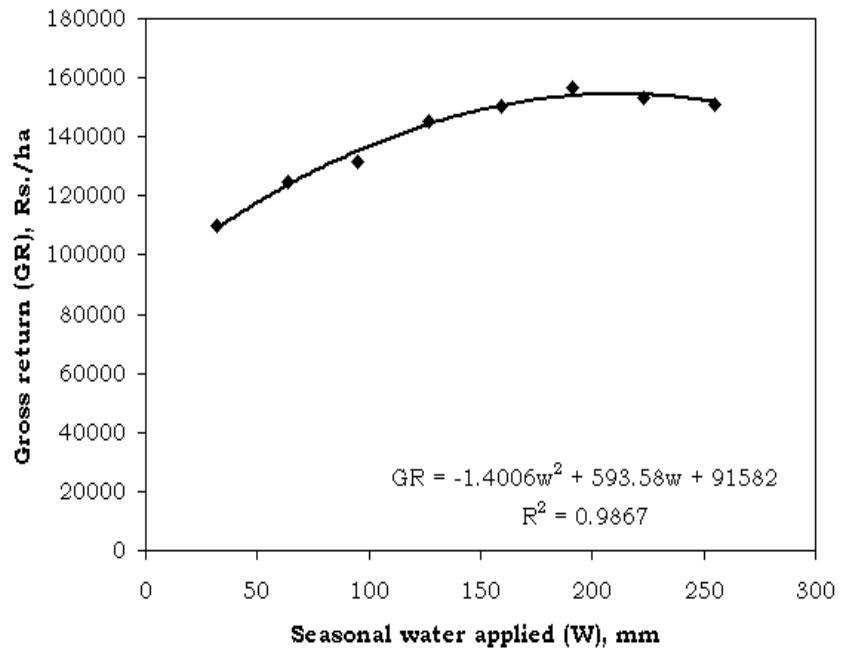
Fig. 2: Seasonal water applied vs. Gross Return

Within the figure:
$$GR = -1.4006w^2 + 593.58w + 91582$$
$$R^2 = 0.9867$$
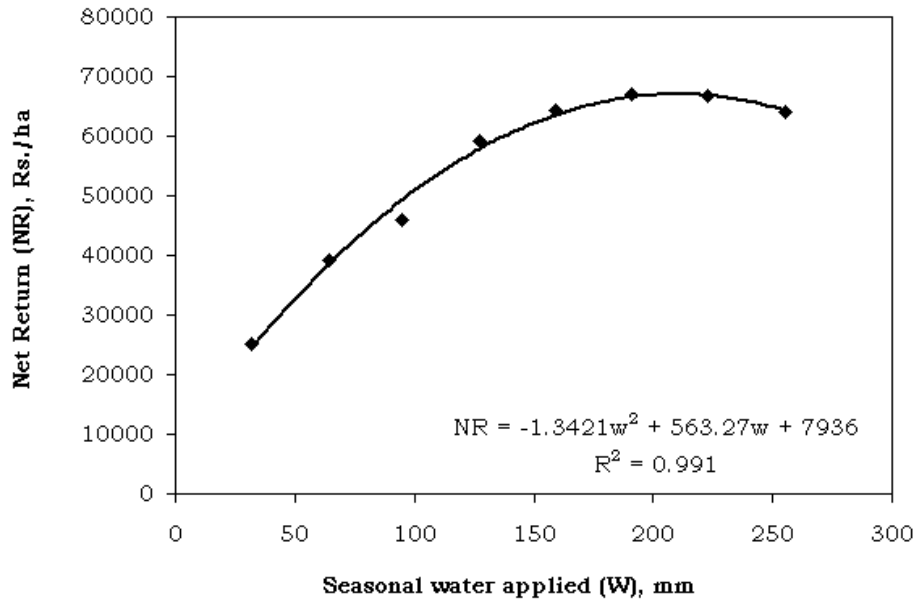
Fig. 3: Seasonal water applied vs. Net Return
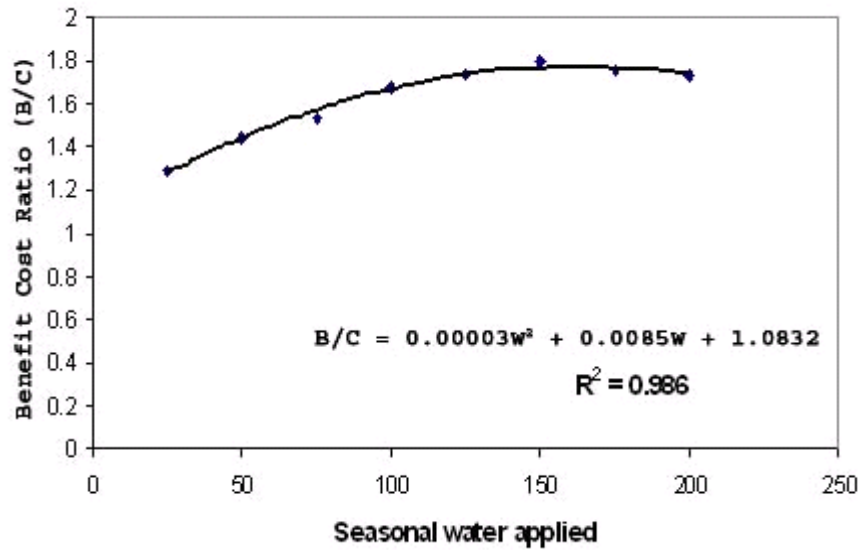
Fig. 4: Seasonal water applied vs. Benefit Cost Ratio

Table 3: Economic analysis of potato under different irrigation levels (average data for 2 years)

Treatment (pan evaporation replenishment,%)	Total cost of production, Rs./ha	Gross Return, Rs./ha	Net Return, Rs./ha	Benefit Cost ratio
25	84965	110080	25115	1.29
50	85279	124576	39297	1.45
75	85604	131552	45948	1.53
100	85909	145088	59179	1.68
125	86224	150592	64368	1.74
150	86539	156736	70197	1.80
175	86854	153504	66650	1.76
200	87169	151136	63967	1.73

Note: 1 US$ is approximately Rs. 41(INR)

9. James, L. D. and R. R. Lee (1971). Economic of water resources planning. McGraw Hill, New Delhi, p 20.
10. Jensen, M. E., Rob, D. C. N. and C. E. Franzoy (1970). Scheduling irrigation using climatic crop soil data. J. Irrig. Drain 96: 25 – 38.
11. Misra, R. D. and P. C. Pant (1981). Criteria for scheduling irrigation of wheat. Exp. Agric. 17: 157 – 162.
12. Shrivastava, P. K., Parikh, M. M., Swani, N. G. and S. Raman (1994). Effect of irrigation and mulching on tomato yield. Agric Water Manage 25: 179 – 184.
13. Singh, B. P. (1987). Effect of irrigation on the growth and yield of Okra. Hort Sci 22: 879 – 880.
14. Singh, P. N. and S. C. Mohan (1994). Water use and yield response of sugarcane under different irrigation schedules and nitrogen levels in a subtropical region. Agric Water Manage 26: 253 – 264.
15. Singh, S., Ram, M., Ram, D., Sharma, S. and D. V. Singh (1997). Water requirement and productivity of palmarosa on sandy loam soil under subtropical climate. Agric Water Manage 35: 1 – 10
16. Theodore, W. S. (1980). Comparison of Sprinkler, trickle, subsurface and furrow irrigation methods for row crops. Agron. J. 72: 701 – 704.
17. Wanjura, D. F., Upehurch, D. R. and J. R. Mahan (1990). Evaluating decision criteria for irrigation scheduling in cotton. Trans ASAE 33: 512 – 518.
18. Tiwari, K. N. and K. Y. Reddy (1998). Economic analysis of trickle irrigation system considering planting geometry. Agric. Water Management. 34: pp. 195 – 206.

EFFECTS OF MOISTURE CONTENT ON SOME ENGINEERING PROPERTIES OF TWO VARIETIES OF SAFFLOWER SEED

Mahdi Kashaninejad[*] and Maryam E. Rezagah[*]

ABSTRACT

The physical and engineering properties of bulk materials such as safflower are important to design the equipment for processing, transportation, sorting, separation and storing. In this study some engineering and physical properties of two varieties of safflower seed including principal dimensions, sphericity, geometric mean diameter, kernel volume, unit mass, bulk density, true density, porosity, terminal velocity and coefficient of static friction against different surfaces were evaluated as a function of moisture content in the range of 7 to 30% (w.b.). The results showed that all the physical properties of safflower seed to be dependent on their moisture content. An increasing relationship was found between principal dimensions, geometric mean diameter, unit mass, true density, porosity and moisture content in safflower seed while bulk density decreased with increase in moisture content. Terminal velocity and the coefficient of static friction increased linearly against all the tested surfaces as the moisture content increased. Individual volume and angle of repose for filling and emptying increased linearly with increasing of moisture content for both varieties.

Keywords: *Angle of repose; Density; Dimensions; Porosity; Safflower; Static coefficient of friction; Terminal velocity. © 2007 AAAE*

1. INTRODUCTION

Safflower (*Carthamus tinctorius* L.) is a thistle-like annual plant mainly grown in dry hot climates as an oilseed or birdseed. It has many red, orange or yellow flowers on bushy plants. Flower heads are on the ends of stiff branches, with 15 to 30 seeds developing within each head. The seed is about the size of plump barley, either white or brownish and white with grey, brown or black stripes. The crop is seeded and harvested with the same equipment as is used for cereal grains. Safflower was originally grown in the Middle East and south Asia for the red/orange pigment in the flower petals which was used for colouring rice and bread, and dyeing cloth. After synthetic aniline dyes took over this market in the 1800's the crop was grown as an oilseed (Weiss, 1971).

Today this crop supplies oil, meal, birdseed and foots (residue from oil processing) for the food and industrial products markets, although this crop is now primarily grown for the oil. There are two types of safflower varieties, the type that produces oil which is high in monounsaturated fatty acids (oleic acid), and those with high concentrations of polyunsaturated fatty acids (linoleic acid) (Weiss, 1983).

The meal that remains after oil extraction is used as a protein supplement for livestock. The meal usually contains about 24% protein and much fiber. Decorticated meal (most of hulls removed) has about 40% protein with a reduced fiber content. Foots are used to manufacture soap. The birdseed industry buys a small portion of the seed production. Sheep and cattle can graze succulent safflower and stubble fields after harvest (Giayetto *et al.*, 1999; Mohseni *et al.*, 2006).

Currently, the estimated world production is about 680 thousand tonnes of safflower seed from an area of 899 thousand ha land (FAOSTAT, 2005). Although Iran has a small share in the world production of safflower seed (about 500 tonnes), areas under safflower seed cultivation have lately increased in recent years because oilseed crops are in extensive demand in Iran to meet the lack of the country's oil.

There has been much effort and progress in developing the measurement techniques and accumulating data on physical properties of biological and agro food materials for the last three decades

[*] Department of Food Science & Technology, Gorgan University of Agricultural Sciences and Natural Resources, Gorgan, Iran, Corresponding author E-mail: kashaninejad@yahoo.com, kashani@gau.ac.ir.

(Sessiz *et al.*, 2007). The major moisture-dependent physical properties of biological materials are shape and size, bulk density, true density, porosity, mass, friction against various surfaces, terminal velocity and angle of repose (Mohsenin, 1980). These properties have been studied for various crops such as terebinth fruits (Aydin and Ozcan, 2002), pigeon pea (Baryeh and Mangope, 2002), rapeseed (Çalışır *et al.*, 2005), lentil (Scanlon *et al.*, 2005), caper seed (Dursun and Dursun, 2005), green soybean (Sirisomboon *et al.*, 2007), pistachio nut (Kashaninejad *et al.*, 2006), rice (Corrêa *et al.*, 2007), peanut (Aydin, 2007), pomegranate seeds (Kingsly *et al.*, 2006) and sorghum (Mwithiga and Sifuna, 2006).

Although some selected mechanical and compression properties of safflower seed have been reported by Baümler *et al.* (2006), the most important physical properties of safflower seed such as coefficient of static friction against various surfaces, terminal velocity and angle of repose have never been reported. This information is valuable not only to engineers but also to food scientists, processors and breeders.

Size, shape and physical dimensions of safflower seed are important in sizing, sorting, sieving and other separation processes. Densities of safflower seed are necessary to design the equipment for processing and storing such as hullers, dryers and bins. The porosity affects the resistance to airflow through bulk safflower seed. Terminal velocity is very critical in the design of a pneumatic conveyor, transporting safflower seed using air and separating the safflower seed from undesirable materials. The terminal velocity is affected by the density, shape, size and moisture content of samples. During the harvesting, handling, processing and storage of safflower seed, the product exerts frictional forces on machinery components or storage structures. The magnitude of these frictional forces affects the amount of power required to convey the material. Static friction between the safflower seed and conveyor belt affects the maximum angle with the horizontal which the conveyor can assume when transporting safflower seed. The angle of repose for emptying can be used to calculate the quantity of safflower seed that will remain in a bin with a flat bottom when the bin is emptied through an outlet in the floor. The angle of repose for filling can be used to estimate the amount of material that can be placed in piles or in a storage structure with flat floors (Mohsenin, 1980; Rameshbabu *et al.*, 1996; White

and Jayas, 2001). Therefore, the objective of this study was to determine some physical properties of two varieties of safflower seeds, IL111 (Iran Local) and LRV5151 (Long Rosette Varamin), as a function of moisture content in the range of 7 to 30% (w.b.). In this research, dimensions, geometric mean diameter, sphericity, unit mass, kernel volume, true density, bulk density, porosity, static coefficient of friction against various surfaces, filling and emptying angles of repose and terminal velocity for two varieties of safflower seeds were investigated at 5 levels of moisture content.

2. MATERIALS AND METHODS

2.1 Sample Preparation

The safflower seeds used in this research (IL111 and LRV5151 varieties) were prepared from the Seed and Plant Breeding Institute of Ministry of Agriculture in Karaj, Iran. These are the most important varieties that are cultivated in Iran and their chemical composition and fatty acid distribution are represented in Tables 1 and 2 (Omidi, 2005). These varieties produce oil with a high concentration of polyunsaturated fatty acids (linoleic acid) which is primarily used for edible oil products such as salad oils and soft margarines. The seeds were manually cleaned to remove all foreign materials and broken

Table 1: Average composition (%) of safflower seed varieties

Composition	Variety	
	IL111	LRV5151
Moisture	8	7
Oil	32	31
Protein	15	14
Ash	1.5	1.6
Fiber	34	32

Table 2: Average fatty acid composition (%) of safflower oil

Fatty acid	Variety	
	IL111	LRV5151
Palmitic acid	6.2	7.6
Stearic acid	1.8	1.4
Oleic acid	7.6	6.1
Linoleic acid	78.4	74.9
Linolenic acid	1.0	0.9
Arachidic acid	1.2	1.5

seeds. The initial moisture content of the seeds was determined by using standard methods. Some samples were placed in an air convection oven drying at 103 ± 2 °C for 72 h. The samples were then cooled in a desiccator, weighed and when a constant weight was reached the moisture content of the seeds was calculated (USDA, 1970). In order to obtain samples with higher moisture content, a calculated quantity of distilled water was added to the sample.

The sample was then sealed and kept at 5°C in a refrigerator for at least one week to enable the moisture to distribute uniformly throughout the product. It is necessary to let the samples warm up to room temperature before starting each test (Kashaninejad *et al.*, 2006). All the physical properties of the seeds were measured at five moisture contents in the range of 7-30% (w.b.) for two varieties.

2.2 Dimensions, Sphericity and Unit Mass

In order to determine dimensions, sphericity and unit mass, one hundred safflower seeds were randomly selected and for each, the three principal dimensions, namely minor diameter (thickness), intermediate diameter (width) and major diameter (length), were measured using an electronic digital caliper (GUANGLU) having at least count of 0.01 mm at each moisture level. Fig. 1 illustrates the principal dimensions of the safflower seed.

To obtain the unit mass, each seed was weighed on a precision electronic balance (Sartorius, TE313S,
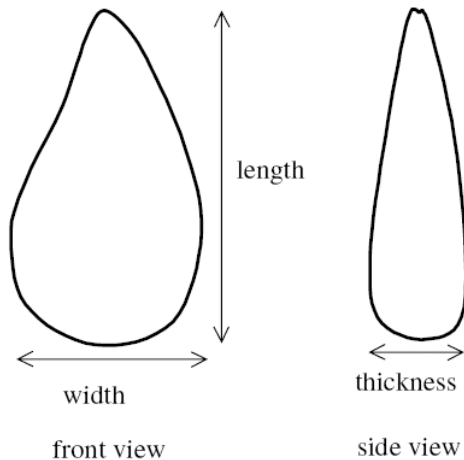
Canada) reading to 0.001 g. Geometric mean diameter and degree of sphericity of safflower seeds were calculated at each moisture level by the following equations (Mohsenin, 1980):

$$D = (LWT)^{1/3} \tag{1}$$

$$\phi = \frac{(LWT)^{1/3}}{L} \times 100 \tag{2}$$

2.3 Volume, Bulk Density, True Density and Porosity

Bulk density was calculated from the mass and volume of the circular container with known volume that was filled with the safflower seed. After filling the circular container, excess seeds were removed by passing a stick across the top surface using five zigzag motions. The samples were not compacted in any way (Kashaninejad et al., 2006).

The true density, defined as the ratio of the mass of the seed to the true volume occupied by the sample, was determined using an electronic balance reading to 0.001 g and a pycnometer (Baümler et al., 2006). Safflower seed volume was determined using the liquid displacement method. Toluene (C7H8) was used instead of water because it is absorbed by seeds to a less extent and because of its low surface tension it can fill even shallow deeps in a seed (Mohsenin, 1980).

The porosity (ε) of the bulk is the ratio of spaces in the bulk to its bulk volume and was determined by the following equation (Mohsenin, 1980):

$$\varepsilon = \frac{\rho_t - \rho_b}{\rho_t} \times 100 \tag{3}$$

2.4 Coefficient of Static Friction

Coefficient of static friction for safflower seeds was determined against surfaces of galvanized iron, plywood, concrete, fiberglass and rubber at different moisture content. A wooden box of 100 mm length, 100 mm width and 40 mm height without base and lid was filled with the sample and placed on an adjustable tilting plate, faced with the test surface. The sample container was raised slightly (5–10 mm) so as not to touch the surface. The inclination of the test surface was increased gradually with a screw device until the box just started to slide down and the angle of tilt (α)

Fig. 1: Characteristic dimensions of safflower seed from different views.

was read from a graduated scale. For each replication, the sample in the container was emptied and refilled with a new sample (Joshi *et al.*, 1993; Olajide *et al.*, 2000, Kashaninejad *et al.*, 2006). The coefficient of static friction was calculated from the following relationship:

$$\mu = tg\alpha \tag{4}$$

2.5 Angle of Repose

In general, the angle of repose in situations where the material is being emptied from a bin called the angle of repose for emptying (θ_e) (Mohsenin, 1980). In order to obtain this angle, samples were filled in a 15×15×15 cm handmade wooden box with a slide side door. After quickly opening the door, the angle of the shaped bulk was calculated by measuring the height of seeds (h) using the following equation:

$$\theta_e = \tan^{-1}\left(\frac{h}{a}\right) \tag{5}$$

Where a was 15 cm in this work.

To obtain the angle of repose for filling (θ_f) samples were poured from 15 cm height on a wooden horizontal surface. The height of seed pile above the floor (H) and the diameter of the heap (D) was measured and used to determine the angle of response for filling with the following relationship:

$$\theta_f = \tan^{-1}\left(\frac{2H}{D}\right) \tag{6}$$

2.6 Terminal Velocity Measurement

The terminal velocities of safflower seed varieties (IL111 and LRV5151) at different moisture content were measured using an air column. For each test, a sample of each variety was dropped from the top of a 100 mm diameter, 2 m long glass tube. The air flowed upwards in the tube from bottom to the top and the air velocity at which the sample suspended was recorded by a hot wire anemometer having at least 0.01 m/s sensitivity. Ten replications were taken for each moisture content level (Joshi, *et al.*, 1993; Aydin and

Ozcan, 2002; Gezer *et al.*, 2002; Kashaninejad *et al.*, 2006).

2.7 Data Analysis

All experiments were replicated five times, unless stated otherwise, and the average values are reported. Mean, maximum, minimum, standard deviation and correlation coefficient of dimensions and unit mass of safflower seed were determined using Microsoft excel (2003) software program. The effect of moisture content on different physical properties of safflower seed were determined using the analysis of variance (ANOVA) method and significant differences of means were compared using the Duncan's test at 1% significant level using SAS software (2001) program. The best relationship between moisture content and physical properties of safflower seed were determined using linear and non linear (NLIN procedure) regression analysis of SAS software (2001) program. The best model was chosen as the one with the highest coefficient of determination and the least residual mean square and the mean relative percent error.

3. RESULTS AND DISCUSSION

3.1 Dimensions and Unit Mass

Table 3 shows the dimensions and unit mass of two safflower varieties at different moisture contents in the range of 7 to 30% (w.b.). Increasing moisture content had significant effect on dimensions and unit mass of safflower varieties (P<0.0001). Table 3 shows these significant differences were observed among measured parameters with increase in moisture content and the increasing of moisture content caused an increase in safflower seed size. Dimensions (length, width and thickness) of both varieties increased linearly with moisture content. The reason for this increase was probably due to water absorption by hull and hydration of starch in the seeds. Similar results were found by Deshpande *et al.* (1993) for soybean, Gezer *et al.* (2002) for apricot pits and kernel and Carman (1996) for lentil seeds. The effect of variety on dimensions and unit mass of safflower seed was highly significant (P<0.0001) and as observed in Table 3 the values for length, width, thickness and unit mass of the IL111 variety are higher than values of LRV5151 variety. Frequency distribution of seed dimensions for variety IL111 is given in Fig. 2 at the

Table 3: Dimensional properties and unit mass of safflower seed varieties

Variety	Moisture content (w.b.)	Length (mm)	Width (mm)	Thickness (mm)	Mass (g)
IL111	6.94	7.42±0.32 bc	4.35±0.20 cd	3.57±0.13 cd	0.047±0.007 ef
	11.71	7.52±0.07 b	4.47±0.05 c	3.67±0.05 c	0.054±0.002 d
	18.97	7.61±0.10 ab	4.79±0.05 b	3.83±0.03 b	0.063±0.003 c
	23.23	7.80±0.18 a	4.99±0.11 a	3.98±0.10 a	0.067±0.003 b
	28.77	7.81±0.10 a	5.03±0.13 a	4.02±0.11 a	0.077±0.006 a
LRV5151	7.05	7.10±0.37 d	4.02±0.13 g	3.37±0.10 f	0.033±0.003 h
	13.92	7.20±0.08 cd	4.07±0.05 fg	3.35±0.06 f	0.038±0.001 g
	17.18	7.35±0.15 bcd	4.17±0.11 ef	3.44±0.07 ef	0.041±0.003 g
	22.17	7.53±0.09 b	4.26±0.06 de	3.54±0.05 de	0.046±0.001 f
	29.28	7.54±0.09 b	4.29±0.05 de	3.57±0.04 cd	0.051±0.002 de

Superscript letters indicate that means with the same letters designation in a column are not significantly different at P=0.01.

moisture content of 6.94% (w.b.). Eighty four percent of safflower seeds have a mass ranging from 0.05 to 0.08 g, 85% of safflower seeds have a length from 7.20 to 9.00 mm, 88% of safflower seeds have a width from 3.7 to 5.10 mm and 92% of safflower seeds have a thickness from 3.30 to 4.05 mm at a moisture content of 6.94% (w.b.). The relationship between length, width, thickness, unit mass and moisture content of safflower seed for IL111 variety were given by following equations:

$$L= 1.74 \ W= 2.23 \ T= 126.48 \ M \quad (7)$$

$$L= 0.0189 \ M_c +7.2909, \ (R^2 = 0.942) \quad (8)$$

$$W= 0.0342 \ M_c + 4.1145, \ (R^2 = 0.962) \quad (9)$$

$$T= 0.0222 \ M_c + 3.4172, \ (R^2 = 0.979) \quad (10)$$

$$M= 0.0014 \ M_c + 0.0375, \ (R^2 = 0.996) \quad (11)$$

Fig. 3. shows the frequency distribution of seed dimensions for variety LRV5151 at the moisture content of 7.05% (w.b.). Eighty nine percent of safflower seeds have a mass ranging from 0.035 to 0.055g, 90% of safflower seeds have a length from 7.50 to 8.40 mm, 87% of safflower seeds have a width from 4.0 to 4.80 mm and 89% of safflower seeds have a thickness from 3.20 to 3.80 mm at a moisture content of 7.05% (w.b.). The relationship between length, width, thickness, unit mass and moisture content can be represented by the following regression equations for LRV5151 variety:

$$L= 1.86 \ W= 2.28 \ T= 184.71 \ M \quad (12)$$

$$L= 0.0221 \ M_c +6.9473, \ (R^2 = 0.898) \quad (13)$$

$$W= 0.0133 \ M_c + 3.9255, \ (R^2 = 0.918) \quad (14)$$

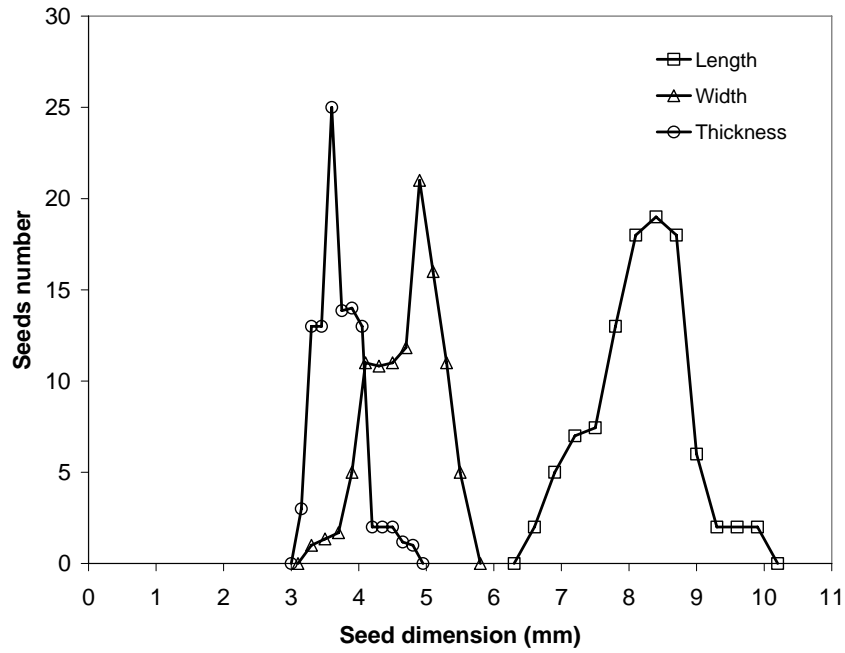$$T= 0.0106 \ M_c + 3.2639, \ (R^2 = 0.833) \quad (15)$$

Fig. 2: Frequency distribution curves for safflower seed (IL111 variety) dimensions at 6.94% moisture content (w.b.).
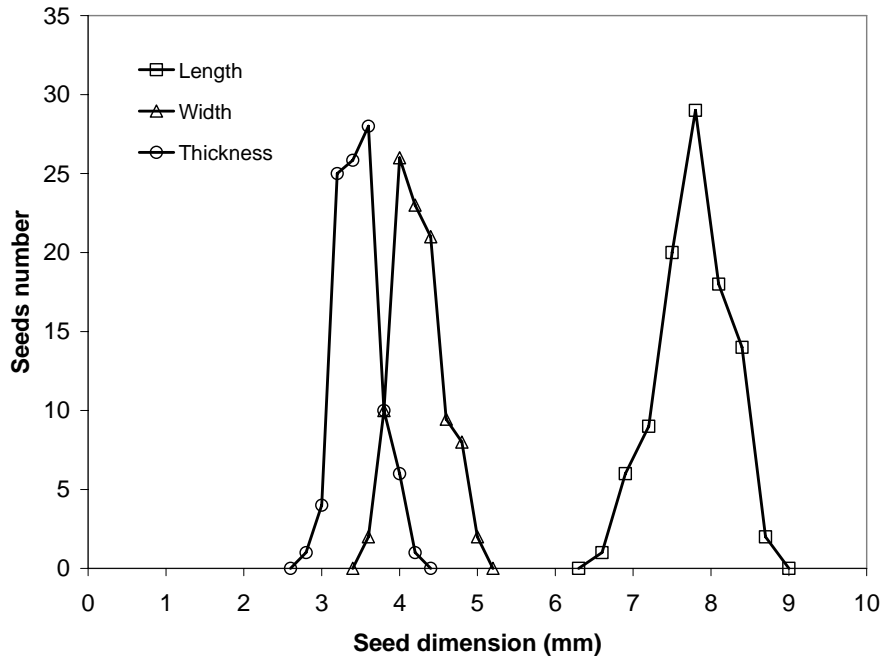
Fig. 3: Frequency distribution curves for safflower seed (LRV5151 variety) dimensions at 7.05% moisture content (w.b.).

$$M = 0.0008\,M_c + 0.0272, \quad (R^2 = 0.995) \tag{16}$$

Table 4 shows the relationship and correlation coefficients between safflower seeds. The correlation coefficients show that all ratios are significant at 1% level but L/M ratio is more significant than L/W and L/T ratios for safflower seeds (due to higher correlation coefficients). It indicates that the mass shows more association with the length of seeds than width and thickness. Similar relationships were reported for pistachio nut and its kernel (Kashaninejad *et al.*, 2006), lentil seeds (Carman, 1996), sunflower seeds (Gupta and Das, 1997) and pumpkin seeds (Joshi *et al.*, 1993).

3.2 Geometric Mean Diameter and Sphericity

Table 5 shows the sphericity and geometric mean diameter of safflower seeds at different moisture contents. This table indicates that the sphericity and geometric mean diameters of both varieties increased with increasing moisture content. Analysis of data shows significant differences were observed among sphericity and geometric mean diameter with increase in moisture content (P<0.0001). The sphericity of the safflower seed increased from 65.61 to 69.16% and 64.07 to 64.63% for IL111 and LRV5151 varieties respectively when the moisture content increased. It was observed that sphericity of IL111 variety is affected by moisture content more than LRV5151 variety. Geometric mean diameter of safflower seeds was higher than those reported for pigeon pea (Shepherd and Bhardwaj, 1986), muskmelon and longmelon seed (Ramakrishana, 1986) and was found close to sunflower seeds (Gupta and Das, 1997), soybean (Deshpande *et al.*, 1993) and watermelon seeds (Ramakrishana, 1986). However, it was considerably lower than those reported for oilbean (Oje and Ugbore, 1991) and pumpkin seed (Joshi *et al.*, 1993). Sphericity of safflower seed was much lower than those reported for soybean (Deshpande *et al.*, 1993), pigeon pea (Shepherd and Bhardwaj, 1986), pistachio nut and its kernel (Kashaninejad *et al.*, 2006) but higher than sunflower seed (Gupta and Das, 1997). The relationship between sphericity and moisture content as well as geometric mean diameter

and moisture content was found to be the following for IL111 and LRV5151 varieties, respectively:

$$\phi = 0.1798\,M_c + 64.349, \quad (R^2 = 0.955) \tag{17}$$

$$\phi = 0.0273\,M_c + 63.874, \quad (R^2 = 0.904) \tag{18}$$

$$D = 0.0268\,M_c + 4.676, \quad (R^2 = 0.970) \tag{19}$$

$$D = 0.0145\,M_c + 4.465, \quad (R^2 = 0.897) \tag{20}$$

3.3 Bulk Density

The experimental results of the bulk density for safflower seed at different moisture levels are presented in Fig. 4. Increasing moisture content had a significant effect (P<0.0001) on bulk density of safflower seed by lowering it. IL111 variety represented higher bulk density values than the LRV5151 variety with significant differences (P<0.0001) at all moisture content levels. The bulk density of LRV5151 and IL111 varieties decreased from 587.90 to 536.00 and from 595.11 to 556.15 kg/m^3 respectively as the moisture content increased from 7 to 30%. The decrease in bulk density of both safflower seed varieties with increase in moisture content indicates that the increase in mass owing to moisture gain in the sample is less than the accompanying volumetric expansion of the bulk. Deshpande *et al.* (1993) for soybean, Carman (1996) for lentil seed, Gupta and Das (1997) for sunflower seed and Konak *et al.* (2002) for chick pea also observed the negative linear relationship of bulk density with moisture content. Baümler *et al.* (2006) reported the lower values for bulk density of safflower seeds than values obtained in this study. They also reported that the bulk density of the safflower seeds decreased from 450 to 427 kg/m^3 with increase in moisture content. The following equations were obtained to show the relationship between moisture content and bulk density of IL111 and LRV5151 varieties, respectively:

$$\rho_b = 607.69 - 1.7915\,M_{c,,} \quad (R^2 = 0.994) \tag{21}$$

$$\rho_b = 605.08 - 2.3756\,M_c, \quad (R^2 = 0.908) \tag{22}$$

Table 4: Safflower seed varieties dimensions ratio at initial moisture content (w.b.)

Variety	Particulars	Mean value	Standard deviation	Degree of freedom	Correlation coefficient (r)
IL111 (6.94% w.b.)	L/W	1.74	0.149	98	0.62[a]
	L/T	2.23	0.212	98	0.70[a]
	L/M	126.48	32.644	98	0.93[a]
LRV5151 (7.05% w.b.)	L/W	1.86	0.145	98	0.70[a]
	L/T	2.28	0.187	98	0.66[a]
	L/M	184.71	31.012	98	0.92[a]

[a] significant at 1% level.

Table 5: Sphericity and geometric mean diameter of safflower seed varieties

Variety	Moisture content (w.b.)	Sphericity (%)	Geometric mean diameter (mm)
IL111	6.94	65.62±0.58 [c]	4.87±0.18 [cd]
	11.71	66.18±0.22 [c]	4.98±0.06 [c]
	18.97	68.19±0.34 [b]	5.19±0.05 [b]
	23.23	68.89±0.51 [ab]	5.37±0.12 [a]
	28.77	69.24±0.66 [a]	5.41±0.12 [a]
LRV5151	7.05	64.11±0.48 [d]	4.58±0.09 [g]
	13.92	64.05±0.44 [d]	4.61±0.05 [fg]
	17.18	64.32±1.23 [d]	4.72±0.09 [ef]
	22.17	64.28±0.38 [d]	4.84±0.04 [de]
	29.28	64.58±0.43 [d]	4.87±0.04 [cd]

Superscript letters indicate that means with the same letters designation in a column are not significantly different at P=0.01.

3.4 True Density and Kernel Volume

Fig. 5 shows kernel volume changes of safflower seeds at different moisture contents. Increasing moisture content had a significant effect on true density and kernel volume of safflower varieties (P<0.0001). The kernel volume of both varieties of safflower seed was observed to increase linearly from 0.053 to 0.069 and 0.036 to 0.050 cm³ for IL111 and LRV5151 respectively when the moisture content

increased from 7 to 30% (w.b.). The volume increase of safflower seeds during increasing moisture content may be related to water absorption of hull and kernel components. It should be noted that the hull has a tremendous potential for absorbing moisture. The kernel volume of IL111 variety was higher than that of LRV5151 variety at all moisture contents (P<0.0001). The following equations are obtained to show the relationship between moisture content and
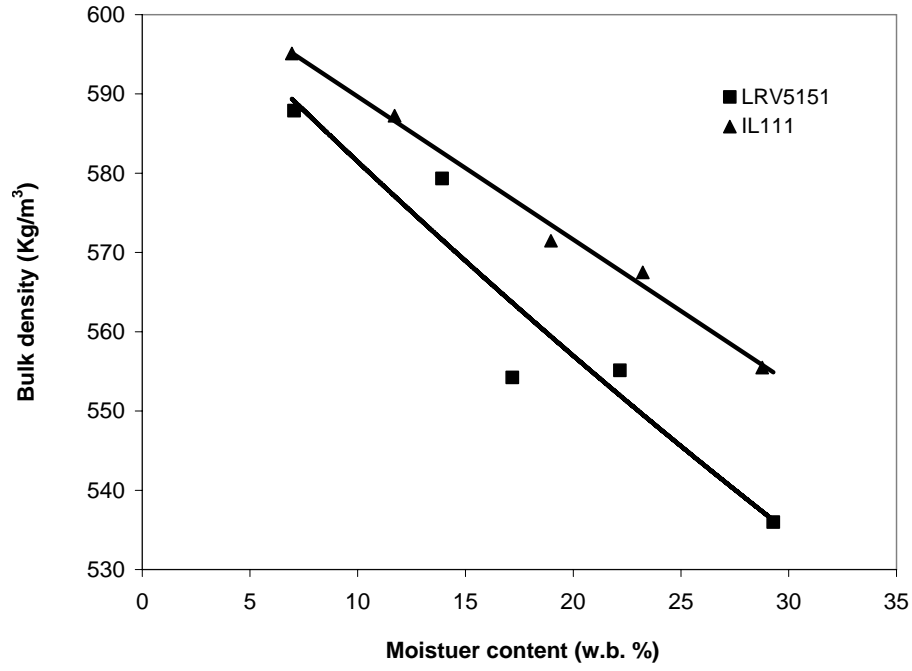
Fig. 4: Effect of moisture content on bulk density of safflower seed.
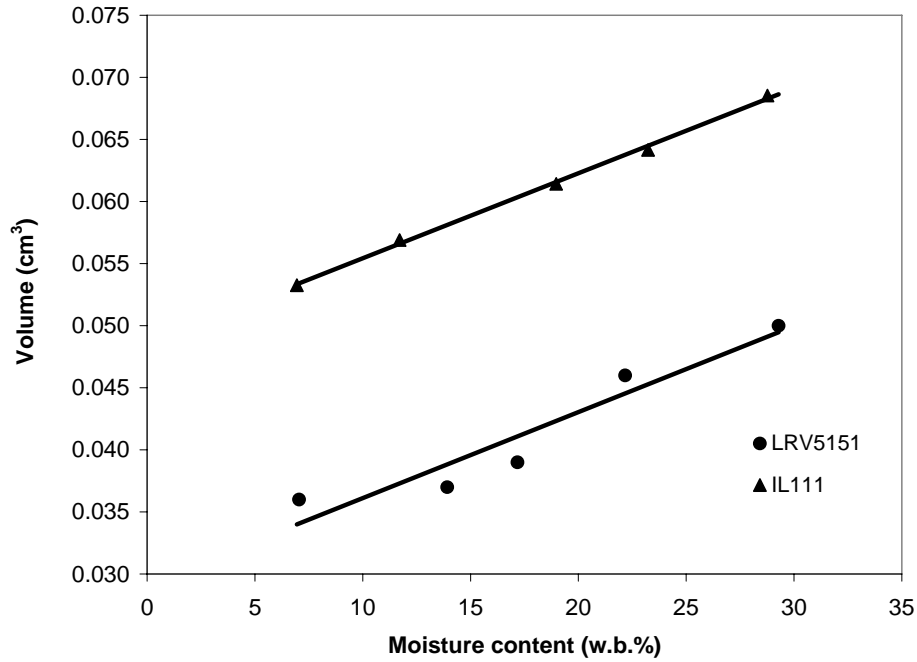

Fig. 5: Effect of moisture content on volume of safflower seed.

kernel volume of IL111 and LRV5151 varieties, respectively:

$$V = 0.0007M_c + 0.0483 , (R^2 = 0.992) \qquad (23)$$
$$V = 0.0007M_c + 0.0292 , (R^2 = 0.907) \qquad (24)$$

The variation of true density with moisture content for both varieties of safflower seed is shown in Fig. 6. True density of safflower seeds at different moisture levels varied from 975.31 to 1199.60 and 916.67 to 1016.80 kg/m^3 for IL111 and LRV5151 respectively. Although variation of true density with moisture content for IL111 variety was linear, the LRV5151 variety showed quadratic trend. In the IL111 variety the increasing trend of the true density of safflower seed may be attributed to the higher moisture gain of the seeds as compared with their volumetric expansion. The increase in true density of LRV5151 variety from initial moisture content to 23% (w.b.) indicates that kernel volume increasing is lower than mass increasing up to this moisture content. The trend reverses when the seed is moistened to higher moisture contents. These discrepancies between two varieties could be due to the cell structure and the volume and mass increase characteristics of the samples, as the moisture content of seeds increases. These changes are related to structural properties of the seeds.

The relationship existing between moisture content and true density (ρ_t) appears linear for IL111 but non-linear for LRV5151 which can be represented by the following equations:

$$\rho_t = 10.602M_c + 874.98 , (R^2 = 0.943) \qquad (25)$$

$$\rho_t = -0.7716M_c^2 + 32.417M_c + 728.46 ,$$
$$(R^2 = 0.991) \qquad (26)$$

An increase in true density with an increase in moisture content was reported for cumin seeds (Singh and Goswami, 1996), sunflower (Gupta and Das, 1997), pigeon pea (Baryeh and Mangope, 2002), pistachio nut and its kernel (Kashaninejad et al., 2006). However, Deshpande et al. (1993), Ozarslan (2002) and Konak et al. (2002) have found that the true density of soybean, cotton seed and chickpea respectively decreases as the moisture content increases.

3.5 Porosity

Since the porosity depends on the bulk as well as true densities, the magnitude of variation in porosity depends on these factors only. The values of porosity were calculated using the data on bulk and true densities of the safflower seed and the results are presented in Fig. 7. It increased from 38.98 to 50.65% and from 35.87 to 47.29% for IL111 and LRV5151 varieties respectively when the moisture content changed from 7 to 30% (w.b.). The relationship between moisture content and porosity appears linear for IL111 but quadratic for LRV5151. This difference between the two varieties could be due to the cell structure and volume and mass increase characteristics of the samples, as the moisture content of seeds increases. A similar trend was reported for sunflower seed (Gupta and Das, 1997), lentil seed (Carman, 1996) and pigeon pea (Baryeh and Mangope, 2002), but different to that reported for pistachio nut and its kernel (Kashaninejad et al., 2006), soybean (Deshpande et al., 1993) and pumpkin seed (Joshi et al., 1993). The relationship existing between moisture content and porosity appears linear for IL111 variety and quadratic for LRV5151 variety which can be represented by the following regression equations:

$$\varepsilon = 0.5927M_c + 34.303, (R^2 = 0.967) \qquad (27)$$

$$\varepsilon = -0.0463M_c^2 + 2.1859M_c + 22.831,$$
$$(R^2 = 0.994) \qquad (28)$$

3.6 Static Coefficient of Friction

Table 6 shows the static coefficient of friction for IL111 and LRV5151 varieties determined with respect to galvanized iron, plywood, fiberglass, concrete and rubber surfaces at different moisture contents. At all moisture contents, the static coefficient of friction was the highest for both varieties on rubber and the least for plywood. It was observed that the static coefficient of friction for safflower seeds increased linearly with increasing of moisture content on all surfaces and effect of moisture content on static coefficient of friction was highly significant (P<0.0001). The relationships between these coefficients against various surfaces and moisture contents of safflower seed varieties are shown in Table 7. It was observed that the moisture content had a more significant effect
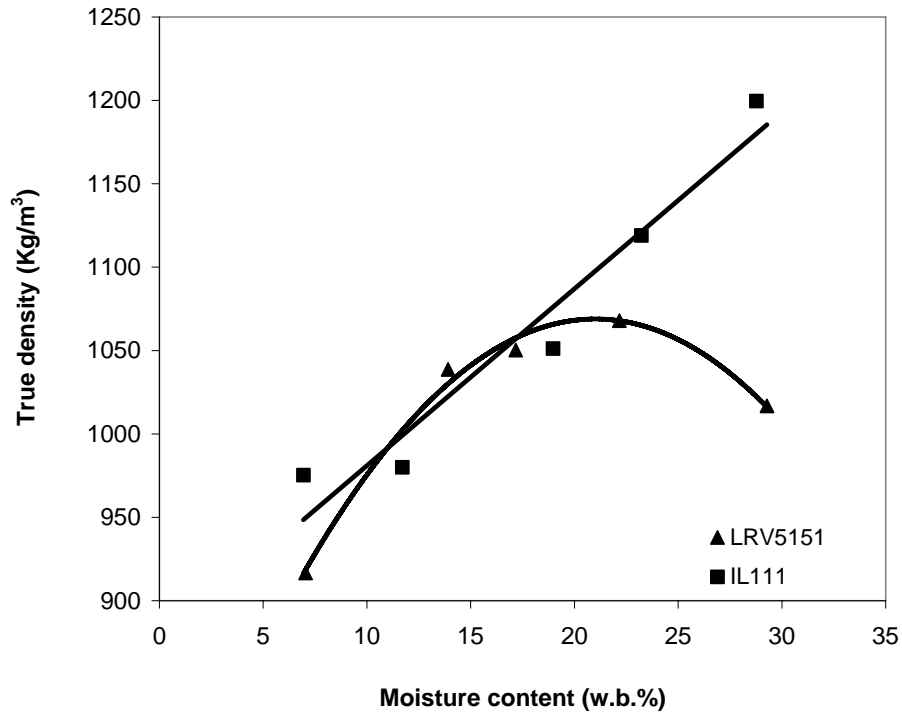
Fig. 6: Effect of moisture content on true density of safflower seed.
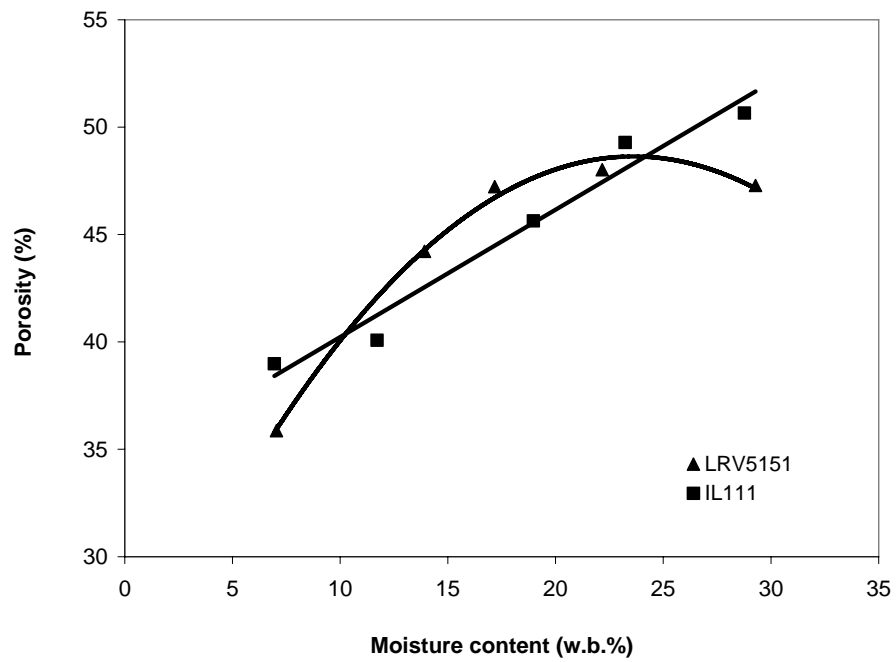
Fig. 7: Effect of moisture content on porosity of safflower seed.

Table 6: Static coefficient of friction of safflower seed varieties at different moisture contents

Variety	Moisture content (w.b.)	Galvanized iron	Plywood	Fiberglass	Concrete	Rubber
IL111	6.94	0.29±0.013 [e]	0.23±0.014 [f]	0.29±0.022 [d]	0.31±0.001 [e]	0.37±0.018 [d]
	11.71	0.30±0.009 [e]	0.23±0.009 [f]	0.30±0.013 [d]	0.32±0.001 [e]	0.37±0.009 [d]
	18.97	0.34±0.027 [d]	0.29±0.009 [d]	0.38±0.009 [c]	0.35±0.011 [d]	0.39±0.013 [cd]
	23.23	0.39±0.018 [bc]	0.35±0.018 [c]	0.44±0.034 [ab]	0.39±0.011 [c]	0.43±0.037 [abc]
	28.77	0.45±0.018 [a]	0.42±0.018 [a]	0.43±0.016 [b]	0.41±0.011 [b]	0.45±0.036 [a]
LRV5151	7.05	0.33±0.026 [d]	0.25±0.017 [f]	0.29±0.029 [d]	0.32±0.009 [e]	0.38±0.024 [d]
	13.92	0.38±0.017 [c]	0.27±0.009 [e]	0.36±0.009 [c]	0.35±0.009 [d]	0.40±0.040 [bcd]
	17.18	0.41±0.011 [b]	0.30±0.011 [d]	0.42±0.027 [b]	0.39±0.023 [c]	0.43±0.022 [ab]
	22.17	0.45±0.009 [a]	0.37±0.011 [b]	0.45±0.031 [ab]	0.42±0.014 [ab]	0.46±0.011 [a]
	29.28	0.46±0.011 [a]	0.42±0.009 [a]	0.47±0.017 [a]	0.43±0.016 [a]	0.46±0.026 [a]

Superscript letters indicate that means with the same letters designation in a column are not significantly different at P=0.01.

Table 7: Relationships between static coefficient of friction and moisture content of safflower seeds

Surface	IL 111	LRV5151
Plywood	$\mu = 0.0092\,M_c + 0.1431$, ($R^2 = 0.933$)	$\mu = 0.0086\,M_c + 0.1658$, ($R^2 = 0.930$)
Concrete	$\mu = 0.005\,M_c + 0.2677$, ($R^2 = 0.985$)	$\mu = 0.0052\,M_c + 0.2915$, ($R^2 = 0.887$)
Fiberglass	$\mu = 0.008\,M_c + 0.2245$, ($R^2 = 0.919$)	$\mu = 0.008\,M_c + 0.2539$, ($R^2 = 0.882$)
Galvanized iron	$\mu = 0.0075\,M_c + 0.2173$, ($R^2 = 0.944$)	$\mu = 0.006\,M_c + 0.3006$, ($R^2 = 0.920$)
Rubber	$\mu = 0.0035\,M_c + 0.3415$, ($R^2 = 0.918$)	$\mu = 0.0035\,M_c + 0.3638$, ($R^2 = 0.854$)

(P<0.0001) than the material surface on the static coefficient of friction (P<0.0023). This is due to the increased adhesion between the seed and material surface at higher moisture values.

The reason for the increased friction coefficient at higher moisture content may be due to the water present in the seeds offering a cohesive force on the surface of contact. As the moisture content of the seeds increases, the surface of the samples becomes more sticky. Water tends to adhere to surfaces and the water on the moist seed surface would be attracted to the surface across which the sample is being moved. Other researchers found that as the moisture content increased, the static coefficient of friction increased also (Joshi *et al.*, 1993; Carman, 1996; Gupta and Das, 1997; Ogut, 1998; Gezer *et al.*, 2002; kashaninejad *et al.*, 2006).

3.7 Angle of Repose

The experimental results for the angle of repose for safflower seeds at various moisture levels are shown in Fig. 8. It was observed that the angles of repose for filling and emptying increased linearly with increase in moisture content for both varieties of safflower seed. The analysis of variance revealed that the effect of moisture content on angles of repose for filling and emptying was highly significant (P<0.0001).
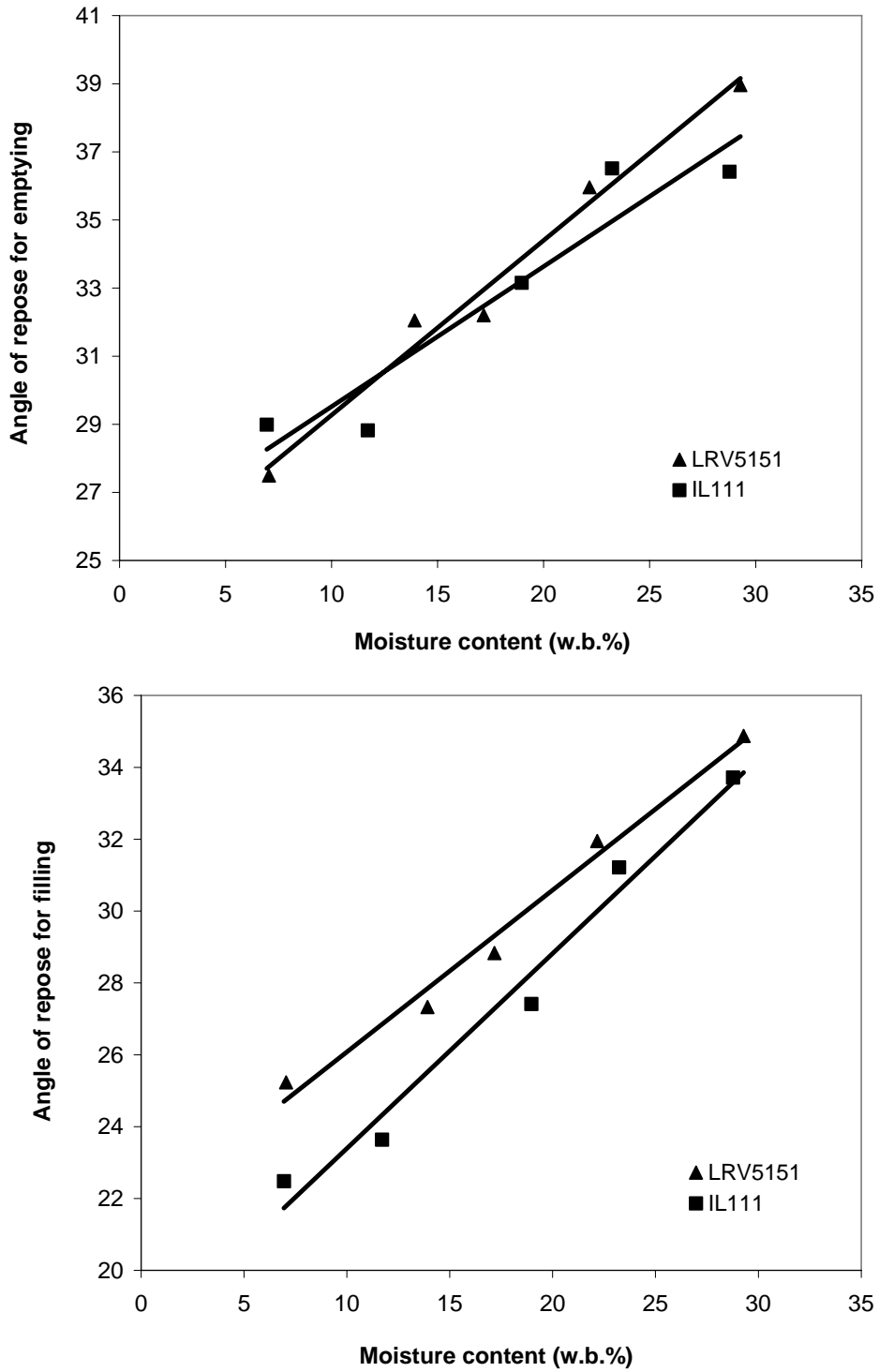
Figs. 8: Effect of moisture content on angle of repose of safflower seed.

Angle of repose for filling increased from 22.48 to 33.71 and 25.23 to 34.88° for IL111 and LRV5151 varieties and angle of repose for emptying increased from 28.99 to 36.42 and 27.49 to 38.96° for IL111 and LRV5151 varieties respectively in the moisture range of 7-30% (w.b.). The angle of repose for safflower seed was close to values reported for gram (Dutta *et al.*, 1988), pigeon pea (Shepherd and Bhardwaj, 1986), fababean (Fraser *et al.*, 1978) and oil bean (Oje and Ugbore, 1991) but lower than sunflower seed (Gupta and Das, 1997) and pumpkin seed (Joshi *et al.*, 1993). The relationship existing between moisture content and angle of repose appears linear and can be formulated as following:

Variety IL111

$$\theta_f = 0.5428\, M_c + 17.962,\, (R^2 = 0.976) \qquad (29)$$

$$\theta_e = 0.4114\, M_c + 25.406,\, (R^2 = 0.903) \qquad (30)$$

Variety LRV5151

$$\theta_f = 0.4508\, M_c + 21.567,\, (R^2 = 0.985) \qquad (31)$$

$$\theta_e = 0.5127\, M_c + 24.^{147},\, (R^2 = 0.981) \qquad (32)$$

3.8 Terminal Velocity

The variation in terminal velocity of safflower seed varieties (IL111 and LRV5151) with moisture content of the sample are presented in Fig. 9. Increasing moisture content had significant effect on terminal velocity of safflower varieties (P<0.0001). The terminal velocity was found to increase from 7.65 to 8.91 and 6.80 to 7.41 m/s for IL111 and LRV5151 respectively in the moisture range of 7 to 30% (w.b.). Variety had a significant effect on terminal velocity (P<0.0001) and the terminal velocity was lower for LRV5151 than IL111 variety at all moisture levels. As the moisture content increased, the terminal velocity was found to increase linearly and the following equations give these relationships:

$$V_t = 0.0586M_c + 7.17,\, (R^2 = 0.958) \qquad (33)$$

$$V_t = 0.028M_c + 6.65,\, (R^2 = 0.941) \qquad (34)$$

The increase in terminal velocity with increase in moisture content can be attributed to the increase in mass of an individual sample per unit frontal area presented to the air stream. The other reason is that the drag force is affected by the moisture content of particle. However, it is not possible to comment on the relative significance of these effects, except to say that the shape factor has an effect. Joshi *et al.* (1993) for pumpkin seeds, Carman (1996) for lentil seeds, Gupta and Das (1997) for sunflower seed, Gezer *et al.* (2002)
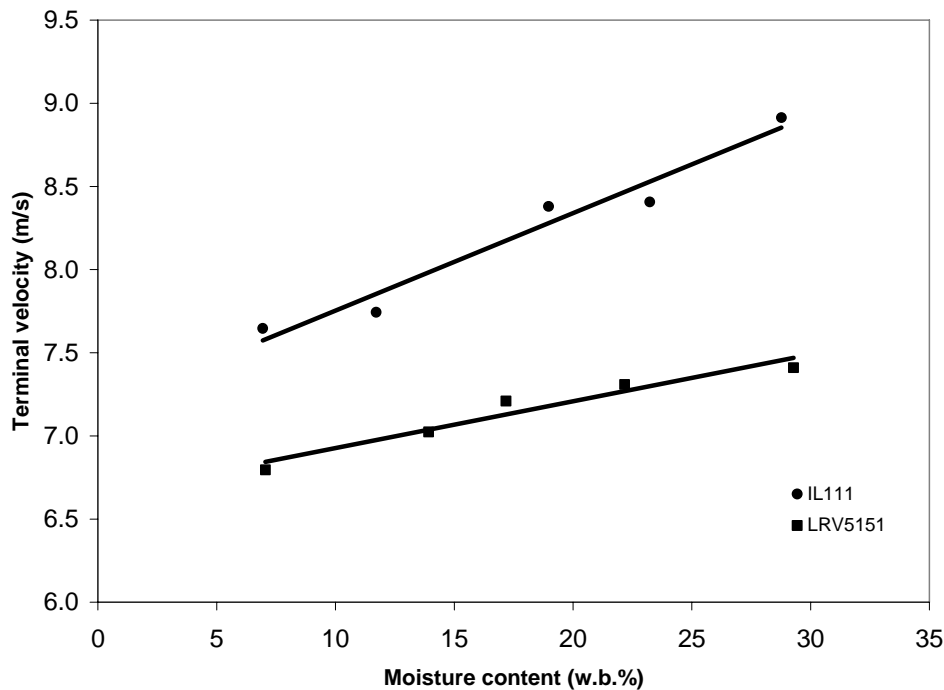
Fig. 9: Effect of moisture content on terminal velocity of safflower seed.

for apricot pit and kernel and Kashaninejad *et al.* (2006) for pistachio nut and kernel found similar results.

4. CONCLUSIONS

Some engineering properties of two varieties of safflower seeds were investigated in the range of moisture content from 7 to 30% (w.b.). These properties are very useful to design equipment for planting, harvesting, processing, transportation, aeration, drying, dehulling, separation and storing. The following conclusions are drawn from this investigation into the properties of safflower seed:

1. All the physical properties of safflower seed varieties to be dependent on their moisture contents.
2. At the moisture content of 6.94% (w.b.), the average length, width and thickness of 100 safflower seed of IL111 variety were 7.42, 4.35 and 3.75 mm respectively, while the corresponding values for LRV5151 variety were 7.10, 4.02 and 3.37 mm. At initial moisture content the average unit mass of IL111 and LRV5151 varieties was 0.047 and 0.033 g, respectively.
3. An increasing relationship was found between sphericity as well as geometric mean diameter and moisture content in both varieties of safflower seed.
4. As the moisture content increased from 7 to 30% (w.b.), bulk density of IL111 and LRV5151 varieties decreased from 595.11 to 555.50 kg/m^3 and from 874.90 to 536.00 kg/m^3 while true density increased from 975.31 to 1199.60 kg/m^3 and from 916.67 to 1016.80 kg/m^3 for IL111 and LRV5151 varieties, respectively.
5. The porosity of both varieties of safflower seed increased with increase in moisture content.
6. The static coefficient of friction of both varieties of safflower seed increased linearly with moisture content irrespective of surfaces employed. At all moisture contents, the static coefficient of friction was the highest for both varieties on rubber and the least for plywood.
7. As the moisture content increased from 7 to 30% (w.b.), the terminal velocity was found to increase linearly from 7.65 to 8.91 m/s and from 6.79 to 7.41 m/s for IL111 and LRV5151 varieties, respectively.
8. Angle of repose for filling increased from 22.48 to 33.71 and 25.23 to 34.88° for IL111 and LRV5151 varieties and angle of repose for emptying increased from 28.99 to 36.42 and 27.49 to 38.96° for IL111 and LRV5151 varieties respectively in the moisture range of 7-30 (w.b.%).

ACKNOWLEDGMENTS

Nomenclature	
D	Geometric mean diameter (mm)
H	Height of seed (mm)
L	Length of seed (mm)
M	Mass of seed (g)
M_c	Moisture content (w.b.)
R	Coefficient of determination
T	Thickness of seed (mm)
V	Volume of seed (cm^3)
V_t	Terminal velocity of seed (m/s)
W	Width of seed (mm)
ε	Porosity (%)
μ	Coefficient of static friction
ρ_b	Bulk density (kg/m^3)
ρ_t	True density (kg/m^3)
ϕ	Sphericity (%)
θ_e	Angle of repose for emptying
θ_f	Angle of repose for filling

REFERENCES

1. Aydin, C. (2007). Some engineering properties of peanut and kernel. Journal of Food Engineering,

79(3):810-816.

2. Aydin, C. and M. Ozcan (2002). Some physico-mechanic properties of terebinth fruits. Journal of Food Engineering, 53: 97-101.

3. Baryeh, E. A. and B. K. Mangope (2002). Some physical properties of QP-38 variety pigeon pea. Journal of Food Engineering, 56: 59-65.

4. Baümler, E., Cuniberti, A., Nolasco, S. M. and I. C. Riccobene (2006). Moisture dependent physical and compression properties of safflower seed. Journal of Food Engineering, 72: 134-140.

5. Çalışır, S., Marakoğlu, T., Öğüt, H. and Ö. Öztürk (2005). Physical properties of rapeseed (*Brassica napus oleifera* L.). Journal of Food Engineering, 69: 61-66.

6. Carman, K. (1996). Some physical properties of lentil seeds. Journal of Agricultural Engineering Research, 63: 87-92.

7. Corrêa, P. C., da Silva, S. F., Jaren, C., Afonso Júnior, P. C. and I. Arana (2007). Physical and mechanical properties in rice processing. Journal of Food Engineering, 79(1):137-142.

8. Deshpande, S. D., Bal. S. and T. P. Ojha (1993). Physical properties of soybean. Journal of Agricultural Engineering Research, 56: 89-98.

9. Dursun, E. and I. Dursun (2005). Some physical properties of caper seed. Biosystems Engineering, 92(2): 237-245.

10. Dutta, S. K., Nema, V. K. and R. K. Bhardwaj (1988). Physical properties of Gram. Journal of Agricultural Engineering Research, 39: 259-268.

11. FAOSTAT. (2005). Safflower production. Available from http://faostat.fao.org.

12. Fraser, B. M., Verma, S. S. and W. E. Muir (1978). Some physical properties of fababeans. Journal of Agricultural Engineering Research, 23: 53–57.

13. Gezer, I., Haciseferogullari, H. and F. Demir (2002). Some physical properties of hacihaliloglu apricot pit and kernel. Journal of Food Engineering, 56: 49-57.

14. Giayetto, O., Fernandez, E. M., Asnal, W. E., Cerioni, G. A. and L. Cholasky (1999). Behavior of safflower (*carthasmus tinctorius* L.) cultivars in Rio IV, Córdoba, Argentina. Investigation of Agricultural Products and Protection of Vegetation, 14: 203–215.

15. Gupta, R. K. and S. K. Das (1997). Physical properties of sunflower seeds. Journal of Agricultural Engineering Research. 66: 1–8.

16. Joshi, D. C., Das, S. D. and R. K. Mukherjee (1993). Physical properties of pumpkin seeds. Journal of Agricultural Engineering Research, 54: 219-229.

17. Kashaninejad, M., Mortazavi, A., Safekordi, A. and L. G. Tabil (2006). Some physical properties of Pistachio (*Pistacia vera* L.) nut and its kernel. Journal of Food Engineering, 72: 30–38.

18. Kingsly, A. R. P., Singh, D. B., Manikantan, M. R. and R. K. Jain (2006). Moisture dependent physical properties of dried pomegranate seeds (*Anardana*). Journal of Food Engineering, 75: 492-496.

19. Konak, M., Çarman, K. and C. Aydin (2002). Physical properties of chick pea seeds. Biosystems Engineering, 82(1): 73-78.

20. Mohseni, M., Ohe, T., Fazeli, M. R., Ostad, S. N., Hamedi, M., Jamalifar, H. and E. Azizi (2006). Studying the mutagenicity of red florets safflower IL111 using Ames Test. Journal of Pharmacology and Toxicology, 1(6): 545-551.

21. Mohsenin, N. N. (1980). Physical properties of plants and animal materials. New York: Gordon and Breach Science Publishers, NW.

22. Mwithiga, G. and M. M. Sifuna (2006). Effect of moisture content on the physical properties of three varieties of sorghum seeds. Journal of Food Engineering, 75: 480-486.

23. Ogut, H. (1998). Some physical properties of white lupin. Journal of Agricultural Engineering Research, 56: 273-277.

24. Oje, K. and E. C. Ugbore (1991). Some physical properties of oilbean seed. Journal of Agricultural Engineering Research, 50: 305- 313.

25. Olajide, J. O., Ade-Omowaye, B. I. O. and E. T. Otunola (2000). Some physical properties of shea kernel. Journal of Agricultural Engineering Research, 76: 419-421.

26. Omidi, A. H. (2005). Safflower production in Iran. Technical report, Seed and Plant Breeding Institute, Karaj, Iran.

27. Ozarslan, C. (2002). Physical properties of cotton seed. Biosystems Engineering, 83: 169-174.

28. Ramakrishana, P. (1986). Melon seeds-Evaluation of physical characteristics. Journal of Food Science and Technology, 23: 158-160.

29. Rameshbabu, M., Jayas, D. S., Muir, W. E., White, N. D. G. and J. T. Mills (1996). Bulk and handling properties of hulless barley. Canadian Agricultural Engineering, 38(1): 31-35.

30. Scanlon, M. G., Cenkowski, S., Segall, K. I. and S. D. Arntfield (2005). The physical properties of micronised lentil as a function of tempering moisture. Biosystems Engineering, 92(2): 247-254.

31. Sessiz, A., Esgici, R. and S. Kizil (2007). Moisture-dependent physical properties of caper (*Capparis* ssp.) fruit. Journal of Food Engineering, 79(4): 1426-1431.

32. Shepherd, H. and R. K Bhardwaj (1986). Moisture dependent physical properties of pigeon pea. Journal of Agricultural Engineering Research, 35: 259-268.

33. Singh, K. K. and T. K Goswami (1996). Physical properties of cumin seed. Journal of Agricultural Engineering Research, 64: 93-98.

34. Sirisomboon, P., Pornchaloempong, P. and T. Romphophak (2007). Physical properties of green soybean: criteria for sorting. Journal of Food Engineering, 79(1): 18-22.

35. USDA. (1970). Official grain standards of the United States, US Department of Agricultural Consumer and Marketing Service Grain Division, Revised.

36. Weiss, E. A. (1971). Castor, sesame and safflower. Barnes & Noble, Inc., New York.

37. Weiss, E. A. (1983). Tropical Oilseed crops. Tropical Agriculture Series, Longman, London and New York.

38. White, N. D. G. and D. S. Jayas (2001). Physical properties of canola and sunflower meal pellets. Canadian Biosystems Engineering, 43: 49-52.

UTILIZATION OF WOOD RESIDUES IN RENEWABLE ENERGY PROJECTS - DETERMINANTS OF PREFERENCE FOR WOOD-PROCESSING COMPANIES IN MATSUSAKA CITY

Naveeda Qaseem[‡], Tomohiro Uchiyama[§] and Kotaro Ohara[§]

ABSTRACT

As a result of recent policies by the Japanese government, the utilization of biomass, particularly wood residues, in renewable energy projects is becoming an important issue. However, the practical implementation of biomass energy involves challenges that range from financial, economic and technical to secure supply of the residues for the projects. Although advanced studies have been conducted related to these challenges, research is limited on the issue of secure supply of available residues. Therefore, a case study of a renewable energy project in Matsusaka City, located in the central part of the Japan, was conducted to address the issue. Despite the characteristics of the project, the wood-processing company's reluctance to supply wood residues to the proposed power generation plant remains a serious challenge. This study employs a logit model to analyze the factors responsible for this reluctant behavior and identify the determinants of the wood company's preferences in managing their residues. Estimated results of the model indicate that the economic factor is the most dominant along with geographical and social factors. It is concluded that government policies for residue management and dioxin control could contribute significantly to determining the preferences of the wood-processing companies.

Keywords: *Wood residues; Renewable energy projects; Residue management; Preference; Logit model.*
© 2007 AAAE

1. INTRODUCTION

Biomass utilizes carbon dioxide, a major greenhouse gas, thus helps in reducing the potential increase in atmospheric warming (Hall, 1991). Available bioenergy in Japan is estimated as 5% of the Japanese energy supply (Matsumura, 2005). It indicates that bioenergy can assist in the 6% reduction of greenhouse gas emissions that Japan agreed to in the Kyoto Protocol. Therefore, in the year 2001, the Japanese government, for the first time, officially defined biomass as one of the new energy resources in the "Law Concerning Special Measures for Promotion of the Use of New Energy." Later, in December 2002, Biomass Nippon Strategy was designed by the government of Japan to utilize the biomass resources in an effective and efficient way.

Biomass resources can be classified as virgin resources and residues (Minami *et al.* 2005). Virgin resources are primarily biomass produced through photosynthesis while residues are by-product resources that are generated from biomass-based materials. A study by Minami and Saka (2005) indicates that in Japan the available quantities of residues, estimated at 46 Mty^{-1}, are larger than the virgin resources, 30 Mty^{-1}. Among the residues, a share of wood is significantly large (21%) as compared to other forms of residues (Minami *et al*, 2005). Therefore, initialization of projects for utilization of wood residues in producing renewable energy has become common practice in many parts of the country. These projects have been proposed considering the social, economic and technical specifications of the site. Practical implementation, however, still involves several challenges that range from financial, technical and economic factors to secure an adequate supply of the available residues. Studies have been conducted on technical, financial and economic aspects (Yoshioka, *et al.*, 2005, Rodrigues *et al.* 2003, Dornburg *et al.*, 2001, Bridgwater, 1995), however, limited research has been done on the issues of possible supply of residues, despite the availability. Recent studies also indicate that it is non-technical challenges, rather than

technical, which hinder the support for bioenergy projects (McCormick, 2007). Therefore, a case study of a renewable energy project in Matsusaka City was conducted to address the issue of secure supply of available wood residues. The city is located in Mie Prefecture, a central part of Japan. The project has the characteristics that it is initiated in the region which is rich with forest resources. Moreover, number of wood-processing companies, operating in the area, is one of the largest in Japan, similar to the areas of Nakatsugawa in Gifu Prefecture, Maniwa in Okayama Prefecture, Tanba in Hyougo Prefecture and Noshiro in Akita Prefecture. The project is also unique in the sense that it is initiated by Wood Biomass Utilization Cooperative. Examples of such projects are few in Japan, as most of the projects are owned by the public authorities. If the project could be successfully implemented, it could be followed by other regions. However, information on actual estimation of available volume and kinds of wood residues produced in wood-processing companies and their present methods of managing the wastes is not available. Besides that, the major challenge of the project is the issue of secure supply of wood residues due to less likely preference of the supplying agents to participate in the project. Therefore, based on the questionnaire survey, the study first estimated the available volume, kinds of wood residues produced by wood-processing companies and the practices used to manage the residues. Moreover, considering the level of commitment through cooperation of the parties of biomass suppliers as an important factor for the feasible implementation of the project, the study attempts to analyze the factors responsible for the reluctant behavior. It also identifies the determinants of preferences for the wood companies to manage their residues.

Wood residues, in this study, are defined in terms of mill residues, which are generated in timber, sawmill and plywood companies.

Wood Biomass Utilization Cooperative (WBUC) was established, jointly, in May 2006, to utilize the wasted wood residues in Matsusaka City. Members of the Cooperative include Matsusaka Woodpia Cooperative, cooking oil company in Matsusaka city, owners of few wood companies and forestry industry of the city. The cooking oil company is particularly taking a risk in promoting the renewable energy project. The Cooperative proposed the direct combustion based power plant, which will produce 26 ton/hour of steam and 2000KW of electricity. The power plant contains two sections. The first section, known as pre-processing plant, is proposed to be established at Matsusaka Woodpia Cooperative. Wood residues from the sources would be transported to this section where the residues will be converted into chip. In the second stage, converted chip will be transported to the private cooking oil company, where the chip will be burned in a boiler and a generator will be run using steam from the boiler. Produced steam and electricity will be used to meet energy needs of the cooking oil company which is estimated to cover more than 50% of the company's electricity.

2. DESCRIPTION OF METHODOLOGY AND BASIC SURVEY RESULTS

The research was conducted from August 2005 to July 2006. Data for this study were collected through questionnaires, and telephone and in-person surveys of representatives of wood-processing companies in Matsusaka City, particularly in Iitaka and Iinan towns where most of the companies are located, as well as municipal authorities and Cooperative officials.

Table 1 reports the amount of production of residues by the wood-processing companies in the region. The major types of waste are bark, chip, sawdust and edge cuttings. Figures also indicate that bark accounts for the largest volume, followed by chip, sawdust and edge cuttings, respectively.

Table 1: Production of Biomass in the Region

Type of residues	Production quantity/day	
	m^3	ton
Bark	199.83	57.95
Chip	103.29	28.92
Sawdust	80.27	12.04
Edge cuttings	77.94	14.03
Total	**470.58**	**115.71**

Source: Survey by the authors, 2006

It has been estimated that chip and edge cuttings are reused or recycled, whereas, a large percentage of bark and sawdust are lost in the form of burning. This is evident from Figure 1, which shows the present disposal methods of bark and other residues by wood-processing companies. Results indicate that 81% of the companies dispose of bark through burning, while
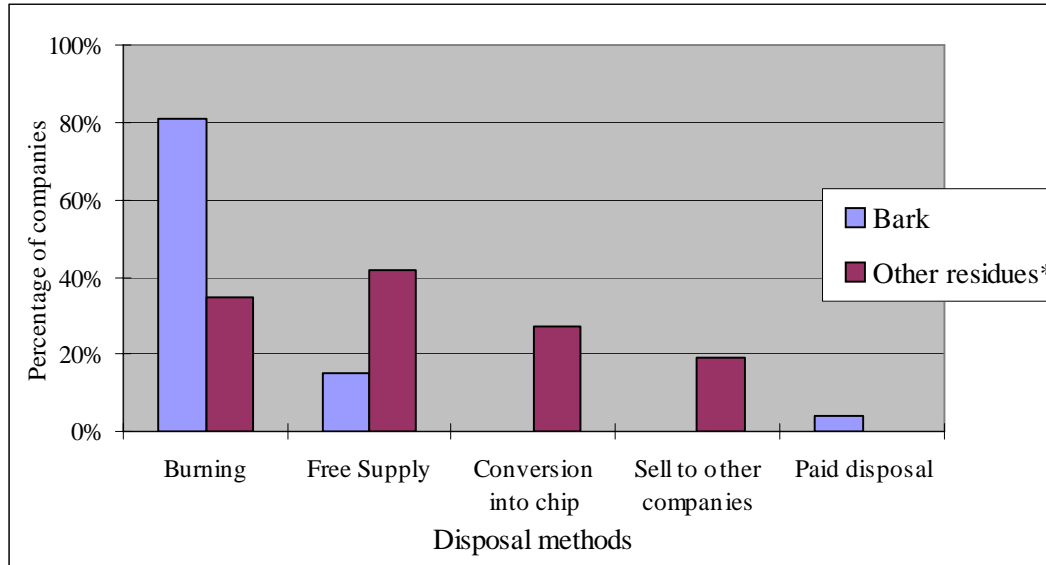
Source: Survey by the authors, 2006
 *Other residues include saw dust and edge cuttings

Fig. 1: Present Disposal Methods of Residues by Wood-Processing Companies

the percentage for free supply and paid disposal methods is 15% and 4%, respectively. The disposal methods for edge cuttings and saw dust are burning (35%), free of charge supply to wood chip merchandisers and to stock farmers for compost and liter (42%), conversion into chip (27%) and selling to other companies (19%), respectively. Total percentage of companies for other residues is more than 100, which is due to multiple disposal methods used by one company.

Therefore, the amount which is disposed of through burning and paid consignment has been considered as the available amount for a biomass energy project while the amount of selling and free supplying is not included due to the reuse of the residues. Available amounts of the wood residues are presented in Table 2.

Table 2: Available Supply of Biomass in the Region

	Quantity/day, ton
Bark	57.95
Others*	6.92
Total	**64.87**

Source: Survey by the authors, 2006
*edge cuttings and sawdust

It can be seen that about 65 tons of unused residues are available, which can be utilized to generate energy. This is explained in Figure 2, which shows the present scenario of disposal of wood residues and the structural shift from disposal to effective utilization for energy generation from local woody biomass.

However, the reluctant behavior of the wood-processing companies towards supplying biomass resources for the renewable energy project poses a serious issue for the possible availability of wood residues. Survey results indicate that more than 70% of the companies are not willing to supply the residues. A quantitative analysis was conducted to investigate the factors and determinants responsible for management preferences of residue for the wood-processing companies. This analysis considers socio-economic, environmental and geographical characteristics which differ from one company to the other.

3. MODEL SPECIFICATION

In analyzing the survey data, it is estimated how different attributes of the companies affect the choice of a specified residue management method. The analysis assumes that the data distinguish only whether observations are in one category,

management preference to supply residues to the power plant, or in a second category, incineration. Thus, the dependent variable is a dummy variable taking the value 1 if the company chooses participation in power plant project and the value 0 if the company chooses otherwise (incineration) and as a result, a qualitative response model is used for the quantitative analysis.

Hence, logit model is presented as:

$$Z_i = ln\ \{Pi/(1- P_i)\} = a + b_1X_{i1} +......b_kX_{ik}$$

where $i= 1,........N$

Z_i is the log of odds ratio-the ratio of the probability of an individual company preferring participation in the project to the probability of not participating and preferring incineration. Z_i is not only linear in X_i but linear in parameters also (Gujrati, 2002).

Prior to presenting the estimation results of the model, a brief summary of the surveyed data is presented in Table 3. The figure for total production indicates that 46% of the wood companies produce less than or equal to 100 tons per month. The percentage of companies which produce a quantity of waste less than or equal to 100 tons/month is estimated at 81%. To burn the produced waste, 85% of the companies use incinerators while 11% burn in open air. The detailed explanation for the rest of the surveyed variables, which are estimated quantitatively, is presented in section 4.

4. ESTIMATION RESULTS OF LOGIT MODEL

As can be seen from resulting parameter estimates (Table 4), coefficients of company size and quantity of waste are negative and significant at 5 and 1 percent, respectively. The choice of incineration for smaller companies is due to the low cost associated with it, and less awareness of environmental issues and regulations. The higher the quantity of waste produced, the more the companies would prefer incineration, due to less cost, easy on site handling, the possibility of daily management and thus, no requirement of a storage facility. The higher the cost of waste management through participation in the program, the more likely it will be rejected by the

Table 3: Summary of Surveyed Data

Variable	Mode of choices		Frequency	
Production (ton/month)	1.	0-100	1.	18
	2.	101-200	2.	2
	3.	201-300	3.	3
	4.	More than 300	4.	3
Quantity of waste (ton/month)	1.	0-100	1.	21
	2.	101-200	2.	3
	3.	201-300	3.	1
	4.	More than 300	4.	1
Cost of disposal (Yen/year)	1.	0-100,000	1.	14
	2.	100,001-200,000	2.	7
	3.	200,001-300,000	3.	2
	4.	More than 300,000	4.	3
Type of company	1.	Individual	1.	18
	2.	Limited Corporation	2.	8
Age of company owner	1.	Less than 40	1.	1
	2.	40-49	2.	4
	3.	50-59	3.	11
	4.	more than 60	4.	10
Education level of company owner	1.	Secondary Level	1.	8
	2.	High level	2.	13
	3.	University level	3.	5
Location of the company	1.	In residential area	1.	12
	2.	Far from residential area	2.	14
Presence of successor	1.	Yes	1.	12
	2.	No	2.	9
	3.	Don't know	3.	5
Number of employees	1.	Permanent employees	1.	25
	2.	Part timers	2.	9
Method of burning	1.	In open air	1.	3
	2.	Using incinerators	2.	22
	3.	Others	3.	1
Number of burning/month	1.	1-5 times	1.	8
	2.	6-10 times	2.	8
	3.	more than 10 times	3.	10

companies. Hence, this variable is negative and significant at 1%.

The incurred cost for waste management through participation in the power plant is in the form of disposal charge which companies are supposed to pay, and is fixed at about 2000 Japanese yen/ton, by the Wood Biomass Utilization Cooperative (WBUC). Presently, a large number of companies in the region have installed incinerators for burning the residue. Field survey results show that the companies consider the average annual cost of disposing of residue in an incinerator to be about 100-120 thousand yen, depending upon the type, capacity and scale of the

incinerator. The estimated cost figure includes installation, operation and ash disposal cost. However, it does not include the annual dioxin inspection cost, which is defined as the cost involved in dioxin inspection of incinerators. An inspection is conducted annually by the local officials to check the working condition of the incinerators according to environmental standards. Most of the companies, in the present case, have not registered their incinerators with the municipal government to avoid the dioxin inspection cost and the renewal cost of replacement or maintenance, if applicable. Therefore, such costs are not involved in the decision of preference for project participation.

Results by location are significant with positive signs, indicating that the companies, which are located in residential areas, are more willing to use their residues as a resource for energy generation than the companies who are far from residential areas. This is due to the issue of safety of the residents from fire and other environmental effects such as smoke, which have adverse effects on their health. Such conscious behavior of the companies developed after the occurrence of two major incidents in this area due to burning the residues, which produced a large fire. As a result, smoke that spread into the residential area contained ash which produced adverse health effects on the residents. Local people did not complain openly to the municipal authorities to take action against the companies to stop burning, which is a common Japanese attitude. It is expected that increased awareness of health issues and resulting
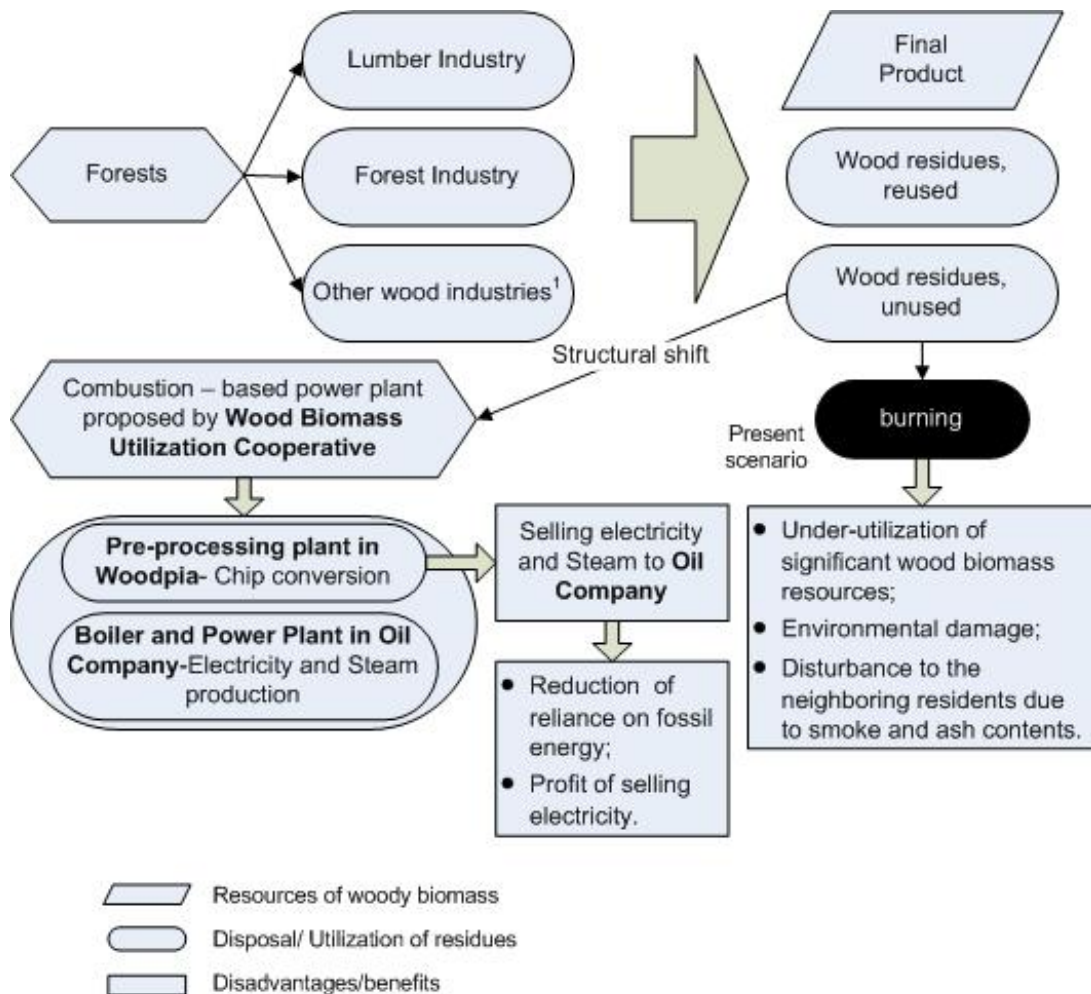
Fig. 2: Structure of Disposal/Utilization of Wood Residues

serious steps by the concerned authorities has made the wood companies conscious of alternative management methods.

The estimation also indicates that the continuation of business to the next generation (successor) is a significant variable in choosing participation in the project. This is due to the future vision of the companies when other options for waste management will be more expansive, as well as sensitive, and environmental regulations will be more strict. The decision to participate, at this stage, would have a positive impact on the companies' economic, social and environmental fronts. Education level and consideration of neighboring residents are positive but insignificant, whereas owner age is significant at 10 percent. The value of Pseudo-R^2 shows that 67.9% of the companies' preferences are explained by the selected exogenous variables, and hence, suggests a good efficiency of the model. Further, the results of the model suggest the statistically significant and theoretically justified relationships between the preferences of participation by power plant and explanatory variables.

5. CONCLUSIONS

Reluctant behavior of wood processing companies to supply wood residues is a serious challenge for the implementation of the renewable energy project in Matsusaka City. Therefore, a quantitative analysis was carried out to identify the determinants of preferences for the wood-processing companies to manage the residues. Results indicate that the primary preference for non-participation in the project is due to economic factors. A cost is involved in the form of a disposal charge that wood-processing companies have to pay per unit of ton and is specified by the Wood Biomass Utilization Cooperative. Companies consider the disposal charge higher than the cost of their presently adopted disposal methods. However, the companies would reconsider the cost associated with the disposal charge if the annual dioxin inspection of the incinerators was carried out regularly by the municipal authorities. If the dioxin inspection cost paid by the company were more than the disposal charge, then it might be less costly to participate in the biomass renewable energy program.

Table 4: Maximum Likelihood Estimation of Logit Model, Dependent Variable: Supply residues to the power plant

Variable Name	Logit Model	
	Coeff.	t-statistic
constant	0.028	1.925*
Size of the company, Large-1, Small-0 [a]	-2.314	-2.867**
Location of the company, In residential area-1, Otherwise-0	2.331	1.878*
Quantity of waste, ton	-2.246	-3.898***
Cost of disposal/month, Japanese Yen	-0.36	-4.435***
Age of company's owner, Below 50-1, Above 50-0	1.980	3.227*
Education level of company's owner, Above Secondary-1, Otherwise-0	1.852	0.005
Continuation of business to the successor, Yes-1, Otherwise-0	1.849	3.745***
Consideration of neighboring residents, Yes-1, Otherwise-0	1.324	0.065
log likelihood	145.214	
Pseudo-R^2	0.679	

***0.01, **0.05, *0.10. Two-tailed test
Units of account are in parenthesis
[a] Large companies are defined as those who have employees, including part timers, whereas, small companies are family based, i.e. only family members are running the company and there are no additional employees

Environmental regulations for dioxin inspection are therefore, contributory in determining the preference of the wood companies. Moreover, the voluntary approach is gaining increasing trend as a new approach to environmental regulation. The analysis provides clues into incentives for firms to volunteer to participate. Presence of successor is positively related to the preference of supply through understanding the importance of utilization of residues in renewable energy projects. This provides evidence that social and public recognition is a key element in improving the results of participation along with additional incentive systems in terms of company performance awards and encouragement for effective use of residues. Regulators should consider the important role of these awards and other forms of recognition as a major design feature of preference in renewable energy programs.

Moreover, rules should be made in such a way that companies are responsible for the health problems of the residents due to smoke and pollutant emissions as a result of burning. Civil and public interest groups should be established to promote awareness to the residents regarding their attitude towards the environment and health issues and the understanding of their rights.

REFERENCES

1. Bridgwater, A. V. (1995). 'The Technical and Economic Feasibility of Biomass Gasification for Power Generation'. Fuel, 74 (5): 631-653.
2. Decision at the Cabinet Meeting, Government of Japan, Biomass Nippon Strategy. December 27, 2002.
3. Dornburg, V. *et al*. (2001). 'Efficiency and Economy of Wood-fired Biomass Energy Systems in relation to Scale regarding Heat and Power Generation using Combustion and Gasification Technologies'. Biomass and Bioenergy, 21(2), 91-108.
4. Gujarati, D. N. (2002). Basic Econometrics, 3rd ed., McGraw-Hill, Inc., New York.
5. Hall, W. Carl (1991). 'Biomass and Global Implications for Food and Energy'. Material prepared for the seminar supported by Japan Society for the Promotion of Science.
6. Matsumura, Y. *et al*. (2005). 'Current Situation and Prospect of Biomass Utilization in Japan'. Biomass and Bioenergy, 29 (5): 304-309.
7. Mc Cormick, Kes *et al*. (2007). 'Key Barriers for Bioenergy in Europe: Economic Conditions, Know-how and Institutional Capacity, and Supply-chain Co-ordination'. Biomass and Bioenergy. 31(7): 443-452.
8. Minami, E. and S. Saka (2005). 'Biomass Resources Present in Japan-Annual Quantities Grown, Unused and Wasted'. Biomass and Bioenergy, 29 (5): 310-320.
9. Rodriguez, M. *et al*. (2003). 'Techno-economic Analysis of Co-fired Biomass Integrated Gasification / Combined Cycle Systems with inclusion of Economies of Scale'. Energy, 28(12): 1229-1258.
10. Yoshioka, T. *et al*. (2005). 'Woody Biomass Resources and Conversion in Japan: The Current Situation and Projections to 2010 and 2050'. Biomass and Bioenergy, 29 (5): 336-346.

A COMPARATIVE STUDY ON PULLOUT BEHAVIOR OF REINFORCEMENTS FOR EFFECTIVE DESIGN OF REINFORCED SOIL STRUCTURES

Md. Zakaria Hossain[*]

ABSTRACT

Pullout behavior of reinforcement embedded in soil is one of the major phenomena towards the effective design of many agricultural and civil engineering structures such as reinforced-soil, slopes and embankments. It is evident that the success of reinforced soil structures depends not only on the strength and performance of reinforcements but also on the pullout resistances of reinforcement such as interfacial friction between the backfill material and the reinforcement under any service conditions. This paper presents a comparison of the pullout resistances of different types of reinforcing materials for effective design of reinforced soil structures. For this purpose, a series of pullout tests on various reinforcing materials such as geogrids, geosynthetics, wires meshes and composite reinforcements that are commonly used in Japan as well as in the world were carried out in the laboratory with two types of backfill materials. It is observed that the pullout stress of the geogrid reinforcement is larger than that of the geosynthetic reinforcement and the pullout stress of the geosynthetic reinforcement is larger than that of the wire mesh reinforcement. The pullout stress of the composite reinforcement is the highest among the types of reinforcement tested in this research works. The analyses of the data also revealed that the composite reinforcement made of cement mortar reinforced by wire mesh achieved the desired performance with a synergetic action from two components where interfacial friction between the soil and the cement matrix provides adequate frictional capacity and the wire mesh in mortar provides the required tensile strength enabling an optimum design of reinforced soil structures.

Keywords: *Reinforced soil; Reinforcing materials; Pullout test; Backfill; Sandy soil; Clayey soil; Tensile strength. © 2007 AAAE*

1. INTRODUCTION

Success of reinforced soil structures depends not only on the strength and performance of reinforcements but also on the pullout resistances of reinforcement such as interfacial friction between the backfill material and the reinforcement under any service conditions. There are mainly two stages, namely: i) internal analysis and ii) external analysis for the design of reinforced soil structures. The selection of suitable backfill materials, and durability, spacing, number of reinforcement as well as mechanisms of mobilization of internal forces are related to internal analysis, whereas the stability of the reinforced soil structures, including safety against sliding, tilt/bearing failure and overturning are related to external analysis (Sivakumar *et al.*, 2002). For the reinforcement to be effective, two conditions need to be satisfied (Sivakumar *et al.*, 2003). That is, it must possess enough strength to withstand: i) tension failure and ii) adhesion failure (Milligan and Palmeria,

1987; Jones, 1996). To date, a number of efforts have been made to ensure enough tensile strength and frictional resistance, simultaneously, for the reinforcements. For improvement of the reinforcement's functions, bearing capacity, pullout and shear resistances; various types of geosynthetics are reported in literature. Among these, study on material properties and pullout resistances on some major geogrids used in Japan were made by Kuwano *et al.* (1999); and Izawa *et al.* (2003). Composite reinforcement made of strip and grid; strip and anchor (Jones, 1996); steel bars and anchor plates (Fukuoka, 1998); z-type reinforcement and triangular anchor (Murray and Irwin, 1981); fiberglass and steel (Koerner, 1994); steel and cement mortar (Sridharan *et al.*, 1991) are also used.

Literature review clearly indicates that many types of reinforcing materials are widely used all over the world for soil reinforcement applications. A reinforced earth slope containing horizontal reinforcement is shown in Fig. 1 as a field application

---

[*] Graduate School of Bioresources, Mie University, 1577 Kurima Machiya-cho, Tsu, Mie 514-8507, Japan
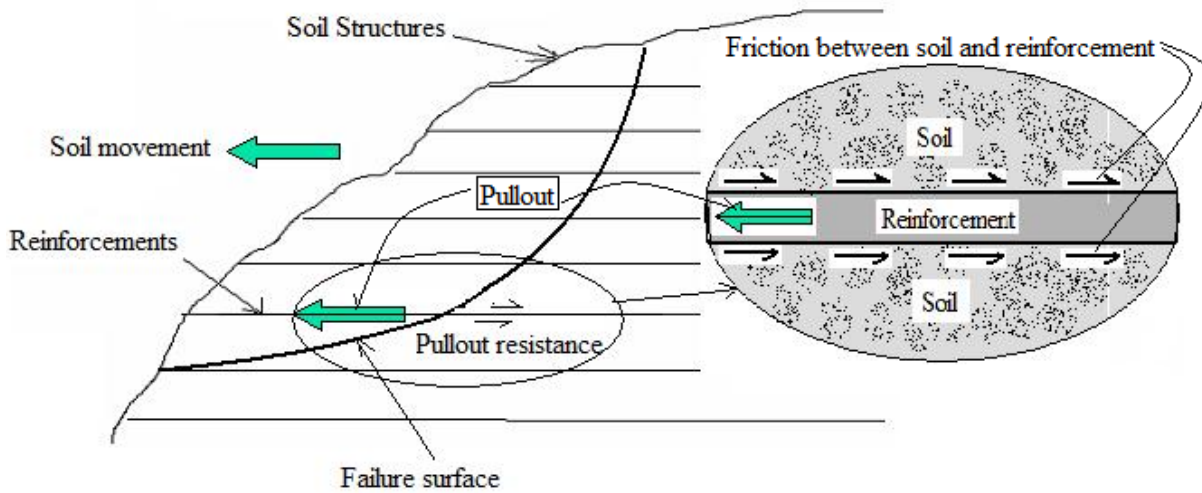
Fig.1: Application of soil reinforcing material in reinforced earth structure/slope

of soil reinforcing material. This figure also indicates the location and pullout direction of reinforcing material as well as frictional force acted between the soil and the reinforcing material.

It is known that the researchers have, extensively, used pullout tests to evaluate interface interactions and failure mechanism of reinforcements. Madhab *et al.* (1998) and Gurung and Iwao (1999) illustrated the general applicability of bilinear shear stress-displacement model for soil reinforcement interaction during pullout tests with extensible and inextensible geo-reinforcements. Richards and Scott (1985); Lafleur *et al.* (1987); Williams and Houlihan (1987); Miyamori *et al.* (1988); and Lauwers (1991) have studied the geotextiles/cohesionless soil interfaces and have adopted a suitable test method to simulate field conditions. A soil-geosynthetic reinforcement interface model based on rigid plastic shear stress mobilization has been reported by Sobhi and Wu (1996) for extensible reinforcement (geotextiles). Mahmood *et al.* (2000) have studied geotextiles/soil interface shear behavior with two types of soils namely sandy soil and organic clay.

Owing to the versatility of the reinforcement and backfill materials, none of the achievements stated above is ever unique to be used as the effective guideline for reinforcement of soil structures. Comparison of the pullout behavior and frictional resistances of different reinforcing material with commonly used backfill materials is therefore, utmost important for effective selection of the better reinforcing material and its suitability with backfill materials as it presents considerable versatility in the

effective design of reinforced soil structures. It should be pointed out here that the objective of this research is to compare different types of reinforcements used for reinforced soil structures. In order to fulfill the objective of this study, it is necessary to include almost all types of soil reinforcement materials either extensible or inextensible those are available in the market. In view of this objective of comparative study, the paper depicted the results of extensible (geosynthetics) and inextensible (steel grids, concrete slabs) reinforcements. It is noted that the HDPE (high density poly ethylene) sheet is being in use in the field in Japan especially in water storage structures such as ponds. By drawing analogy with other conventional soil reinforcement materials, one may argue that such HDPE will behave in a manner similar to geosynthetics. However, this needs to be substantiated by evidence requiring experimentation as well as theoretical analysis, if necessary. For this purpose, a comparison of HDPE as soil reinforcement along with conventional soil reinforcing materials is also depicted for its effective and safe application in the field. An attempt is made in this paper to compare the pullout behavior and frictional resistances of various types of reinforcements that are commonly used in Japan as well as in the world. The paper presents the stress-displacement relationships, variation of cohesion and internal friction of expanded metal mesh (EMM), square steel mesh with 3 mm openings (SSM3), square steel mesh with 10 mm openings (SSM10), chicken mesh (CM), high density poly ethylene (HDPE), geogrid mat (geocomposite) (GM), fortrac geogrid mesh (FGM), nilon geogrid mesh (NGM),

stabilanka geosynthetic sheet (SGS), soft geogrid mat (geocomposite) (SGM), cement composite with rough surface (CCRS), cement composite with smooth surface (CCSS), cement composite with 4 channels (CCC4) and cement composite with 6 channels (CCC6) from pullout test results.

2. PROPERTIES OF MATERIALS

2.1 Properties of Backfills

The particle size distribution curve of sandy soil (Fig. 2) reveals that nearly 9% of the soil is coarse clay, 7% is fine silt, 6% is coarse silt, 14% is fine sand, 44% is medium sand and more than 20% is coarse sand, which means that more than 90 percent of the soil is in the silt and sand fraction. The particle size distribution curve of clayey soil plotted in Fig. 2 indicates that, nearly, 33% of the soil is clay, 24% is fine silt, 5% is medium silt, 4% is coarse silt, 12% is fine sand, 14% is medium sand and 6% is coarse sand, which means that more than 66% percent of the soil is in the clay and silt fraction. The other properties of sandy and clayey soils used in these tests are depicted in Table 1.

2.2 Properties of Reinforcements

Four types of wire mesh reinforcements, 6 types of geogrid and geosynthetics reinforcements, and 4 types of composite reinforcements those are widely used in Japan and all over the world are taken into

Table 1: Properties of backfill materials

Parameters	Sandy soil	Clayey soil
Dry unit weight (γ_d)	1.83 t/m^3	1.53 t/m^3
Optimum water content (W$_{opt}$)	15.3%	25.0%
Specific gravity (ρ_s)	2.64	2.7
Cohesion (c)	5.01 kN/m^2	64.3 kN/m^2
Angle of internal friction (ϕ)	32.19°	16.01°
Sand, >75μm	78%	34%
Silt, 5-75μm	13%	33%
Clay, <5μm	9%	33%
Liquid limit	-	56.2%
Plastic limit	-	29.3%
Plasticity index	-	26.9

consideration in this article for a comparative study. The physical appearances, identities, names and description are depicted in Tables 2-4.

3. EQUIPMENT AND METHODOLOGY

3.1 Test Apparatus

The apparatus used in this study is shown in Fig. 3 which is capable of performing both pullout and direct shear tests. For convenience of the readers, the important components of the testing equipment are
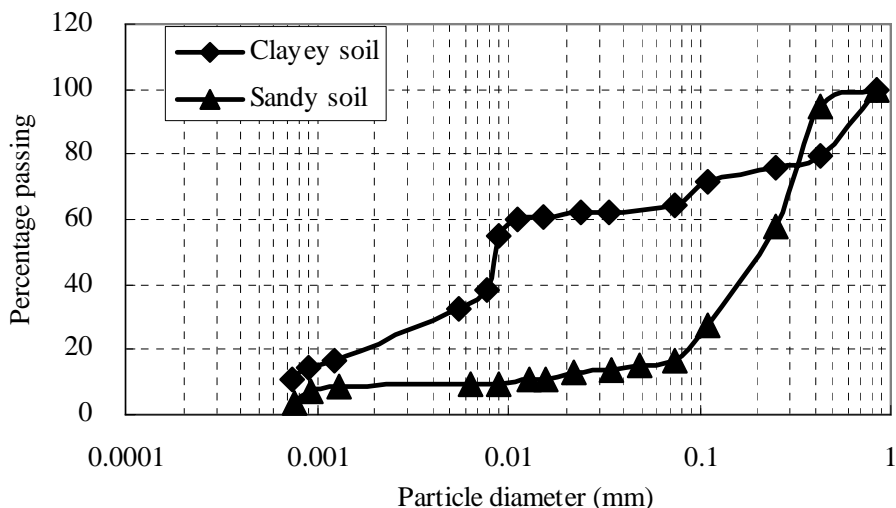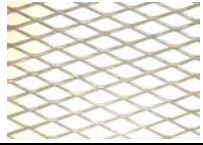

Fig. 2: Particle size distribution curve of sandy and clayey soil

Table 2: Properties of wire mesh reinforcements

Reinforcement	Identity	Name	Description
	EMM	Expanded metal mesh	It is made of steel wires by electrical welding. The cross section of wire is 1.5×1.7 mm with grid opening of 9.6×28.8 mm. Young's modulus is 138 kN/mm^2 and Poisson's ratio is 0.3.
	SSM3	Square mesh with 3mm opening	The SSM3 is made of steel wire of diameter of 0.8 mm and center-to-center mesh opening is 3 mm. The Young's modulus is 138 kN/mm^2 and Poisson's ratio is 0.3.
	SSM10	Square mesh with 10mm opening	The SSM10 is made of steel wire of diameter of 1.2 mm and center-to-center mesh opening is 10 mm. The Young's modulus and Poisson's ratio of SSM10 are same as SSM3.
	CM	Chicken mesh	The cell is 9×11.2 mm in size with 59.53^o angle of diagonal wire. Wire diameter, Young's moduli and Poisson's ratios of the CM are 0.8 mm, 104 kN/mm^2 and 0.3, respectively

numbered, numerically, starting from top-left to right-down in the increasing way, such as, the number from [1] to [8], where the number [1] is the normal load application plate for upper box, [2] is the pullout stress measuring device, [3] is the upper box filled with soil, [4] is the reinforcement, [5] is the lower box filled with soil, [6] is the electrically operated pullout jack, [7] is the displacement measuring dial gauge and [8] is the device taking normal load which acted on the upper box.

3.2 Testing Procedures

The reinforcements were cut to make a piece of 316 mm width and 500 mm length. The cement composite panels were made to obtain rectangular pieces of 316 mm by 380 mm in size with 120-mm extended mesh. The specified length of the pieces was selected in order to facilitate clamping with the pullout apparatus. The reinforcements were clamped in the box in such a way that the embedded length of the panel is 380 mm in the loading direction and 316 mm in the transverse direction. Water was added, gradually, to the soil, and mixed up to obtain desired water content, uniformly, throughout the soil. After placing the reinforcements on the soil filled in lower box, the upper part was set on the panel, and then the soil was filled in the upper box also. The tests were carried out in the way of pulling out the reinforcements with constant speed of 1 mm /min by means of screw jack under electrically operated constant pressure. The pullout force was measured using a tension load cell with the least count of 5 N. The displacements were measured by means of a dial gage with least count of 0.001mm. All the tests were carried out under normal stresses of 40, 60, 80 and 100 kPa. The soil was compacted in three layers for all the tests to obtain uniform density of backfill for all the pullout tests. The tests were carried out with 14.63% water content of sandy soil and 26.54% water content of clayey soil, whereas the optimum water contents were calculated as 15.3% and 27.0% for sandy and clayey soils, respectively. All the pullout tests were conducted according to the standard of the Japanese Geotechnical Society (JGS), T941-199X (Kenju, *et al.*, 1985).

The pullout box was divided into two parts namely upper and lower boxes, both were 110 mm in depth. The apparatus was designed in such a way that the mobility of soil parallel to the pullout surface was restricted completely by the four side walls along with its girder during the test. The friction between the boxes and the reinforcement was eliminated with the help of the vertical screws that were set at both sides of the upper and lower boxes. The normal stress at the top surface of the upper box applied through the upper jack in the downward direction which was balanced by the opposite stresses of the lower box. The normal

Table 3: Properties of geogrid and geosynthetic reinforcements

Reinforcement	Identity	Name	Description
	HDPE	High density polyethylene	The HDPE is made of poly ethylene and looks like a sheet of 2 mm thickness. One surface of it is covered by bentonite layer of 3 mm thickness. However, it was taken off before the pullout test. Therefore, both surfaces were directly come in contact to the backfill materials.
	GM	Geogrid mat	The GM is made of polyester yarns and looks like a porous sheet of 5 mm thickness.
	FGM	Fortrac geogrid mesh	It is made from polyester yarns of cross-section 2×6mm. Mesh opening 20×24 mm. Tensile strength of 150 kN/m in the longitudinal direction and 30 kN/m in the transverse direction.
	NGM	Nilon geogrid mesh	The filament of NGM is circular in cross section. This mesh is made by weaving the filament with each other and the junctions are not sheathed nor connected. The diameter of the filament is 0.5 mm and the center-to-center opening is 2 mm in both directions.
	SGS	Stabilanka geosynthetic sheet	This is made of polyester yarns (2 mm dia.) by interweaving each other in such a way that there is no gap among the filaments. Tensile strength of 800 kN/m in the longitudinal direction and 100 kN/m in the transverse direction.
	SGM	Soft geogrid mat	The SGM made of polyester yarns and looks like a porous sheet of 5.0 mm thickness. It is comparatively softer than GM.

Table 4: Properties of composite reinforcements

Reinforcement	Identity	Name	Description
	CCRS	Cement composite with rough surface (made by stone)	The rough surface of CCRS is made by applying small stone (size varying from 4.0 to 8.0 mm) into the mortar. The thickness and size of the panels are 10.0 mm and 31.5× 38.0 mm, respectively.
	CCSS	Cement composite with smooth surface	CCSS are prepared according to the same way as of the CCRS except applying small stone on it. Therefore, the surface is plain in nature.
	CCC4	Cement composite with rough surface (4-channels)	The rough surface of CCC4 is made with 4 small channels of 15 mm width and 5 mm depth. The channel-to-channel spacing is 50 mm.
	CCC6	Cement composite with rough surface (6-channels)	The rough surface of CCC6 is made with 6 small channels of 15 mm width and 5 mm depth. The channel-to-channel spacing is 50 mm.
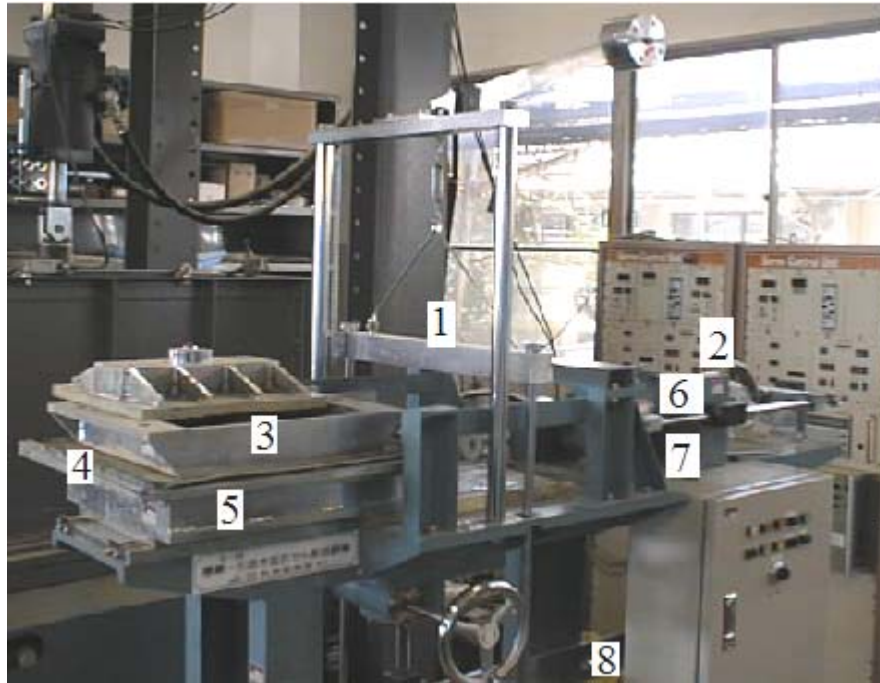
a. Photograph
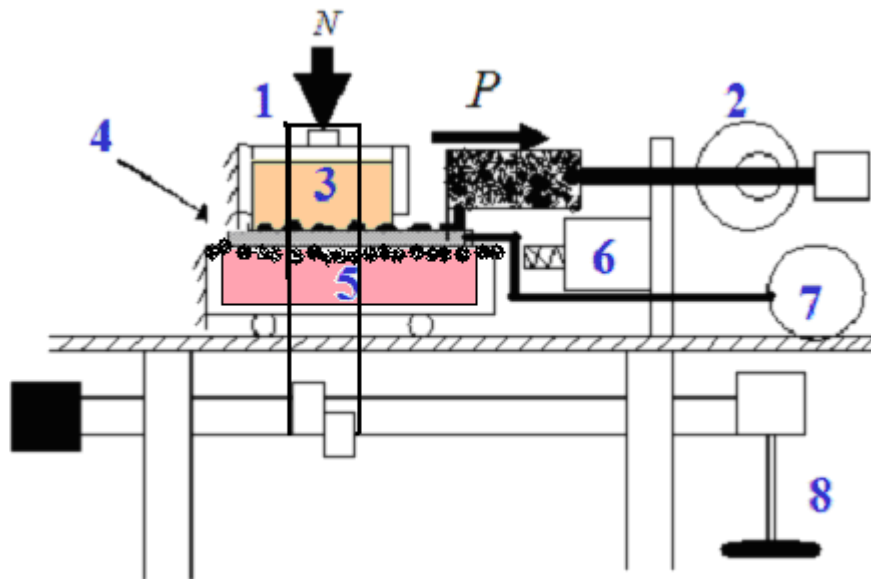
b. Drawing

Fig.3: Pullout testing apparatus

stresses such as consolidation pressures were applied in the soil of upper and lower boxes through vertical

pistons inserted nearly 10 mm into the upper and lower boxes. Therefore, the depths of the soil in the upper and lower boxes were 100 mm each. The soil inside the boxes could move freely in the vertical direction towards the reinforcement to clamp it from both (top and bottom) sides. A clearance between the boxes and the reinforcements was provided by the adjusting screws of the boxes. The lower and upper boxes are set in such a way that there is no friction between the box wall and the reinforcement. The load cell was set between the reinforcement and the

clamping jack to facilitate direct load measurement on the cell avoiding any frictional discrepancy on the machine components. The depth of the soil used in the laboratory (100 mm at bottom and top of the reinforcements) is lower than that used practically in the filed (usually 500 mm soil layers between the reinforcements). However, the test equipment was made following the standard of JIS (Japanese Industrial Standards) and the tests were performed according to the standard of Japanese Geotechnical Society. The normal stresses applied during the experiment are able to simulate exactly the field conditions. Also the soil conditions were same for all the tests.

After embedding the reinforcement on the soil in the lower box, the upper box was fastened on the reinforcement and then additional soil was filled in the upper box having further compaction manually according to the proctor tests. Finally, the normal stresses such as consolidation pressures were applied on the soil through the vertical pistons in order to get the soil a required compaction in the lower and upper boxes and waited until the change of dilatancy becomes close to zero or negligible range. Usually, it took nearly 30 minutes to obtain the required compaction which is a measure of density. It was confirmed based on the dilatancy measurement after applying the consolidation pressure. The wire mesh used as soil reinforcing material was also pulled out from soil in the same way as of other conventional reinforcements. The wire mesh was clamped throughout its width by the clamping device to apply pullout stress uniformly over the mesh width in order to minimize the mesh squeeze during pullout tests. The detail of the pullout mechanism of wire mesh is shown in Fig.3. All the samples used for the pullout tests were of same size in both pullout and transverse directions i.e. in both length and width. However, the thickness of the reinforcements varied depending on the type of material such as composite reinforcements were of 10 mm in thickness whereas the wire meshes were of 2-3mm thickness and geogrids /geosynthetics were of 3-6mm thickness. Although, composite reinforcement was heavier than the wire mesh and conventional geogrids /geosynthetics, it did not affect the pulling force. Because the weight of the reinforcements was not only negligible as compared to the normal stress applied to the soil in the pullout boxes but also it was balanced by the opposite stress through the pistons placed at the bottom soil of lower

box and top soil of the upper box. The composite reinforcements were placed in such as way so that the channels were in transverse direction (across the pull) during the pullout tests.

4. RESULT AND DISCUSSION

4.1 Stress-Displacement Relationships

The relationships between the pulling stress and the displacement of different reinforcements under normal stress of 40, 60, 80 and 100 kPa for sandy soil with water content of 14.63% are given in Figs. 4 - 6. It can be seen from this figure that the pullout stresses increase with the increase in displacement for all types of reinforcements. The EMM reinforcement shows its ultimate pullout stresses at pullout displacement of nearly 10 mm. After that the pullout stresses decreases linearly with the increase in displacement. Similar trends for the SSM3 reinforcement are observed, however, the decreasing trend is comparatively smoother than that of EMM. Also, the range of the ultimate stresses is more for SSM3 than EMM. Unlike the trend of EMM and SSM3, the SSM10 shows different stress-displacement relationships, depending on applied normal stresses. At lower normal stress condition, the stress-displacement curves are almost horizontal and smooth nature, whereas, at higher normal stress condition, it shows a pick value and then decreases with the increase in displacement. There are some scatters in the stress-displacement curves owing to the slip and rearrangement of mesh-wires. For woven nature and larger grid of SSM10, the transverse wires of the mesh are getting to slip after a certain amount of pressure acted on it, which causes a decrease of pullout stress at higher normal stress. On the other hand, for the lower normal stress, there is not enough pressure to cause the slippage of the transverse wire strands. The trend of the stress-displacement curves that are observed in the case of EMM, SSM3 and SSM10 is conspicuously absent for the case of CM. The pullout stress increases, gradually, with the increase in pullout displacement due to the extension of the mesh.

The HDPE, on the other hand, shows a sudden peak at the increase in displacement for all normal stress conditions. The differences of the pullout stresses with the change of normal stress are also significant as compared to above reinforcements. The stress-displacement behavior of GM can be taken as

a. EMM

b. SSM3

c. SSM10

d. CM
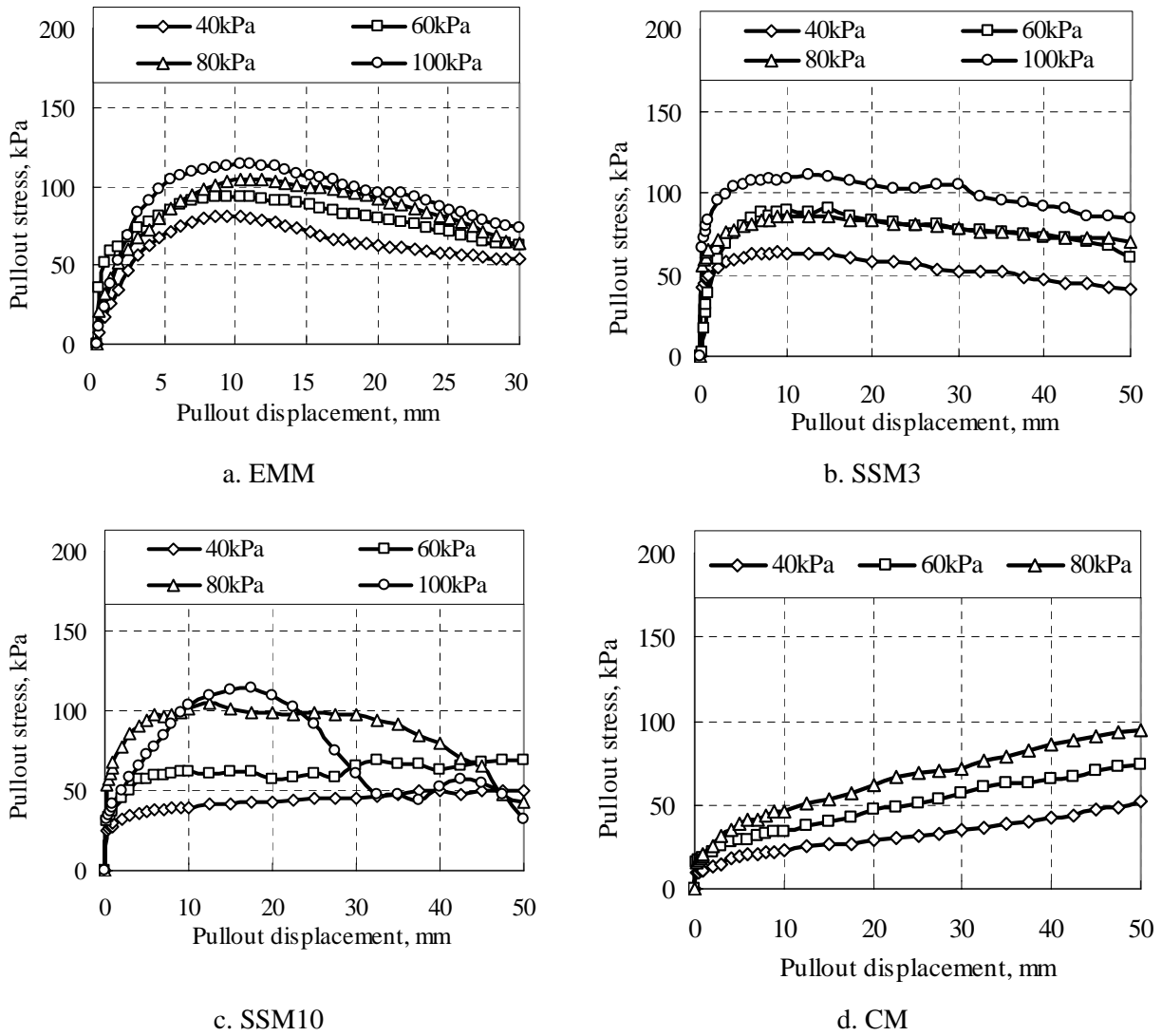
Fig. 4: Pullout stress-displacement relationships for wire mesh reinforcements

the similar behavior of SSM3. The pullout stress fluctuates with displacements after 10 mm and continued in the same fashion of up to 50 mm for FGM. This may be due to variation of stress distribution along the reinforcement in the pullout direction. Because of rectangular cross section of FGM reinforcement, there may be accumulation of some soils in the front side of filament section which gives an increase in soil pressure and after accumulation of certain amount of soil i.e. while accumulation exceeds the limit to cause failure, pullout stress decreases due to slippage of soil particles. The increase in pullout stress for NGM with the increase in displacement is very quick owing to its

small grid size, which gives good grip between the backfill and the reinforcement. This also provides a notable difference among the values of pullout stresses with the differences of applied normal stresses. A close inspection of the plotted results indicates that the stress displacements are bi-linear fashion at lower normal stress. It is noted here that bi-linear trend is also observed for the SGM reinforcement under any normal stress condition. Nonetheless, the curves are closer to each other as compared to NGM.

Dissimilarity to above observation, in the case of SGM, all the three graphs at higher normal stresses is of flat parabolic shapes and can be taken in a group
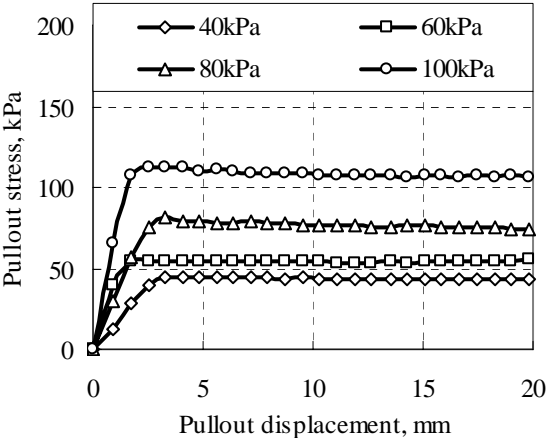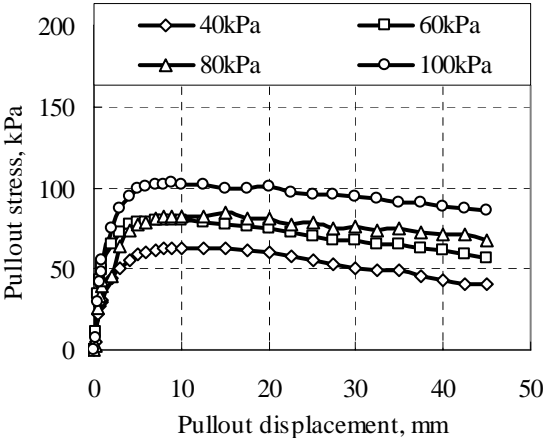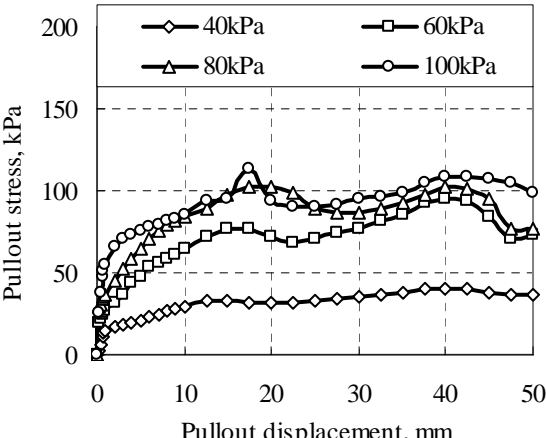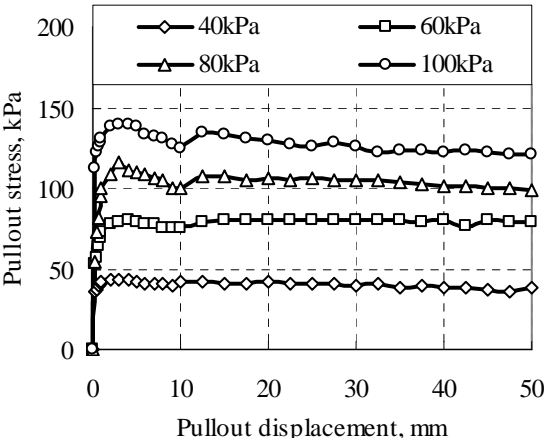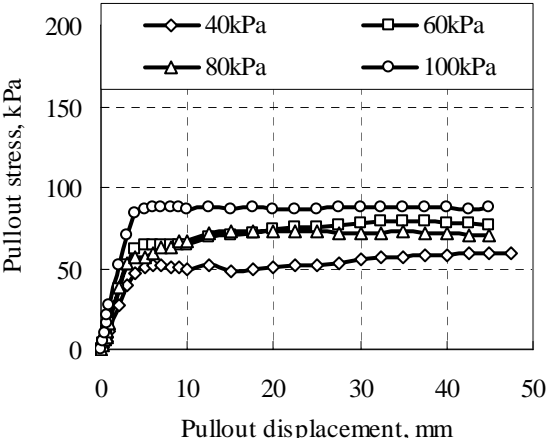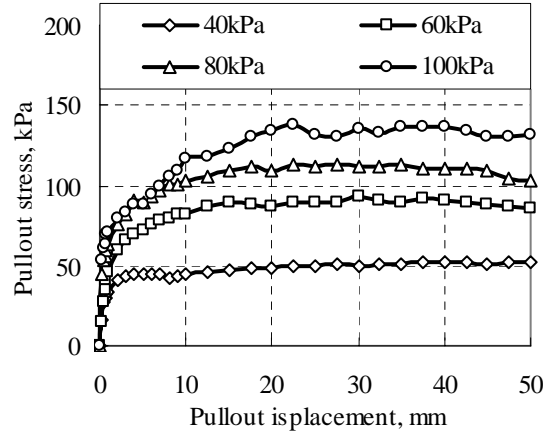
Fig. 5: Pullout stress-displacement relationships for geogrid /geosynthetic reinforcements

a. CCRS

b. CCSS

c. CCC4

d. CCC6
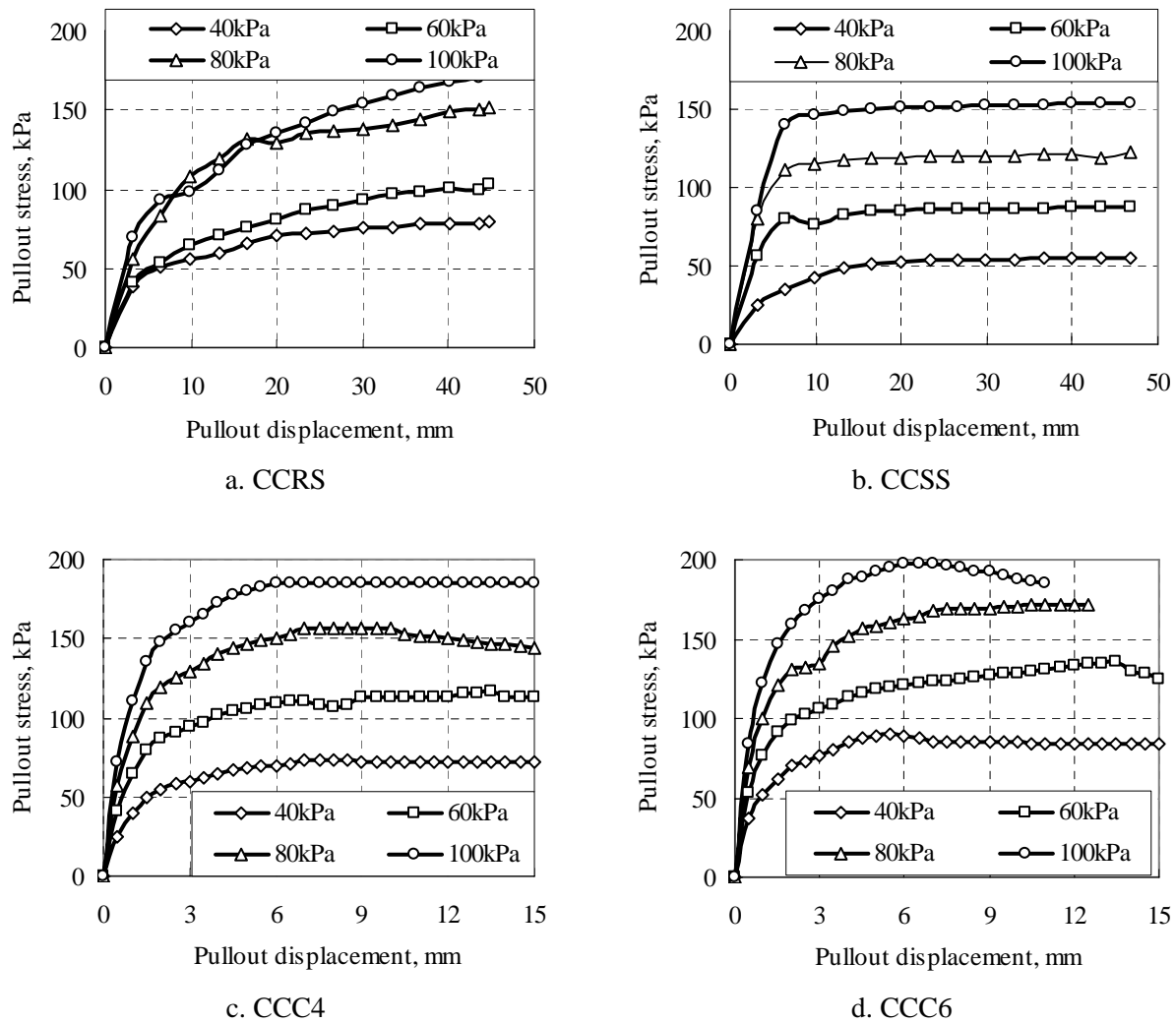
Fig. 6: Pullout stress-displacement relationships for composite reinforcements.

with the linear portion restricted to the displacement of about 2 mm. After that all the curves become non-linear. The non-linearity, at the lower limit, starts with displacement of nearly 2 mm and then continues downswing until the displacement of 50 mm. The pullout stress at the lower normal stress is almost constant and resumes its bi-linear characteristics.

Pullout stress-displacement relationships for CCRS indicate that all the four graphs belong to the same characteristic like the combination of flat curvilinear shape, initially, and linear pattern, finally. The curvilinear portion can be taken in a group with a linear portion restricted to pullout displacement of about 15 mm. After that, all the curves become linear. The linearity, at the lower limit, starts with a pullout displacement of nearly 15 mm, and then continues

upward direction until a displacement of 45 mm. Unlike the curves for other reinforcements stated above, pullout stress-displacement curves for CCRS are almost showed their gradually increasing resistance owing to the effect of small stone on the surface.

For the case of CCSS, an inspection of the plotted results of the stress-displacement relationships indicates that they are, in general, of bi-linear characteristics. However, a resemblance of linearity is seen for smaller part of the relationships (between 0.0 mm to 6 mm displacement). A greater part of linearity can be taken from 7 mm to 45 mm displacement. It is also found from this figure that there is more or less no variation of the pullout stress with the increase in displacement. This phenomenon mainly depends on

the plain surface of the CCSS, and failure of bonding stresses between the CCSS's surfaces and the backfill materials. It is evident from the pullout stress-displacement relationships of CCC4 and CCC6 that they are, in general, of curvilinear characteristics. The pullout stress is more for higher normal stress and higher number of channels. The distinction of the pullout stresses is clearly visible corresponding to each applied normal stress condition. This is due to the effect of existence of channels on the surface of composite and number of channels.

4.2 Interaction Resistances (Cohesion and Internal Friction)

The pullout stresses acted on both sides of reinforcement are measured directly, and plotted in Figs. 7 and 8 with the applied normal stresses as abscissa and pullout out stresses as ordinate. The least square linear lines obtained by the regression analysis for different types of reinforcements are similar to that from the method of failure envelope for direct shear test, but having the resistance at two surfaces of the reinforcements. Two surfaces of reinforcement means two times of pullout stresses as compared to direct shear test which gives double intercept on Y axis, but there is no effect on the angle of the linear lines, because all the normal stresses will increase in the same fashion when the resistance acted on two surfaces. These points should be taken into account in calculating the cohesion and internal frictional resistances under pullout test for safe design of reinforced soil structures. The following design equations (Table 5) are obtained as a result of pullout tests for different reinforcements from the straight lines as plotted in Figs. 7 and 8.

4.3 Ultimate Pullout Strength

For the sake of clear perception of the bearing capacity of reinforced soil under pullout test, the ultimate pullout strength corresponding to the different overburden pressures (normal stresses) of the reinforced soil with different types of reinforcements are plotted in Figs.7 and 8 for sandy and clayey backfills, respectively. It is evident that the ultimate pullout strengths are increasing with the increase in overburden pressure containing any type of reinforcements and backfill materials. There was more scatter on the ultimate pullout strength with the

increase in normal stress for sandy backfill than for clayey backfill. This may be the effect of the particle size of the backfill, properties of backfill and surface characteristics of the reinforcements.

For the sake of clarity, relationships between the interaction resistances in terms of cohesion and frictional angle as well as types of reinforcement are plotted in Figs. 9 and 10 as the bar diagram. It is evident from these figures that, in general, both the cohesion and frictional angle are more for composite reinforcement than for any other reinforcements. The cohesion values of EMM, SSM10, GM, FGM, NGM, SGS, CCRS, CCC4 and CCC6 are higher in clayey backfills whereas it is higher for SSM3, CM, HDPE and CCSS in sandy backfills. A slight variation of the frictional angle depending on the reinforcements is observed. It can be noticed that EMM, SSM3, SSM10, CM, HDPE, GM, FGM, NGM and SGS show higher frictional angle in clayey backfill whereas SGM, CCRS, CCSS, CCC4 and CCC6 show higher frictional angle in sandy backfills.

It is interesting to note that the cementitious composites can deform at the joint of panels depending on the design of joint and field requirement, Therefore, the reinforced soil structures containing composite reinforcements can deform and possesses flexibility. Moreover, results indicates that it has more cohesion and frictional resistance which give more reliable design of reinforced soil structures as compared to conventional reinforcements, and thus it increases the resistance even against the seismic loads that may occur during earthquakes.

It is noted here that the backfill materials used in this study are not absolutely sand or clay i.e. neither the sandy soil is pure sand nor the clayey soil is pure clay. Grain size curve given in Fig. 2 and data depicted in Table 1 indicate that the sandy soil contain nearly 24% clay and silt fractions which is mainly responsible for obtaining the cohesion intercept of the sandy soil. On the other hand, clayey soil used in this research contains nearly 34% sand which is mainly responsible to obtain frictional resistance of clayey soil. When these particles are come in contact to the reinforcements, they give a synergetic action between the soil and the reinforcement producing a cohesion intercept at the interface between the soil and the reinforcement depending on the type of materials. These are the main reasons of obtaining the closer values of cohesion given in Table 3 for sandy and clayey soils used in this research.
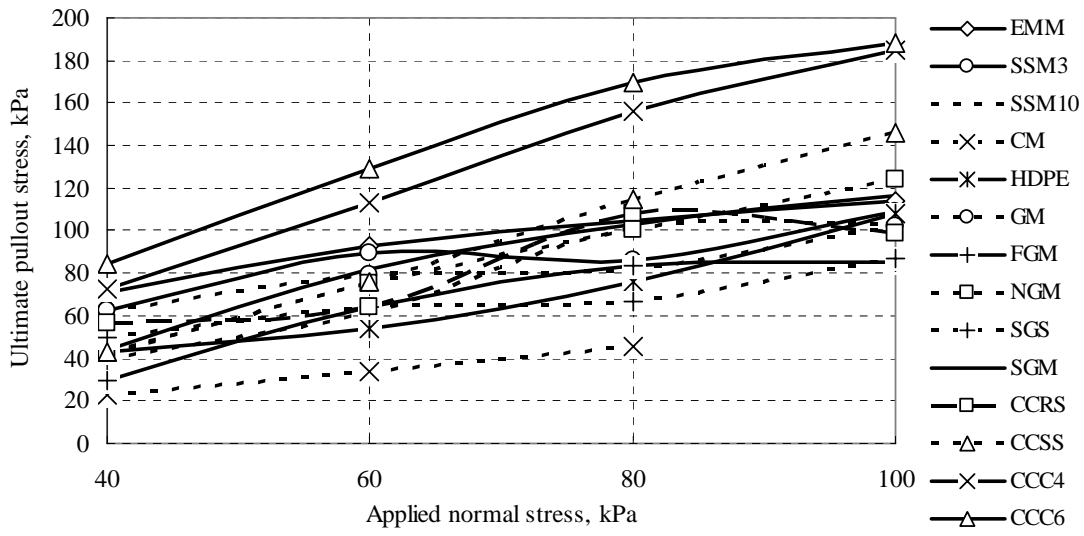
Fig. 7: Ultimate pullout strengths vs. applied normal stress for various reinforcements in sandy soil.
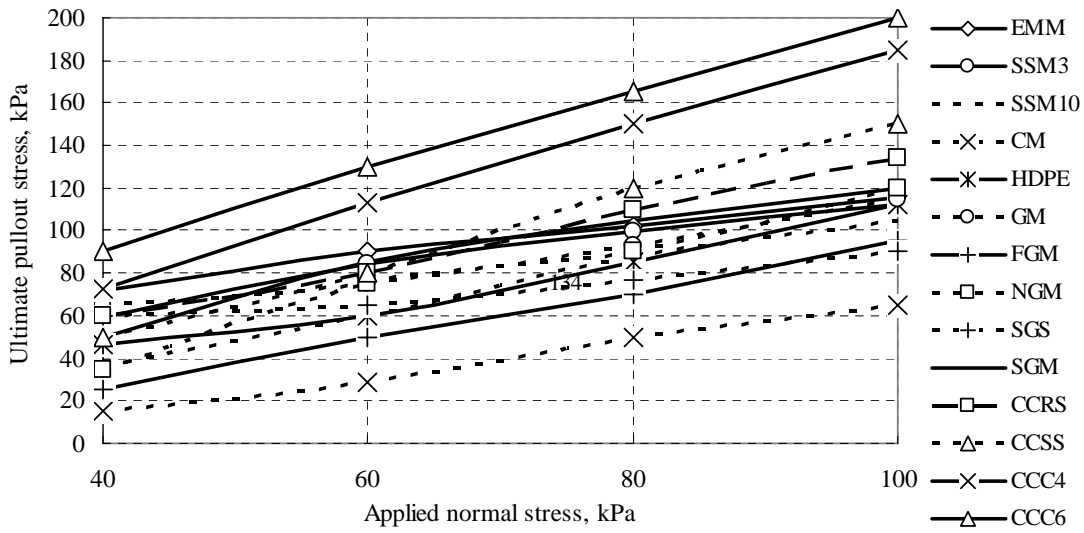
Fig. 8: Ultimate pullout strengths vs. applied normal stress for various reinforcements in clayey soil.
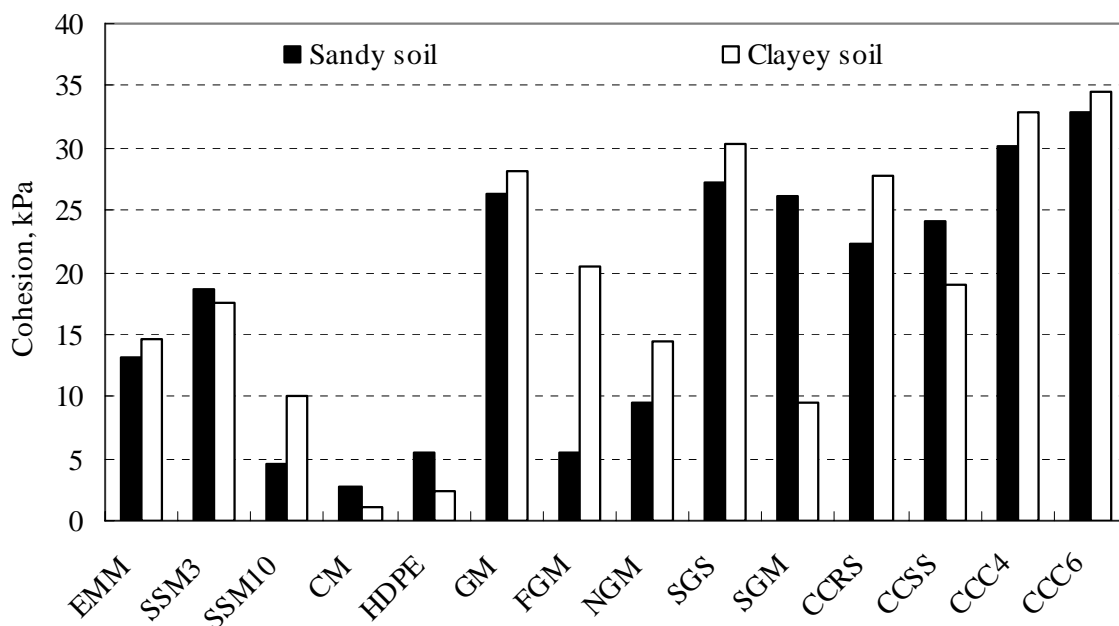
Fig. 9: Comparison of cohesion values under pullout tests with sandy and clayey backfills
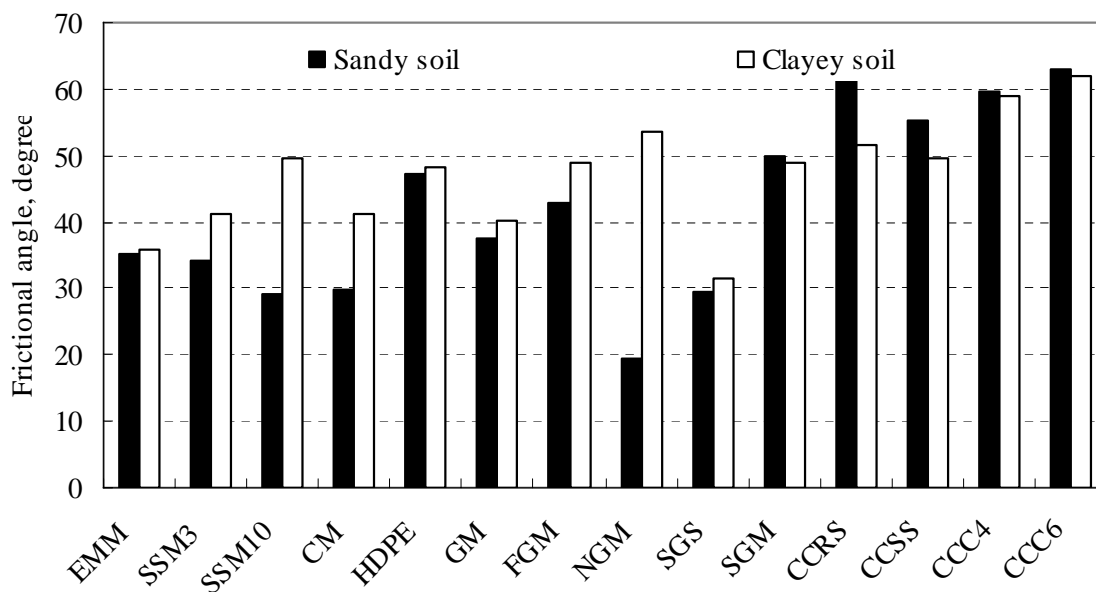
Fig. 10: Comparison of frictional angle under pullout tests with sandy and clayey backfills

It is obvious that the research presented in this paper mainly deals with the comparative study of pullout resistance of different reinforcements in two types of backfill materials. Therefore, the two failure modes such as pullout and slippage of reinforcements only were taken into account in this study. Other failure modes such as tensile failure or breakage of

reinforcement were not indicated in this article because these were not observed in this investigation. After the tests, it was observed that there was no tensile failure or breakage of reinforcement occurred during the tests.

As depicted above, the tests were performed according to the standard of the Japanese

Table 5: Design equations of pullout stresses for various reinforcements in
sandy and clayey backfills

Reinforcements	Sandy backfill	Clayey backfill
EMM	$\tau = 0.70\sigma + 13.13$	$\tau = 0.72\sigma + 14.60$
SSM3	$\tau = 0.68\sigma + 18.69$	$\tau = 0.87\sigma + 17.50$
SSM10	$\tau = 0.56\sigma + 04.52$	$\tau = 1.17\sigma + 10.00$
CM	$\tau = 0.57\sigma + 02.71$	$\tau = 0.87\sigma + 01.16$
HDPE	$\tau = 1.08\sigma + 05.45$	$\tau = 1.11\sigma + 02.30$
GM	$\tau = 0.76\sigma + 26.23$	$\tau = 0.84\sigma + 28.20$
FGM	$\tau = 0.93\sigma + 05.56$	$\tau = 1.15\sigma + 20.50$
NGM	$\tau = 0.35\sigma + 09.47$	$\tau = 1.35\sigma + 14.50$
SGS	$\tau = 0.56\sigma + 27.30$	$\tau = 0.61\sigma + 30.30$
SGM	$\tau = 1.19\sigma + 26.20$	$\tau = 1.15\sigma + 09.50$
CCRS	$\tau = 1.85\sigma + 22.34$	$\tau = 1.26\sigma + 27.80$
CCSS	$\tau = 1.44\sigma + 24.17$	$\tau = 1.17\sigma + 19.00$
CCC4	$\tau = 1.70\sigma + 30.20$	$\tau = 1.67\sigma + 32.92$
CCC6	$\tau = 1.95\sigma + 32.95$	$\tau = 1.88\sigma + 34.50$

Where, τ is the shear resistance of reinforced soil on both surface of reinforcement
under pullout test in kPa and σ is the normal stress (overburden pressure) on
reinforcement in kPa.

Geotechnical Society (JGS), T941-199X which used the clamping system between the loading cell and pullout box apparatus out-side the soil. It is noted here that all the reinforcements were clamped in the same way and thus the errors of the test results if any, would be in the same trend, which might be neglected because it is a comparative study.

It is evident that reinforcement of soil with different materials still remains a science in its infancy, and ideas are evolving towards assessing the optimal material for soil reinforcement applications. Although, the researches on in-soil clamping system are beyond the scope of this research article and field applications of this works have not been thoroughly examined, it can be considered a good start to achieve the goal towards the development of composite reinforcement as supplementary construction materials made with mesh and mortar. It was observed that the composite reinforcements gained maximum strength than the ordinary reinforcements indicating that the composite reinforcement performed much better than the ordinary reinforcement alone.

5. CONCLUSIONS

From the above compilation of the test results, we can arrive at the following conclusions:

1. The results of the pullout test given in various charts and diagrams in terms of stress-displacement and comparison of cohesion values as well as interaction resistances may be helpful to aid in effective design of reinforced soil structures.
2. For all types of reinforcements under pullout test in this study, the common feature is that there is an increase in pullout stress with the increase in displacement and normal stress.
3. Equations for strength parameters of reinforced soil such as cohesion and internal friction of the individual reinforcement given in this paper will be useful in the design of reinforced soil structures.
4. Among various reinforcement reported in this paper, composite reinforcement made of cement mortar reinforced by wire mesh shows the best performance with a synergetic action from two components, where interfacial friction between backfill and cement matrix provides adequate frictional capacity, and wire mesh in mortar

provides required tensile strength, enabling effective design of reinforced soil structures.

5. It is observed that both cohesion and frictional resistance of EMM, SM3, SM10, CM and NGM are very low in both sandy and clayey soils. Therefore, use of these reinforcements is not so effective for the design of reinforced soil structures. Soil structures that need to be more strength but permeable such as road embankments, the use of GM, FGM, SGS and SGM can be recommended for it depending on the type of backfill materials. On the other hand, soil structures that need to be impervious and more strength such as water storage structures e.g. dam; the use of HDPE and composite reinforcements may be recommended in this case. Results depicted in this research indicate that the degree of compaction does not make a given material more effective.

6. Composite reinforcements made of non-corrosive material may be more durable than the wire mesh and conventional geogrids /geosynthetics. The cost of the composite reinforcement depends on the materials to be used, such as, sand, cement and reinforcements plus labor. As it is known that the cost of the mortar is much cheaper than the reinforcing materials, it is expected that the total cost of the composites would be minimum which will balance the labor charge. In addition to this, it is observed that the composite reinforcement provides much strength in reinforced soil; it would be more stable than any other reinforcements. Although, the durability performance and the cost analysis have not been performed in this research article; it can be considered a good start to achieve the goal towards the development of the composite reinforcement system as soil reinforcement applications.

REFERENCES

1. Fukuoka, M. (1998). Earth Reinforcement-West and East, Int. Geotech. Symp on Theory and Practice of Earth Reinforcement, 1, 33-47.

2. Gurung, N. and Y. Iwao (1999). Pullout Test Analysis for Georeinforcement, Geotextiles and Geomembranes, 17, 157-170.

3. Izawa, J. Ishihama, Y., Kuwano, J., Takahashi, A. and H. Kimura (2003). Effects of Geogrid Properties on Pullout Resistance, Landmarks in Earth Reinforcement, 1, 55-60.

4. Jones, C. F. W. B. (1996). Earth Reinforcement and Soil Structures, Buterworths Advanced Series in Geotech. Eng, London, 379.

5. Kenju M., Shigeo I. and M. Katsuhiko (1985). Geotekisutairu to suna no masatsu teikou ni tsuite (Frictional Resistance of Geotextile and Soil), Proc. of the 30th Geotechnical Engineering Symposium, 87-92.

6. Koerner, R. M. (1994). Designing with Geosynthetics, Third Edition, Prentice Hall Inc. 781.

7. Kuwano, J., Takahashi, A. and J. Kimura (1999). Mechanical Properties and Pullout Characteristics of Geogrids Used in Japan, Geosynthetics Engineering Journal, 14, 195-204.

8. Lafleur, J., Sall, M. S. and A. Ducharme (1987). Frictional Characteristics of Geotextiles with Compacted Lateritic Gravels and Clays, Geosynthetics, New Orleans, 205-215.

9. Lauwers, D. C. (1991). PVC Geocomposite for Improved Friction and Performance Properties, Geosynthetics, IFAI, Atlanta, GA, 101-112.

10. Madhab, M. R., Gurung, N. and Y. Iwao (1998). A theoretical Model for the Pullout Response of Geosynthetic Reinforcement, Geosynthetic International, 5(4): 399-424.

11. Mahmood, A. A., Zakaria, N. and F. Ahmad (2000). Studies on Geotextiles/Soil Interface Shear Behavior, Electronic Journal of Geotechnical Eng., 13: 1-14.

12. Milligan, G. W. E. and E. Palmeria (1987). Prediction of Bond Between and Reinforcement, Int. Conf. on Prediction and Performance in Geotech. Eng, Calgary, 1: 147-153.

13. Miyamori, T., Iwai, S. and J. K. Makiuchi, (1988). Frictional Characteristics of Non-Woven Fabrics, Proc. 3rd. Int. Conf. on Geotextiles, Osterreichischer Ingenieur-und Architekten, Vienna, 701-705.

14. Murray, R. T. and M. J. Irwin (1981). A Preliminary Study of TRRL Anchored Earth, Transport and Road Research laboratory Report SR, 674.

15. Richards, E. A. and J. D. Scott (1985). Soil Geotextile Frictional Properties, Proc. 2nd. Canadian Sym. on Geotextile and Geomembrane, Canadian Geotechnical Society, Edmonton. Alberta, 13-24.

16. Sivakumar B. G. L., Srinivasa, R. B. M. and A.

Sridharan (2002). Evaluation of Bearing Capacity Improvement Using Composite Geogrids, Journal of Testing and Evaluation, ASTM, 30(4): 362-366.

17. Sivakumar B. G. L., Shridharan, A. and B. K. Kishor (2003). Composite Reinforcement for Reinforced Soil Applications, Soils and Foundations, 43(2): 123-128.

18. Sobhi, S. and J. T. H. Wu (1996). An Interface Pullout Formula for Extensible Sheet Reinforcement, Geosynthetic International, 3(5): 565-582.

19. Sridharan A., Srinivasa, M., Bindumadhava, B. R. and K. Revanasiddappa (1991). A Technique for Use of Fine Grained Soil in Reinforced Earth, Journal of Geotech Eng, ASCE, 117(8): 1175-1190.

20. Williams, N. D. and M. R. Houlihan (1987). Evaluation of Interface Friction Properties Between Geosynthetics and Soils, Geosynthetics, New Orleans, 616-627.

DISTINGUISHING VARIETIES OF PADDY SEEDS BASED ON Vis/NIRS AND CHEMOMETRICS

Xiao-li Li[*] and Yong He[*†]

ABSTRACT

The potential of visible and near infrared reflectance spectroscopy (Vis/NIRS) was investigated for its ability to nondestructively distinguish the varieties of paddy seeds. A total of 150 samples were prepared for spectra collecting from spectroradiometer (325-1075 nm). Then principal component analysis (PCA) was performed on the spectra of all the samples. PCA compressed hundreds of spectral data into several new variables, which can explain the most variance of original spectra. The 2-dimension plot was drawn with the scores of the first 2 PCs, it provided the clustering information of the varieties of paddy seeds. Principal component analysis showed that the cumulative variance of first 4 principal components (PCs) were 99.6%. So, the first 4PCs were used to replace the original spectra. The first 4 PCs were used as inputs of a back propagation artificial neural network (ANN). One hundred and twenty five samples were selected from five varieties randomly (25 for each variety), then they were used as train samples to develop ANN model. The optimal topology structure was 4-7-1 for three-layer neural network. This model was used to predict the varieties of 25 unknown samples, and the recognition rate was 100%. This model was reliable and practicable, and Vis/NIRS has substantial potential for distinguishing varieties of paddy seeds.

Keywords: *Vis/NIRS; Principal component analysis (PCA); Artificial neural network (ANN); paddy seed; Distinguish; Variety.* © 2007 AAAE

1. INTRODUCTION

Paddy is the most important food crop in the world. In China, the planting area of paddy is one quarter of that of entire food crop, and the output of paddy is half of all the output of the entire food crop. With the development of paddy breeding, the discrimination of different varieties of seeds becomes more and more important. But the methods to distinguish the different varieties are still traditional. The traditional methods are mainly based on the morphological characteristics or chemical experiments. In morphological methods, appraiser needs expert training, and accuracy depends on the skills of the appraiser. In chemical methods, the sample must be destructed, and it spends much time (Yan and Huang, 1996). So a simple, rapid, non-destructive, accuracy and cost effective method determination of paddy seed needs to be developed.

The modern NIRS analytical technique has the advantages of speediness, high-level efficiency, low cost and non-destruction, so it has widely been applied in estimate rice quality characteristics (Wu and Shi,

2007; Lu *et al.*, 2007). Lu *et al*. evaluated eating quality of Chinese indica rice based on visual and near-infrared reflectance spectroscopy (Lu *et al.*, 2007). Bao *et al.* (2007) studied the property of rice starch using near infrared reflectance spectroscopy. Natsuga and Kawamura (2006) studied the potential of near-infrared reflectance spectroscopy for determination of moisture content, appearance and amylogram characteristic of rice. And the discrimination of coffee varieties (Esteban-Diez, Pizarro and Gonzalez-Saiz, 2004), the varieties of waxberry (He and Li, 2006), and wheat varieties (Utku, 2000) have been studied based on the visible/near infrared spectroscopy. The spectral absorbance peaks overlap in Vis/NIRS wavelength range, and the analysis of spectral datum is very difficult. So, proper chemometrics tools should be employed.

Principal component analysis (PCA) is a way of data digging. A few new variables can be extracted to replace original vast variables after PCA, and the principal information of spectrum can be preserved, then the analysis of spectral datum becomes easy.

---

[*] College of Biosystems Engineering and Food Sciences, Zhejiang University, Hangzhou 310029
[†] Corresponding Author : Fax: 086-571-86971143, Email: yhe@zju.edu.cn

Back propagation artificial neural network (ANN) model is a powerful learning system. A good non-linear mapping can be found between input and output variables based on the ANN. It has already been proven that this kind of model could approach any consecutive non-linear curve (Clifford and Lau, 1992). So, it is used for studying non-linear system extensively.

The objective of this study is to put forward a rapid and non-destructive method to discriminate the variety of paddy seeds based on visible/near infrared reflectance spectroscopy (NIRS) technique. The new method not only can qualitatively analyze the variety of paddy seeds in the PCs space, but also can accurately discriminate the variety of unknown samples based on ANN classifier.

2. MATERIALS AND METHODS

2.1 Reflectance Measurements of Paddy Seeds

In the research, a handheld FieldSpec (Analytical Spectral Device) spectroradiometer was used to collect spectrum of paddy seed. The spectroradiometer measures reflectance from 325 to 1075 nm at 3.5-nm bandwidth. Then all data are interpolated to 1-nm intervals. Five varieties of paddy seeds were selected randomly as objects, which were IIYou46, IIYou63, Shanyou10, Shanyou63 and Zhongjiajing21 (Table 1). A total of 150 samples of paddy seeds were prepared for reflectance measurement. Uniform glass vessel (diameter: d=95 mm, height: h=14 mm) was adopted

to load the seeds, which covered the bottom of the vessel (He, Li and Shao, 2005). The spectroradiometer was fixed 100 mm above the surface of the sample with the field of view (FOV) of 25º. A 150W halogen lamp was fixed 150 mm above the sample, and the angle between the incident light and the spectroradiometer detector was about 45º (Fig. 1). In order to reduce the operating error, for each sample, three reflection spectra were taken for three equidistant rotation positions of approximately 120º around the center of the sample. For each reflection spectra the scan number was 10 at exactly the same position, a total scan for each example was 30. A 65 mm^2 BaSO$_4$ white reference disk was used for the relative reflectance (R) by comparing near infrared energy reflected from the target with the standard optical reference. The software was ASD View Spec Pro, Unscramble V9.5 (CAMO, PROCESS, AS, OSLO, Norway) and DPS (data procession system for practical statistics) (Tang and Feng, 2002).

2.2 Pretreatment of the Optical Data

To reduce the noise, the smoothing way of Savitzky-Galay smoothing was used. After trying, the segment size of 3 was chosen with better performance compared with other sizes. The second type of pretreatment was the use of the multiplicative scatter correction (MSC). The technique was used to correct additive and multiplicative scatter effects in the spectra. Due to the asymmetry of sample granule and light scattering in sample, the light did not always
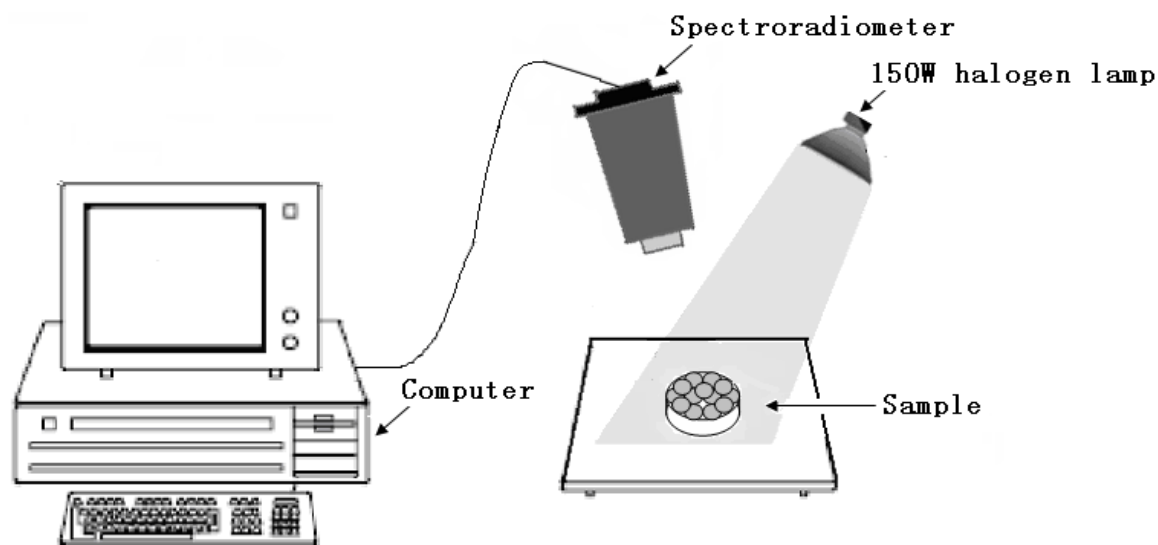
Fig. 1: Simple diagram of the experiment setup

Table 1: Description of samples

Varieties	Sort	Producing area	No.
IIYou46	Hybridization indica type rice	Zhejiang of China	30
IIYou63	Hybridization indica type rice	Sichuan of China	30
Shanyou10	Hybridization indica type rice	Zhejiang of China	30
Shanyou63	Hybridization indica type rice	Jiangshu of China	30
Zhongjiajing21	Non glutinous rice	Zhejiang of China	30

travel the same distance in the sample before it was detected. A longer light traveling path corresponds to a lower relative reflectance value, since more light is absorbed. This causes a parallel translation of the spectra. This kind of variation was not useful for the calibration models and was eliminated by MSC-technique. The pretreatments and calculations were carried out by using 'The Unscrambler V9.5 (CAMO, PROCESS, AS, OSLO, Norway), a statistical software package for multivariate calibration. To avoid low signal-noise ratio, only the wavelength ranging from 400 to 1000 nm was used in this investigation (Qi *et al.*, 2003).

2.3 Methodology

Neural network is known as useful tool for pattern recognition, identification, and classification (Mouwen, 2006). A neural network model can determine the input-output relationships for a complicated system, and such a model can provide data approximation and signal-filtering functions beyond optimal linear techniques, it is more adaptable than conventional statistical models to provide more robust results in analyzing a complicated system. Artificial neural network with back propagation algorithm was used for developing neural classifiers for sorting paddy seeds based on varieties. A schematic diagram of multi-layer neural network architecture is shown below (Fig. 2). However, if all the spectral data were used as the input of the ANN classifier, the classifier would be difficult to converge and training time will be too long. So, extraction diagnostic information is an importance step. The artificial neural network was implemented by the neural networks toolbox of Matlab.

Principal component analysis is a very effective way of data reduction. It summarizes data by forming new variables, which are linear composites of the original variables. The new variables (principal components) are uncorrelated and represent the most common variations of the data. Score is the estimated value for a principal component (PC). Each spectrum has a score along each principal component. Before the calibration, the spectra range from 400 to 1000 nm was analyzed by principal component analysis (PCA). The original set of variables is transformed into a set of orthogonal variables. PCA was implemented by the "Unscrambler V9.5" software package. In this paper, principal component analysis was used to extract information and reduce the dimension of spectral data. And the PCs from PCA were used as input variables of ANN classifier. The whole samples were separated randomly into two parts, one part that contained 125 samples was used as reality calibration samples, and the other was used as predicting samples.

3. RESULTS AND DISCUSSIONS

3.1 Features of Vis/NIRS

Fig. 3 shows the reflectance spectra of five varieties: IIYou46 seed, IIYou63 seed, Shanyou10 seed, Shanyou63 seed and Zhongjiajing21 seed. The five samples were selected randomly from each variety. It can be found that spectral curves of five
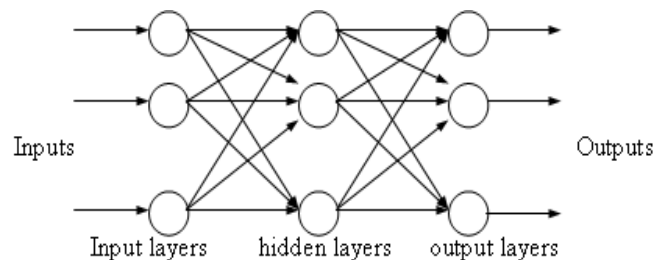
Fig. 2: Diagram of the topological structure of BP neural network

varieties paddy seeds have similar trend. From 400 to 950 nm, the reflectance values increase along with the wavelength adding. There is a valley at 975 nm in these curves of reflectance spectra. It indicates that there is an absorbance peak at around 970 nm. This absorbance peak relates to N-H bond, and may represent protein content (Shenk, Workman and Westerhaus, 2001). There are crossovers and overlapping among the curves of other four varieties. In other words, the reflectance spectrum of each variety is similar with other varieties. So it was difficult to distinguish these varieties directly based on reflectance spectra.

3.2 Principal Components Analysis of Full Spectrum

The principal components analysis was adopted to reduce the dimensionality. PCA was performed on the data matrix which was composed with 600 wavelength variables (from 400 to 1000 nm) and 150 samples. After PCA, many principal components could be generated which were the linear combination of original wavelength variables. Each sample was described with scores in the new principal components space. If samples were plotted in principal components spaces based on the scores. The new image is then called 'PCA scores image'. If the first principal component (PC1) scores and the second principal component (PC2) scores were manipulated, the resultant image was then call PC1 and PC2 scores image, just as Fig. 4. The advantage of using principal components scores image was that it could display the clustering information of varieties from multiple wavelength.

The scatter plot of PC1 (variability; 88.7%)×PC2 (variability; 9.5%) is shown in Fig. 4. The plot gives distributing information about varieties of paddy seeds. In this scatter plot, the five varieties of paddy seeds are composed as five well-defined groups. In short, Zhongjiajing 21 seed samples closely cluster in the quadrant where PC1 and PC2 are negative. All of the II You43 seed samples are closely situated in the quadrant where PC1 is negative and PC2 is positive, while almost all of the II You63 seed samples are scattered in the same quadrant with II You43, but they do not mix with each other. The samples of Shanyou10 and Shanyou63 seed are located at the side of the positive of abscissa, but the boundary of the two varieties is clear. It can be found that the location of

Zhongjiajing21 samples is far from the other four varieties, because the Zhongjiajing21 seed is non glutinous rice, the other varieties seed are hybridization indica type rice; the II You43 and II You63 seed are located in the same quadrant, because the two varieties have the same hybridization female parent II You-32A; and Shanyou10 seed are situated beside Shanyou63 seed, because their same hybridization female parent is Zhenshan97-A. The distributing information shown in Fig. 4 is consistent with the varieties and genic information of paddy seeds. So the discrimination of different varieties become easier in PCs space than in original wavelength space.

3.3 Classification of Paddy Seeds by ANN

PCA found an alternative set of coordinate axes, principal components (PCs), about which data set might be represented. The PCs were orthogonal to each other and they were ranked so that each one carried more information than any of the following ones. The number of principal components was set as 20 in program of Unsrambler software package. Fig. 5 shows the cumulative variance of the first 10 PCs. The first 4 PCs were enough to explain the 99.62% of the total variance. So the 4 new variables were used to replace the 600 wavelength variables. The new matrix was generated that was composed with 150 rows (samples) and 4 columns (variables).

The training of the ANN was done with a basic error back propagation algorithm, in which the neural network processed example patterns and the network output expressed the likelihood that an object corresponded with a training pattern, i.e. the output was a measure of resemblance. The difference between the desired (i.e. 0 or 1) and calculated network output was employed to alter the weight factors between the neurons. Initially network output was random, as all the weight factors were set to random values. However, the difference between desired and calculated network output, defined as the network output error, will gradually became less after every epoch of a training pattern and adjustment of the weight factors. The network output error was defined as $E = \frac{1}{2} \sum_{i=1}^{n} (y_i - \hat{y}_i)^2$, where $\hat{y}_i$ - predicted value of the each sample, y_i - measured value of the each sample, n – number of samples for analysis. One cycle
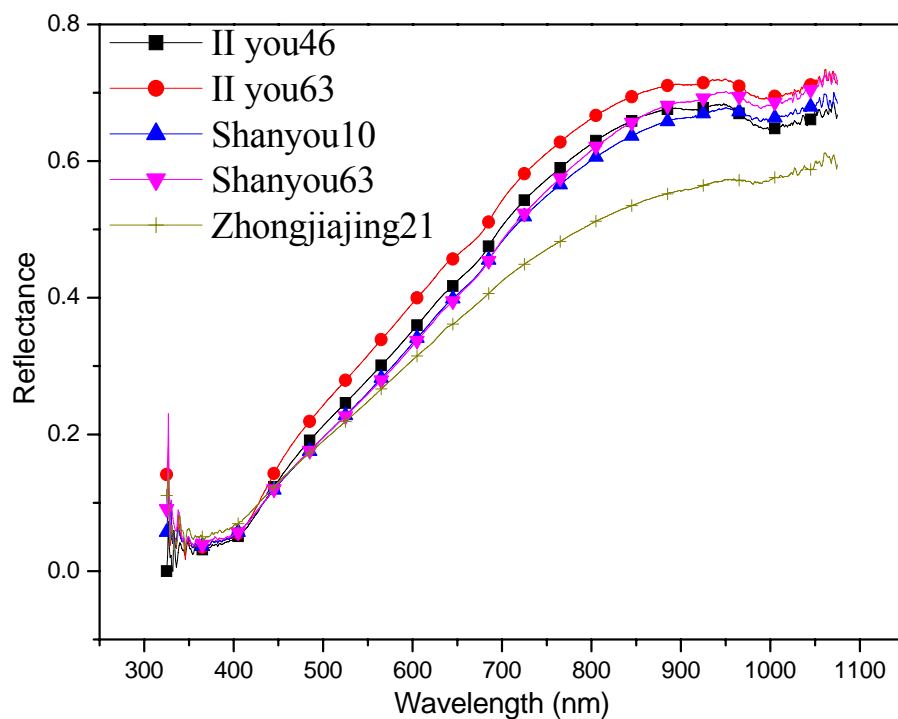
Fig. 3: Vis/NIR spectra of five different varieties paddy seeds
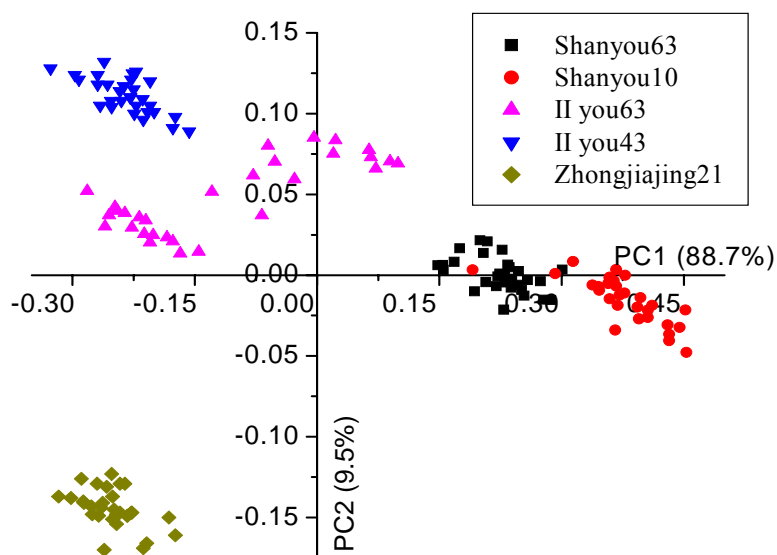
Fig. 4: Scores plots obtained from the PCA (PC1×PC2) of 150 samples
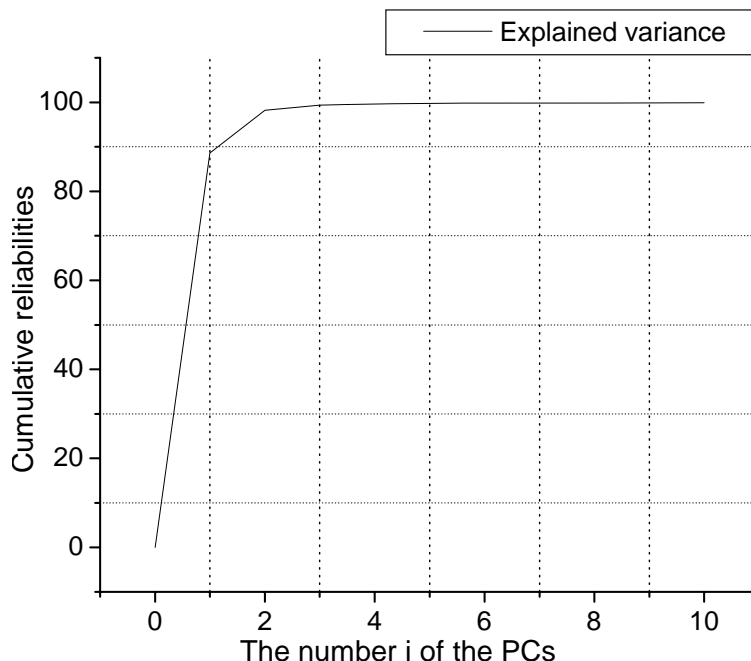
Fig. 5: Ability of explained variance of the first 10 PCs

through all the training patterns was defined as an epoch, and back propagation required many epochs before optimal accordance between desired and calculated network output was established for all training patterns.

The total wavelength was replaced by the 4 characteristic variables. The optimal architecture of neural network could be achieved by adjusting the number of nodes in the hidden layer (Zhao, Qu and Cheng, 2004). A three-layer ANN was built. The structure parameters of ANN were listed in Table 2. The variety of paddy seeds were coded with constant values of 1, 2, 3, 4 and 5, respectively (Wang, Ram and Dowell, 2002) and the same value was used in assigning the class. Network output error was 2.917×10^{-4}. And, 25 unknown samples were distinguished by this model; the recognition rate was 100% (Fig. 6). This model got high correlation coefficient (0.9962) between measured variety and predicted variety of paddy seed.

The result was superior to those obtained by Galvao (2005) in sugarcane varieties with `87.5% classification accuracy, and better than those obtained by Utku (2002) in wheat varieties with recognition of unknown samples (82%, 81%) based on orthonormal transformation. The traditional classification methods including PCA, linear discriminate analysis (LDA) and PCA+LDA can make qualitative discrimination of variety; however they don't get high accuracy at prediction step with unknown sample.

4. CONCLUSION

The above results indicate that it is possible to develop a non-destructive technique for discriminating the varieties of paddy seeds. In this research, a new application of PCA-ANN was developed focused on paddy seed. By means of this new method a close relation was established between reflectance spectra and paddy seed varieties. The model for discrimination the varieties of paddy seeds showed an excellent prediction performance. The network output

Table 2: Structure parameters of ANN model

Transfer function of each layer	sigmoid
Node number of input layer	4
Node number of hidden layer	7
Node number of output layer	1
Goal error	0.001
Momentum	0.2
Epoch	1000
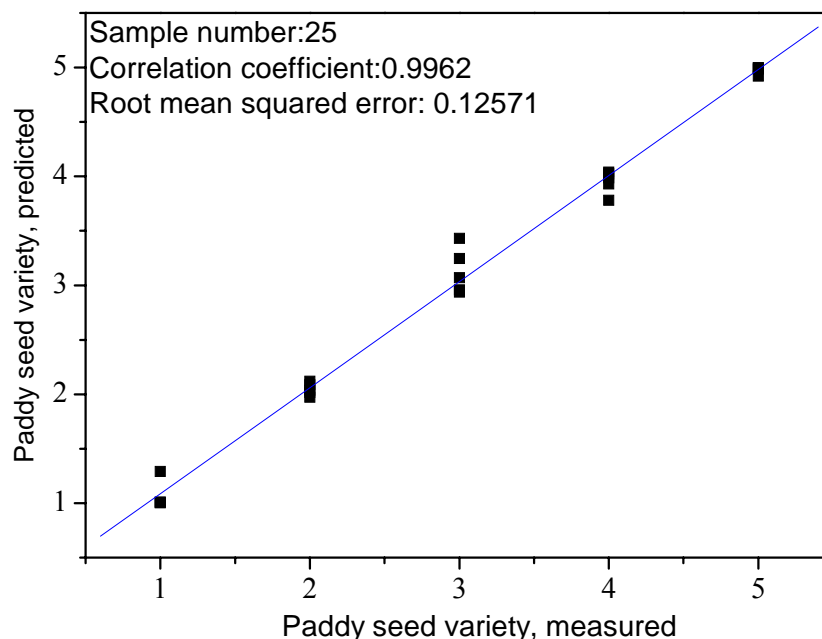
Fig. 6: Prediction result for unknown samples by ANN model (1-IIYou46 seed; 2-IIYou63 seed; 3-Shanyou10 seed; 4-Shanyou63 seed; 5-Zhongjiajing21)

error for the calibration samples was 2.917×10^{-4}. The recognition rate of 100% was achieved. The method combined with PCA-ANN is very suitable for dealing with spectral data, and it will be a very good way in pattern recognition. The describe method can be applied for variety identification and protection. The future ultimate goal of our studies is to expand the varieties and the number of samples and to enhance the applicability of the method.

ACKNOWLEDGEMENTS

REFERENCES

1. Yan, Qi-chuan and Y. J. Huang (1996). Handbook of identification the variety of crop. Beijing: Chinese agriculture Press (in Chinese).

2. Wu, J. G., and C. H. Shi (2004). Prediction of grain weight, brown rice weight and amylose content in single seeds of rice using near-infrared reflectance spectroscopy. Field Crops Research, 87: 13–21.

3. Wu, J. G. and C. H. Shi (2007). Calibration model optimization for rice cooking characteristics by near infrared reflectance spectroscopy (NIRS). Food Chemistry, 103: 1054–1061.

4. Lu, Q.Y., Chen, Y.M., Mikami, T., Kawano, M. and Z. G. Li (2007). Adaptability of four-samples sensory tests and prediction of visual and near-infrared reflectance spectroscopy for Chinese indica rice. Journal of Food Engineering, 79: 1445–1451.

5. Bao, J. S., Shen, Y. and L. Jin (2007). Determination of thermal and retrogradation properties of rice starch using near-infrared spectroscopy. Journal of Cereal Science, 46: 75–81.

6. Natsuga, M. and S. Kawamura (2006). Visible and near-infrared reflectance spectroscopy for determing physicochemical properties of rice. Transactions of the ASABE, 49: 1069−1076.

7. Esteban-Diez, I., Pizarro C. And J. M. Gonzalez-Saiz (2004). An evaluation of orthogonal signal correction methods for the characterisation of arabica and robusta coffee varieties by NIRS. Analytica Chimica Acta, 514: 57-67.

8. He, Y. and X. L. Li (2006). Discriminating

varieties of waxberry using near infrared spectra. Journal of Infrared and Millimeter Waves, 25(3): 192-194 (in Chinese).

9. Utku, H. (2000). Application of the feature selection method to discriminate digitized wheat varieties. Journal of Food Engineering, 46, 211-216.

10. Clifford, G. and Y. Lau (1992). Neural Networks: Theoretical Foundations and Analysis. IEEE, New York, NY, USA.

11. He, Y., Li, X. L. and Y. N. Shao (2005).Quantitative Analysis of the Varieties of Apple Using Near Infrared Spectroscopy by Principal Component Analysis and BP Model. Lecture Notes in Artificial Intelligence, 3809: 1053 – 1056.

12. Tang, Q.Y. and M. G. Feng (2002). DPS Data Processing System for Practical Statistics. Science Publication. Beijing (in Chinese).

13. Qi, X.M., Zhang, L. D., Du, X. L., Song, Z. J., Zhang, Y. And S. Y. Xu (2003). Quantitative Analysis Using NIR by Building PLS-BP Model. Spectroscopy and Spectral Analysis 23 (5): 870-872 (in Chinese).

14. Mouwen, D.J.M., Capita, R., Alonso-Calleja, C., Prieto-Gómez, J., M. Prieto (2006). Artificial neural network based identification of Campylobacter species by Fourier transform infrared spectroscopy. Journal of Microbiological Methods, 67: 131–140.

15. Shenk, J. S., J. J. Workman, and M. O. Westerhaus (2001). Application of NIR spectroscopy to agricultural products. In Hand Book of Near–Infrared Analysis, 419–474. D. A. Burnes and E. W. Ciurczak, eds. New York, N.Y.: Marcel Dekker.

16. Zhao, C., Qu, H. B. and Y. Y. Cheng (2004). A New Approach to The Fast Measurement of Content of Amino Acids in Cordyceps Sinensis by ANN-NIR. Spectroscopy and Spectral Analysis, 24 (1): 50-53.

17. Wang, D., Ram, M. S. and F. E. Dowell (2002). Classifications of damaged soybean seeds using near-infrared spectroscopy. Transactions of the ASABE, 45: 1943−1948.

18. Gãlvao, L. S., Formaggio, A. R. And D. A. Tisot (2005). Discrimination of sugarcane varieties in southeastern Brazil with EO-1 hyperion data. Remote Sensing of Environment, 94: 523-534.

19. Krzanowski, W. J., Jonathan, P., McCarthy, W.V. and M. R. Thomas (1995). Discriminant Analysis with Singular Covariance Matrices. Methods and Applications to Spectroscopic Data Applied Statistics, 44: 105-115.

ERGONOMIC EVALUATION OF MANUALLY OPERATED SIX-ROW PADDY TRANSPLANTER

Rajvir Yadav[*], Mital Patel[†], S.P. Shukla[‡] and S. Pund[§]

ABSTRACT

India is one of the major rice producing and consuming countries in the world. In India, transplanting of the paddy crop depends completely on human labour. In changing scenario of agricultural mechanization, ergonomics plays crucial role for effectiveness of the operation. Therefore the study was undertaken to evaluate the paddy transplanting operation on ergonomic basis and to work out the energy expenditure rate involved in the operation. Manually operated six row paddy transplanter was selected for the study and the male and female subjects selected randomly in the age group of 25-35 years operated it. The heart rate (HR) of the subjects was measured by computerized polar heart rate monitor (HRM) and it was taken as a base to work out energy expenditure rate. A Novatech load cell with digital indicator was used for the measurement of push-pull force. The field capacity of six row manually operated paddy transplanter was found to be 0.38 ha day^{-1} while for transplanting by hand it was found to be 0.04 ha day^{-1}. The average energy expenditure for male and female workers for transplanting operation by manually operated paddy transplanter was found to be 30.70 and 32.58 kJ min^{-1}, respectively. The operation was graded as 'heavy work' on the basis of heart rate. The rest pause, for achieving functional effectiveness during transplanting the paddy by six-row transplanter, was found to be 14.30 min followed 30 minutes of work. More force in pulling the transplanter in forward direction is required by the subjects as compared to handle up and handle down operation. The average force required for pulling the trasplanter was 130.32 and 145.12 N for male and female subjects, respectively. More force is required for female workers as compared to male workers because of males are taller and thus exerted a more upward-oriented force on the unit thus reducing the drag force on the runners.

1. INTRODUCTION

India is one of the major rice producing and consuming countries in the world. Rice is also the single most important crop in Indian agriculture. Paddy is grown in about 44.55 Mha in India (22.8% of the total cropped area) and has the largest acreage in the world after China. It is the staple food for two-thirds of Indian population and provides 20-25% of agricultural income (De and Babu, 2004). Rice can also be grown in dry-fields, but from the twentieth century paddy field agriculture became the dominant form of growing rice. Paddy fields are typical in feature of rice-growing countries of east and southeast Asia, including Malaysia, Nepal, China, Sri Lanka, Myanmar, Thailand, Korea, Japan, Vietnam, Taiwan, Indonesia, India, and Philippines. They are also found in other rice-growing regions such as Piedmont (Italy), the Camargue (France) and the Artibonite Valley (Haiti). Paddy is generally grown by transplanting under wetland conditions or direct seeding depending upon the availability of water. Transplanting essentially refers to the planting of 20-35 days old and 20-30 cm high seedlings raised in nurseries and uprooted for transplanting either manually or mechanically (Mehta *et al.*, 1990).

Presently in India, transplanting of the paddy crop completely depends upon manual labour. Manual paddy transplanting is a labour-intensive operation comprising nursery raising, uprooting of the seedlings, transporting and transplanting the uprooted seedlings in the main fields, with a total labour requirement of about 250-320 man-hour ha^{-1} (Jain and Philip, 2003). High labour demand during the peak periods

---

[*] Professor, and Corresponding Author, College of Agril. Engg. & Technology, Junagadh Agril. University, Junagadh 362001, India. E-mail: ryadav61@gmail.com and rajvir_yadav1961@yahoo.co.in

[†] Design Engineer, Jain Irrigation Ltd., Gitanjali-2 Chikuwadi, Jetalpur Road, Vadodara, India. E-mail: mb_patel81@yahoo.co.in

[‡] Associate Professor, Department of Agril. Engineering, Navsari Agril. University, Navsari, India

[§] Dy. Manager, R&D Centre, Mahindra & Mahindra Ltd., Satpur, Nashik – 422 007, India. E-mail : pund.s@mahindra.com

adversely affects the timeliness of operation, thereby reducing the crop yield. To offset these problems, mechanical transplanting is the solution. There are more than 200 million agricultural workers of which more than 35% are female workers (Gite and Singh, 1997). These workers are exposed to all kind of machine and environmental hazards. Mechanization not only changes the structure of labour in agriculture, but also influences the nature of the workload. Farm implements and machinery hitherto have not been ergonomically designed. Hence there is an urgent need to study the ergonomic aspects to quantify the drudgery involved in agricultural operations especially in rice farming.

Physiological cost of work is influenced by the health of the operator, nutrition, basal metabolic rate (BMR) and energy expended while working. These measurements are also important from the safety point of view because whenever physical capacity of a person in exceeded, it is bound to cause considerable fatigue and decrease in the degree of alertness of the subject, making the operation unsafe. Heart rate bears a linear relationship with the intensity of physical exercise and oxygen consumption especially if the steady state is reached. Moreover heart rate monitor can measure instantaneous heart rate continuously over a period of time under field condition. Therefore, several research workers have used heart rate for assessment of physical and physiological workload on the workers (Le Blanc, 1957; Suggs and Splinter, 1961). Keeping in view the above aspects, ergonomic evaluation of manually six-row paddy transplanter is undertaken.

2. REVIEW OF LITERATURE

Christensen (1953) and Zander (1969) suggest the physical workload on the basis of energy expenditure and heart rate as given in the Table 1.

It was therefore evident that estimation of EER by measuring HR under field or laboratory conditions would be an acceptable and fairly accurate method for operator's performance assessment.

Lehmann (1958) stressed upon the need to figure out the reasonable ceiling of energy expenditure over the period of conventional working day. He found that the maximum energy output, a normal man can afford in long run, is about 4800 kcal day^{-1} subtracting his estimate of basal and leisure requirements of about 2300 kcal day^{-1}, leaves a maximum of about 2500 kcal day^{-1} available for the working day. Although he proposed a maximum of about 2000 kcal day^{-1} as a normal load. In continuation to this, Murrell (1965) developed equation (1) for total amount of rest required during a certain work period based on average energy cost

$$R = \frac{T(K-5)}{K-1.5} \qquad (1)$$

Where, R= Rest time (min);
       T= Total working time (min) and
       K= Average kilocalories per minute of work and value 5 kcal min^{-1} adopted as standard. The value 1.5 is an approximation of resting level in kcal min^{-1}.

Morehouse and Miller (1963) concluded that a period of 3-5 minutes is considered suitable for pulse rate to stabilize depending upon the nature of exercise. Tomilson (1970) reported that a rapid increase occurs in the heart rate at the start of work and highest

Table 1: Grade of physical work based on EER, HR and OCR

Sl. No.	EER, kcal min^{-1}	HR, beats min^{-1}	OCR, 1 min^{-1}	Grade of work
1	<2.5	<75	<0.5	Very light
2	2.5-5.0	75-100	0.5-1.0	Light
3	5.0-7.5	100-125	1.0-1.5	Moderately heavy
4	7.5-10.0	125-150	1.5-2.0	Heavy
5	10.0-12.5	150-175	2.0-2.5	Very heavy
6	>12.5	>175	>2.5	Unduly heavy

increase takes place within the first 15 seconds of exercise and it gradually becomes constant. For better muscular efficiency, the dynamic effort of a repetitive nature should not exceed 30% of maximum (Van Wely, 1970). Therefore, the tools should be such that the operator does not have to exert more than 7.5 kg push or 6.0 kg pull.

Martin and Chaffin (1972), Ayoub and McDaniel (1974), and Chaffin *et al.* (1983) found that the height at which push-pull forces were applied was the most important variable in affecting the force output. Chaffin *et al.* also reported volitional postures during maximal push and pull exertions in sagital plane of 67 cm, 109 cm, and 152 cm heights. They concluded that the foot placement, handle height and body postures all affected the push-pull strength.

McCormick (1976) reported that the posture of workers while performing some tasks is another factor that can influence energy requirements. Transplanting in bending posture required the highest energy than any other posture. Saha *et al.* (1979) reported that acceptable workload for average young Indian worker varies between 30 - 40% of an individual maximum aerobic power under comfortable environment conditions. The corresponding heart rate and energy expenditure reported by the author were 110 beats min^{-1} and 18 kJ min^{-1} respectively. Considering the limit for acceptable workload (AWL) for Indian workers is considered as 14.6 kJ min^{-1} they worked out the relation between energy expenditure rate (EER) and heart rate (HR) as presented by equation (2).

$$EER = \frac{(HR - 66.0)}{2.4} \qquad (2)$$

Nag and Dutt (1980) concluded that, the transplanting of rice by hand demanded higher energy as the workers have to immerse their feet in mud (mid calf to knee depth). As a result it requires 240 man-hours to transplant paddy in one hectare area. Walking in a puddle field itself required 22% more oxygen uptake and the heart rate was higher by 11 beats min^{-1}. Baqui and Latin (1982) studied human energy expenditure in rice transplanting using IRRI manual rice transplanter in comparison with traditional hand transplanting by indirect calorimetry. The maximum energy expenditure in machine and hand transplanting were 3.79 and 3.09 kcal min^{-1} respectively. Singh and Gangwar (1999) reported that 70% labour and 48% cost might be save by using mechanical transplanting

as compared to hand transplanting. Mechanically transplanted seedling gave 13.34% higher yield compared to hand transplanted and 50% higher yield compared to direct seeded fields. The benefit/cost ratio for mechanically transplanted fields (2.55) was maximum followed by 2.04 for hand transplanted and 1.88 for direct seeded fields.

An improved version of power tiller operated paddy transplanter developed in Kerala has been reported to achieve a field capacity of 0.13 ha per hour with saving of 50% in cost and 85% in labour (Anonymous, 2001). An eight row self-propelled paddy transplanter (Model: 2ZT-238-8 power driven rice transplanter) being introduced for transplanting of paddy seedlings in India. Field trials for performance evaluation of this planter have been conducted at different places in India (Chhuneja and Ahuja, 2001; Swain, 2002 and Varma, 2002). Performance of an eight-row self propelled paddy transplanter with respect to the technological feasibility, economic merits, and energetic was compared with manual transplanting (Baruah *et al.*, 2001). Cost of machine transplanting was found to be only Rs 1310/ha in comparison to Rs 2463/ha for manual transplanting. The energy requirements for mechanical and manual methods of transplanting were found to be 1074 and 757 MJ/ha, respectively.

Ergonomical evaluation of paddy transplanter was carried out and they observed that the mean heart rate and energy expenditure of the male subjects were 136.03 beats min^{-1} and 24.45 kJ min^{-1}. The corresponding oxygen consumption for this heart rate was 1.171 l min^{-1} and the operation of paddy transplanter was graded as 'heavy' (Anonymous, 2002). Karunanithi and Tajuddin (2003) studies the energy expenditure of male workers varied from 2.4 to 4.9 kcal min^{-1} whereas that of female workers varied from 2.3 to 3.5 kcal min^{-1}. Male workers consumed 2 to 10% more energy than female workers for performing the same task.

Sharma and Singh (2004) developed a mat type nursery-raising device for rice planter. They reported that 72.02 and 33.33% saves the time and labour respectively, over the manual method of raising type nursery. The cost of raising mat type nursery for 1 ha was Rs. 299.50 with the developed device where as it was Rs. 1608.75 with manual method. Sivaswami and Anie John (2004) found that nearly 85% of labour cost was reduced by the introduction of paddy transplanters compared to manual transplanting. The

labour shortage has been overcome by the use of transplanters and also the total cost of paddy cultivation was reduced by 50% as Japanese and Cono weeders were also used for weeding. The yield in machine transplanted fields had shown an increase of 10-18% because of maintaining the correct hill density, no. of seedlings/hills and depth of planting, increased tillering, easy wind passage and shock free transplanting of seedlings. However paddy transplanter are considerably expensive for almost all Asian small hold farmers. Paddy transplanters are popular in industrialized countries where labour cost is high like South Korea.

3.   MATERIALS AND METHODS

3.1 Selection of Subjects for the Transplanting Operation

Three male and three female subjects were randomly selected for the ergonomic study. The due care was taken that the subjects are medically fit to under go the trials and they are true representative of the user's population for the operation of paddy transplanter. For the selection of the subjects, his age as the main criterion was used. The age group of the subjects varied in the range of 25 – 35 years because in this range maximum strength level is attained (Gite, 1997).

3.2 Growing of Seedlings

Seedlings were grown on raised bed in wooden compartment of 200 x 100 cm. Ordinary plastic sheets was laid on the raised bed surrounded by open ditch and the wooden frames were kept on plastic sheets. The paste of soil, farm yard manure (FYM) and sand was prepared 4:1:1 proportion respectively and adding required quantity of water. The paste was laid over the plastic sheet in the form of bed (1.5 cm high). Pre-germinated seeds of paddy were placed over the bed and then pressed slightly by hand for uniform coverage. Water was sprinkled very frequently for three days to avoid any crack in the soil. From forth day, the open channel around beds was filled with water to maintain 2 cm water above the bed surface. After 12 to 15 days good quality seedlings were ready for transplanting.

3.3 Preparation of the Field for Transplanting

Through ergonomic evaluation point of view, test plot of 21 x 20 m was chosen. The texture of the field soil was 62.86% clay, 21.16% silt and 8.83% sand. The field was prepared with mould board plough and then it was flooded with water. After a period of 24 hours, the field was puddled thoroughly using power tiller operated rotavator. The puddle field was leveled using a bullock drawn wooden leveler. The leveled field was left undisturbed for natural settlement of soil particles forming a relatively impermeable layer to retain water on the surface. A thin layer of water was maintained in the field for conducting the trial with manually operated paddy transplanter and hand transplanting.

3.4 Transplanting of Paddy Seedlings

Paddy seedlings were transplanted by manually operated six row paddy transplanter which is generally used in the region and also by hand transplanting. Fig. 1 discloses a manually operated six row paddy transplanter used in the study. The study was conducted at the farm of Department of Soil and Water Conservation, Navsari Agricultural University, Navsari. Single person can carry it comfortably. Table 2 shows the specifications of the planter.

3.5 Ergonomic Evaluation

The ergonomic evaluation of paddy transplanter was conducted to work out energy expenditure rate, rest pause required and force required during the operation. The transplanter was loaded seedlings mats and kept ready for the operation. The subjects were acclimatized with experimental protocol and asked to take sufficient rest before start of the operation. Both mechanical and hand transplanting operations were replicated thrice by male and female operators to avoid the error in data recording (Figs. 2 and 3).

3.5.1 Heart Rate Measurement

During transplanting, heart rate was measured by computerized polar heart rate monitor (Series–S610). It consists of polar coded transmitter, elastic strap, wristwatch type receiver and interface. The sensor of heart rate monitor was fixed on the chest of the operator and its display was fixed on wrist of the
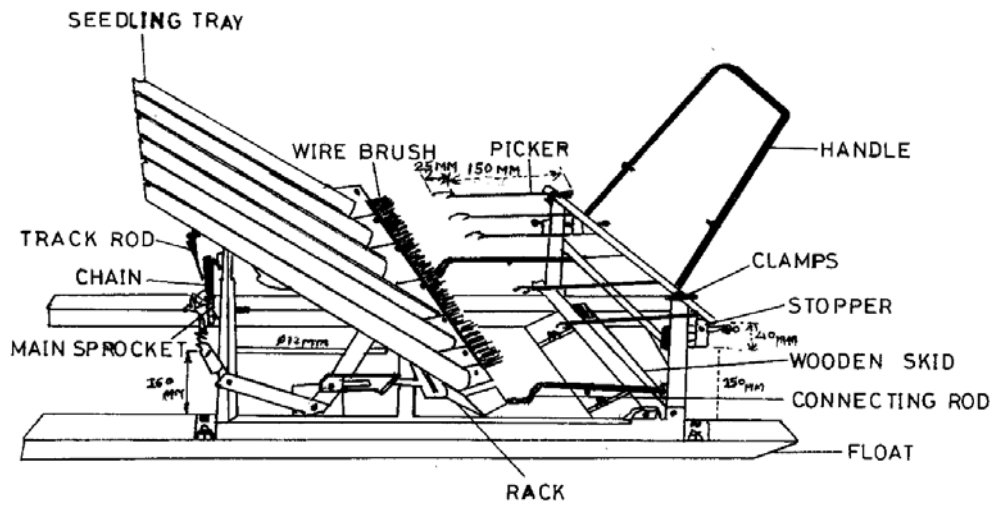
Fig 1: Six row manually operated paddy transplanter

Table 2: Specifications of six row manually operated paddy transplanter

Sl. No.	Details	Specification
1	Type	Manually operated six-row transplanter
2	Dimensions (L x W x H)	91.5 cm x 96.0 cm x 63.5 cm
3	Weight	33.0 kg
4	Planting mechanism	Fixed fishing hook type fingers actuated by hand operated lever mechanism
5	No. of rows	Six
6	Row spacing	19.0 cm
7	Power source	One person
8	Effective width	114.0 cm
9	No. of floats	2
10	Float Size	90.5 x 5.0 cm
11	Seedling tray dimensions	123 x 53.5 cm
12	No. of person needed for the operation	Two (alternate operation and bring seedlings)
13	Cost of paddy transplanter	Rs. 7500

operator, i.e., within the signal range of the device. After the data was downloaded for analysis.

3.5.2 Energy Expenditure Rate

As suggested by Tewari and Gite (1998), the recorded heart rate values at resting level and 6th to 15th minute of operation were taken for calculating the physiological responses of the subjects. The stabilized values of heart rate for each subject from 6th to 15th minute of operation were used to calculate the mean

heart value. Energy expenditure rate was calculated by using the equation (3) developed by Saha *et al.*, 1979.

$$EER = \frac{(HR - 66.0)}{2.4} \tag{3}$$

Where, EER= Energy expenditure rate (kJ min^{-1}) and
HR= Heart rate (beats min^{-1})

The energy cost of the subjects for transplanting operation by paddy transplanter and by hand was worked out and the operation was graded as per the classification of physical work based on EER, HR and OCR (Christesen, 1953 and Zander, 1969).

3.5.3 Rest Pause During Work

During every strenuous work in field, adequate rest is required to have an optimum work output. Better performance results can be expected from both the operator only when proper attention is given for the work rest schedule for different operations. The rest time was measured from the cease of the operation till the heart rate of the subject reaches resting level. The rest pause for paddy transplanting operation in both the cases was calculated by using Murrel's equation:

$$R = \frac{T(K-5)}{K-1.5} \qquad (4)$$

Where, R= Rest time (minute);
   T= Total working time (minute) and
   K= Average kilocalories per minute of work and value 5 kcal min^{-1} adopted as standard. The value 1.5 is an approximation of resting level in kcal min^{-1}.

3.5.4 Measurement of Force Required in Paddy Transplanting Operation

During transplanting operation, the force on the implement is applied through the handle of the implement. During transplanting, the implement experiences sequence of different operations viz.

| Male | Female |

Figs. 2: Transplanting operation by male and female subjects with paddy transplanter

| Male | Female |

Figs. 3: Transplanting operation by male and female subjects with hand

planting, pulling to next planting position without moving the leg, pulling while stepping backward, and end of pulling. Based on the above sequence of operation, there are three types of forces coming in the transplanting process. The force pushing the handle to pick the seedling and planting, force in pulling the fork back from the soil to the next planting position and the force in pulling the tranplanter in forward direction is experienced. So the arrangement was made on the handle to accommodate the load cell. A Novatech load cell (0-40 kg) with digital indicator was used for the measurement of push-pull force.

4. RESULTS AND DISCUSSION

4.1 Selection of Subjects

For the ergonomic evaluation of manually operated six-row paddy tranplanter, three male and three female agricultural workers were randomly selected. The average anthropometric data of selected subjects are shown in Table 3.

4.2 Performance of Paddy Transplanter

The paddy transplanter was tested for its performance. The transplanting efficiency, field capacity and cost of operation was found to be 94.2%, 0.38 ha day^{-1} and 1020 Rs day^{-1}, respectively (Table 4).

4.3 Ergonomic Evaluation of the Subjects

4.3.1 Heart Rate Variation

Three male and three female subjects were participated in the study and the energy expenditure was worked out from heart rate measured during transplanting operation. Transplanting trials were carried out for a period of 30 minutes because of the fact that, the time taken for emptying the seedling tray matched with the same. The average heart rate of the male subjects was 139.68 while for female subjects was 144.19 beats min^{-1} during transplanting operation by paddy transplanter. The heart rate of the male subjects increased steeply from the beginning of the operation and stabilized in the range of 141.0 beats min^{-1} after 6th minute of the operation while female subjects it was 145.0 beats min^{-1}.

The mean value of heart rate of the male and female subjects was found 119.90 and 115.09 beats min^{-1} respectively during transplanting by hand. The heart rate of the male and female subjects was stabilized in the range of 121.0 and 116.0 beats min^{-1} after 6th minute of the operation. It can be concluded that the heart rate of the operator is almost stabilized after 5 min of the start of the operation.

4.3.2 Energy Expenditure Rate

The energy expenditure for transplanting operation by paddy transplanter and by hand for all the subjects was worked out on the basis of mean heart rate during the operation. The mean heart rate was calculated after 6th min of the operation starts. The mean heart rate was found to be 139.68 beats min^{-1} for a male subject and 144.19 beats min^{-1} for female subjects. The energy expenditure rate as worked out from equation (3) for the operation of transplanting by six row transplanter was found to be 30.70 kJ min^{-1} for male subjects while 32.58 kJ min^{-1} for female subjects. On the basis of heart rate, operation was categorized as 'heavy' work. Fig. 4(a) shows the comparison of heart rate and energy expenditure rate for male and female subjects during transplanting operation by paddy transplanter. It is clear from the figure that the energy expenditure of the female subjects is more as compared to male subjects because in transplanting operation heart rate of the female subjects is more than the male subjects. Further, the male workers were taller, and thus exerted a more upward-oriented force on the unit thus reducing the drag force on the runners. It was observed that energy expenditure rate varies among the subjects for the same implement under the similar conditions and it may be due to the variation of strength and skill level of the subjects.

During hand transplanting, the mean heart rate of male and female subjects was found to be 119.90 and 115.09 beats min^{-1} respectively. The energy expenditure rate for male subject was found to be 22.46 kJ min^{-1} whereas it was 20.45 kJ min^{-1} for female subjects. Therefore, the operation of hand transplanting was categorized as 'moderately heavy' work. Fig. 4(b) shows the comparison of heart rate and energy expenditure rate between male and female subjects during transplanting operation by hand. Again in hand transplanting also, the energy expenditure of male subjects is more than that of
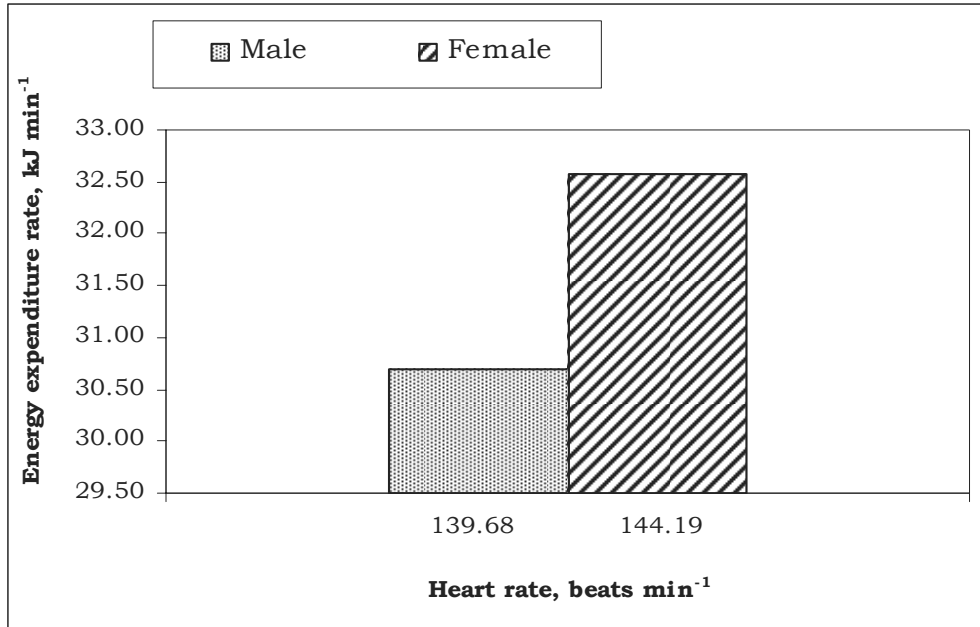
(a) By Paddy Transplanter
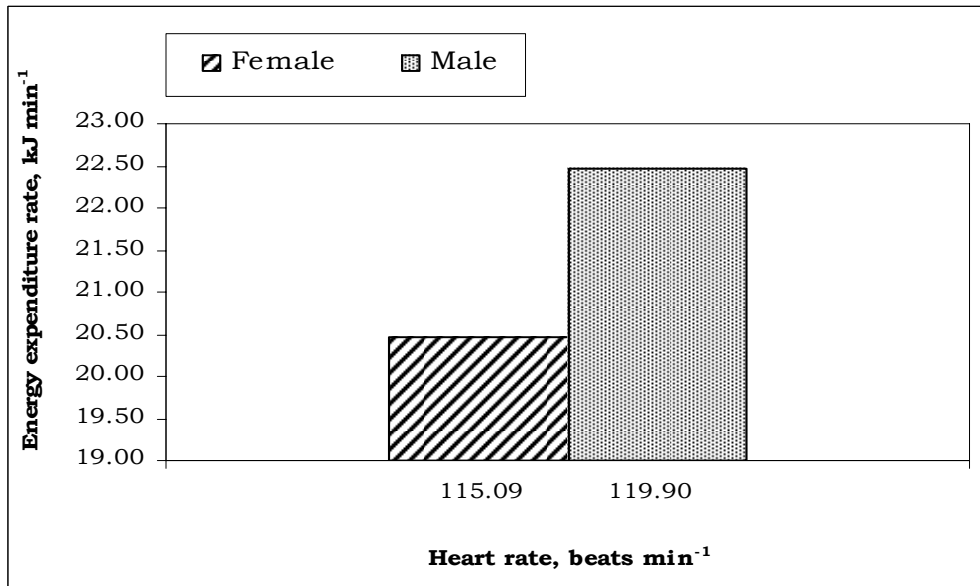
(b) By Hand

Figs. 4 (a and b): Comparison of heart rate and energy expenditure rate between male and female subjects during transplanting operation

female subjects. During hand transplanting the major portion of energy expended is consumed in walking in the puddle field. The workers had to spend more energy for taking out their legs out of the puddle field at each and every step. It was also found that the female subjects were more habituated to transplanting by hand in puddle field as compared to male subjects and therefore, the level of energy expenditure rate is comparatively less in females.

4.3.3 Rest Pause

The rest pause for the transplanting operation was worked out as explained in section 3.5.3 and it is presented in Table 5. The calculated rest pause was compared with the actual rest pause taken by the subjects in the field to reach the heart rate to normal level. It was observed that, the actual rest time taken for transplanter (14.30 min) was in agreement with the computed value of rest pause. Two operators were employed in cyclic system for transplanting to enhance the comfort of the subjects and to maintain the efficiency of the implements.

Table 3. Average anthropometric dimensions of subjects under test

Subject	Age (Year)	Height (cm)	Weight (kg)	Elbow height (cm)	Metacarpal-III height (cm)
Male	30.0	159.7	49.7	100.0	67.0
Female	29.0	153.7	44.0	95.9	66.3

Table 4. Performance data of paddy transplanter in the puddle field during planting

Sl. No.	Item of observation	Observed data
1	Time of transplanting	1 day after puddling
2	Total numbers of seedling per hill	3.0 to 5.0
3	Depth of planting, cm	3.0 to 4.0
4	Hill to hill spacing, cm	15.0 to 18.0
5	Row to row spacing, cm	19.0 to 20.0
6	Missing hills, %	5.0 to 6.0
7	Transplanting efficiency, %	94.2
8	Field capacity, ha day^{-1}	0.38
9	Labour requirement, man-hr ha^{-1}	35 to 40
10	Cost of operation, Rs ha^{-1}	1020/-
11	Saving in transplanting cost, Rs ha^{-1}	1480/-
12	Percent saving in transplanting cost, %	59.2

Table 5. The rest pause calculated for the subjects during transplanting operation

Subject	Total work time, min	Mean energy cost, kJ min^{-1}	Rest time, min	Proposed work rest cycle
Male	30	30.70	12.00	30 minutes of work followed by 14 min rest with two operators.
Female	30	32.58	13.29	30 minutes of work followed by 14 min rest with two operators.

4.3.4 Transplanting Force

The average force for handle down, handle up and pulling was found to be 101.93, 94.61 and 130.32 N respectively for male subjects whereas for female subjects it was 117.08, 109.34 and 145.12 N respectively. More force was required in pulling the transplanter by female workers as compared to male workers because the male workers were taller, and thus exerted a more upward-oriented force on the unit thus reducing the drag force on the runners.

5. CONCLUSIONS

1. The field capacity of six row manually operated paddy transplanter was found to be 0.38 ha day^{-1} while for transplanting by hand it was found to be 0.04 ha day^{-1}.
2. The average heart rate for operating six-row paddy transplanter was found to be 139.68 and 144.19 beats min^{-1} for male and female subjects, respectively. Whereas for transplanting paddy by hand, it was found to be 119.90 and 115.09 beats min^{-1} for male and female subjects, respectively.
3. The average energy expenditure of male and female workers for transplanting operation by manually operated paddy transplanter was found to be 30.70 and 32.58 kJ min^{-1}, respectively. The operation of six row paddy transplanter was graded as 'heavy' on the basis of heart rate.
4. The average energy expenditure of male and female workers for transplanting paddy by hand was found to be 22.46 and 20.45 kJ min^{-1}, respectively. The operation was graded as 'moderately heavy'.
5. The rest pause, for achieving functional effectiveness during transplanting the paddy by six row paddy transplanter, was found to be 14.30 min followed by 30 minutes of work.
6. More force in pulling the transplanter in forward direction is required by the subjects as compared to handle up and handle down operation. The average force required for pulling the trasplanter was 130.32 and 145.12 N for male and female subjects, respectively. More force was required for female workers as compared to male workers because the male workers were taller, and thus exerted a more upward-oriented force on the unit thus reducing the drag force on the runners.

List of Symbols

Agril.	Agricultural
AICRP	All India Co-coordinated Research Project
AWL	acceptable workload
BMR	basal metabolic rate
EER	energy expenditure rate
FYM	farm yard manure
HR	heart rate
IRRI	International rice research institute
OCR	oxygen consumption rate
Sl	serial number

REFERENCES

1. Anonymous (1984). Recommended dietary intakes for Indians. ICMR, Delhi, pp. 58-59.
2. Anonymous (2001). Website based report of Kelappaji College of Agricultural Engineering and Technology, Kerela Agricultural University, Kerela.
3. Anonymous (2002). Progress Report of AICRP on Ergonomic and Safety in Agriculture Submitted by TNAU- Coimbatore Centre to ICAR, New Delhi.
4. Ayoub, M. M. and J. W. McDaniel (1974). Effect of operator stance and pushing and pulling tasks. Transactions of Institute of Industrial Engineering, 6(3): 185-195.
5. Baqui, A. and R. M. Latin (1982). Human energy expenditure in manually operated rice transplanter. AMA, 14(1): 14-16.
6. Baruad, D. C., Goswami, N. G. and R. Saikia (2001). Manual transplanting vs. mechanical transplanting of paddy: a techno-economic analysis in Assam. Journal of Agricultural Engineering, 38(3): 66-72.
7. Chaffin, D. B., Andres, R. O. and A. Garg (1983). Volitional postures during maximal push/pull exertions in the sagital plane. Human Factors, 25(5): 541-550.
8. Christensen, E. H. (1953). Physical evaluation of work in the Nykroppa iron works in N. Floyd and A. T. Walfort. Ergonomics Society Symposium on Fatigue, Lewis, London.
9. Chhuneja, N. K. and S. S. Ahuja (2001). Field

performance of self-propelled paddy trasplanter. A Paper Presented in XXXV Annual Convention of ISAE held at OUAT, Bhubeneswar, January, 22-24.

10. De, D. and B. V. Babu (2004). Energy consumption patterns in transplanted paddy cultivation in India. Journal of Agricultural Engineering (ISAE), 41(4): 16-26.

11. Gite, L. P. and G. Singh (1997). Ergonomics in agricultural and allied activity in India. CIAE Technical Bulletin No. CIAE/97/70, pp: 12-14.

12. Jain, S. C. and G. Philip (2003). Sowing and Planting Machines. Farm Machinery – An Approach. Standard Publishers Distributors, Delhi, pp: 36-70.

13. Karunanithi, R. and A. Tajuddin (2003). Physiological response of agricultural workers in rice farming operation. Journal of Agricultural Engineering (ISAE), 40(1): 33-40.

14. Le Blanc, J. A. (1957). Use of heart rate as an index of workload. J. Applied Physiology, 38: 275-280.

15. Lehmann, G. (1958). Physiology measurement as a basis of work organization in industry. Ergonomics, 29(7): 903-912.

16. Martin, J. B. and D. B. Chaffin (1972). Biomechanical computerized simulation of human strength in sagital plane activities. American Institute of Industrial Engineering Transactions, 4: 19-28.

17. McCormick, E. J. (1976). Human Factors in Engineering and Design. New York: McGraw-Hill, pp: 242-243.

18. Mehta, M. L., Varma, S. R., Mishra, S. K. and V. K. Sharma (1990). Testing and evaluation of rice transplanter. Testing and Evaluation of Agricultural Machinery. U. S. G. Publishers, Ludhiana, pp: 80-88.

19. Morehouse, L. E. and T. A. Miller (1963). Physiology of Exercise. 93rd Edition C. V. Mosby Co. St. Louis, USA.

20. Murrell, K. F. H. (1965). Human Performance in Industry. Reinhold Publishing Corporation, New York, USA.

21. Nag, P. K. and P. Dutt (1980). Cardio-respiratory efficiency in some agricultural work. Applied Ergonomics, 11: 81-84.

22. Saha, P. N., Datta, S. R., Banerjee, P. K. and C. G. Narayane (1979). An acceptance workload for Indian workers. Ergonomics, 22(9): 1059-1071.

23. Sharma, S. C. and T. P. Singh (2004). Pantnagar developed a mat type nursery raising device for rice transplanter. Agricultural Engineering Today, 28(1-2): 70-72.

24. Singh, K. K. and K. S. Gangwar (1999). Performance evaluation of self-propelled rice transplanter and comparison of yield and economic returns of mechanically and hand transplanted and direct seeded rice. A Paper Presented in XXXIV Annual Convention of ISAE held at CCSHAU, Hisar, December, 16-18.

25. Sivaswami, M. and S. Anie, John (2004). Comparative studies on self propelled paddy transplanter with manual transplanting in Kerala. A Paper Presented in XXXVIII Annual Convention of ISAE held at Dapoli, January, 16-18.

26. Suggs, C. W. and W. E. Splinter (1961). Effect of environment on the allowable workload of man. Transaction of ASAE, 4: 48-51.

27. Swain, S. (2002). Evaluation of eight-row self-propelled rice transplanter in farmers field for adoption in Central and North-Eastern India. A Paper Presented in XXXVI Annual Convention of ISAE held at IIT, Kharagpur, January, 28-30.

28. Tomilson, R. W. (1970). Assessment of workload in agricultural task. Proceeding of Institute of Agricultural Engineers, 25(1): 18-29.

29. Tiwari, P. S. and L. P. Gite (1998). Human energy expenditure during power tiller operation. Paper presented during XXXIII Annual Convention of ISAE held at CIAE, Bhopal, September, 21-23.

30. Van Wely, P. (1970). Design and disease. Applied Ergonomics, 1(5): 262-269.

31. Varma, S. R. (2002). Field performance evaluation of Chinese self-propelled rice trasplanter under different pattern of hill transplanting of rice. A Paper Presented in XXXVI Annual Convention of ISAE held at IIT, Kharagpur, January, 28-30.

32. Zander, J. (1969). Ergonomics in Machine Design. Wageningen, H. Veeman and Zones, New York.

MOISTURE SORPTION ISOTHERMS AND HEAT OF SORPTION OF MANGO
(*Magnifera Indica* L. cv. NAM DOK MAI)

S. Janjai[*#]**, B. K. Bala**[†]**, K. Tohsing**[*]**, B. Mahayothee**[‡]**,**
M. Haewsungcharern[§] **and J. Müller**[**]

ABSTRACT

The equilibrium moisture contents of the Thai mango variety 'Nam Dok Mai' were determined using the dynamic method at temperatures of 30-50 °C and water activity from 0.11-0.97. The sorption isotherm curves obtained displayed an inverse relationship with temperature at constant relative humidity. Six selected isotherm models were tested against the experimental isotherm data and the models were compared using standard error of estimate, mean relative error, coefficient of determination and residual plots. Among the models tested, GAB model was the best fitting for the temperatures of 30, 40, and 50 °C. The fitting of the Day and Nelson model, and the modified Smith model was very close and it is next to the GAB model. These models can be considered and used with good predictive accuracy to determine the equilibrium moisture contents of the Thai mango variety 'Nam Dok Mai'. The isosteric heats of sorption were also determined from the equilibrium data using the Clausius-Clapeyron equation and were found to be exponential functions of moisture content. This equation is suggested for use in the computation of heat of sorption of mango slices.

*Keywords***:** *Mango; Sorption models; Dynamic method; Isosteric heat. © 2007 AAAE*

1. INTRODUCTION

Mangoes are economically important tropical fruit in Thailand. They are grown in all regions of this country. Both ripe and unripe mangoes are consumed fresh. Drying of the ripened mangoes during harvesting season minimizes post-harvest losses, increases income by value addition to the quality dried products and ensures the year round availability of mangoes. Furthermore, dried mangoes are becoming more popular as an alternative to fresh fruits due to the particular taste and flavour of the dried mangoes. Moisture isotherm and isosteric heat of adsorption data are essential information for understanding the drying process of mangoes.

Moisture sorption isotherms describe the relation between the equilibrium moisture contents and relative humidity at constant temperatures (Bala, 1997). Moisture isotherm data of the mango slices are required for drying, predicting shelf life, as well as determining packaging and moisture accumulation during storage. The quality of a dried product is particularly related to equilibrium moisture content. Most foods have a critical moisture content below which the rate of quality loss is negligible (Gal, 1983; Rahman and Lubuza, 1999).

The net isosteric heat of sorption is also important information for drying. It can be used to determine the energy requirements and provide information on the state of water within the dried product. The moisture content level of a product at which the net isosteric heat of sorption reaches the value of latent heat of sorption is often considered as the indication of the amount of bound water existing in the product (Wang and Brennan, 1991).

In the past 20 years, many sorption isotherm models have been formulated for various agricultural products. More than 200 purely empirical EMC/ERH equations have been developed for cereal grains and food materials (Sun and Woods, 1994). However, no single equation accurately describes the EMC/ERH relationship for various crops over a broad range of

---

[*] Department of Physics, Faculty of Science, Silpakorn University, Nakhon Pathoom 73000, Thailand

[†] Department of Farm Power and Machinery, Bangladesh Agricultural University, Mymensingh 2202, Bangladesh

[‡] Department of Food Technology, Silpakorn University, Nakhon Pathom 73000, Thailand

[§] Department of Food Engineering, Chiang Mai University, Chiang Mai 50200, Thailand

[**] Institute of Agricultural Engineering, University of Hohenheim, Stuttgart 70593, Germany

[#] Corresponding author. Tel.: +66-34-270-761; Fax.: +66-34-271-189 Email address: serm@su.ac.th

relative humidity and temperature. It is believed that no universal equation for sorption isotherms of agricultural products exists (Chen and Morey, 1989). The modified Henderson equation and Chung-Pfost equation are the best existing models for starchy grains and fibrous materials.

Many investigators have developed mathematical equations - theoretical, semi-theoretical and empirical - to describe the sorption isotherms of agricultural and food materials. Previously, 23 isotherm equations, theoretical and empirical, and their use for fitting sorption isotherms of foods and food products were reviewed (Chirife and Iglesias, 1978). None of these equations described adequately the sorption isotherms over the whole range of relative humidity and for all types of food materials tested. Two two-parameter equations and one three-parameter equation for 163 food materials including fruits, vegetables, spices and starchy foods were also evaluated (Lomauro *et al.*, 1985). It was found that the three parameter Guggenheim, Anderson and de Boer (GAB) equation (Van den Berg, 1984) describes the sorption isotherms for most food better than two-parameter equations.

Recently the GAB model has been proposed by food engineers as the universal model to fit the sorption data for all foods (Lomauro *et al.*, 1985; Van den Berg, 1984). Lomauro *et al.* (1985) reported that moisture sorption of foods can be described by more than one sorption model and the GAB gives the best fit for more than 50% of the fruits, meats and vegetables analyzed (Lomauro *et al.*, 1985). However, the GAB model can not be used to describe the sorption isotherms of starchy grains (Chen and Jayas, 1978). Furthermore, it is difficult to extend the model by adding a temperature parameter.

Five isotherm models (BET, GAB, Henderson, Oswin and Smith) were fitted to the sorption isotherm data of three types of mango bars (plain mango bar, mango-coconut bar and mango-soya protein concentrate bar) (Mir and Nath, 1995). The BET and GAB models were found to accurately predict the moisture content only for the plain mango bar, whereas the Oswin model was applicable to all the three types of the mango bars. Models for pineapple, including six two-parameter and one three-parameter, were tested to fit the observed data from experiments and the modified BET model was found to be the best fit (Hossain *et al.*, 2001).

Lahsasni *et al.* (2004) determined the equilibrium moisture contents of prickly pear fruit at three temperatures of 30, 40, and 50 °C over a range of relative humidity from 5-90%. The GAB, modified Halsey, modified Chung-Pfost, modified Oswin and modified Henderson models were tested to fit the experimental data. The GAB model was found to be the most suitable for describing the sorption curves.

Kaymak-Ertekin and Gedik (2004) determined the moisture isotherms of grapes, apricots, apples and potatoes at 30, 45, and 60 °C and fitted six two-parameter and five three-parameter sorption models to fit the experimental data. The Halsey equation was found to be the best fit to the experimental data for all the materials tested over the range of temperatures and water activities investigated. The GAB model also resulted in the closest fit to sorption data for potatoes and grapes.

Although sorption isotherms for mango bars have previously been reported (Mir and Nath, 1995), no data on sorption isotherms of a Thai mango slices have been reported in scientific literature. However, the GAB model, BET model and Halsey model are reported to have fit experimental isotherm data of apple and pineapple accurately, therefore, in this study six isotherm models were tested (GAB, Day and Nelson, modified Smith, modified Chung-Pfost, modified Halsey, and modified Oswin).

Tsami (1991) proposed an empirical exponential relationship between the net isosteric heat of sorption and material moisture content for some fruits. Janjai *et al.* (2006) also reported the net isosteric heat of sorption to be an exponential function of moisture content for longan. Hossain *et al.* (2001) found isosteric heat to be a power function of equilibrium moisture content for pineapple.

The overall objective of the study was to conduct experimental measurements to determine the isotherms for Thai mango slices at various temperatures and relative humidities, to fit isotherm models to sorption isotherm data, to calculate the net isosteric heat of sorption from the experimental data and to develop an equation for calculating the net isosteric heat of sorption for the mango slices.

2. MATERIALS AND METHODS

The mango samples used in this study were of the variety 'Nam Dok Mai,' which is popular in Thailand because of its favourable taste and texture and it was collected from a fresh market of Nakhon Pathom, Thailand and it was stored at 5 °C in the Department

of Food Engineering, Silpakorn University, Nakhon Pathom. The initial moisture content of fresh mango was about 82% (w.b.). Before starting an experiment the fruits were left in the room temperature in the laboratory in the Department of Physics, Silpakorn University for about 16 hours to attain a temperature in equilibrium with the room temperature. The mangoes were peeled and sliced into thickness of 10 mm. It was dried in a laboratory dryer to prepare the samples for determination of equilibrium moisture contents of mango slices.

2.1 Determination of the Sorption Isotherm of Mango

There are two general methods for determining the equilibrium moisture content: (i) static method and (ii) dynamic method. In static method the product is allowed to come to equilibrium in still and moist air while in dynamic method the air is mechanically moved around the product in a closed chamber containing either salt or acid solution (Bala, 1997). Equilibrium moisture contents of the mango slices were determined experimentally in the Department of Physics, Silpakorn University, Nakhon Pathom, Thailand using dynamic method. To determine the equilibrium moisture contents three sets of equipment were constructed and each set consists of a hot air chamber containing six sample boxes in three trays. The sample box was essentially an airtight plastic box containing saturated salt solution to maintain constant relative humidity inside the sample box. Each sample box is divided by plastic wall into two sections for holding two samples separately and simultaneously. The sample boxes were half filled with salt solution. The samples were placed inside the perforated sample containers of 3 cm diameter and 2 cm height and the sample containers were placed on the perforated plastic supports just above the salt solution. Two small electric fans were fitted to circulate the air inside the sample box to accelerate moisture transfer between the samples and air inside the sample box. The sample boxes were placed inside the hot air chamber. The hot air chamber was equipped with a 3 kW electrical heater and an electronic temperature controller to maintain the temperature and the relative humidity was maintained by saturated salt solution.

In conducting the experiments, 50 g of the mango slices was placed inside the sample containers which were placed inside the sample boxes and the sample boxes were placed inside the hot air chamber. The samples were weighed regularly until they reached equilibrium. It took 2-4 days to reach the equilibrium. The final moisture contents of the product were determined by standard oven method (temperature of 103° C for 24 hours). The selected temperatures for sorption isotherm determination were 30, 40, and 50 ^{o}C and the water activity was 0.11 to 0.97.

2.2 Selection of the Equilibrium Moisture Content Models

Six isotherm models listed in Table 1 were tested to fit the sorption isotherms of the mango slices. These models were selected on the basis of their effectiveness for describing isotherms of several food and plant materials and simplicity of computation. The parameters of the models were determined by Marquardt-Levenberg optimization method (SPSS 11.5). Reduced mean relative error (RMRE), value of the root mean square error (RMSE) and randomness of residuals (ei) were computed as:

$$RMRE = \frac{100}{N} \sum_{i=1}^{N} \left| \frac{M_o - M_P}{M_o} \right| \tag{1}$$

$$RMSE = \sqrt{\frac{\sum_{i=1}^{N} (M_o - M_P)^2}{N}} \tag{2}$$

$$ei = M_o - M_P \tag{3}$$

2.3 Determination of Isosteric Heat of Sorption of Mango

The net isosteric heat of sorption phenomena can be explained by the Clausius-Clayperon equation (Iglesias and Chirife, 1976; Okos *et al.*, 1992; Mohamed., 2005) as follows:

$$\frac{\partial \ln(\text{RH})}{\partial T_{ab}} = \frac{Q_{st}}{R_0 T_{ab}^{2}} \tag{4}$$

Integrating Eq. (4) and assuming that the isosteric heat of sorption (Q_{st}) is independent of temperature, gives the following Eq. (5):

$$\ln(RH) = -\left(\frac{Q_{st}}{R_0} \right) \frac{1}{T_{ab}} + K \tag{5}$$

Table 1: Selected isotherm models for fitting experimental data

Sl. No.	Model	Mathematical expression
1.	Day and Nelson Equation	$a_w = 1 - \exp(-b_o T^{b_1} M_e^{b_2 T^{b_3}})$
2	Smith Equation	$M_e = (b_o + b_1 T) - (b_2 + b_3 T)\ln(1 - a_w)$
3.	Modified Halsey Equation	$a_w = \exp\left[\dfrac{-\exp(b_o + b_1 T)}{M_e^{b_2}}\right]$
4.	Modified Chung-Pfost Equation	$a_w = \exp\left[\dfrac{-b_o}{T + b_1}\exp(-b_2 M_e)\right]$
5.	Modified Oswin Equation	$a_w = \dfrac{1}{1 + \left[\dfrac{b_o + b_1 T}{M_e}\right]^{b_2}}$
6.	GAB Equation	$M_e = \dfrac{b_0 b_1 b_2 a_w}{(1 - b_2 a_w)(1 - b_2 a_w + b_1 b_2 a_w)}$

where K is a constant. The value of Q_{st} is calculated from the slope of the Eq. (5).

3. RESULTS AND DISCUSSION

3.1 Sorption Isotherm of Mango

Experimental data (points) on sorption isotherm of mango determined using dymanic method are shown in Fig. 1. The isotherm curves have similar patterns for each temperature and the EMC values decrease with increase in temperature at constant equilibrium relative humidity. This indicates that the mango slices become less hygroscopic when temperature is increased. This may be explained by the fact that the kinetic energy associated with water molecules present in mango slices increases with increase in temperature. This, in turn, resulted in decreasing attractive forces and consequently escape of water molecules. This leads to a decrease in EMC values with increase in temperature at a contant relative humidity. Several researches have reported similar trends for plant and food materials (Iglesias and Chirife, 1982; McLaughlin and Magee, 1998; Hossain and Bala, 2000 a and b; Hossain *et al.*, 2001; Shivhare

et al., 2004 and Mohammed, 2005). The temperature dependence of the equilibrium moisture content has an important bearing upon the chemical and microbiological reactions associated with spoilage (Al-Muhtaseb *et al.*, 2004). At a constant moisture content, higher temperatures entail a higher water activity and consequently faster rates of deterioration (Van den Berg and Bruin, 1981).

Six isotherm models, presented in Table 1, were
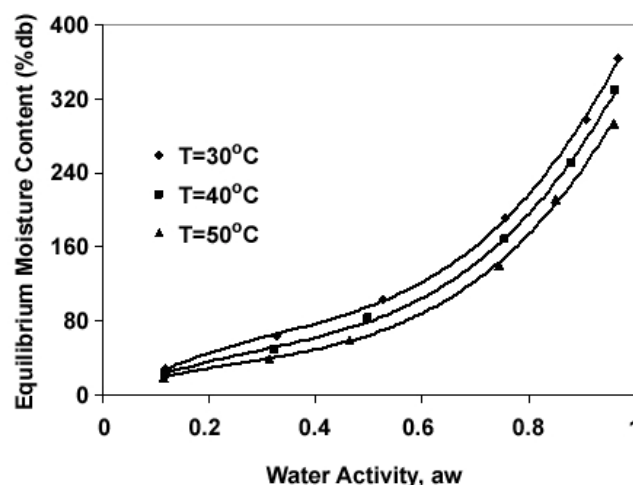
Fig. 1: Sorption isotherms of mango at 30, 40, and 50 °C.

tested to fit the sorption isotherm data of the mango slices. Fitted coefficients and accuracy of parameters for sorption isotherms of the mango slices are given in Table 2. Among the isotherm models tested, the GAB model fitted the best to the experimental isotherm data of the mango slices for the temperature levels of 30, 40, and 50 °C with the lowest values of standard estimate of error and mean relative error, and the highest value of coefficient of determination. The fitting of the Day and Nelson model, and the modified Smith model was very close in terms of standard estimate of error and mean relative error, and coefficient of determination and the Day and Nelson model, and the modified Smith model were next to the GAB model. Fig. 2 shows the comparison between the observed and predicted values of the isotherms of the mango slices for the GAB model, the Day and Nelson model, and the modified Smith model. The agreement between the observed and predicted values is very good. Fig. 3 shows the residuals of the predicted equilibrium moisture contents for the GAB model, Day and Nelson model, and the modified Smith model. The residuals are random in pattern and hence these models are suitable to define the sorption isotherms. However, it must be mentioned that the goodness of fit of a sorption model to experimental data does not describe the nature of the sorption process, it only reflects on the mathematical quality of

the model (Samapundo *et al.*, 2007). Also as water is associated with the food matrix by different mechanisms in different water activity regions, no single model can be considered accurate over the entire water activity range (Labuza, 1975).

3.2 Isosteric Heat of Sorption of Mango

The plot of ln(RH) as a function of 1/Tab at constant moisture content is shown in Fig. 4. The slopes of the lines at constant moisture contents were determined by regression analysis to find the net isosteric heat of sorption of the mango.

The isosteric heat of sorption were calculated from the slope of the curves and the heat of sorption for mango at different moisture content is shown in Fig. 5. The net isosteric heat of sorption was found to decrease with increase in moisture content. This trend is similar to those reported by other researchers for agricultural produce, food, and medicinal and aromatic plants (Iglesias and Chirife, 1976; Swami *et al.*, 2005; Soysal and Oztekin, 2001; Hossain *et al.*, 2001; Corzo and Fuentes, 2004; Lahsasni *et al.*, 2004 and Mohamed *et al.*, 2005). The rapid increase in the heat of sorption at low moisture content was due to the existence of highly active polar sites on the surfaces of the food material, which were covered with water molecules forming a mono-molecular layer

Table 2: The coefficients of the selected models, relative error (RMRE), standard error of estimate (RMSE) and the coefficient of determination (R^2) for mango.

Model	Temperature °C	Coefficients				RMRE	RMSE	R^2
		b_0	b_1	b_2	b_3			
Day and Nelson	30,40 &50	0.000029	1.3261	1.3855	-0.0432	9.4589	26.7751	0.9858
Smith	30,40 &50	49.8255	-0.7896	157.7409	-1.6234	10.8863	15.0733	0.9809
Modified Halsey	30,40 &50	6.2221	-0.0294	1.2665		34.2042	181.3293	0.9702
Modified Chung-Pfost	30,40 &50	110.0299	3.0232	0.0151		20.4994	30.9906	0.9658
Modified Oswin	30,40 &50	150.1736	-1.7852	1.8031		15.7368	74.3472	0.9865
GAB	30	91.389	3.04	0.799		4.4114	8.2843	0.99
	40	95.01	1.88	0.78		6.3339	5.1179	0.99
	50	39.108	8.266	0.878		8.8694	8.5691	0.987
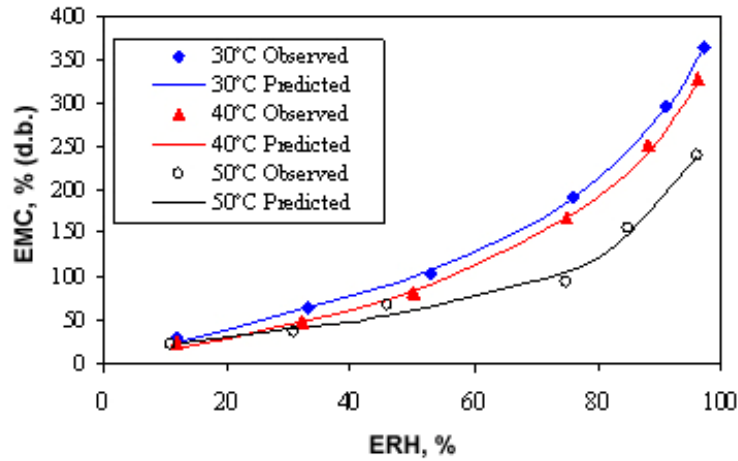
Fig. 2(a): Predicted and measured sorption isotherms of mango at 30, 40, and 50 °C (GAB model).
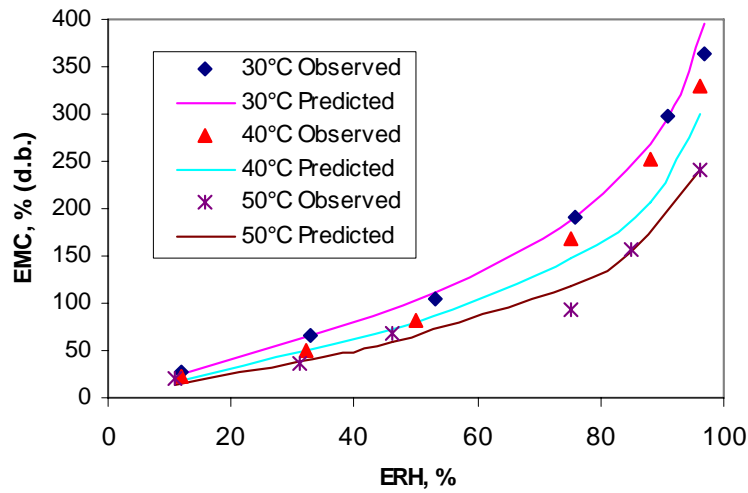
Fig. 2(b): Predicted and measured sorption isotherms of mango at 30, 40, and 50 °C (Day and Nelson model).
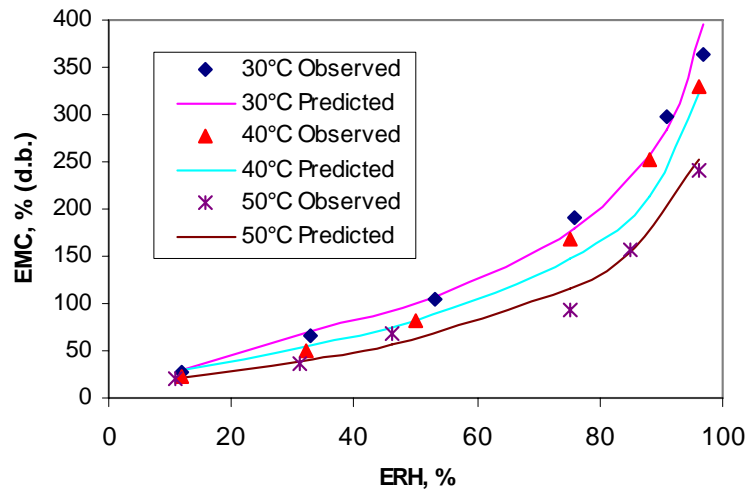
Fig. 2(c): Predicted and measured sorption isotherms of mango at 30, 40, and 50 °C (modified Smith model).
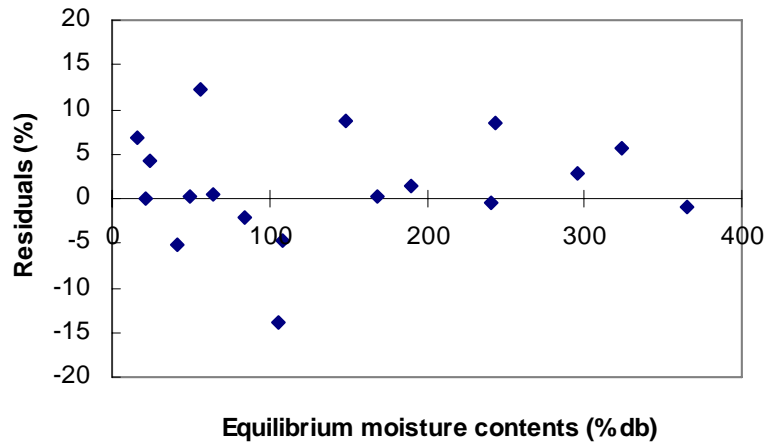
Fig. 3(a): Residuals of the predicted equilibrium moisture contents (GAB model).
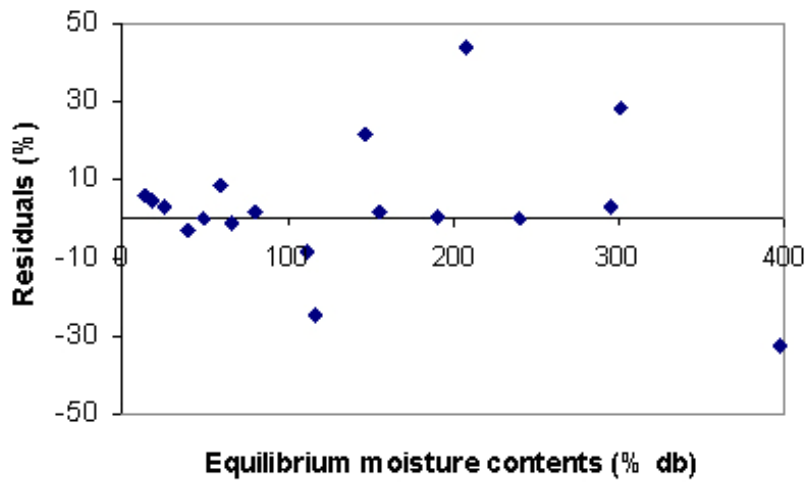
Fig. 3(b): Residuals of the predicted equilibrium moisture contents (Day and Nelson model).
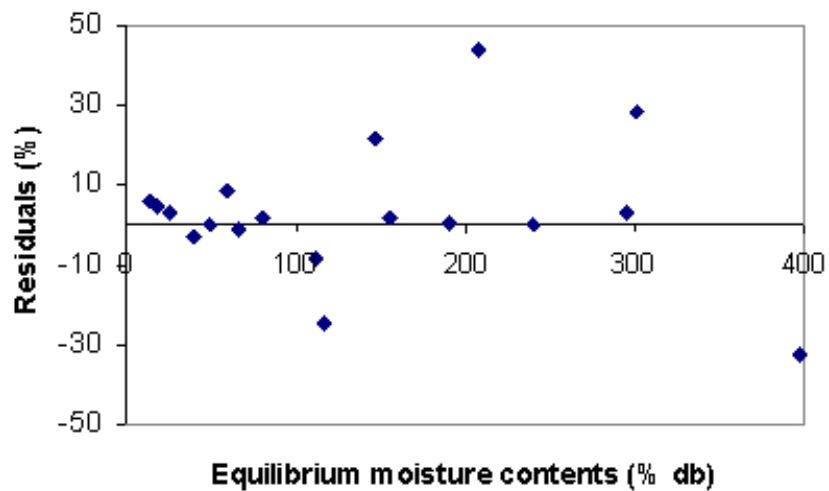
Fig. 3(c): Residuals of the predicted equilibrium moisture contents (modified Smith model).
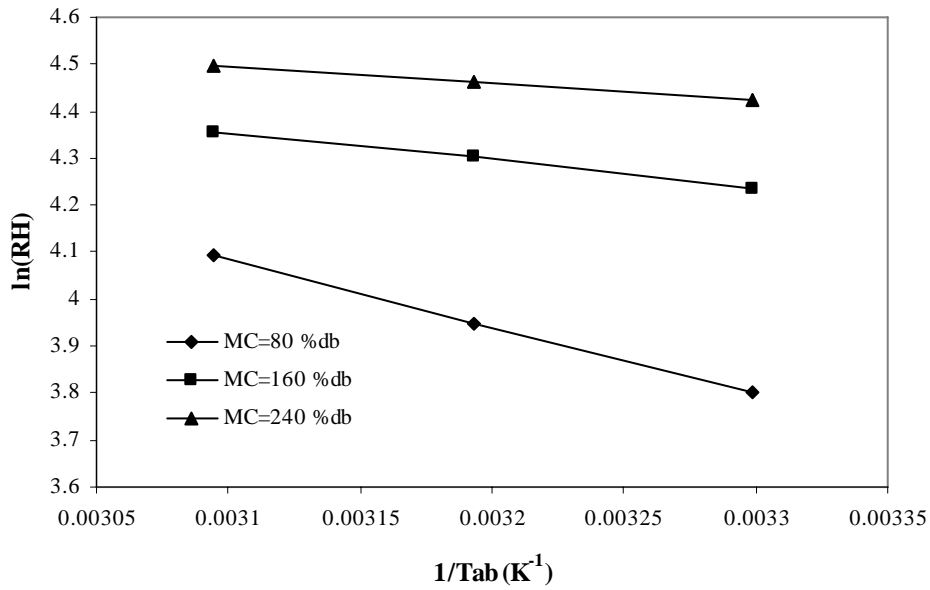
Fig. 4: Plot of ln(RH) as a function of $1/T_{ab}$ at different moisture contents, MC (% db).
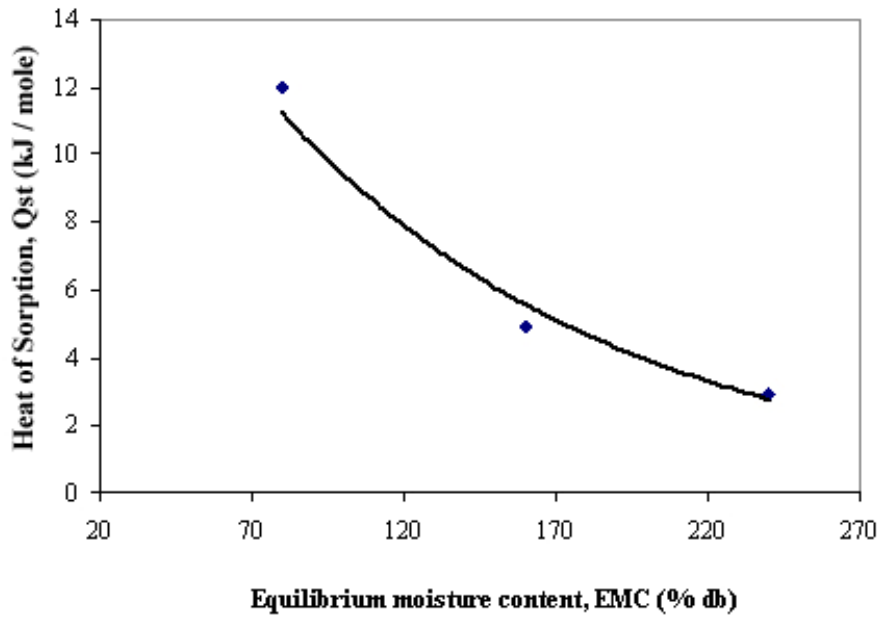
Fig. 5: Net isosteric heat of sorption of mango at various equilibrium moisture contents.

(Lahsasni *et al.*, 2003). The net isosteric heat of sorption was found to be a function of equilibrium moisture content and the following equation was developed:

$$Q_{st} = 50.465\, e^{-0.0239\, M_e} \qquad (R^2 = 0.97) \qquad (6)$$

This relation showed that the net isosteric heat of sorption of mango decreased exponentially with the increase in equilibrium moisture content. This mathematical relationship may be used to calculate the heat of sorption of mango slices for various moisture contents.

4. CONCLUSSIONS

The equilibrium moisture contents of mango slices have been determined experimentally using dynamic method at the temperature levels of 30, 40, and 50 °C and a relative humidity in the range of 11-97%. The equilibrium moisture content decreases with increase in temperature at constant water activity. Six sorption isotherm models were used to fit the experimental data of the mango slices. Among them, GAB model fitted the best to the experimental data at the temperature levels of 30, 40, and 50 °C and the Day and Nelson, and Modified Smith model were next to the GAB model. These three models are suggested for use in drying, storing and packaging of mango slices.

The isosteric heats of sorption were determined from the equilibrium data using the Clausius-Clapeyron equation and the net isoteric heat of sorption of mango slices was found to decrease with increase in moisture content and it was also found to be an exponential function of moisture content. The resulting equation, Eq. (6), is suggested for use in the computation of heat of sorption of mango slices.

Nomenclature	
aw	Water activity
b_0, b_1, b_2…	Parameters of isotherm equation
EMC	Equilibrium moisture content (% db)
ERH	Equilibrium relative humidity (%)
M_e	Equilibrium moisture content (% db)
Q_{st}	Heat of sorption (kJ/mole)
RH	Relative humidity (% db)
R	Coefficient of determination (%)
R_0	Universal gas constant (kJ/mol. K)
T	Temperature (°C)
T_{ab}	Absolute temperature (K)

REFERENCES

1. Al-Muhtaseb, A. H., McMinn, W. A. M. and T. R. A. Magee (2004). Water sorption isotherms of starch powders Part 1: mathematical description of experimental data. Journal of Food Engineering, 61: 297-307.
2. Bala, B.K. (1998). Drying and Storage of Cereal Grains. Oxford and IBH Publishing Co. Pvt. Ltd.
3. Chen, C. and D. S. Jayas (1998). Evaluation of the GAB equation for the isotherms of agricultural products. Transactions of the ASAE, 41: 1755-1760.
4. Chen, C. and R. V. Morey (1989). Comparison of four EMC/ERH equations. Transactions of the ASAE, 32: 983-990.
5. Chirife, J. and H. A. Iglesias (1979). Equations for fitting water sorption isotherms of foods, 1. A review. Journal of Food Technology, 13: 159-174.
6. Corzo, O. and A. Fuentes (2004). Moisture sorption isotherms and modeling for pre-cooked flours of pigeon pea (Cajanus ensiformis) and lima bean (Canavalia ensiformis). Journal of Food Engineering, 65: 443-448.
7. Gal, S. (1983). The need for, and practical applications of sorption data. In: Physical Properties of Foods, (eds). Jowitt, Ronald *et al.*, Published by Applied Science Publishers, London, 425.
8. Hossain, M. D., Bala, B. K., Hossain, M. A. and M. R. A. Mondol (2001). Sorption isotherms and heat of sorption of pineapple. Journal of Food Engineering, 48: 103-107.
9. Hossain, M. A. and B. K. Bala (2000a). Moisture isotherms characteristics of red chilli. Drying Technology, 18(1-2): 503-515.
10. Hossain, M. A. and B. K. Bala (2000b). Moisture sorption isotherms of green chilli. International Journal of Food Properties, 3(1): 93-104.
11. Iglesias, H. A. and J. Chirife (1982). Handbook of Food Isotherms: Water Sorption Parameters for Food and Food ComponentsEd.; Academic Press: New York, pp.
12. Iglesias, H. A. and J. Chirife (1976). Prediction of the effect of temperature on water sorption

isotherms of food materials. Journal of Food Technology, 11(2): 109-116.

13. Janjai, S., Bala, B. K., Tohsing, K., Mahayothee, B., Haewsungcharern, M., Muhlbauer, W. and J. Muller (2006). Equilibrium moisture content and heat of sorption of longan (Dimocarpus longan Lour.). Drying Technology, 24: 1691-1696.

14. Kaymak-Ertekin, F., and A. Gedik (2004). Sorption isotherms and isosteric heat of sorption for grapes, apricots, apples and potatoes. Lebensmittel-Wissenschaft und Technologie, 37: 429-438.

15. Labuza, T. P. (1975). Interpretation of sorption data in relation to the state of constituent water. In Water Relations in Foods; Duckworth, R. Ed.; Academic Press: 155-172.

16. Lahsasni, S., Kouhila, M., Mahrouz, M. and M. Fliyou (2003). Moisture absorption desorption isotherms of pickly pear cladode (Opuntia ficus-indica) at different temperatures. Energy Conservation and Management, 44: 923-936.

17. Lahsasni, S., Kouhila, M. and M. Mahrouz (2004). Adsorption-desorption isotherms and heat of sorption of pickly pear fruit (Opuntia ficus-indica). Energy Conservation and Management, 45: 249-261.

18. Lomauro, C. J., Bakshi, A. S. and T. P. Labuza (1985). Evaluation of food moisture sorption isotherm equations, Part I: Fruit, vegetable and meat products. Lebensmittel-Wissenschaft und Technologie, 18: 111-117.

19. Mir, M. A. and N. Nath (1995). Sorption isotherms of fortified mango bars. Journal of Food Engineering, 25: 141-150.

20. McLaughlin, C. P. and T. R. A. Magge (1998). The determination of sorption isotherm and the isosteric heats of sorption for potatoes. Journal of Food Engineering, 35: 267-280.

21. Mohamed, L. A., Kouhila, M., Lahsasni, S., Jamali, A., Idlimam, A., Rhazi, M., Aghfir, M. and M. Mahrouz (2005). Equilibrium moisture content and heat of sorption of Gelidium sesquipedale. Journal of Stored Products Research, 41: 199-209.

22. Okos, M. R., Narsimhan, B., Singh, R. P. and A.C. Weimauer (1992). Food Dehydration. In Hand Book of Food Engineering; Heldman, D.R., Lund, D.B. Eds.; Marcel Dekka: New York, 437-562.

23. Rahman, M. S. and T. P. Labuza (1999). Water activity and food preservation. In Handbook of Food Preservation; Rahman, M.S. Eds.; Marcel Dekker: New York, 339-382.

24. Samapundo, S., Devlieghere, F., De Meulenaer, B., Atukwase, A., Lamboni, Y. and J. M. Debevere (2007). Sorption isotherms and isosteric heats of sorption of whole yellow dent corn. Journal of Food Engineering, 79: 168-175.

25. Shivhare, U. S., Arora, S., Ahmed, J. and G. V. S. Raghavan (2004). Moisture adsorption isotherms for mushroom. Lebensmittel-Wissenschaft und Technologie, 37: 133-137.

26. Soysal, Y. and S. Öztekin (2001). Sorption isosteric heat for some medicinal and aromatic plants. Journal of Agricultural Engineering Research, 78: 159-166.

27. Sun, D. W. and J. L. Woods (1994). The selection of sorption isotherm equations for wheat based on the fitting of available data. Journal of Stored Products Research, 30(1): 27-43.

28. Swami, S. B., Das, S. K. and B. Maiti (2005). Moisture sorption isotherms of black gram nuggets (bori) at varied temperatures. Journal of Food Engineering, 67: 477-482.

29. Tsami, E. (1991). Net isosteric heat of sorption in dried fruits. Journal of Food Engineering, 14: 327-335.

30. Van den Berg, C. (1984). Description of water activity of foods for engineering purpose by means of the GAB model of sorption. In Engineering and Food; McKemenne, B.M. Eds.; Elsevier: 147-177.

31. Van den Berg, C. and S. Bruin (1981). Water activity and its estimation in food system. In Water Activity: Influences on Food Quality; Rockland, L. B. and Stewart, G. F. Eds.; Academic Press: 311-321.

32. Wang, N. and J. G. Brennan (1991). Moisture sorption isotherm characteristics of potatoes at four temperatures. Journal of Food Engineering, 14: 269-282.

VELOCITY OF ULTRASOUND AS AN EFFECTIVE INDICATOR OF THE SUGAR CONTENT AND VISCOSITY OF WATERMELON JUICE

Feng-Jui Kuo[*], Chung-Teh Sheng[†] and Ching-Hua Ting[‡§]

ABSTRACT

This paper presents the application of a low-intensity ultrasonic system to measure the sugar content and viscosity of reconstituted watermelon juice. The system, which operates in pulse-echo (PE) mode, detects the above two properties using responsive velocity of ultrasound and power attenuation. Experimental results show that the power attenuation is ineffective for such a purpose, and that the velocity of ultrasound tends to respond linearly to sugar content ($R^2 = 0.996$) and viscosity ($R^2 = 0.992$).

Keywords: *Ultrasonic velocity; Sugar content; Viscosity; Watermelon juice.* © 2007 AAAE

1. INTRODUCTION

In Taiwan, the juice production industry plays an important role in the harvest season as fresh fruits are usually in excess of demand. To maximize the profit and balance the market, fresh juice may be stored as a concentrated solution and later delivered to the market as reconstituted bottle juice. Bottled juices, either fresh or reconstituted, may be blended with additives, diluted with water, or have added sugar to arrive at a specific flavor.

The sweetness and viscosity are two important quality factors for providing juice products with quantifiable attributes. The sweetness is a taste sensation that is difficult to measure directly and hence the sugar content is metered alternatively (Harker *et al.*, 2002). Practical methods currently used for measuring sugar contents include Brix refractometer probing, chemical analysis, and near-infrared (NIR) detection. Brix refractometer probing and chemical analysis are traditional, accurate and effective, but can only be manually operated (Lynnworth, 1989). NIR spectrum analysis is accurate and efficient in distinguishing the concentrations of individual sugar components (Rodriguez-Saona *et al.*, 2001). However, the equipment and consumables are costly and cannot be operated in real time. The viscosity is measured in another ways such as a

manual viscometer that infers the viscosity through detecting the shear force of the fluid. These manual operations impair their exploitation in measuring system responses for automated juice processing.

Low-intensity ultrasonic waves which are emitted from equipment isolated from the target material are a well-studied means of measuring material properties in food processing, as they do not introduce extraneous contamination nor alter the properties of the substance (Cartwright, 1998b; Bhardwaj, 2001). Ultrasonic waves are normally emitted in pulse trains of a short period and the responses occur after a short duration propagation. This means that the interaction of sound with matter will provide information in a limited time. The nature of non-contact sensing and prompt provision of information makes ultrasonics an effective quality detector for real-time applications (Cartwright, 1998a; Bhardwaj, 2001). The energy of high-intensity ultrasound passes to the medium resulting in cavitation, which may cause a rapid change of heating to 5000 $^{\circ}$C, about the temperature of the sun's surface, and pressure increase to 50 MPa (Suslick, 1990). The sudden heating up and the pressure change can be used to alter the microorganisms in foodstuffs (Knorr *et al.*, 2004; Valero *et al.*, 2007) and to generate new chemical compositions from the substrate (Suslick, 1990; Mason *et al.*, 1996).

[*] Lecturer, Department of Biomechatronic Engineering, National Chiayi University, Chiayi, Taiwan

[†] Professor, Department of Bio-Industrial Mechatronics Engineering, National Chung Hsing University, Taichung, Taiwan

[‡] Associate Professor, Department of Biomechatronic Engineering, National Chiayi University, Chiayi, Taiwan

[§] Corresponding author: 300 University Road, Chiayi 600, Taiwan; Email:cting@mail.ncyu.edu.tw; Tel: +8865-2717642; Fax: +886-5-2717647.

Ultrasonic velocity measurement is a widely used and indispensable method for determining the adiabatic compressibility of fluids (Nölting, 1995) and a wide range of thermodynamic parameters (Ewing, 1993). The simple theory together with the cost reduction in ultrasonic transducers spur the use of ultrasonics in measuring and processing of biological properties in the food industry (McClements, 1995). These industrial applications, for example, include the measurements of texture, viscosity, and concentration of many solid or fluid foods (Contreras Montes de Oca *et al.*, 1992; Fox *et al.*, 2004); composition determination of dairy products (Ay and Gunasekaran, 2003; Dukhin *et al.*, 2005); and non-destructive inspection of whole fruits, vegetables and meats (Hachiya *et al.*, 1991; Mizrach, 2000; Verlinden *et al.*, 2004). In aqueous sugar solutions, the velocity of sound appears to correlate with the temperature, sugar concentration, and solution density (McClements, 1995; Harker *et al.*, 2002) and with the viscosity (Zhao *et al.*, 2003).

In low-attenuation fluids, the velocity of sound and the properties of solution is linked with the so-called Wood equation (Wood, 1964):

$$\upsilon = \frac{1}{\sqrt{\kappa\rho}} \qquad (1)$$

where κ is adiabatic compressibility and ρ is density of solution. The Wood equation is analogy to:

$$\upsilon^2 = \frac{B + \mu\omega}{\rho} \qquad (2)$$

where B is the bulk modulus, ω is the acoustic angular frequency, and μ is the viscosity for Newtonian fluids and apparent viscosity for non-Newtonian fluids (Zhao *et al.*, 2003). This equation indicates that a denser fluid (with a larger ρ) or a more compressible fluid (with a larger κ or smaller viscosity) will reduce the velocity of sound propagation in the fluid. However, the propagation velocity of sound traveling in a fluid is a competing factor between density ρ and compressibility κ. The relationship between the two variables is described with the concept of "concentration increments" (Sarvazyan, 1991):

$$[\kappa] = -2[\upsilon] - [\rho] \qquad (3)$$

where the bracketed notations are defined by

$$[\kappa] = \frac{\Delta\kappa}{\kappa}$$

$$[\upsilon] = \frac{\Delta\upsilon}{\upsilon}$$

$$[\upsilon] = \frac{\Delta\rho}{\rho}$$

as the relative ratios of change. In organic solution the compressibility (κ) decreases to a greater degree if its density (ρ) increases (Sarvazyan, 1991). The combined effect of a considerably decreased compressibility subject to an increased density will increase the velocity of ultrasound (v) in solution. This fact of physics elucidates the use of ultrasonic velocity in determining the density and compressibility of a solution, the sugar content and viscosity.

Based on the Wood equation and the concept of concentration increments, we developed a pulse-echo (PE) ultrasonic measurement system for assessing the sugar content and viscosity in watermelon juice. The exploitation was initially carried out on aqueous sugar solutions of various concentrations. The responsive velocity and power attenuation of ultrasound propagation were investigated before adopting either as the instrumental indicator. The preliminary investigation on aqueous solutions provides a macroscopic point of view of ultrasonic velocity in response to various sugar concentrations. Based on the preliminary study, the approach was extended to screened watermelon juice blended with various amounts of sugar solutions.

2. THE ULTRASONIC MEASUREMENT SYSTEM

2.1 Theoretical Assumption

The sugar in solution is assumed to be completely soluble and the resultant density ρc is:

$$\rho c = \frac{W_\omega + W_s}{W_\omega \cdot \rho_\omega^{-1} + W_s \cdot \rho_s^{-1}} \qquad (4)$$

where W_ω is the weight of water, W_s the weight of sugar, ρ_ω the specific gravity of water, and ρ_s the specific gravity of sugar.

The sugar content of solution provides an alternative, indirect measurement of sweetness sensation supposing the solution to be free of artificial sweetener (Harker *et al.*, 2002). Additional sugar dissolved in a solution alters the sensation of sweetness. The sugar content (S_c) in 88 water (W_ω) is a fraction of the dissolved sugar (W_s):

$$S_c = \frac{W_s}{W_\omega + W_s} \qquad (5)$$

The food industry uses "Brix" to measure S_c. For fruit juices, one degree Brix is about 1 - 2% sugar by weight. This usually correlates well with perceived sweetness. Eq. (4) provides a correlation between ultrasonic velocity of Eq. (3) and Brix of Eq. (5). Increasing the sugar content in the solution increases the Brix index S_c and the density ρ_c. The added sugar composition induces a descent in adiabatic compressibility κ. These effects accelerate the propagation of ultrasound in the solution, as the concept of concentration increments predicts. The Brix index of fluid is directly linked with the concentration of the dissolved sugar. Hence, we may expect a correlation between the Brix index of fluid and the behavior of the ultrasound traveling in the fluid.

A similar correlation can also be expected on viscosity since a fluid with more sugar becomes tackier and hence has a higher viscosity (Greenwood *et al.*, 2006). A fruit juice contains other chemical compounds rather than the added sugar. The inherent chemical compounds influence the ultrasonic velocity (Dukhin *et al.*, 2005) and the viscosity (Zhao *et al.*, 2003). In theory, the chemical compounds change the modulus, i.e. the compressibility, and hence the ultrasonic velocity. This phenomena is to be demonstrated by the experimental results.

2.2 The Apparatus

Fig. 1 shows the structure of the in-house developed pulse-echo ultrasonic measurement system. The sample chamber accommodates 400 ml of fluid being detected and is immersed in water kept at a constant temperature to mitigate temperature effects on acoustic propagation. Acoustic velocity is very sensitive to temperature. In water, it changes about 2.4 m/s per degree Celsius. A 1 MHz ultrasonic transducer (Western NDE, Canada) is mounted onto the sample chamber. A computer-controlled ultrasonic instrument (WT-UT-001A, Western NDE, Canada) excites the transducer to emit ultrasound into the fluid and amplifies the received ultrasonic waves at a gain of 60 dB. Ultrasonic responses and inferred data are displayed on-line for human intervention and recorded for subsequent off-line analysis. The transducer was calibrated using reverse osmosis (RO) water as the reference solution.

The transducer ($\varphi 20$ mm) was excited to emit ultrasound at a maximum power of 800 mW/m^2 (0.25 W in total) and a duty duration of 60 μs. In food processing using ultrasonics, the ultra sound is
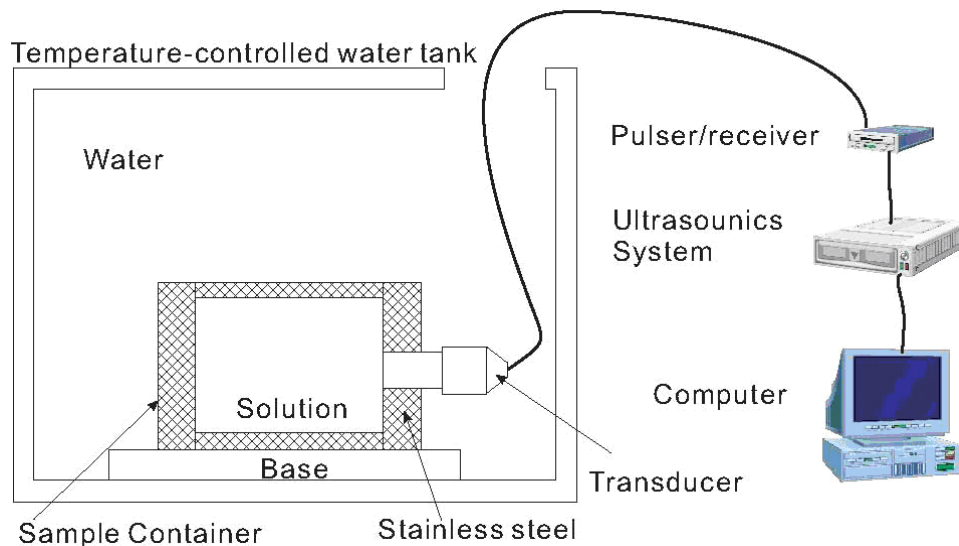
Fig. 1: The ultrasonic measurement system developed in house

designed with a power intensity much higher than 1 kW/m^2 to heat up the material or alter the micro-organisms because of the cavitation effects induced by acoustic vibration in the medium (Suslick, 1990; Knorr et al., 2004). Ultrasound irradiation to orange juice at 500 kHz/240W for 15 min inhibited the growth of microbial organisms effectively and did not cause detrimental effects on the quality attributes of juice (Valero et al., 2007). In this study, the employed transducer emits a very low intensity (0.25 W @ 60 μs = 15 μJ) of acoustic stimulation to the medium. In comparison with the intensity used in food processing, this intensity is too small to introduce substantial heat or sonochemical effects on the juice, i.e. the thermodynamic attributes of juice can be considered unchanged during the course of ultrasonic measurement. This assumption is essential since the thermodynamic attributes forms the essence of ultrasonic measurement, as the Wood equation describes.

The sample chamber was designed with a dimension within the ultrasonic near field ((Fresnel field). The near field is the ideal region for measurement of highest accuracy because of maximum beam power. Ultrasonic waves diverge while propagating beyond the designated near-field distance. Thus, ultrasonic waves propagate within the near field having a stronger power than that beyond the near field. The near field, Z_m, is defined as the distance within:

$$Z_m = \frac{r^2 \cdot f}{\upsilon} \tag{6}$$

where r is the radius of the probe, f the ultrasonic frequency, and v the velocity of ultrasound.

The adopted transducer has a radius of 10 mm and an operating frequency of 1 MHz. For aqueous sugar solution at a reasonable temperature around 25 ^{o}C, the expected ultrasonic velocity ranges from 1465 m/s in water to 1714 m/s in dense aqueous sugar solution (Contreras Montes de Oca et al., 1992). This gives a maximum allowable near-field distance of 58 mm to assure a minimum resistance to ultrasound propagation in fluid. In this study, the inner space of the sample chamber is chosen to be 33 mm giving a safety factor of 1.75 to account for uncertain mechanical variations in materials and devices.

2.3 Measurement of Ultrasonic Velocity

The ultrasonic system, as shown in Fig. 2, emits a chirp of ultrasound (wave "a") through the solution until the acoustic waves impinge on the steel wall of the container. Part of the acoustic energy is reflected (wave "b") depending on the size of the interface and the relative impedance difference (Lynnworth, 1989). The reflection process continues until the ultrasound decays in the fluid. All reflected waveforms ("b" and "d") are picked and converted by the transducer to electric signals, with peak amplitudes A_b and A_d. The waveform remains a chirp shape but with an attenuated amplitude after reflection. The velocity of acoustic propagation in a medium is only a function of the properties of the medium, especially the density and adiabatic compressibility as shown in Eq. (1). Unlike in food processing, the acoustic intensity for property detection is small and the produced heat and cavitation effect is negligible. Therefore, it is reasonable to assume that the medium has fixed adiabatic compressibility and density during the short period of measurement (McClements, 1995).

The two reflected waveforms in Fig. 2 show conceptually that the magnitudes are attenuated after reflection, with the same frequency. The attenuation is understandable since part of the ultrasonic energy is turned to numerous bubbles which cause cavitation effect on the fluid (Suslick, 1990). A portion of the acoustic energy is consumed by cavitation, which can be seen as being absorbed by the solution. The velocity of ultrasound is measured by counting the time elapsed between the peak amplitudes of two consecutive reflections. The ultrasonic velocity in the sample solution is calculated as:
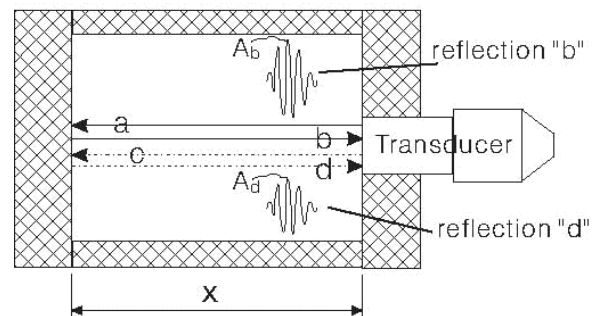
Fig. 2: The sample chamber and waveform propagation

$$\upsilon = \frac{2x}{t_d - t_b} \tag{7}$$

where t_d and t_b denote the occurrence times of peaks A_d and A_b; $x=33$ mm (within near field 58 mm) is the inner space of the sample chamber.

The power attenuation (α, dB/m) is calculated by:

$$\alpha = \frac{1}{2x}\log_{10}(\frac{A_b}{A_d}) \tag{8}$$

This equation states that the propagation route x is a significant factor in ultrasound attenuation. A larger coefficient indicates a more attenuated propagation.

2.4 Measurement of Physical Characteristics

The bath water was kept at 30±0.5 ^{o}C to alleviate possible temperature influence on fluid properties and ultrasonic propagation. The sugar content was quantitatively measured using a Brix refractometer (N-50E, Atago, Tokyo, Japan) with a reference temperature of 20 ^{o}C. The actual Brix indices were calibrated to fit the ambient (bath water) temperature at 30 ^{o}C. The viscosity of solution was measured using an LVDV-II+ Brookfield Cone and Plate Viscometer (Brookfield, MA, USA). A measurement was completed within 1 minute to avoid possible degrading effects on the juice.

3. PRELIMINARY EXPERIMENTS ON AQUEOUS SUGAR SOLUTIONS

3.1 Preparation of Aqueous Sugar Solutions

Different quantities of white refined cane sugar were dissolved in RO water to obtain 25 sample solutions with concentrations ranging from 2% to 50% at incremental steps of 2%. The sample chamber of Fig. 2 was filled with sample solution and then covered with a lid to avoid environmental influence on acoustic transmission in the chamber. The ultrasonic velocity, attenuation, Brix, and viscosity of each sample solution were measured and recorded. Fig. 3 records Brix and density measurements as functions of sugar contents S_c of Eq. (5). The Brix index is an alternative measurement of solution density ρ_c of Eq. (4). The relation between S_c and ρ_c can hence be considered ideally as a linear function. This

relationship reveals that the Brix index of a solution can be easily altered by regulating the amount of added sugar. It also allows us to investigate the sugar content using the Wood equation, Eq. (1), by means of the velocity of ultrasound.

3.2 Ultrasonic Velocity and Brix

The equations Eq. (1) and (3) state that an increased ultrasonic velocity in response to an increased density can be expected. Rewriting Eq. (3) in the form:

$$[\upsilon] = \frac{-[\kappa]-[\rho]}{2} \tag{9}$$

A positive $[\rho]$ is associated with a more negative $[\kappa]$ thus giving a positive $[v]$, i.e. the velocity increases. Experimental results in Fig. 4 show that there is a linear correlation between ultrasonic velocity and Brix. The experimental data deviate slightly from the regression line at around 30 Brix. The discrepancy because of experimental variation is considered acceptable as the standard deviation of the regression error is about 68 m/s comparing to the average velocity of 1550 m/s. This preliminary result on aqueous sugar solutions demonstrates the possibility of ultrasonic velocity as an effective indicator of Brix index and density in fluid.

3.3 Ultrasonic Velocity and Viscosity

The viscosity of solution is a function of the sugar content (Harker *et al.*, 2002), which alters the chemical composition and hence the modulus of the solution. The relation between the two variables is nonlinear as shown in Fig. 5. The viscosity is linearly proportional to Brix at values less than 35 and is exponential beyond 35. This behavior shows that a solution containing more sugar is much tackier than a light solution. The relationship between the ultrasonic velocity and the viscosity is nearly exponential, as shown in Fig. 6. The tomato and the orange juices have the same ultrasonic velocity profile in responses to the viscosity (Zhao *et al.*, 2003). There exists a nearly linear correlation for viscosity less than 3 mPas. The ultrasonic velocity almost saturates for viscosity values beyond 3 mPas. This is understandable as a tackier solution exhibits a larger

shear resistance to the employed rotary viscometer in fluid mechanics.

3.4 Ineffective Ultrasonic Attenuation

The ultrasound attenuation is a complicated function of wave propagation in a fluid. Factors that may affect ultrasound attenuation include the viscosity, compressibility, wall material, and scattering and adsorption effects (Povey, 1997). No meaningful correlation was found between the attenuation coefficient and Brix (Fig. 7) and viscosity (Fig. 8) in the experimental results. Thus, ultrasound attenuation was not considered in subsequent studies.

3.5 Summary from Preliminary Experiments

The ultrasonic velocity in solution is an effective, non-destructive indicator of Brix and viscosity. In theory, ultrasound propagating in a fluid is attenuated and hence distinguishable attenuation coefficients can be expected (McClements, 1995). However, the laboratory study revealed a non-applicable attenuation coefficient profile. This means that the velocity of ultrasound is a more reliable indicator for instrumentation in food processing. The characteristics of the inspected solution will not be altered by the ultrasound as the measurement uses low intensity ultrasound.

Though the preliminary study was carried out on water dissolved with various amounts of sugar. The result may be used as a guide for studies relating to juice production. Encouraged by the good correlation between ultrasonic indices and physical properties, the experimental study was extended to detect the Brix index and viscosity of watermelon juice blended with sugar solutions of various concentrations.

4. APPLICATION TO WATERMELON JUICE

4.1 Preparation of Sample Solutions

A juice sample consists of 300 ml of fresh watermelon juice and 600 g of sugar solution. Watermelon juice was obtained from fresh watermelons with pulps being screened out using a stainless steel mesh filter with an aperture size of 0.061 mm^2. Aqueous sugar solutions were prepared having concentrations ranging from 0% to 22% at incremental steps of 2%, which gave a Brix range

from 4.7 to 20. This Brix range is adequate for commercial reconstituted juices that normally have an maximum Brix index between 10.6 and 11.6 (USDA, 1995). The sample chamber of Fig. 2 was filled with the blend and was tightly covered with a lid. The laboratory work was the same as that used in the previous study on aqueous sugar solutions.

4.2 Measurement of Sugar Content and Viscosity

Fig. 9 shows the responses of ultrasonic velocity to pure watermelon juice blended with solutions of various sugar concentrations. The ultrasonic responses show a good linear correlation between the ultrasonic velocity and the Brix index in watermelon juice. The reconstituted juice can be blended to any expected Brix and the Brix can be easily detected by the non-contact ultrasonic system.

Fig. 10 shows a nearly linear relationship for viscosity below 2.6 mPa·s, i.e. a sugar content less than 20 Brix. The watermelon juice is too tacky and sweet to drink for a viscosity beyond 2.6 mPa·s or a Brix index bigger than 20. When the sugar content in solution is increased, the viscosity increases proportionally in two different rates (Fig. 6): linear for viscosity below 3 mPa·s and exponential for the beyond. This linear zone is large enough in juice control processing.

5. DISCUSSION

The Brix indices of both aqueous solution and watermelon juice can be effectively indicated by the ultrasonic velocity. The aqueous sugar solution expresses a slower ultrasonic velocity (υ = 1434 m/s) than watermelon juice (υ = 1470 m/s) when the Brix indices of both fluids are set to zeros, i.e. x = 0 in Fig. 4 and 9. This is because the watermelon juice contains more chemicals than the aqueous sugar solution. Acoustic velocity is very sensitive to chemical composition, changing roughly 100 m/s at a concentration of 1 mol/L of a simple salt (Dukhin et $al.$, 2005). The addition of sugar increases the Brix index in a linear trend (Fig. 3) but may change the viscosity dramatically (Fig. 5). This facts indicates that the modulus (reciprocal compressibility) of solution is a strong function of the chemical composition. According to Eq. (1) and Eq. (3), the offset difference indicates that the chemicals diminish the compressibility κ at a larger degree than increase

the density ρ. The combined effect results in a faster ultrasonics velocity in watermelon juice. The offset value provide valuable macroscopic information about the chemical composition in a fluid, although the exact chemical formula is still unveiled. However, the information is useful in juice producing if the concentration of chemical composition 264 is the variable to be controlled.

Though the juice was screened, there were still residual pulps that attenuated ultrasound propagation by scattering effects. A same phenomenon was observed in orange juice but not in apple juice (Rodriguez-Saona et al., 2001). Hence, the velocity of ultrasound is a more robust and reliable measurement than the coefficient of power attenuation. This behavior is implied in Eq. (1), where the formula accounts for propagation velocity depending only on the occurrences of reflected waveforms. The velocity is only a function of adiabatic compressibility and density. These two thermodynamic properties of fluid are not affected by any attenuation related variables. This explains why the ultrasonic velocity is more robust and reliable than the attenuation coefficient.

In high-intensity ultrasonics, the extreme heat and pressure by ultrasonic cavitation at a spot is an effective energy in disintegrating the chemical structure of a substance (Suslick, 1990) and is therefore used in food processing for food preservation and product modification (Knorr et al., 2004). Such a degree of cavitation effect is unlikely to develop in ultrasonic measurement that exploits low-intensity ultrasound, though the development of cavitation is inevitable. The inherent cavitation effect in ultrasonic measurement is beneficial to altering micro-organisms in fluid although the effect is trivial. Hight-intensity ultrasonic irradiation of orange juice effectively suppressed the growth of micro-organisms in the juice and the sensory properties and color of the juice were not negatively affected (Valero et al., 2007). The study is positive, constructive to the use of ultrasound in measuring the properties of juice since the induced sonochemistry is positive and and the sensory properties of juice are intact.

The application of ultrasound for the determination of composition relies on there being a significant change in the ultrasonic properties of a food as its composition varies. The greater the magnitude of the change, the more accurately the composition can be determined. The ultrasonic velocity of the aqueous sugar solution increases by ~5 m/s for each 1 Brix increase in the sugar concentration (Fig. 4); and by ~3 m/s in the blended watermelon juice (Fig. 9). It is simple to measure the ultrasonic velocity of a solution to 0.3 m/s, the Brix measurement can be determined to within 0.1 Brix. This approach has been used successfully to determine the sugar concentration of various fruit juices and drinks (Contreras Montes de Oca et al., 1992). The regression equations in Fig. 9 and 10 give analogue measurements of sugar content and viscosity in watermelon juice. This is valuable and important for real-time applications of ultrasound in juice production. The measurements can be used as a feedback signal in automatic regulating the sugar content and viscosity during the production of reconstituted juice.

6. CONCLUSIONS

An ultrasonic measurement system has been developed for determination of sugar content and viscosity in filtered watermelon juice. The velocity of ultrasound tends to respond linearly to sugar content ($R^2 = 0.996$) and viscosity ($R^2 = 0.992$) when the Brix index is less than 30. The power attenuation of ultrasound in watermelon juice is ineffective for such a purpose. Both the sugar content and the viscosity can be described with good linear regression equations. These regression equations are valuable in the use of ultrasonic measurement as a alternative solution to tradition refractometers and viscometers, particularly in real-time applications.

The measurement system was operated in a static manner and the sample solution was confined in an isolated chamber. For the purpose of industrial applications, the measurement should be capable of dealing with flowing fluids and other juices should be investigated. This subject is challenging as flowing fluids will alter the propagation of the impinging ultrasound. Dynamic measuring allows us to build an automated inspection system that will lead to an automatic juice quality control system for the juice industry.

It is obvious from the experimental results that ultrasonic velocity can be influenced by other compounds rather than just sugar. The difference between sugar and other compounds could be determined by the differences in the offset and slope of the regression equation (Fig. 9). For example, the ultrasonic velocity in watermelon juice has a larger
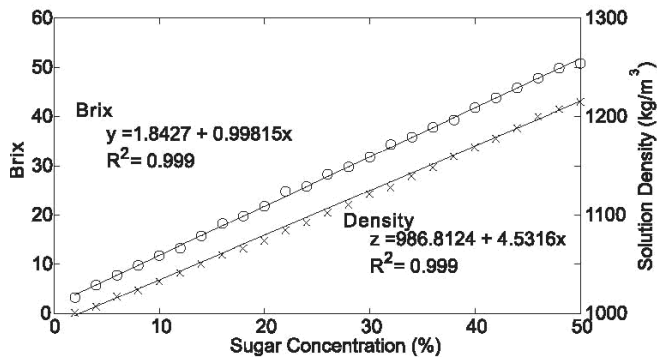
Fig. 3: Prepared aqueous sugar solution samples
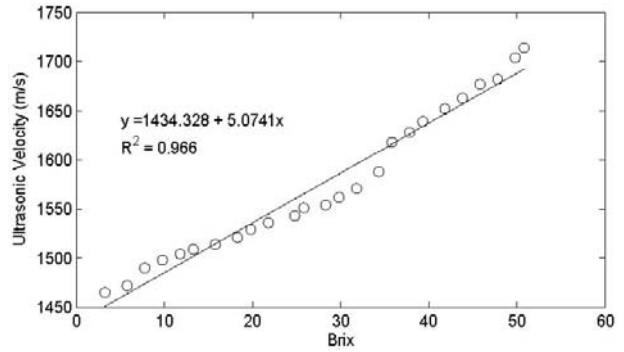
Fig. 4:   Ultrasonic velocity and Brix in aqueous sugar solution
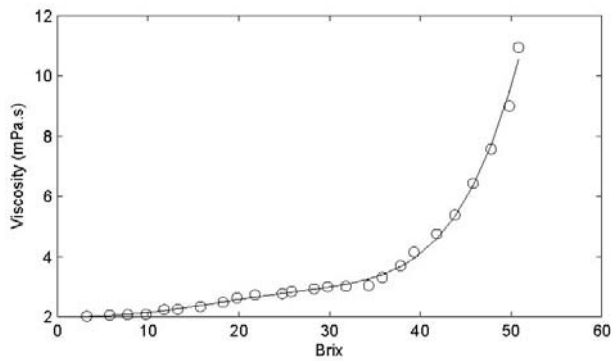
Fig. 5: Viscosity as a function of Brix
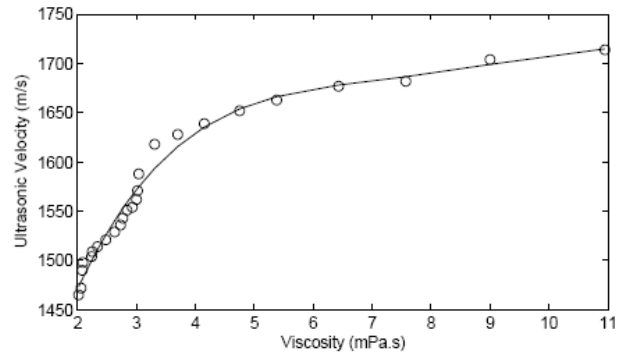
Fig. 6:   Ultrasonic velocity and viscosity in aqueous sugar solution
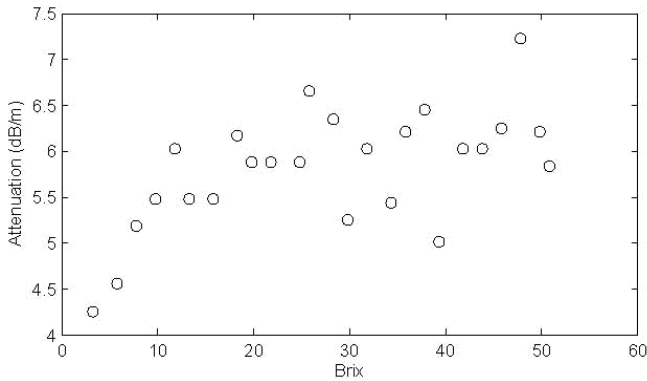
Fig. 7:   Ultrasonic attenuation and Brix in aqueous sugar solutions
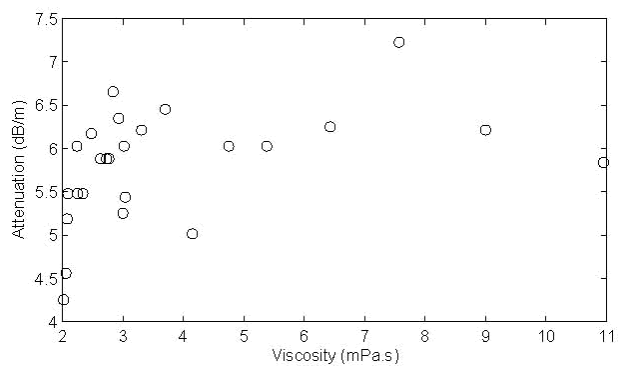
Fig. 8:   Ultrasonic attenuation and viscosity in aqueous sugar solutions
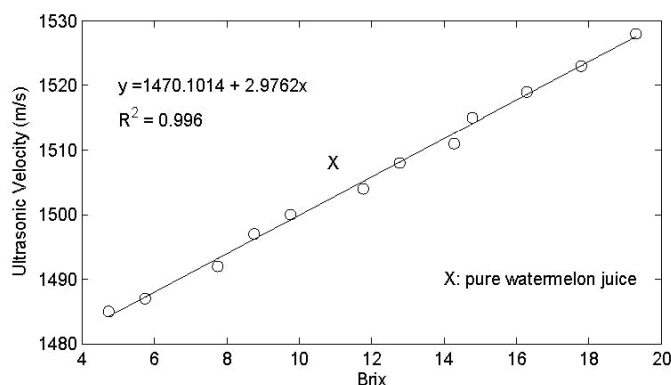
Fig. 9: Ultrasonic velocity and Brix in watermelon juice
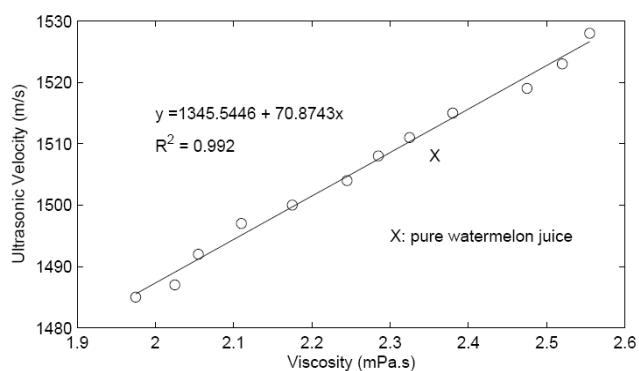
Fig. 10: Ultrasonic velocity as a function of the viscosity of watermelon juice

offset and a small slope in the on different juices or chemical solutions.

REFERENCES

1. Ay, C. and S. Gunasekaran (2003). Numerical method for determining ultrasonic wave diffusivity through coagulating milk gel system. Journal of Food Engineering, 58: 103–110.
2. Bhardwaj, M. C. (2001). Non-contact ultrasound: the final frontier in nondestructive testing and evaluation. In Biderman, A., editor, Encyclopedia of Smart Materials. Wiley, New York.
3. Cartwright, D. (1998a). Off-the-shelf ultrasound instrumentation for the food industry. In Povey, M. J. W. and Mason, T. J., editors, Ultrasound in Food Processing, chapter 2. Blackie, London.
4. Cartwright, D. (1998b). Rapid determination of food material properties. In Povey, M. J. W. and Mason, T. J., editors, Ultrasound in Food Processing, chapter 3. Blackie, London.
5. Contreras Montes de Oca, N. I., Fairley, P., McClements, D. J. and M. J. W. Povey (1992). Analysis of the sugar content of fruit juices and drinks using ultrasonic velocity measurements. International Journal of Food Science and Technology, 27: 515–529.
6. Dukhin, A. S., Goetz, P. J. and B. Travers (2005). Use of ultrasound for characterizing dairy products. Journal of Dairy Science, 88(4): 1320–1334.
7. Ewing, M. B. (1993). Thermophysical properties of fluids from acoustic measurements. Pure and Applied Chemistry, 65: 907–912.
8. Fox, P., Smith, P. P. and S. Sahi (2004). Ultrasound measurements to monitor the specific gravity of food batters. Journal of Food Engineering, 65: 317–324.
9. Greenwood, M. S., Adamson, J. D. and L. J. Bond (2006). Measurement of the viscosity– density product using multiple reflections of ultrasonic shear horizontal waves. Ultrasonics, 44(Supplement): e1031–e1036.
10. Hachiya, H., Ohtsuki, S. and M. Tanaka (1991). A method for measurement of sound speed in biological tissues without deformation. Japanese Journal of Applied Physics, 30(1, Supplement): 235–237.
11. Harker, F. R., Marsh, K. B., Young, H., Murray, S. H., Gunson, F. and S. Walker (2002). Sensory interpretation of instrumental measurements 2: sweet and acid taste of apple fruit. Postharvest Biology and Technology, 24(3): 241–250.
12. Knorr, D., Zenker, M., Heinz, V. and D. Lee (2004). Applications and potential of ultrasonics in food processing. Trends in Food Science and Technology, 15: 261–266.
13. Lynnworth, L. C. (1989). Ultrasonic measurements for process control techniques: applications. Academic Press, New York.
14. Mason, T. J., Paniwnyk, L. and J. P. Lorimer (1996). The uses of ultrasound in food technology. Ultrasonics Sonochemistry, 3: S253–S260.
15. McClements, D. J. (1995). Adavances in the application of ultrasound in flood analysis and processing. Trends in Food Science and Technology, 6: 293–299.

16. Mizrach, A. (2000). Determination of avocado and mango fruit properties by ultrasonic technique. Ultrasonics, 38:717–722.

17. Nölting, B. (1995). Relation between adiabatic and pseudoadiabatic compressibility in ultrasonic velocimetry. Journal of Theoretical Biology, 175:191–196. Povey, M. J. W. (1997). Ultrasonic Techniques for Fluids Characterization. Academic Press, London.

18. Rodriguez-Saona, L. E., Fry, F. S., McLaughlin, M. A. and E. M. Calveyb (2001). Rapid analysis of sugars in fruit juices by FT-NIR spectroscopy. Carbohydrate Research, 336(1):63–74.

19. Sarvazyan, A. P. (1991). Ultrasonic velocimetry of biological compounds. Annual Review of Biophysics and Biophysical Chemistry, 20:321–342.

20. USDA (1995). United States Standards for Grades of Concentrated Tangerine Juice for Manufacturing. Technical Report 20 FR 7281, U.S. Department of Agriculture, Washington D.C., USA.

21. Valero, M., Recrosio, N., Saura, D., Munõz, N., Martí, N. and V. Lizama (2007). Effects of ultrasonic treatments in orange juice processing. Journal of Food Engineering, 80:509–516.

22. Verlinden, B. E., Smedt, V. D. and B. M. Nicolaï (2004). Evaluation of ultrasonic wave propagation to measure chilling injury in tomatoes. Postharvest Biology and Technology, 32(1):109–113.

23. Wood, A. B. (1964). A Textbook of Sound. Bell, London, 3rd edition.

24. Zhao, B., Basir, O. A. and G. S. Mittal (2003). Correlation analysis between beverage apparent viscosity and ultrasound velocity. International Journal of Food Properties, 6(3):443–448.

THIN LAYER DRYING MODEL FOR NATURAL CONVECTION DRYING OF PARBOILED PADDY

C. B. Singh[*], S. Bal[†], P. K. Ghosh[*] and D. S. Jayas[*‡]

ABSTRACT

Parboiling of paddy and subsequent drying to remove moisture are the major energy intensive operations in rice milling industry. In forced convection drying of paddy considerable amount of energy is consumed to heat and pump hot air through grain. In this study an attempt was made to establish drying characteristics of parboiled paddy for natural convection drying at elevated temperatures. A series of thin-layer drying experiments on parboiled paddy were performed at 70, 80, 100, 110, 120, and 130 °C for single-kernel thick layers. Several thin layer drying models were evaluated from which a model based on Page's equation predicted the moisture ratios well at all the drying temperatures investigated. Activation energy of the drying process in this study was calculated to be 28.7 kJ/g mol, which is lower than the literature values for forced convection drying.

Keywords: *Parboiled paddy; Natural convection drying; Thin layer drying; Modeling.* © 2007 AAAE

1. INTRODUCTION

Rice (*Oriza sativa* L.) is a staple food for most of the world's population. On average the global production of paddy is 600 Mt (FAO, 2002). Paddy is subjected to various processing and handling operations namely cleaning, soaking in cold or hot water, steaming, drying, and milling. During milling considerable amount of breakage occurs, which reduces the quantity and quality of head rice yield, defined as the mass percentage of unbroken rice after milling. Head-rice yield is reduced due to increased stress cracks occurred due to improper drying (Jayas and Ghosh, 2006), therefore, maximizing the head rice yield is always a priority (Abud-Archila *et al.*, 2000). To achieve that, a pre-milling hydrothermal treatment is usually given to paddy, which is commonly known as parboiling of paddy. During parboiling irreversible swelling and fusion of starch granules occur that changes the starch from crystalline to an amorphous form. The orderly polyhedral structure of starch molecules changes into coherent mass due to this transformation (Rao and Juliano, 1970). The major advantages of parboiling of paddy are high head rice yield, hard and translucent rice, and higher cooking quality (Bhattacharya, 1985). During the parboiling process paddy attains the moisture content of about 33

to 38% wet mass basis (w.b.). Paddy usually contains husk and bran layers, therefore, during drying paddy is not considered to be a single homogeneous material (Noomhorm and Verma, 1986). Drying of parboiled paddy is an important and desirable step before the milling operation. Drying of parboiled paddy with forced air convection has been studied by several researchers to improve the head rice yield (Bhattacharya and Swamy, 1967; Bal *et al.*, 1976; Prasad 1988; Bakshi and Singh, 1980; Sharma and Kunze, 1992). However a large amount of mechanical or electrical energy is needed for blowing hot air into the dryer if dried under forced convection with air. The introduction of natural convection drying system seems to be the most promising alternative to reduce the energy requirement in the drying operation.

Natural convection drying is the process in which water is removed from the grain by the buoyancy force arising from the density differences at the air-grain interface. Only limited efforts have so far been made to study the natural convection air drying of paddy. Zaman and Bala (1989) and Basunia and Abe (2001) studied thin layer drying characteristics of rough rice under natural convection using solar dryer. However the control of solar drying process is difficult due to weather uncertainties, high labour cost, possibility of insect infestation, or mixing of foreign

---

[*] Department of Biosystems Engineering, University of Manitoba, Winnipeg, Manitoba, R3T 5V6, Canada.
[†] Department of Agricultural and Food Engineering, Indian Institute of Technology, Kharagpur, 721 302, India.
[‡] Corresponding author: Digvir_Jayas@Umanitoba.ca.

particles. Basunia and Abe (1998) studied the natural convection drying characteristics of parboiled paddy with a mechanical air dryer operated at a negligible airflow. However, their study was restricted to low temperature drying (11-50 ^{o}C) which took approximately five days to dry the paddy samples. This process would limit practical applicability for drying of parboiled rice. Due to such slow drying rate, high moisture parboiled rice not only can produce foul odour but also this long process would increase the operational cost. Chandra and Singh (1984) demonstrated that high moisture parboiled rice (35-40% w.b.) can be dried at very high temperature in a concurrent flow columnar dryer or a concurrent flow rotary dryer. They conducted thin-layer drying of parboiled rice in a custom-built vertical columnar dryer at 38-158 ^{o}C where a thin layer of grain was placed in the middle of the dryer and hot air was passed from the top to the bottom of the dryer. So far, no studies have been found on the use of natural convection dryers to dry parboiled paddy to verify if the process can be energy efficient. Also, grain variety and grain type have significant effect on the drying behavior and thus parameters needed to design grain drying systems must be determined for specific grain. Therefore, the objectives of this study were to determine thin layer drying characteristics of parboiled paddy during natural convection drying at elevated temperatures and to develop a thin-layer drying model to describe the drying process.

2.   MATERIALS AND METHODS

Medium grain parboiled paddy (variety 'Swarna'), grown in eastern India, was selected as the raw material for this study. Parboiling of paddy was accomplished in a 5 t capacity, industrial parboiling tank at the Mahabir Rice Mill, West Medinipur, West Bengal, India. The parboiled paddy samples were kept in sealed zip-lip low density polyethylene (LDPE) bags in a freezer until used. About 100 g of the parboiled paddy was taken from the freezer at a time and allowed to stabilize for 3 h to room temperature before starting each drying experiment. For each experiment, a sub-sample of 5 g paddy was spread as single-kernel thick layer in each of the 6 to 9 aluminium containers which were removed individually at 15 min interval for drying temperatures of 70 and 80 ^{o}C and at 10 min interval for 100, 110, 120, and 130 ^{o}C. An electronic balance (Sartorius

BM-300S, Sartorius Instruments Pvt. Ltd., Germany) with a resolution of ±0.001g was used to weigh the sample containers to generate the moisture loss data. Triplicate paddy samples of 20 g each were used to determine the initial moisture content by the standard air-oven method before starting each experiment (ASAE, 2003). The initial moisture content of the parboiled paddy was about 35% (w.b.). A natural convection digitally controlled hot air oven (Instruments and Equipments, Calcutta, India) was used for paddy drying experiments. Drying of parboiled paddy was conducted in triplicates for each drying temperatures and the average drying data as a function of drying time were used for the analysis. Higher drying air temperature was limited to 130 ^{o}C because preliminary experiments at temperatures more than 130 ^{o}C produced dark colour rice. Prior to starting the test, the hot air oven was allowed to run with a dummy sample set to stabilize the air conditions. The dummy sample set was then replaced quickly with actual sample containers. The air velocity was very low in the natural convection study (0.2 m/s) so it was not considered a parameter in our study. The relative humidity at high temperature is also negligible, e.g., at 130 ^{o}C and 0.02 humidity ratio, the relative humidity of air is less than 1%. Therefore, relative humidity was not considered a parameter in our study.

The equilibrium moisture content (M_e) was determined by fitting the drying rate (dM/dt) and average moisture content (M_{av}) data to a straight line relationship for each of the drying temperature data sets:

$$\frac{dM}{dt} = P\,M_{av} - Q \tag{1}$$

At equilibrium, $\dfrac{dM}{dt} = 0$ and therefore $M_{av} = M_e$

However, the M_e values determined using this procedure are not true M_e but asymptotic values which give the best fit of the eq. 1 to the drying experimental data.

3.   DATA ANALYSIS

The moisture loss data were first analyzed for determining the dynamic equilibrium moisture content

using eq. 1. Equilibrium moisture content so determined was used to compute the moisture ratios. Chen and Jayas (1998) indicated that the use of dynamic equilibrium moisture content in the drying equations improved the fitting-agreement, especially for drying air with low relative humidity.

Moisture ratio versus time data at drying temperatures of 70, 80, 100, 110, 120, and 130 °C were analyzed to determine the thin-layer drying characteristics of parboiled paddy. Four commonly used thin-layer drying models were evaluated to develop a generalized thin layer drying model to describe the drying behavior of parboiled paddy.

Lewis (1921) developed a simplified drying model based on the Newton's law of cooling that assumes the rate of change in moisture content is proportional to the difference between the grain moisture and its equilibrium moisture content. The mathematical expression of Lewis's equation is:

$$MR = \frac{M_t - M_e}{M_o - M_e} = \exp(-k_1 t) \tag{2}$$

where:
MR = moisture ratio,
M_t = moisture content at time t, (% d.b.),
M_e = equilibrium moisture content (% d.b.),
M_o = initial moisture content (% d.b.),
k_1 = Drying constant determined from experimental data (min^{-1}), and
t = time (min)

Henderson and Pabis (1961) modified the Lewis equation (Eq. 2) by adding another constant as:

$$MR = a \exp(-bt) \tag{3}$$

where:
a = empirical drying constant, and
b = empirical drying constant (min^{-1})

Page (1949) suggested the following equation relating moisture ratio to drying time:

$$MR = \exp(-kt^n) \tag{4}$$

where:
k = empirical drying constant (min^{-n}), and
n = empirical drying constant

A two-term model that uses the first two terms of the general series solution of Fick's diffusion equation can characterize drying of different types of food grains without restrictions of geometric considerations:

$$MR = A \exp(-B t) + C \exp(-D t) \tag{5}$$

where:
A, B = empirical drying constant, and
C, D = empirical drying constant (min^{-1})

The experimental drying data of parboiled paddy were fitted to the Lewis (eq. 2), Henderson and Pabis (eq. 3), Page (eq. 4), and two-term (eq. 5) equations and nonlinear regression analysis was performed using Graphical Analysis 3.0 (Vernier Software and Technology, Beaverton, OR) to determine the parameters of for each equation.

Activation energy which is the minimum energy required for drying operation can be obtained by an Arrhenius-type relationship which relates effective moisture diffusivity to drying temperature (Ozdemir and Derves, 1999).

$$D_{eff} = D_o \exp\left[\frac{-E_a}{RT_{abs}}\right] \tag{6}$$

where,
D_{eff} = effective diffusion coefficient, m^2/s
D_o = effective diffusion coefficient at M_o, m^2/s
E_a = activation energy, kJ/g mol
R = universal gas constant, 8.314 kJ/ g mol K
T_{abs} = absolute temperature, K

Effective diffusion coefficient, D_{eff}, can be calculated using the slope coefficient, b, of Henderson and Pabis model (eq. 3). The b is related to the equivalent radius (R_s) of the paddy kernel (considering spherical shape) by following equation (Mohapatra and Rao, 2004):

$$b = D_{eff} \frac{\pi^2}{R_s^2} \tag{7}$$

4. RESULTS AND DISCUSSION

The parameters of the drying models are presented in Table 1. It can be observed that for the Henderson and Pabis equation (eq. 3), the values of parameter 'a' were approximately equal to 1 and the values of 'b' were approximately equal to the 'k_1' values of the Lewis's equation (eq. 2) for all the investigated drying temperatures. Therefore, it can be said that both the Lewis and Henderson and Pabis equations give similar results for the investigated drying temperatures (70-130 ^{o}C). The values of the parameters were back-substituted into eqs. 2-5 to predict the moisture ratio as a function of drying time, t. The observed and predicted moisture ratio values were compared and statistically analyzed for determining the best-fit equation on the basis of goodness of fit by the correlation coefficient (r), standard error of moisture ratio (SEMR), and root mean square of error (RMSE). The values of r, SEMR, and RMSE for eqs. 2-5 at

temperatures of 70, 80, 100, 110, 120, and 130 ^{o}C are presented in Table 2. Among the four equations, the value of r was the highest ranging from 0.9995 to 0.9999 and the values of SEMR and RMSE were the lowest, ranging from 0.1473 to 0.2497 and 0.0055 to 0.0115, respectively, for the Page's equation (eq. 4). Therefore, Page's equation was considered for further analysis of the drying data.

The Page's equation has been extensively used by many researchers for development of thin layer drying models of other cereal grains (Jayas *et al.*, 1991). Model parameters of the Page's equation, k and n, depend usually on drying air temperature and relative humidity. We compared our parameters of the Page's model with those obtained by Basunia and Abe (1998) for natural convection drying of rough rice at a temperature range of 12-51 ^{o}C and Basunia and Abe (2001) for solar drying of rice at 22-35 ^{o}C (Figs. 1 and 2). It was observed that k value is directly proportional to the drying air temperature. This is

Table 1: Parameter values of four thin-layer drying equations (eq. 2 to 5)

Equations	Temperature (^{o}C)	Parameters
Lewis	70	$k_1 = 0.0288$
	80	$k_1 = 0.0341$
	100	$k_1 = 0.0694$
	110	$k_1 = 0.0841$
	120	$k_1 = 0.1003$
	130	$k_1 = 0.1176$
Henderson and Pabis	70	$a = 1.001, b = 0.029$
	80	$a = 0.992, b = 0.033$
	100	$a = 0.999, b = 0.069$
	110	$a = 0.993, b = 0.084$
	120	$a = 0.995, b = 0.100$
	130	$a = 0.998, b = 0.118$
Page	70	$k = 0.03, n = 0.9893$
	80	$k = 0.0428, n = 0.9373$
	100	$k = 0.0749, n = 0.9738$
	110	$k = 0.1197, n = 0.8781$
	120	$k = 0.1539, n = 0.8405$
	130	$k = 0.1592, n = 0.8821$
Two-term	70	$A = 1.002, B = 0.02913, C = 0.0061, D = -0.006579$
	80	$A = 0.872, B = 0.0308, C = 0.1284, D = 0.0939$
	100	$A = 0.04532, B = 0.02304, C = 0.9567, D = 0.07379$
	110	$A = 0.8311, B = 0.0726, C = 0.1689, D = 0.0967$
	120	$A = 0.7132, B = 0.07803, C = 0.2868, D = 0.2855$
	130	$A = 0.8145, B = 0.1424, C = 0.1856, D = 0.05982$

evident from Fig. 1 which shows that extrapolation of trend line obtained by Basunia and Abe (1998) (low temperature range) has the tendency to merge with the trend line obtained in our study (high temperature range) to create a systematic pattern. The k values obtained for solar drying model are significantly different, which excludes their comparison with the present study. Fig. 2 indicates that n values obtained from our study show a specific sinusoidal pattern with temperature which is very similar to the pattern observed by Basunia and Abe (1998). The n values obtained from the solar drying study were really off and scattered possibly due to inherent complicacy of the process as affected by several other factors.

The values of k were plotted against the temperature (Fig. 3) and were described by a power function of temperature of the following form (R^2 = 0.984):

$$k = 10 \times 10^{-8} T^{2.8756} \tag{8}$$

The new values of n were computed based on k values obtained by eq. 8. Based on several expressions investigated, a regression analysis resulted in the following relationship of drying parameter n with temperature:

$$n = 2.469 - 0.0414T + 0.000415T^2 - 1.441 \times 10^6 T^3 \tag{9}$$

Predicted moisture ratios using eq. 4, 8, and 9 are compared to observed moisture ratios at drying temperatures of 70, 80, 100, 110, 120, and 130 °C in Fig 4. The estimated correlation coefficient between predicted and observed moisture ratios, r, is indicated for all the drying temperatures. It ranged from 0.9981 to 0.9991. Hence thin layer drying model for parboiled paddy developed in this study predicted the moisture ratios in good agreement to that obtained in oven drying experiments.

The activation energy of the drying process was obtained by using eq. 6 and 7. A relationship between $\ln(D_{eff})$ and $1/T_{abs}$ was established (Fig. 5) by a linear plot (r^2 = 0.9824).

$$D_{eff} = 1.71 \times 10^{-11} \exp(-3455.7/T_{abs}) \tag{10}$$

Activation energy of the drying process in our study was calculated to be 28.73 kJ/g mol which is little lower than 31.17 kJ/g mol as reported by Prasad and Singh (1984) for forced-air convection long-grain parboiled paddy drying at 38-158 °C. Activation energy of the drying process of rice was much higher (53-58 kJ/g mol) when dried in forced convection dryers at low temperature range (35-55 °C) (Steffe and Singh 1982; Bakshi and Singh, 1980). Therefore, it can be argued that natural convection drying requires less energy compared to forced convection dryers to dry the parboiled paddy at elevated temperature range. Low energy requirement is beneficial for the rice processing industries which can significantly reduce the operating cost. This area of research needs to be further evaluated in terms of product quality (such as milling characteristics), conventional energy calculation, as well as overall cost analysis.

5. CONCLUSIONS

Natural convection drying of parboiled paddy with negligible air velocity at elevated temperatures was evaluated. Four thin-layer drying equations were used to determine the best-fit model to the experimental data. Page's equation was found to give the best fit. The thin-layer drying model for drying of parboiled paddy for temperatures 70 to 130 °C was described by Page's equation:

$$MR = \frac{M_t - M_e}{M_o - M_e} = \exp(-kt^n)$$

where:
k $= 10 \times 10^{-8} T^{2.8756}$ and
n $= 2.469 - 0.0414T + 0.000415T^2 - 1.441 \times 10^6 T^3$

The activation energy for the drying of parboiled paddy was 28.7 kJ/g mol. This value is lower than the reported values of activation energy for forced convection drying of paddy.

ACKNOWLEDGMENTS
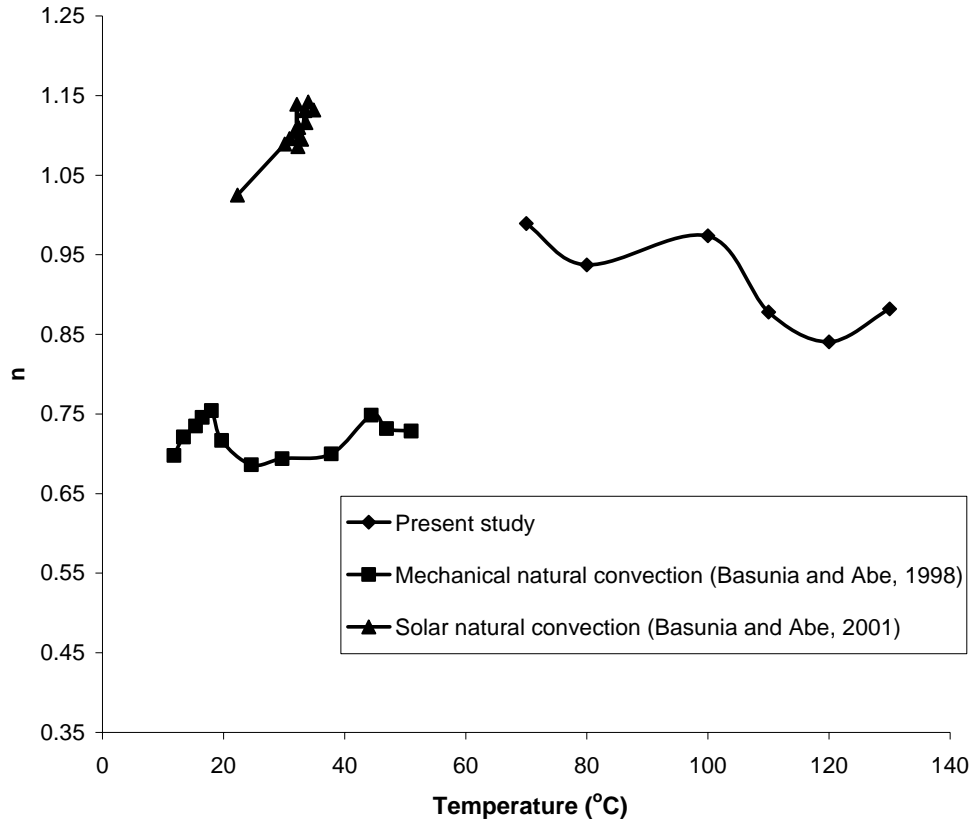
Fig. 1: Plot of drying parameter k in Page equation against temperature obtained from various studies
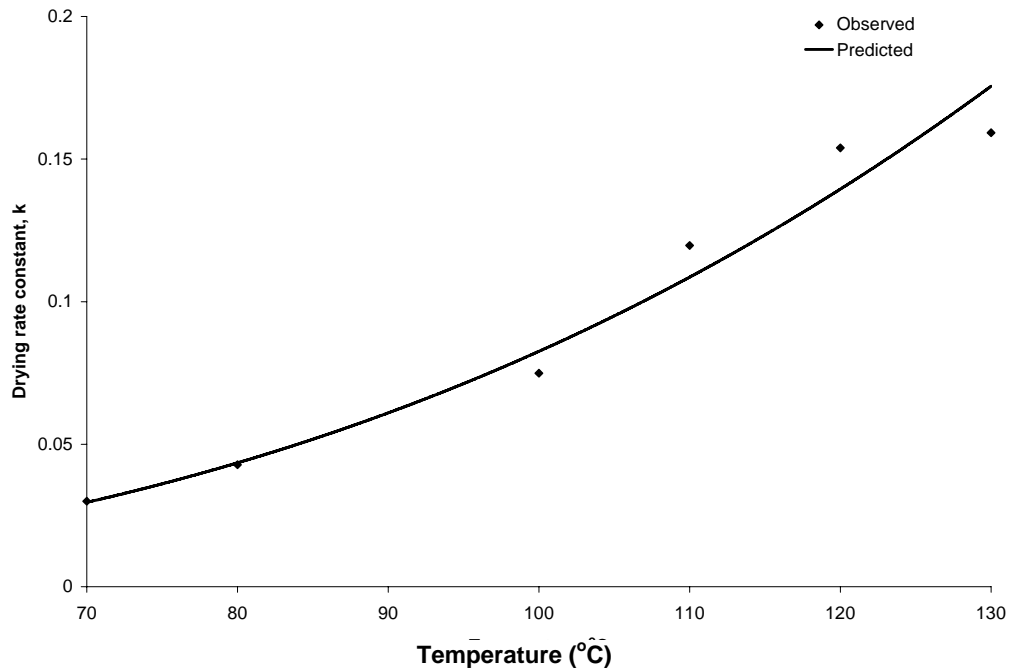
Fig. 2: Plot of drying parameter n in Page equation against temperature obtained from various studies
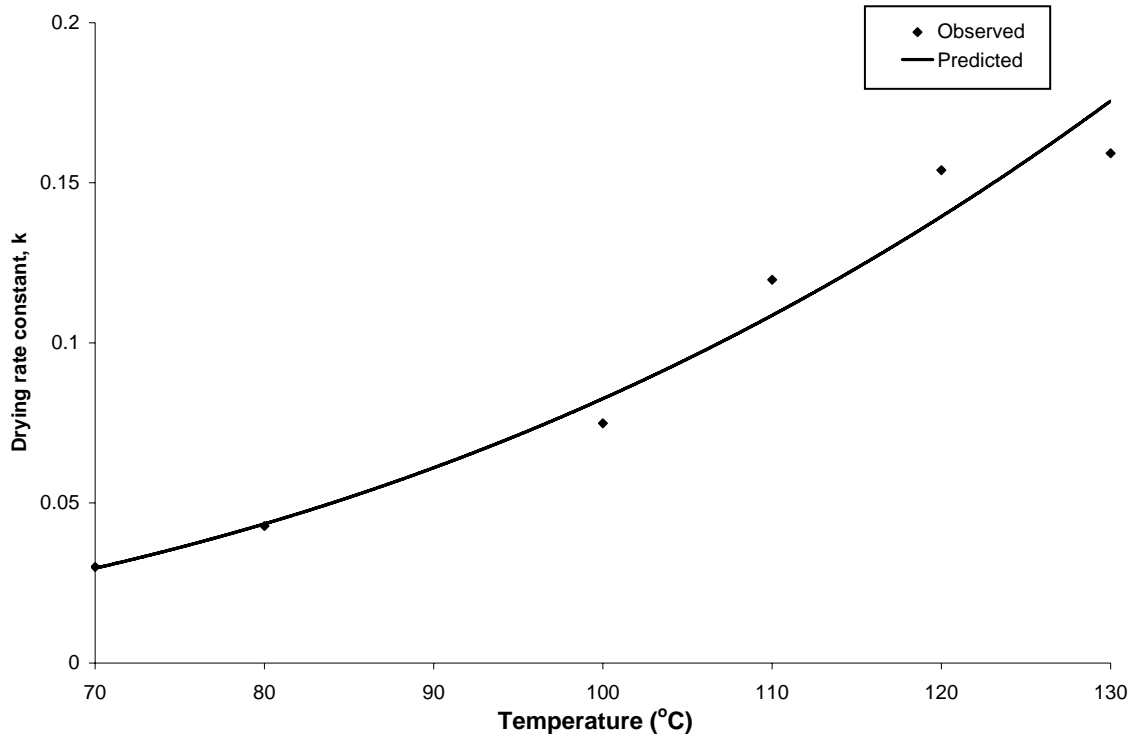
Fig. 3: Plot of k against drying temperature
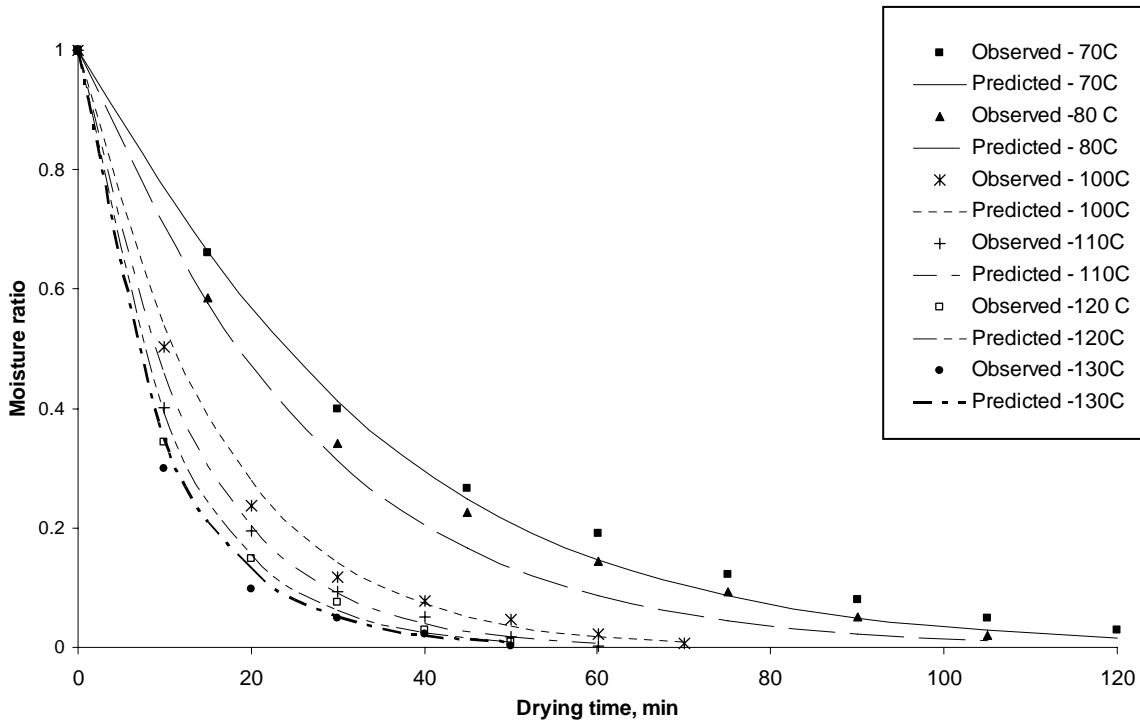
Fig. 4: Predicted and observed moisture ratios. Correlation coefficient: r = 0.9991 at 70 ^{o}C; r = 0.9984 at 80 ^{o}C; r = 0.9983 at 100 ^{o}C; r = 0.9982 at 110 ^{o}C; r = 0.9984 at 120 ^{o}C; r = 0.9985 at 130 ^{o}C

Table 2: Comparison of statistical parameters for four drying equations (eq. 2 to 6) at five drying temperatures

Equations	Temperature (^{o}C)	r	SEMR	RMSE
Lewis	70	0.9994	0.1472	0.0109
	80	0.9993	0.1585	0.0131
	100	0.9996	0.1966	0.0105
	110	0.9992	0.2135	0.0166
	120	0.9992	0.2294	0.0175
	130	0.9997	0.2507	0.0113
Henderson and Pabis	70	0.9995	0.1475	0.0117
	80	0.9993	0.1562	0.0137
	100	0.9996	0.1964	0.0113
	110	0.9991	0.2112	0.0179
	120	0.9992	0.2278	0.0194
	130	0.9997	0.2502	0.0126
Page	70	0.9995	0.1473	0.0115
	80	0.9997	0.1592	0.0096
	100	0.9996	0.1961	0.0100
	110	0.9999	0.2142	0.0067
	120	0.9999	0.2300	0.0055
	130	0.9999	0.2497	0.0070
Two-term	70	0.9995	0.1490	0.0135
	80	0.9997	0.1592	0.0113
	100	0.9997	0.1983	0.0115
	110	0.9999	0.2131	0.0067
	120	0.9999	0.2293	0.0066
	130	0.9999	0.2509	0.0080

r = correlation coefficient
SEMR = standard error of moisture ratio
RMSE = root mean square of error

REFERENCES

1. Abud-Archila, M., Courtois, F., Bonazzi, C. and J. J. Bimbenet (2000). Processing quality of rough rice during drying-modeling of head rice yield versus moisture gradients and kernel temperature. Journal of Food Engineering, 45(3): 161-169.
2. ASAE Standards (2003). S352.2: Moisture measurement – unground grain and seeds., ASAE. St. Joseph, MI.
3. Bakshi, A.S. and R.P. Singh (1980). Drying characteristics of parboiled rice. Proceedings of the 2nd International Symposium, Drying 1980, Vol.2, Ed. Mujumdar, A.S., Hemisphere Publ. Co., Washington, DC, pp. 282-288.
4. Bal, S., Maheswari, R. C., Prasad, S. and R. E. Parker (1976). Effect of drying air temperature on performance of a recirculating batch dryer for drying parboiled paddy. Rice Reporter, Rice Process Engineering Centre, Indian Institute of Technology, Kharagpur.
5. Basunia, M. A. and T. Abe (1998). Thin-layer drying characteristics of rough rice at low and high temperatures. Drying Technology, 16(3-5): 579-595.
6. Basunia, M. A. and T. Abe (2001). Thin-layer solar drying characteristics of rough rice under natural convection. Journal of Food Engineering, 47(4): 295-301.
7. Bhattacharya, K. R. (1985). Parboiling of rice. In: Rice Chemistry and Technology, Ed. Juliano, B.O. AACC. St. Paul, MN. pp. 289-340.
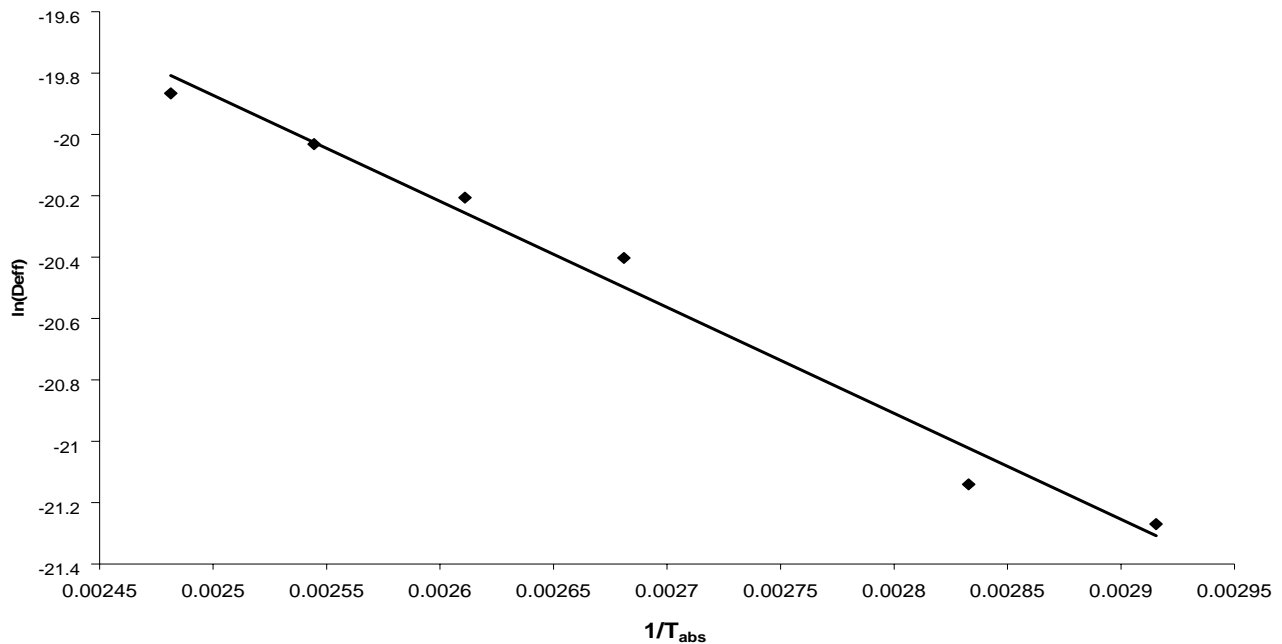
Fig. 5: Plot of $\ln(D_{eff})$ against $1/T_{abs}$ showing an Arrhenius-type relationship

8. Bhattacharya, K. R. and Y. M. I. Swamy (1967). Condition of drying parboiled paddy for optimum milling quality. Cereal Chemistry, 44(6): 592-600.

9. Chandra, P. K. and R. P. Singh (1984). Thin-layer drying of parboiled rice at elevated temperatures. Journal of Food Science, 49: 905-909.

10. Chen, C. and D. S. Jayas (1998). Dynamic equilibrium moisture content for grain drying. Canadian Agricultural Engineering, 40(4): 299-303.

11. FAO (2002). FAO Year Book of Production. FAO, Rome.

12. Henderson, S. M. and S. Pabis (1961). Grain drying theory II: Temperature effects on drying coefficients. Journal of Agricultural Engineering Research, 6(3):169-174.

13. Jayas, D. S. and P. K. Ghosh (2006). Preserving quality during grain drying and techniques for measuring grain quality. In Proceedings of the 9th International Working Conference on Stored Product Protection, 969-981. I. Lorini, B. Bacaltchuk, H. Beckel, D. Deckers, E. Sunfeld, J.P. dos Santos, J. D. Biagi, J.C. Celaro, L. R. D'A. Faroni, L. de O. F. Bortolini, M. R. Sartori, M. C. Elias, R. N. C. Guedes, R. G. da Fonseca, and V. M. Scussel, eds. Campinas, Brazil: Brazilian Post-harvest Association.

14. Jayas, D. S., S. Cenkowski, S. Pabis and W.E. Muir (1991). Review of thin-layer drying and wetting equations. Drying Technology, 9(3): 551-558.

15. Lewis, W.K. (1921). The rate of drying the solid materials. Industrial Engineering Chemistry, 13:427-432.

16. Mohapatra, D. and P. S. Rao (2005). A thin layer drying model of parboiled wheat. Journal of Food Engineering, 66: 513-518.

17. Noomhorm, A. and L. R. Verma (1986). Generalized single-layer rice drying models. Transactions of the ASAE, 29(2): 587-591.

18. Ozdemir, M. and O. Derves (1999). The thin layer drying characteristics of hazelnuts during roasting. Journal of Food Engineering, (42): 225-233.

19. Page, G. E. (1949). Factors influencing the maximum rates of air drying shelled corn in thin layers. Unpublished M.S. thesis. Dept. of Mechanical Engineering, Purdue University.

20. Prasad, P. K. and R. P. Singh (1984). Thin-layer drying of parboiled rice at elevated temperature. Journal of Food Science, 49: 905-909.

21. Prasad, S. (1988). Development of stress cracks in paddy grain during drying. Unpublished Ph.D. Thesis. Post Harvest Technology Centre, Indian Institute of Technology, Kharagpur.

22. Rao, S. N. R. and B. O. Juliano (1970). Effect of parboiling on some physico-chemical properties

of rice. Journal of Agriculture and Food Chemistry, 18(2): 289-294.

23. Sharma, A. D. and O. R. Kunze (1992). Post drying fissures developments in rough rice. Transactions of the ASAE, 25(2): 265-468.

24. Steffe, J. F. and R. P. Singh (1982). Diffusion coefficients for predicting rice drying behavior. Journal of Agricultural Engineering Research, 27: 489.

25. Zaman, M. A. and B. K. Bala (1989). Thin-layer solar drying of rice. Solar Energy, 42(2): 167-171.

DEVELOPMENT OF A TRANSPORTATION DECISION SUPPORT SYSTEM FOR RICE SEEDLING NURSERIES

Yi-Chich Chiu[§], Yi-Jen Chen[**] and Din-Sue Fon[**]

ABSTRACT

A decision-support system for transportation operations has been developed that should assist rice seedling nurseries with optimum planning. This was done using simulation software for five different types of transportation equipment, namely, a single-wheel cart, a dual-rail cart, a fork-lift with dual-rail carts, belt conveyors and a transport gantry Arena and the programming language Visual Basic were employed to develop a model that simulates the process of seedling input and output at a rice seedling nursery. Relevant data such as the size of hardening fields, the number of transporting equipment units and the number of available workers, etc., were inputed into the program in order to obtain the nursery throughput, the operational times and the utilization rate of workers under different conditions; the aim being to allow optimum decision making based on these various factors. An example based on a hardening field (90.4 m by 63.5 m) at 134 m from the sowing room was used to examine the system. The results showed that, for the seedling input operation, a transport gantry provided the best system throughput of 4,164 trays/h using eight workers. If the nursery used belt conveyors or a fork-lift with dual-rail carts, however, the throughputs were 2,549 and 1,725 trays/h, respectively. In output operations, if the number of workers was increased to 15, the transport gantry system throughput increased significantly to 5,885 trays/h. However, the belt conveyor only increased to 3,929 trays/h, which is still significantly lower.

Keywords: *Rice seedling; Nurseries; Decision support system; System simulation.* © 2007 AAAE

1. INTRODUCTION

The growing of rice seedlings in a nursery is an intensive, seasonal and time-limited business and usually requires some type of mechanical assistance to ensure a successful operation. There are about 600 rice seedling centers in Taiwan and these provide all the rice seedlings needed for the country. In the seedling nursing process, machines are required for tray stacking on the pallet, tray transport, tray unloading, tray rearranging and finally the retrieving of the grown seedling from the hardening field. The matured seedlings are then packaged and collected for transplantation. Fig. 1 shows the flow of a rice seedling nursery system. To assess investment in relevant machines and other equipment, factors such as the scale of the rice seedling center, the labor arrangements, the distance between the hardening field and sowing room, the sizes and shapes of the machines as well as their use and operational modes need to be considered. As many transportation operations are involved in a seedling nursery, it has become necessary to investigate the rationalization of

the whole system. Chiu and Fon (1998) analyzed seedling nurseries in terms of the types of transport equipment chosen by nine seedling centers, including a gantry.

Simulation has been frequently applied in operation research and management and can be used as a checkpoint prior to attempts to improve an existing or a newly- built system. It has also been employed to analyze agricultural production systems. One example is the greenhouse plant system developed by Fang *et al.* (1990) using the simulation language SIMAN/CINEMA (Pegden *et al.*, 1995), where the internal transportation system and allocation of resources during year-round production were studied. Another example is the study by Chen *et al.* (1978), who used the simulation language SIMSCRIPT (Kiviat *et al.*, 1973) to simulate a mechanical tray filling operation for potted plants and to analyze existing relationships in the operating system. In a similar way, Jagtap and Verma (1983) used the simulation language SLAM (Pritsker and Pegden, 1979) to set up a soil mixing and tray filling operation to produce consistent seedlings.

[§] Department of Biomechatronic Engineering, National Ilan University, I-Lan, Taiwan.
[**] Department of Bio-industrial Mechatronics Engineering, National Taiwan University, Taipei, Taiwan.

Decision support systems have also been developed using a simulation model to answer broader questions in agriculture, such the development of an integrated crop management of greenhouse cucumbers and tomatoes by Clarke *et al.* (1999). Other examples are the development by Fisher *et al.* (1997a, b) for of recommendations night and day temperature settings to control the timing and height of Easter lilies, the creation of a decision support system by Butts *et al.* (2004) to manage commercial peanut drying facilities and to predict peanut drying time and the development by Throp *et al.* (2007) of a precision agriculture decision support system to evaluate crop growth performance associated with the implementation of CERES-Maize.

The simulation software Arena developed by Rockwell automation (2000) provides an internal graphic environment for users, which allows the building of a simulation/animation model such that the simulation process can be observed on screen and is easy to debug. The Arena software is popular and widely employed for analyzing agricultural systems. Examples include Bechar *et al.* (2007), who developed two simulation models of working procedures in a tomato greenhouse with the aim of suggesting improved working practices by reducing manual labor. Another example is the development by Hansen *et al.* (2002) of a simulation model for sugarcane harvesting and delivery on the scale of a particular mill and its supply area; this model was used to study methods of reducing harvest-to-crush delays in the sugar industry. Furthermore, Halachmi *et al.* (2002) developed a behavior–based simulation model to optimize facility allocation in a robotic milking barn. An example involving a rice seedling nursery was described by Chiu *et al.* (2000), who developed a computer model for a transport gantry system with the aim of simulating and evaluating two transport activities in four seedling centers in Taiwan. Several other recent articles that have been published on model development using Arena software include Herrman *et al.*, 2002; Ingles *et al.*, 2006; Benson *et al.*, 2002 and Hansen *et al.*, 2002).

This study collected data on the various types of transport equipment used in rice seedling nurseries with the aim of creating an interactive decision-support system, which can be used to run a simulation of a rice nursery typical environment, allowing optimum planning of the nursery's transportation system.

2. DESCRIPTION OF THE VARIOUS TRANSPORTATION SYSTEMS

The transportation of seedling trays between sowing room and the hardening field is a major concern in a nursery system, as seed germination needs to be hastened in a stack and then the seedlings exposed to the sunlight in the hardening field. The seedling input process include the moving of seedling trays from sowing room to stacking area and then to hardening field, where seedling trays must be arranged in rows for acclimatization and further growth. The output process, on the other hand, handles the collection of the grown seedlings in form of rolled-mats and moves them out of the field to the truck for shipping. The seedling rolls, usually three in one tray are a convenient method of transportation for the seedlings over the significant distance to the field into which they will to be transplanted. For analysis, the transportation can be divided into three paths as indicated in Fig. 2: S_1 is one from sowing room to hardening field; S_2 is the route around the hardening field and S_3 is the internal transportation in the hardening field. The types of transportation include both batches type and continuous type, as described below.

2.1 Batch Transportation

Transportation in batches implies seedling trays are managed in lots with carriers having a fixed volume. The equipment includes single-wheel carts (SWC) and dual-rail carts with or without fork-lifts (DRC, DRC/F). The single-wheel carts, are simple in structure, are flexible in operation, are highly cost effective and can be pushed by one worker at a rate of about 27 trays per load. To facilitate the moving of the carts during soft field conditions, a pathway is temporarily connected by planks in order to support the cart wheels. However, the dual-rail cart requires a set of sectioned parallel rails supported on the ground. It is sometimes accompanied by a turntable to allow connection turns. The dual-rail carts can carry 80 trays per load in the input mode and this capacity increases to a pallet of 180 trays a time if fork-lifts are also used. The fork-lift is frequently used to help the transportation of pallets from the sowing room to the hardening field ($S_1 + S_2$). In terms of seedling output, the fork-lift's capacity is 75 trays or 225 seedling-rolls per load.

2.2 Continuous Transportation

Continuous transportation is done by belt conveyors, each 6m long, either in series or on a transport gantry. The path of the belt conveyors needs to be planned in advance before connection. They are easy to install at the start of the day and then are removed when the work has been completed. They are characterized by a high transportation rate. Distinct from the belt conveyor system, the transport gantry has two parallel V-belts installed on a longitudinally-moving truss, which rides on two distant parallel tracks located in the hardening field. The span of a gantry ranges from 24m to 30m and can be extended up to 100m in length as long as more spans and tracks added, depending on the hardening field needs. To have synchronous movement, both ends are motor-driven simultaneously under careful control. With the V-belt moving on the top in the horizontal direction, the gantry system allows X-Y movement and provides an internal transport system inside the hardening field.

3. SETTING-UP THE TRANSPORTATION DECISION-SUPPORT SYSTEM

3.1 System Structure

Fig. 3 shows the structural modeling of the transportation decision-support system (TDSS) using Arena 5.0 software for the simulation of the system input and output of seedling trays using the different transportation systems. Since this is graphical simulation with animation, the computer hard disk needs at least 100MB free for the program to smoothly execute. The Arena supports the macro language Visual Basic for Application (VBA), which is used to integrate the control strategy and object manipulations as the Microsoft Access database and its transverse application system are developed. Microsoft Access is used as the platform for data management and recording because it easily operate using strong functions and, through object management of the ActiveX Data Objects (ADO) database, uses Structured Query Language (SQL) to access information for Visual Basic and Arena. Using this approach, the information search results can be obtained in response to the demands of users. Visual Basic is an event driven programming language with a user-friendly graphical interface. During the present

research, Visual Basic 6.0 was used to develop a user-friendly interface that also integrated the Arena and Access database in the background.

3.2 Establishment of the Simulation Models

The models were established for both the input and output operations. In the input mode, six sub-models work involving six transport tools, namely, SWC, DRC, TT, fork-lifts with/without dual-rail cart (FL, FL/DRC), belt conveyor and transport gantry. For details of the developed models, please refer to Chen's thesis (2002).

Three paths are considered in the model, namely S_1, S_2 and S_3, as stated above. Under a discrete event mode, the transportation models are different from each other due to the properties of transportation equipment involved. The events taking place in the seedling input operation include tray supply, rail setting, cart-crossing and tray arranging:

(1) Tray supply: three seeded trays a time are manually loaded from the stacking area in the sowing room onto the transport equipment for forwarding to the hardening field.

(2) Tray arranging: the seeded trays are unloaded from carts and arranged orderly in rows in the field. The event includes: tray unloading; tray carrying to the surrounding distribution sites; setting the trays on the ground and returning for another load. The time of each action can be recorded for simulation purposes.

(3) Rail setting: If rails are used, the cart rails need to be removed to another unfinished line as soon as working on one line is finished.

(4) Cart crossing: cart crossing occurs when two carts meet in the working line. As such, the empty one should divert to avoid the loaded cart and let it pass, then resume motion.

In the output mode for the grown seedlings, the events include inner travel path S_3 and the surrounding route to the truck S_2 (Fig. 4). Four transportation modes, SWC, DRC, belt conveyors and transport gantry, are applicable and include five simulation events, namely, seedling rolling, seedling-roll uploading, rail setting, cart crossing and truck stacking. Fig. 5 shows the output operational flow for the grown seedlings. Chiu and Fon (1998) analyzed
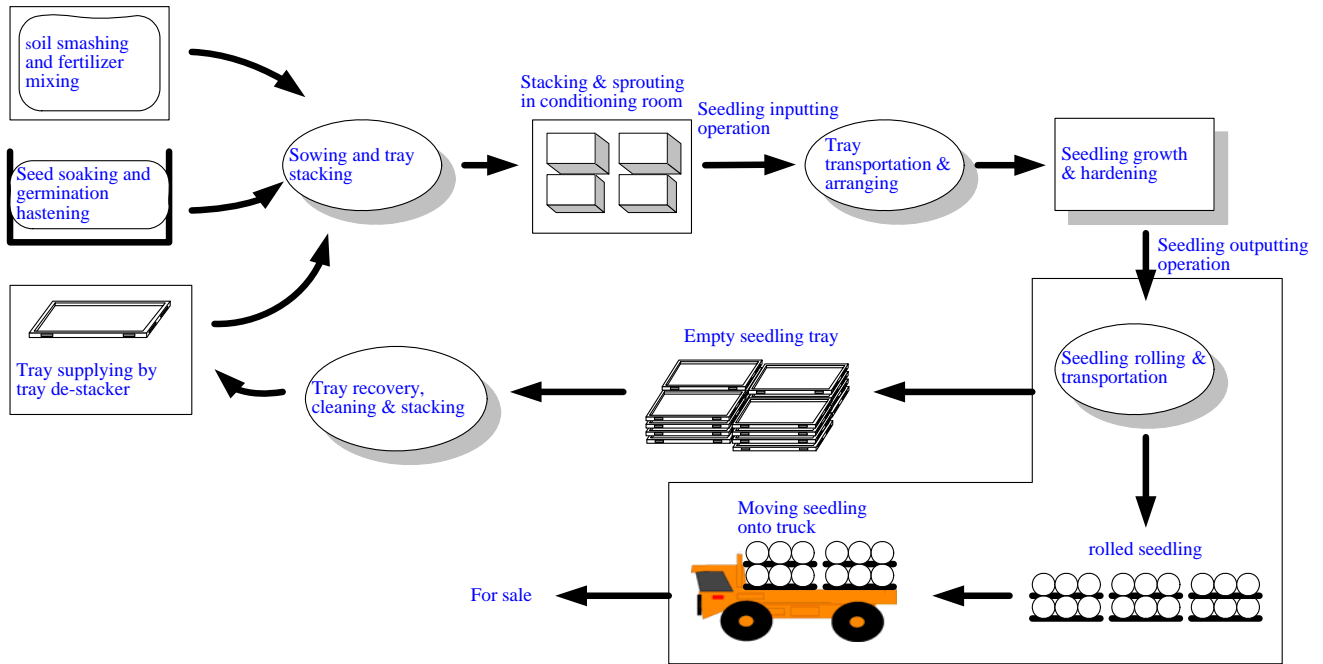
Fig. 1: System flow of a rice seedling nursery
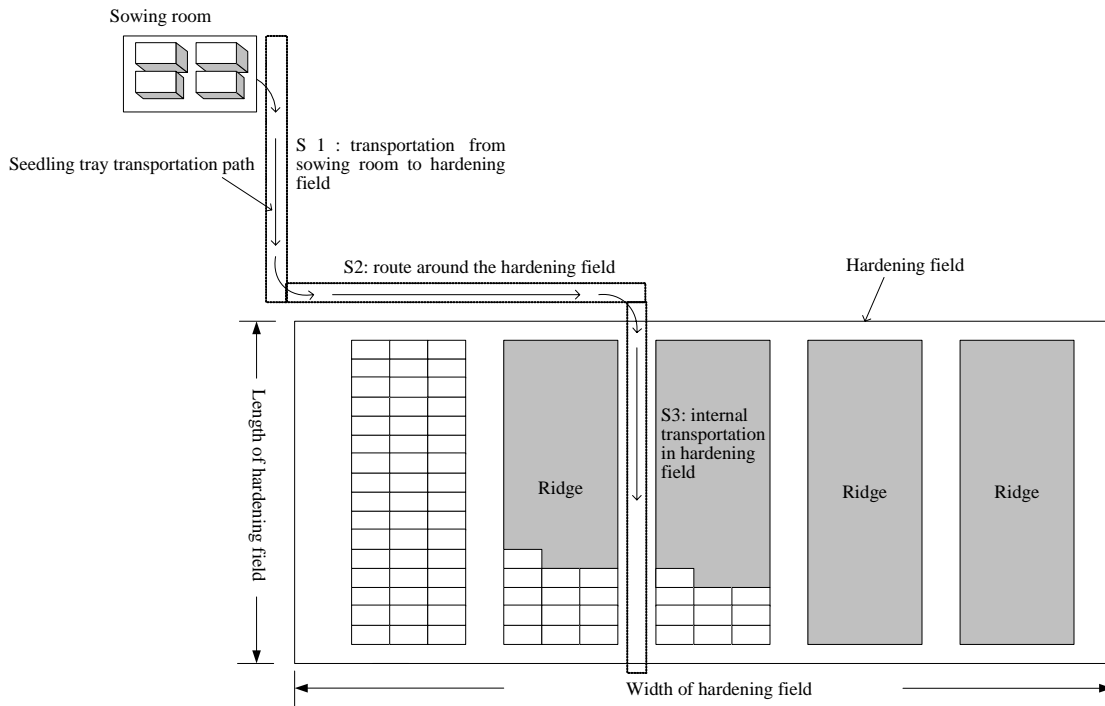
Fig. 2: Schematic diagram of the seedling tray transportation paths
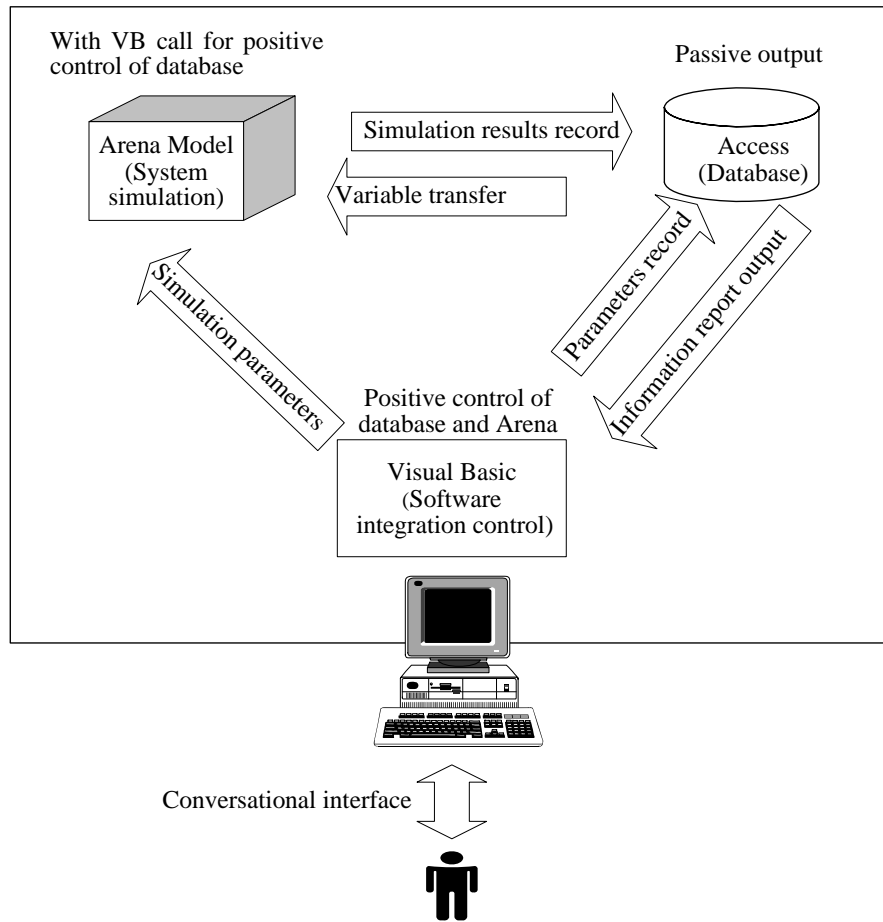
Fig. 3: Structural relationships of the transportation decision-support system
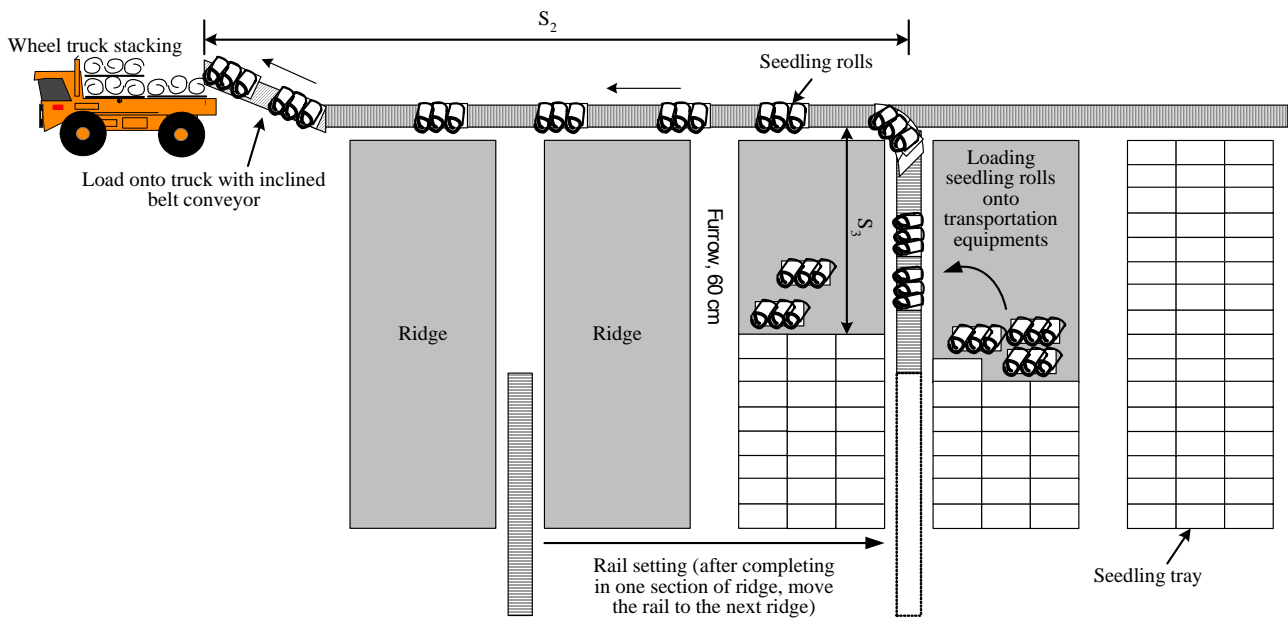
Fig. 4: Schematic diagram of the seedling output transportation system

and measured the operational time for each task (Tables 1 and 2) during transportation operations using a video camera. The results have been included in this study of the operational simulation and assessment.

4. RESULTS AND DISCUSSION

4.1 Operation of TDSS

The TDSS was designed in an interactive manner; with 'Form' as the container of the other objects. This directed the users to use this program step by step and reducing the burden of data entry on the user. The TDSS flow is shown in Fig. 6, with the operational steps being as follow.

(1) Parameter setting and recording
   The main menu of the TDSS displays the data for an individual seedling center and its parameter options involved in this system. The data include distance from sowing room to hardening field, length and width of hardening field. A click on the "Change" button in the right upper corner allows a switch to another nursery center simulation.
   The SSTab control is used to design the volume labels for the user's options in order that the input and output modes can be specified as using the correct equipment. This involves the "transportation operation simulation" label and the results of analysis are provided by "simulation result". The system finally converts the selected options into parameter values for simulation.
(2) Executing the TDSS
   The Visual Basic starts TDSS by using the ADO object to link with the database. Ten simulation runs are executed for each input or output operation case and the results are recorded in the Access database. The Animate function of Arena provides a real-time dynamic simulation and this allows the events that occur to be observed, which is useful for model setup and debugging.
(3) Result report
   A report is generated after the simulation is completed. The content includes the operating time, the system throughput, the hourly productivity per person and the utilization rate of workers.

4.2 Input Mode Analysis

In an example of the simulation, the dimensions used for distance from sowing room to hardening field was 134 m; the hardening field was 90.4 m long by 63.5 m wide; the number of rows per line was 3 rows; the number of concurrent working lines was 2 and the length of the furrow was 50 cm wide. In total, 25,536 seedling trays were processed in this case study.

The input operation had three working units and each required at least one worker. The TDSS is able to adjust the number of workers needed in the operation within a preset range by increasing it according to the utilization rate of the workers or their busy status. The simulation then resumes. In the end, the results obtained include total workers, operating time, system throughput and utilization rate of workers.

4.2.1 Analysis of Batch Input

Tables 3, 4 and 5 show the results for a batch seedling input operation using three transport tools, SWC, DRC and FL/DRC. The results include operating time, number of workers in each unit and the utilization rate of workers for 25,536 trays of grown seedlings. Judged by the utilization rate of workers, the bottlenecks within the system can be identified. Fig. 7 shows the relationships between total workers and the system throughput under the three types of batch input. The FL/DRC system has the highest system throughput, while the SWC has the lowest.

4.2.2 Effect of Batch Transport Tools on Seedling Input

Three batch transport tools (SWC, DRC and FL/DRC) were examined in this study and the simulation results show that when the number of workers is increased to between 7 to 9 persons, both the DRC and FL/DRC mode curves overlap one another (Fig. 8), indicating similarity of the two operational modes. The system bottleneck appears to involve there being too few workers available and thus it would seem that the system throughput is independent of amount of transport equipment used in this situation. In other words, more workers in action

support an increase in system throughput even when different transport tools are involved. However, there does exist a maximum for the system throughput as more workers are added. As long as the amount of batch equipment is fixed, the total productivity of the system is restrained.

4.2.3 Analysis on Continuous Input Operations

Tables 6 and 7 are the simulation results for belt conveyors and a transport gantry in the input mode, respectively. The relationship between the number of workers and the system throughput is shown in Fig. 9. The belt conveyor system has a maximum throughput of about 2,820 trays/h, which occurs when the total worker number reaches ten persons; additional workers have no further effect on the system perhaps due to the limitation imposed by belt conveyor speed. The transport gantry system with 10 workers reaches a throughput limit of 4,164 trays/h, which is significantly higher than the belt conveyor system.

4.3 Analysis of Seedling Output Operation

4.3.1 Batch Seedling Output

Results for the two transport carts (SWC and DRC) for an output of 25,536 seedling-rolls are shown in Tables 8 and 9. The operating time, number of workers and utilization rate of workers are considered and can be used to assess the operational status and system bottleneck. In the SWC case, additional workers are required as they show a high level of utilization; while with the DRC system, however, more workers need to be added to make the seedling rolling run smoothly.

Fig. 10 shows the system throughput for DRC and SWC in terms of the number of workers employed. The system throughput tends to increase as more workers are added. It can be observed that the system throughput for the DRC case is higher than for the SWC case, but that when more than 14 workers are employed, the system throughput of the SWC case is increased only slightly. If we take an example with 20 workers for each system; it requires 8 SWC units to obtain the same throughput as 5 DRC units. This is because the DRC has gates at both ends to prevent seedling trays from falling and as a result the loading procedure takes longer with the SWC system.

4.3.2 Effect of Number of Batch Transporting Tools on Seedling Output

Two simulations using 4 sets each of SWC and DRC were used to estimate seedling output with a limit of 11 total workers and the results indicate that the system throughput using DRCs was inferior to one using SWCs (Fig. 11). However, when the total workers reaches 12, the system throughput for DRCs is higher than for SWCs. Obviously, if the number of total workers is not sufficient, this will be a factor affecting the system throughput. Under a condition of sufficiency in workers, the next significant factor will be the capacity of the transport equipment.

4.3.3 Analysis of a Continuous Seedling Output Transportation Operation

Tables 10 and 11 show the simulation results for output operations using belt conveyors and a transport gantry. The throughput of both modes is related to the total workers as shown in Fig. 12. If fewer than 5 workers employed, the productivity is similar for both systems, but once the worker number increases to more than 5, the throughput of the transport gantry system becomes significantly higher. At 15 workers, the belt conveyor system has a throughput of 4,000 seedling-rolls/h, in comparison with 6,000 for the transport gantry system, which is about 50% higher than the belt conveyor.

5. CONCLUSIONS

A decision-support system using Arena, incorporating Visual Basic and Access was used to establish a rice seedling input model and an output transportation model. In the input operation, which handles seeded trays, five different types of transport equipment, namely, single-wheel cart, dual-rail cart, fork-lift with dual-rail cart, belt conveyor and transport gantry are considered. For the output mode, where seedling mats are shipped as rolls, the transportation modes used in the investigation were single-wheel carts, dual-rail carts, a belt conveyor and a transport gantry. The movement path for input follows the route from sowing room to stacking area and then to the hardening field; while, for the output mode, the move is from hardening field to the shipping truck.

```
                          ┌─────────┐
                          │  Start  │
                          └─────────┘
                               │
                   ┌───────────────────────┐
                   │ Workers collect seedling│
                   └───────────────────────┘
                               │
              ┌────────────────────────────────┐
              │ Workers load seedling-rolls onto│
              │    transporting equipments      │
              └────────────────────────────────┘
                               │
                          ◇ Is
                      all seedling        Yes     ╭─────────────────╮
                      completed for ─────────────→│  Workers stop   │
                      collecting ?                │ Seedling collecting│
                               │                  ╰─────────────────╯
                              No
              ┌────────────────────────────────┐
              │ Transporting equipments transport│
              │   seedling-rolls to the trucks  │
              └────────────────────────────────┘
                               │
              ┌────────────────────────────────┐
              │ Workers move seedling-rolls from the│
              │ transporting equipments onto truck for│
              │             stacking            │
              └────────────────────────────────┘
                               │
                          ◇ Is all
                      Seedling-rolls      Yes     ╭─────────────────╮
                      completed for ─────────────→│ workers stop rolls│
                      stacking ?                  │     stacking    │
                               │                  ╰─────────────────╯
                              No                          │
                          ◇ Is completed              ┌─────────┐
              No          a ridge seedling            │  Stop   │
           ←──────────────  collecting?               └─────────┘
                               │
                              Yes
                   ┌───────────────────────┐
                   │     Rail setting      │
                   └───────────────────────┘
                               │
                   ┌───────────────────────┐
                   │ Continue seedling collecting│
                   └───────────────────────┘
```

Fig. 5: Flowchart of the seedling output operation
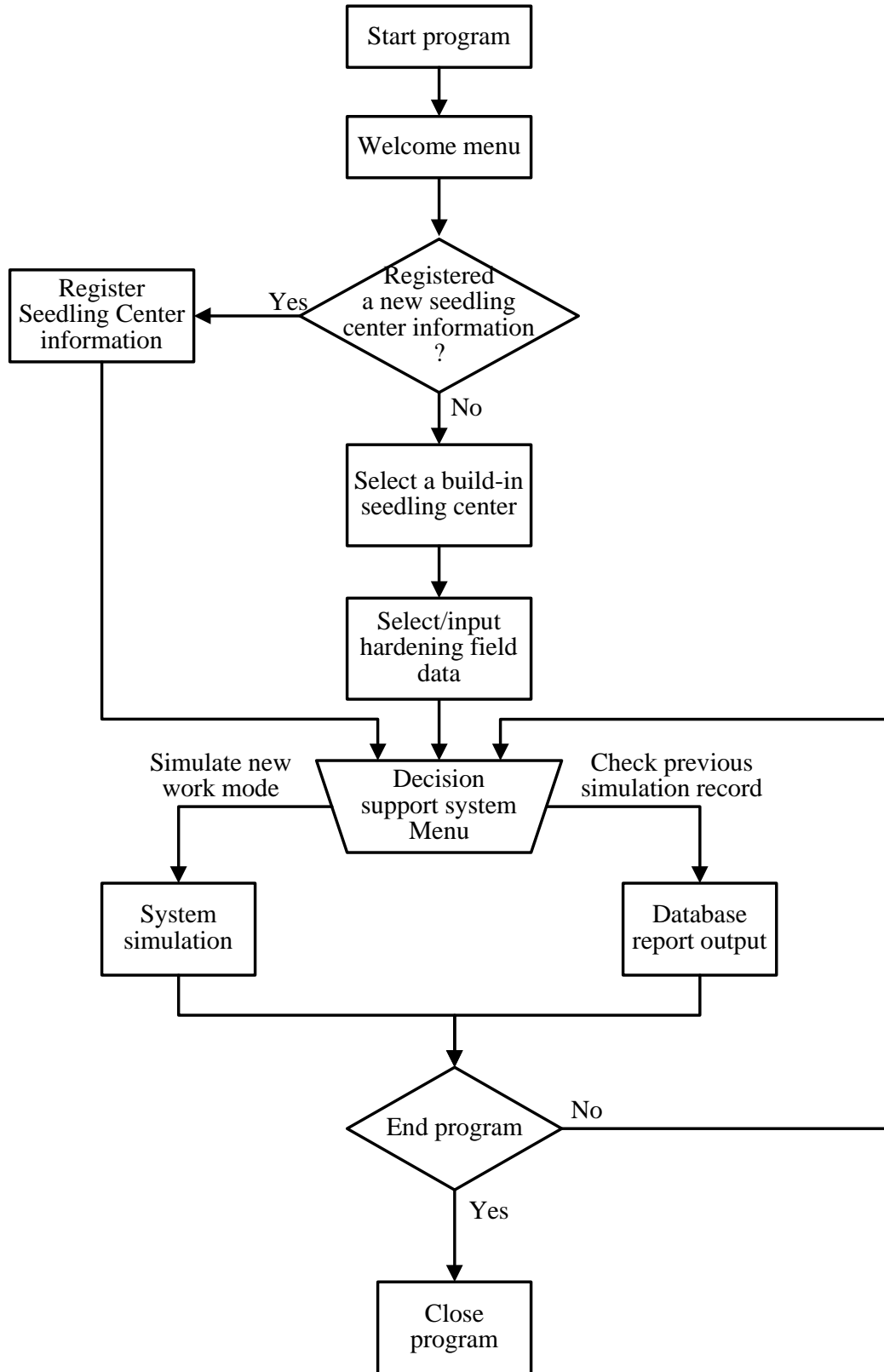
Fig. 6: Operational flow of the transportation decision-support system
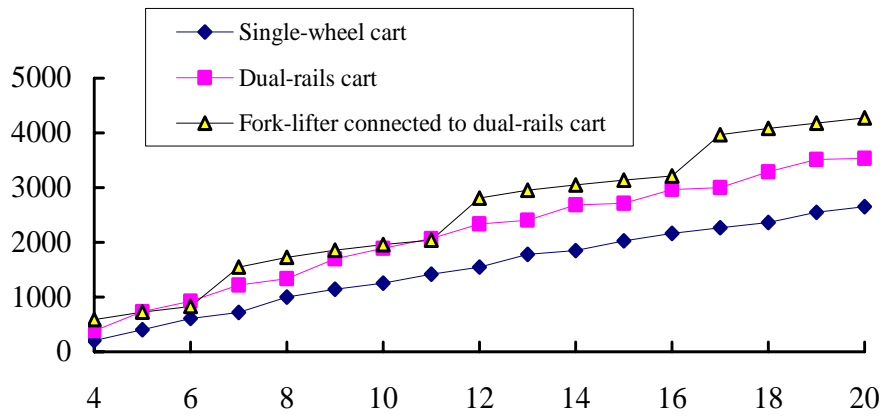
Fig. 7: Relationship between the number of workers and the system throughput under a batch transportation system for a seedling input operation
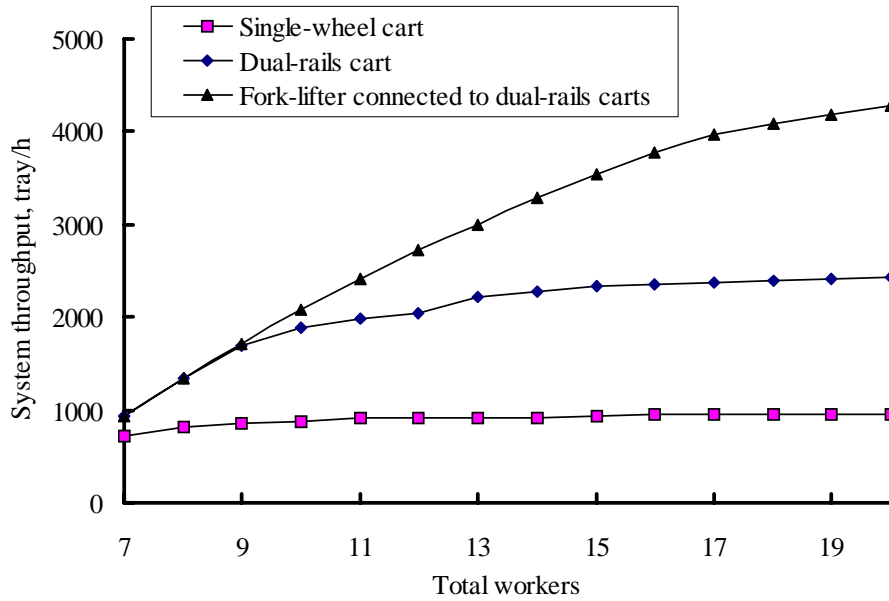
Fig. 8: Simulation results for three batch transportation systems involved in seedling input using three different types of transportation equipment
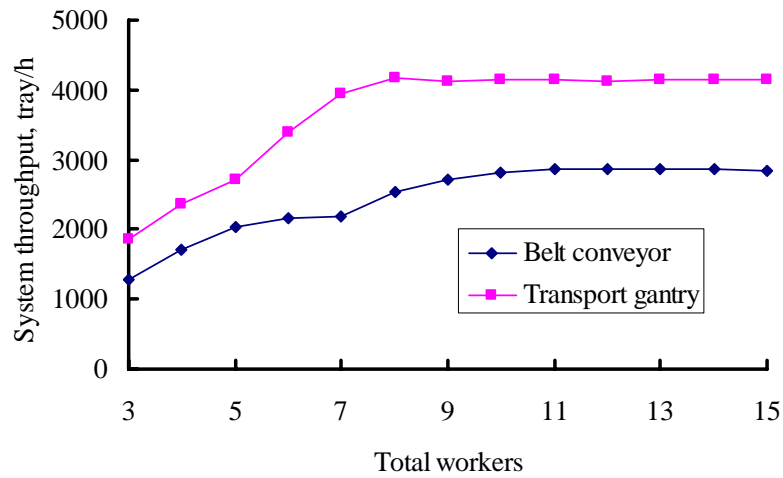
Fig. 9: Relationship between workers and system throughput in a seedling input operation with continuous transporting equipments
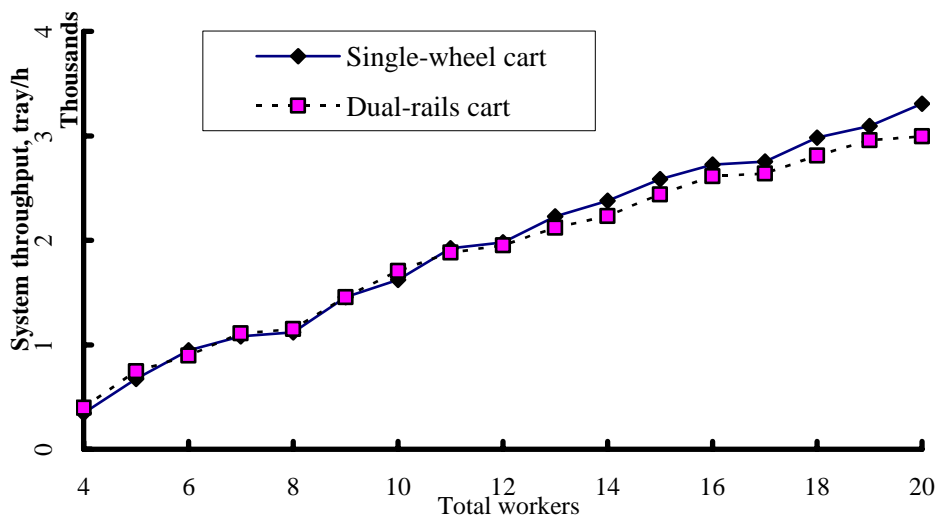
Fig. 10: Relationship between the number of workers and the system throughput under a batch transportation system for a seedling output operation
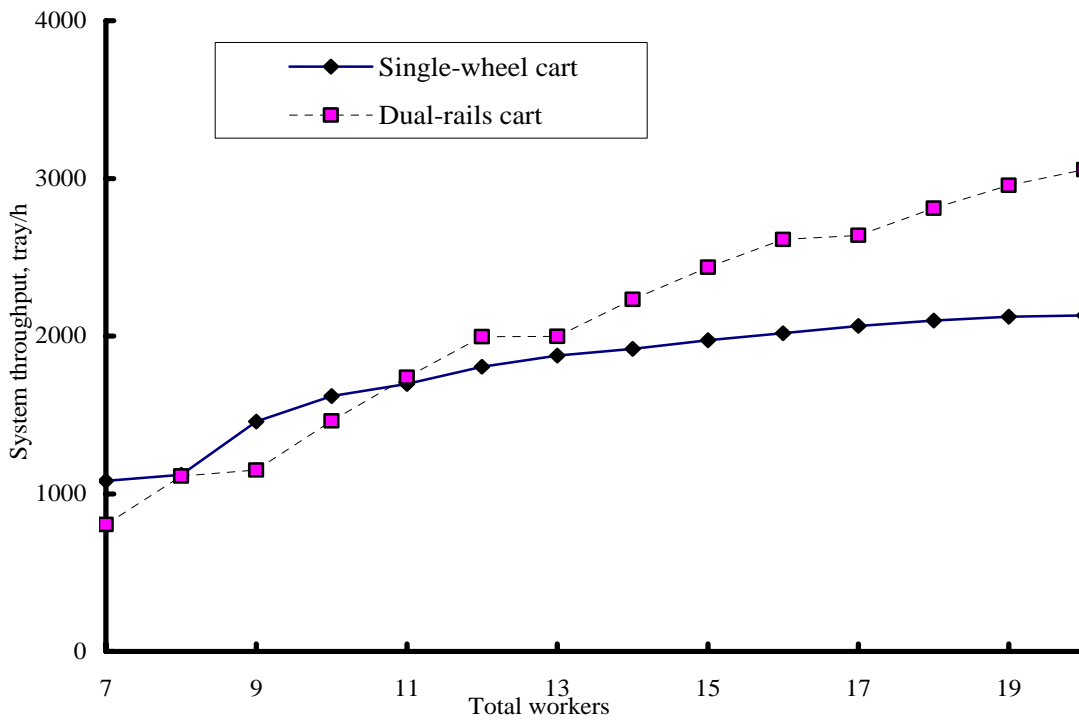
Fig. 11: Simulation results for seedling output using the single-wheel carts and dual-rails cart transportation
systems
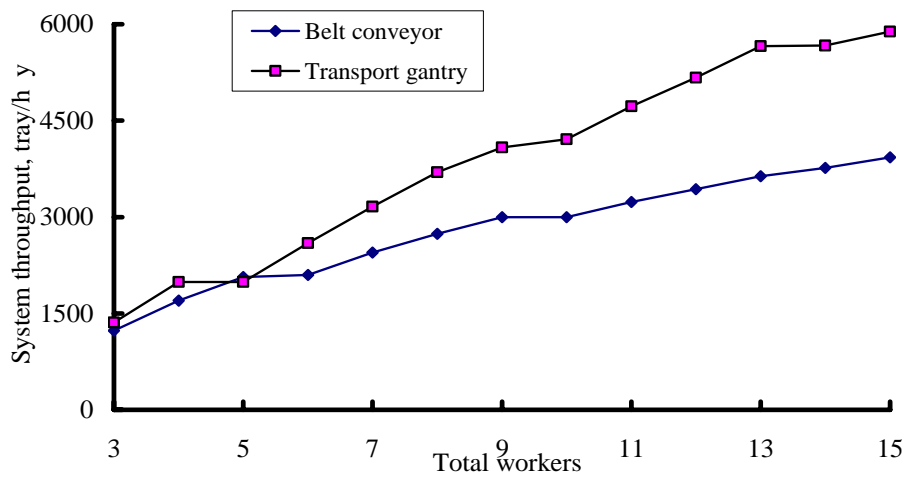
Fig. 12: Relationship between workers and system throughput in a seedling output operation using continuous
transporting equipment

Table1: Activity time data for each task in a rice seedling input operation (Chiu and Fon, 1998)

Transportion equipment	Loading seedling trays onto the transportion equipment, sec/ time	Full-loaded transportion equipment speed, m/sec	Unload seedling trays from the transportion equipment, sec/3 trays	Empty transportion equipment speed, m/sec	Rail setting, sec/m
Single-wheel cart (SWC)	3.69 ± 0.49 (3 trays/time)	1.1 ± 0.15	10.18 ± 2.79	1.15 ± 0.2	6.45 ± 1.11
Dual-rail cart (DRC)	3.69 ± 0.49 (3 trays/time) 49.2 ± 30.8 (180 trays/time)	Turning (sec/time) 6.14 ± 0.62 Direct movement 1.14 ± 0.16	16.84 ± 4.00	1.29 ± 0.46	7.99 ± 1.91
Fork-lift (FL)	17.59 ± 7.17 (180 trays/time)	1.81 ± 0.21	----	3.09 ± 0.62	----
Crawler Truck	44.17 ± 9.28 (72 trays/time)	0.93 ± 0.20	14.47 ± 3.13	1.24 ± 0.55	11.58 ± 1.83
Belt conveyor	2.97 ± 0.87 (3 trays/time)	0.31 ± 0.02	12.98 ± 3.40	----	9.01 ± 2.02
Transport gantry	3.99 ± 0.47 (3 trays/time)	0.31 ± 0.02	10.52 ± 2.66	----	7.99 ± 0.65

Table 2: Activity time data for each task in rice seedling output operation (Chiu and Fon, 1998)

Transportion equipment	Load seedling-rolls onto the transport tool, sec/ 3 rolls	Load seedling-rolls from transport tool onto, sec/3 rolls
Single-wheel cart (SWC)	4.75 ± 0.82	9.68 ± 2.16
Dual-rail cart (DRC)	11.00 ± 4.48	9.68 ± 2.16
Belt conveyor	2.79 ± 0.46	5.25 ± 1.23
Transport gantry	3.42 ± 0.41	5.25 ± 1.23

Table 3: Simulation results for the seedling input operation using a single-wheel cart transportation system

Total workers	Operating time, hr	System throughput, trays/h	Productivity, trays/h-person	Hardening field transportation		Single-wheel carts		Tray arranging	
				Workers	Utilization rate, %	Workers	Utilization rate, %	Workers	Utilization rate, %
4	123.4	207	51.7	1	7.3	1	98.4	2	15.4
5	63.3	403	80.6	1	14.2	2	97.2	2	29.9
6	42.0	608	101.3	1	21.4	3	97.3	2	45.1
7	35.5	720	102.9	1	25.4	4	87.8	2	53.4
8	25.5	1003	125.3	1	35.3	5	97.6	2	74.3
9	22.3	1144	127.1	1	40.3	6	94.3	2	84.8
10	20.4	1253	125.3	1	44.1	7	89.1	2	92.8
11	18.0	1419	129.0	1	49.9	7	96.0	3	70.8
12	16.5	1551	129.2	1	54.6	8	92.5	3	77.2
13	14.3	1782	137.1	1	62.7	9	95.1	3	88.9
14	13.8	1850	132.1	1	65.1	10	90.2	3	92.2
15	12.6	2028	135.2	1	71.4	10	96.1	4	76.5
16	11.8	2162	135.1	1	76.1	11	94.1	4	81.5
17	11.3	2269	133.5	1	79.9	12	91.4	4	85.6
18	10.8	2362	131.2	1	83.1	13	88.4	4	89.1
19	10.0	2546	134.0	1	89.6	13	97.0	5	77.6
20	9.6	2654	132.7	1	93.4	14	97.0	5	80.8

Table 4: Simulation results for a seedling input operation using a dual-rail cart transportation system

Total workers	Operating time, h	System throughput, trays/h	Productivity, trays/h-person	Hardening field transportation		Dual-rails cart		Tray arranging	
				Workers	Utilization rate, %	Workers	Utilization rate, %	Workers	Utilization rate, %
4	67.0	381	95.3	1	13.2	1	95.7	2	40.6
5	34.9	732	146.4	1	25.3	2	92.5	2	78.0
6	27.6	924	154.0	1	31.9	3	79.5	2	98.6
7	20.9	1222	174.6	1	42.2	3	90.7	3	87.4
8	19.1	1335	166.9	1	46.1	4	75.9	3	95.5
9	15.0	1701	189.0	1	58.8	4	89.2	4	91.5
10	13.5	1892	189.2	1	65.3	4	94.2	5	82.1
11	12.3	2069	188.1	1	71.4	5	83.9	5	89.9
12	10.9	2332	194.4	1	80.4	5	90.9	6	85.1
13	10.6	2403	184.9	1	83.0	6	79.7	6	87.5
14	9.5	2688	192.0	1	92.8	6	88.0	7	84.4
15	9.4	2715	181.0	2	46.9	6	79.5	7	85.2
16	8.6	2969	185.6	2	51.3	6	84.8	8	82.0
17	8.5	2999	176.4	2	51.8	7	74.7	8	82.8
18	7.8	3287	182.6	2	56.7	7	79.8	9	81.4
19	7.3	3512	184.8	2	60.7	7	83.6	10	78.5
20	7.2	3533	176.7	2	60.8	8	74.9	10	79.3

Table 5: Simulation results for a seedling input operation using fork-lift and dual-rail cart transportation system

Total workers	Operating time, h	System throughput, trays/h	Productivity, trays/h-person	Dual-rail cart		Tray arranging	
				Workers	Utilization rate, %	Workers	Utilization rate, %
4	43.5	587	195.6	1	35.6	2	62.5
5	35.1	727	181.7	1	44.1	3	51.9
6	30.8	828	165.6	1	50.3	4	44.7
7	16.5	1547	257.8	2	47.2	4	83.4
8	14.8	1725	246.5	2	52.6	5	74.9
9	13.8	1854	231.8	2	56.5	6	67.5
10	13.1	1956	217.3	2	59.6	7	61.4
11	12.5	2041	204.1	2	62.2	8	56.4
12	9.1	2807	255.2	3	57.2	8	77.6
13	8.7	2949	245.8	3	60.1	9	72.9
14	8.4	3051	234.7	3	62.2	10	68.3
15	8.1	3137	224.0	3	64.0	11	64.2
16	8.0	3211	214.1	3	65.5	12	60.6
17	6.4	3964	247.8	4	60.9	12	74.8
18	6.3	4080	240.0	4	62.6	13	71.5
19	6.1	4179	232.2	4	64.1	14	68.4
20	6.0	4273	224.9	4	65.5	15	65.6

Note: total workers include 1 worker to operate the fork-lift.

Table 6: Simulation results for a seedling input operation using a belt conveyor transportation system

Total workers	Operating time, h	System throughput, trays/h	Productivity, trays/h-person	Hardening field transportation		Tray arranging	
				Workers	Utilization rate, %	Workers	Utilization rate, %
3	19.9	1,280	426.8	1	35.2	2	92.8
4	14.9	1,709	427.3	1	47.0	3	83.7
5	12.6	2,023	404.6	1	55.6	4	75.4
6	11.8	2,168	361.3	1	59.6	5	65.5
7	11.6	2,197	313.9	1	60.4	6	56.1
8	10.0	2,549	318.6	2	36.5	6	65.1
9	9.4	2,718	302.0	2	38.6	7	60.3
10	9.1	2,821	282.1	2	39.9	8	55.4
11	8.9	2,857	259.8	2	40.4	9	50.6
12	8.9	2,871	239.2	2	40.6	10	46.3
13	8.9	2,873	221.0	2	40.7	11	42.6
14	8.9	2,873	205.2	2	40.7	12	39.5
15	9.0	2,846	189.7	3	29.4	12	39.2

Table 7: Simulation results for a seedling input operation using a transport gantry transportation system

Total workers	Operating time, h	System throughput, trays/h	Productivity, trays/h-person	Hardening field transportation		Tray arranging	
				Workers	Utilization rate, %	Workers	Utilization rate, %
3	13.7	1,866	622.1	1	68.9	2	93.5
4	10.8	2,356	589.0	1	87.0	3	79.7
5	9.4	2,713	542.5	2	52.1	3	91.9
6	7.5	3,388	564.7	2	64.2	4	87.3
7	6.5	3,936	562.3	2	73.4	5	82.2
8	6.1	4,164	520.4	2	76.9	6	73.4
9	6.2	4,116	457.3	3	53.8	6	72.6
10	6.2	4,139	413.9	3	54.1	7	63.4
11	6.2	4,133	375.8	3	54.0	8	56.1
12	6.2	4,132	344.3	3	54.0	9	50.5
13	6.2	4,148	319.1	4	44.6	9	50.7
14	6.2	4,148	296.3	4	44.6	10	46.2
15	6.2	4,148	276.5	4	44.6	11	42.6

Table 8: Simulation results for a seedling output operation using a single-wheel cart transportation system

Total workers	Operating time, h	System throughput, trays/h	Productivity, trays/h-person	Seedling stacking		Single-wheel cart		Seedling rolling	
				Workers	Utilization rate, %	Workers	Utilization rate, %	Workers	Utilization rate, %
4	73.6	347	86.8	1	31.1	1	96.2	2	30.0
5	38.0	673	134.5	1	60.3	2	94.9	2	58.1
6	27.0	948	157.9	1	84.9	3	91.5	2	81.9
7	23.6	1081	154.4	1	96.9	4	80.5	2	93.4
8	22.8	1120	140.0	2	50.2	4	70.1	2	96.8
9	17.5	1458	162.0	2	65.3	4	81.9	3	84.5
10	15.8	1620	162.0	2	72.6	4	86.9	4	70.9
11	13.3	1925	175.0	2	86.2	5	83.5	4	84.2
12	12.9	1980	165.0	3	59.1	5	78.9	4	86.7
13	11.5	2228	171.4	3	66.6	5	85.5	5	78.4
14	10.7	2377	169.8	3	71.0	6	77.1	5	83.7
15	9.9	2584	172.3	3	77.2	6	82.2	6	76.3
16	9.4	2724	170.3	3	81.4	7	75.3	6	80.4
17	9.3	2755	162.1	4	61.6	7	72.7	6	81.3
18	8.6	2982	165.7	4	66.8	7	77.6	7	75.9
19	8.3	3095	162.9	4	69.3	8	71.1	7	78.7
20	7.7	3307	165.3	4	74.1	8	75.1	8	74.0

Table 9: Simulation results for a seedling output operation using a dual-rail cart transportation system

Total workers	Operating time, h	System throughput, trays/h	Productivity, trays/h-person	Seedling stacking		Dual-rail cart		Seedling rolling	
				Workers	Utilization rate, %	Workers	Utilization rate, %	Workers	Utilization rate, %
4	64.0	399	99.7	1	35.8	1	92.6	2	48.3
5	34.2	747	149.3	1	66.9	2	88.7	2	90.4
6	28.5	897	149.6	1	80.4	2	90.8	3	72.8
7	23.0	1109	158.4	1	99.5	3	76.5	3	89.9
8	22.2	1150	143.7	2	51.5	3	62.0	3	93.2
9	17.5	1456	161.8	2	65.2	3	70.6	4	89.0
10	15.0	1706	170.6	2	76.5	3	77.0	5	83.8
11	13.6	1882	171.1	2	84.3	3	80.3	6	77.3
12	13.1	1953	162.8	3	58.4	3	73.9	6	80.2
13	12.0	2121	163.1	3	63.3	3	76.8	7	74.9
14	11.4	2233	159.5	3	66.7	4	61.5	7	78.9
15	10.5	2437	162.5	3	72.8	4	64.9	8	75.8
16	9.8	2612	163.3	3	78.1	4	68.0	9	72.5
17	9.7	2640	155.3	4	59.2	4	63.6	9	73.1
18	9.1	2811	156.1	4	63.0	4	66.3	10	70.5
19	8.6	2956	155.6	4	66.3	4	68.8	11	67.6
20	8.5	2995	149.8	4	67.0	5	55.7	11	68.6

Table 10: Simulation results for a seedling output operation using a belt conveyor transportation system

Total workers	Operating time, h	System throughput, trays/h	Productivity, trays/h-person	Seedling stacking		Seedling rolling	
				Workers	Utilization rate, %	Workers	Utilization rate, %
3	20.7	1,232	410.5	1	59.5	2	98.8
4	15.0	1,700	425.1	1	81.8	3	91.6
5	12.4	2,066	413.3	1	99.4	4	84.0
6	12.2	2,101	350.1	2	50.5	4	85.4
7	10.4	2,446	349.4	2	58.7	5	80.0
8	9.3	2,741	342.6	2	65.6	6	75.2
9	8.5	3,000	333.3	2	71.6	7	71.0
10	8.5	2,996	299.6	3	47.6	7	71.0
11	7.9	3,235	294.1	3	51.4	8	67.5
12	7.4	3,434	286.2	3	54.5	9	64.0
13	7.0	3,632	279.4	3	57.2	10	61.3
14	6.8	3,766	269.0	3	55.6	11	58.2
15	6.5	3,928	261.9	3	53.9	12	56.0

Table 11: Simulation results for a seedling output operation using a transport gantry transportation system

Total workers	Operating time, h	System throughput, trays/h	Productivity, trays/h-person	Seedling stacking		Seedling rolling	
				Workers	Utilization rate, %	Workers	Utilization rate, %
3	18.8	1,358	452.6	1	66.0	2	98.1
4	12.8	1,990	497.4	1	96.7	3	96.5
5	12.8	1,990	398.0	2	48.4	3	96.5
6	9.8	2,593	432.2	2	63.1	4	95.0
7	8.1	3,163	451.8	2	77.0	5	93.4
8	6.9	3,699	462.4	2	89.8	6	91.9
9	6.3	4,083	453.7	2	99.2	7	87.5
10	6.1	4,212	421.2	3	68.2	7	90.3
11	5.4	4,726	429.6	3	76.6	8	89.3
12	4.9	5,170	430.8	3	83.8	9	87.5
13	4.5	5,657	435.2	3	91.7	10	86.8
14	4.5	5,667	404.8	4	68.9	10	87.0
15	4.3	5,885	392.4	4	71.5	11	82.7

The example was based on a hardening field of 90.4 m length and 63.5 m width, which was 134 m away from the sowing room. The results showed that, for the seedling input operation, the one using a transport gantry yielded the most optimal system throughput of 4,164 trays/h with 8 workers. Under the same circumstances, belt conveyors and fork-lift and dual-rail cart gave throughputs of only 2,549 and 1,725 trays/h, respectively. During output operation with workers increased to 15, the system with transport gantry was also best with a throughput of 5,885 trays/h, while the one with belt conveyor was again significantly lower at 3,929 trays/h.

ACKNOWLEDGEMENTS

REFERENCES

1. Bechar, A., Yosef, S., Netanyahu, S. and Y. Edan (2007). Improvement of work methods in tomato greenhouses using simulation. Transactions of the ASABE, 50(2): 331-338.

2. Benson, E. R., Hansen, A. C., Reid, J. F., Warman, B. L. and M. A. Brand (2002). Development of an in-field grain handling simulation in Arena. ASAE Paper, No. 02-3104, St. Joseph, MI.

3. Butts, C. L., Davidson, J. I., Lamb, M. C. Jr., Kandala, C. V. and J. M. Troeger (2004). Estimating drying time for a stock peanut curing decision support system. Transactions of the ASAE, 47(3): 925-932.

4. Chen, L. H., Willits, D. H. and R. S. Sowell (1978). Computer simulation of nursery potting operations. Transactions of the ASAE, 21(2): 427-430,434.

5. Chen, Y. J. (2002). Development of decision-support system for the transport operation of seedling centers. Master Thesis of Department of Bio-industrial Mechatronics Engineering of Taiwan University, Taiwan.

6. Chiu, Y. C. and D. S. Fon (1998). Analysis on the transportation system for rice seedling centers in Taiwan. Journal of Agricultural Machinery, 7(1): 45-57.

7. Chiu, Y. C., Fon, D. S. and L. H. Chen (2000). Simulation of conveyor transport operations using a gantry system. Journal of Agricultural Engineering Research, 75: 417-428.

8. Clarke, N. D., Shipp, J. L., Papadopoulos, A. P., Jarvis, W. R., Khosla, S., Jewett, T. J. and G. Ferguson (1999). Development of the harrow

greenhouse manager: a decision-support system for greenhouse cucumber and tomato. Computers and Electronics in Agriculture, 24(3): 195-204.

9. Fang, W., Ting, K. C. and G. A. Giacomelli (1990). Animated simulation of greenhouse internal transport using SIMAN/CINEMA. Transactions of the ASAE, 33(1): 336-340.

10. Fisher, P. R., Heins, R. D., Ehler, N. J. and H. Lieth (1997a). A decision-support system for real-time management of Easter lily (*Lilium longiflorum* Thunb.) scheduling and height—I. System description. Agricultural Systems, 54(1): 23-37.

11. Fisher, P. R., Heins, R. D., Ehler, N. J., Lieth, H., Brogaard, M. and P. Karlsen (1997b). A decision-support system for real-time management of Easter lily (*Lilium longiflorum* Thunb.) scheduling and height—II. Validation. Agricultural Systems, 54(1): 39-55.

12. Halachmi I., Metz, J. H. M., van't Land, A., Halachmi, S. and J. P. C. Kleijnen (2002). Case study: optimal facility allocation in a robotic milking barn. Transactions of the ASAE, 45(5): 1539-1546.

13. Hansen, A. C., A. J. Barnes and P. W. L. Lyne (2002). Simulation modeling of sugarcane harvest-to-mill delivery systems. Transactions of the ASAE, 45(3): 531-538.

14. Hansen, A. C., E. R. Benson, J. F. Reid and R. H. Hornbaker (2002). Evaluation and use of an in-field grain handling simulation. ASAE Paper, No. 02-3105, St. Joseph, MI.

15. Herrman, T. J., M. A. Boland, K. Agrawal and S. R. Baker (2002). Use of a simulation model to evaluate wheat segregation strategies for country elevators. Applied Engineering in Agriculture, 18(1): 105-112.

16. Ingles, M. E. A., Casada, M. E., Maghirang, R. G., Herrman, T. J. and J. P. Harner III (2006). Effects of grain-receiving system on commingling in a country elevator. Applied Engineering in Agriculture, 22(5): 713-721.

17. Jagtap, S. S. and B. P. Verma (1983). Computer models of two nursery potting systems. Transactions of the ASAE, 26(4): 983-986.

18. Kiviat, P. J., Villanuena, R. and H. M. Markovitz (1973). SIMSCRIPT II.5 programming language. Los Angeles, California: Consolidated Analysis Centers Ins.

19. Pegden, C. D., Shannon, R. E. and R. P. Sadowski (1995). Introduction to simulation using SIMAN. 2nd Edition, McGraw-Hill, New York.

20. Pritsker, A. A. B. and C. D. Pegden (1979). Introduction to simulation and SLAM. Systems publishing corporation, West Lafayette, IN.

21. Rockwell automation (2000). Arena user's guide. Rockwell software Inc. USA: PA.

22. Thorp, K. R., Batchelor, W. D., Paz, J. O., Kaleita, A. L. and K. C. DeJonge (2007). Using cross-validation to evaluate Ceres-Maize yield simulations within a decision support system for precision agriculture. Transactions of the ASABE, 50(4): 1467-1479.

Volume 16, Contents and Author Index, 2007

International

Agricultural

Engineering

Journal

CONTENTS

AUTHOR INDEX

International Agricultural Engineering Journal

Guidelines for Authors

The International Agricultural Engineering Journal contains original papers only and submission of a manuscript will be taken to imply that the material is original and that no similar paper has been or is being submitted elsewhere. Papers are invited from all disciplines of agricultural engineering.

Copy: Manuscripts must be typewritten in English on A4 size paper (210 mm x 297 mm) on one side of the paper only, in double-spacing with liberal margins. The copies supplied must be complete with all figures, diagrams, drawings, photographs, tables, etc. Original for figures are essential on submission. An original and two copies should be provided. Generally, the length of the manuscript should not exceed 6000 words or about 12 printed pages inclusive of figures and tables.

Headings: The title of the paper should be as short as possible. All principal words should have capital initials. All section headings, table headings and figure captions should have an initial capital letter for the first word of each expression only, while all other words, with the exception of proper names, should be in lower case letters throughout. There should be no stop at the end of any title, footnote, heading, caption, etc., unless the last word is an abbreviation of which the stop is part. To show the hierarchical order of section headings, these should be numbered on the decimal system, e.g. 1, 1.1, 1.1.1 etc. Units in the table headings, legends to illustrations, etc., should follow the expression after a comma, not in parentheses, e.g. Max. output, kW.

Abstract: Each paper should have an abstract, not exceeding 200 words, between the title and the beginning of the paper.

Units, Symbols and Abbreviations: Systeme Internationale (SI) units must be used.

Illustrations: Illustrations, whether line drawings, graphs or photographs, are given a figure number (e.g. Fig. 1) in the same sequence and in ascending numerical order as reference is first made to them in the text. A separate list of figure captions should be supplied. Line drawings should preferably be in Indian ink on tracing paper, Bristol board or faintly lined graph paper. The captions, rather than the illustrations, should contain any explanation or keys, unless already given in the text. Figures should be complete with all legends and captions. As far as possible photos should be avoided. Wherever necessary, supply a black and white photograph on glossy paper.

In general, it is not permissible to give the same information in the form of a photograph and a drawing or in both graphic and tabular form. In each case, the most appropriate presentation should be selected.

Tables: Tables are numbered by Arabic numerals, e.g. Table 2, in ascending numerical order as reference is first made to them in the text. Tabulated data should not duplicate those shown graphically. The most appropriate presentation should be chosen.

Conclusions: Papers should have a final section headed "Conclusions", which succinctly summarizes important conclusions emerging from the work.

References: The references should be made by means of author's names and year in the text. The artifice "Leading author et al." may be used for multiple authorship papers if desired. At the end of paper, there should be a section headed "References" in which the full references should be quoted in alphabetical order including the names of all the authors, year, the title in the original language (and translation, where available), publication, volume, issue number (in parentheses) and page numbers, in that order.

Proprietary Products: In general, it is not desirable to give the names of products, instruments and equipment, model designations, or the names of their manufacturers; exceptions may be allowed, where detailed descriptions can be avoided by indicating the make, etc., or where considerations of accuracy and precision make it desirable that the particular product should be known. Mention of any proprietary product in this way implies no endorsement by this journal.

Refereeing: All papers will be refereed by at least two referees. The Editors collate the referees' reports and add their own comments. Final decisions on papers are made by the Editors.

Proofs: Authors will receive proofs for checking. Proofs will be sent to one author only. These proofs, clearly marked with the corrections, should be returned to the Editor with minimum delay.

Reprints: A total of 20 reprints will be supplied free of charge. Additional reprints can be ordered at current printing prices.

Page charges: To cover the printing and electronic submission process, there is a page charge of US$ 25 per printed page. Upon paper acceptance, the author should pay the charge.
Please make payment either by credit card or by bank draft/cheque in favor of "*ASIAN INST. OF TECH. (AAAE)*" and mail to:

AAAE Secretariat
c/o Agricultural Systems and Engineering
Asian Institute of Technology
P. O. Box 4, Klong Luang, Pathumthani 12120, Thailand
Tel: (66-2) 524-5479, 5450, 5488
Fax: (66-2) 524-6200, Telex: 84276TH

Submission: The original manuscript and two copies should be submitted to the Editor, Inter-national Agricultural Engineering Journal, c/o Agricultural Engineering Department, 218B Davidson Hall, Iowa State University, Ames IA 50011, U.S.A. First submission in electronic form is also encouraged (e-mail: aaae@ait.ac.th).

MEMBERSHIP APPLICATION FORM

ASIAN ASSOCIATION FOR AGRICULTURAL ENGINEERING (AAAE)

I wish to become a member of the AAAE
Membership Categories: (Mark the appropriate box)

☐ LIFE MEMBER   As per the age of a member (minimum US$ 400)
☐ REGULAR MEMBER   US$ 25 within Asia & US$ 35 outside Asia per calendar year[*]
☐ CORPORATE MEMBER   US$ 100 minimum annually (for industries only)

Affix Photo here

PERSONAL DETAILS

NAME (Prof./Dr./Mr./Ms.)...

DATE OF BIRTH : ....

TITLE/POSITION : ....

ORGANIZATION : ....

Mailing Address   : ....

....

Phone: .... Email: ....

Fax:...

QUALIFICATIONS ATTAINED:

....

Number of years of professional experience: ....

....

Special field(s) of interest:...

Affiliation with other society or association: ....

....

Please make payment either by credit card or by bank draft/cheque in favor of "*ASIAN INST. OF TECH. (AAAE)*" and mail to:

> AAAE Secretariat
> c/o Agricultural Systems and Engineering
> Asian Institute of Technology
> P. O. Box 4, Klong Luang, Pathumthani 12120, Thailand
> Tel: (66-2) 524-5479, 5450, 5488, Fax: (66-2) 524-6200, Telex: 84276TH

<u>For Office Use Only</u>... Date received..

Secretariat Acknowledged .... Verification of National Affiliation ....

Membership Grade Approved................................. Membership Number ....

Membership Plaque/Certificate/Card issued ....

---

  * Inclusive of US$ 10 for air mailing of journal and other materials

JOURNAL SUBSCRIPTION FORM

ASIAN ASSOCIATION FOR AGRICULTURAL ENGINEERING (AAAE)

Subscription form for the INTERNATIONAL AGRICULTURAL ENGINEERING JOURNAL published by AAAE.

Subscription rates are as follows:

☐ OUTSIDE ASIA   US$ 150* per annum (four issues)
☐ ASIA   US$ 135* per annum (four issues)
                                 * Including postage

Please make payment either by credit card or by bank draft/cheque in favor of "ASIAN INST. OF TECH. (AAAE)" and mail to:

> AAAE SECRETARIAT
> c/o Agricultural Systems and Engineering
> Asian Institute of Technology
> P. O. Box 4, Klong Luang, Pathumthani 12120, Thailand
> Tel: (66-2) 524 5479/5450 Fax: (66-2) 524 6200

SUBSCRIBER DETAILS

NAME:...

TITLE/POSITION: ....

ORGANIZATION: ....

Address: ....

....

....

Phone:..

Telex:.. Fax: ....

We wish to subscribe for the International Agricultural Engineering Journal for next …………… year(s). We have made arrangements for the subscription fee, a sum of ………... (USD), by Credit card or Bank cheque/Bank draft/Other.

Office Use Only

Date received:..

Secretariat Acknowledged: ....

Verification of Location (Asia/Outside Asia): ....

Subscriber Registration Number: ....

Asian Association for Agricultural Engineering (AAAE)

The Association was established on December 5, 1990 with the objectives, (i) To strengthen the profession of Agricultural Engineering by promoting information exchange, improving communications, minimizing duplication of activities, and optimizing use of resources. (ii) To publish an international peer-reviewed journal, supervised by an editorial board. (iii) To formulate, establish, and promote voluntary academic, professional and technical standards of relevance to the profession of Agricultural Engineering in Asia. (iv) To support, at the international level, the activities of national Agricultural Engineering societies or related associations and to maintain liaison among them. (v) To coordinate and assist in organizing timely international meetings in cooperation with national societies/associations within the region.

Membership Categories: (i) Life Member: Based on the age of the member (Minimum US$ 400); (ii) Regular Member: US$ 25 within Asia and US$ 35 outside Asia per calendar year; (iii) Corporate Member (mainly for industries, institutions or organizations): US$ 100 minimum per calendar year. Payment should be made either by credit card or by bank draft /check in favor of the "Asian Inst. of Tech. (AAAE)" and is to be mailed to the secretariat.

Association Officials:
- Prof. Nobutaka Ito, President, Japan
- Prof. Chen Zhi, Vice President, China
- Dr. Agung Hendriadi, Vice President, Indonesia
- Dr. Tanya Niyamapa, Vice President, Thailand
- Dr. Linus U. Opara, Vice President, Oman
- Prof. Jin Tong, Vice President, China
- Mr. Yoshisuke Kishida, Director, Public Relations, Japan
- Dr. Peeyush Soni, Secretary-General, Thailand
- Dr. Hemantha P.W. Jayasuriya, Treasurer, Thailand

Country Representatives on AAAE Board:
- Prof. B. R. Mulik – India
- Dr. Ida Bagus Suryaningrat – Indonesia
- Prof. Mikio Umeda – Japan
- Prof. Lu-Quan Ren – P. R. China
- Dr. Somposh Sudajan – Thailand

Service to Members:
The following valuable services will be provided by the AAAE to its membership. The Association will publish an "International Agricultural Engineering Journal" regularly. Announce a calendar of events, report on events, people and professional activities, and noteworthy product releases from agro-industry through AAAE Newsletter, published four times a year.

For further information write to: The AAAE Secretariat, c/o Agricultural Systems and Engineering, Asian Institute of Technology, P. O. Box 4, Klong Luang, Pathumthani 12120, Thailand. Tel: (66-2) 524 5450, 524 5479; Fax: (66-2) 524 6200, 516 2126. E-mail: aaae@ait.ac.th